ON THE BENEFIT OF AN ACTIVE HORIZONTAL TAILPLANE TO THE CONTROL OF THE SINGLE MAIN AND TAILROTOR HELICOPTER

by

Stewart S. Houston, B.Sc.

Dissertation submitted to the Faculty of Engineering, University of Glasgow, for the Degree of Doctor of Philosophy.

December, 1984

Table of Contents

Acknowledgements

The author wishes to express deepest gratitude to the following individuals and organisations: Dr. Alastair Caldwell, whose guidance, encouragement and suggestions proved invaluable; Mr. Frank O'Hara, for his enthusiasm and wisdom; Professor Bryan Richards, for his support and encouragement; and Mr. Gerald Wyatt of Westland Helicopters, who acted as external supervisor.

Financial support was provided jointly by the Science and Engineering Research Council and Westland Helicopters through a Cooperative Award in Science and Engineering; and external to this during the initial stage of the research by a University of Glasgow Scholarship.

Thanks are also due to Miss Anne MacKinnon and her staff of the Faculty Computer Service, Mr. David Parry of the Department of Electronics and Electrical Engineering, and Miss Margaret Simpson, Aeronautics and Fluid Mechanics Departmental Secretary. The author would also like to note the outstanding effort of Mrs. Linda McCormick, VAX system manager, who converted simulation and graphics packages under difficult and demanding circumstances.

Thanks are also due to Mr. Douglas Thomson and Mr. John Houston who proof-read the manuscript.

[redacted]

Stewart S. Houston

December 1984.

All aspects of the studies described in this Dissertation are original in content, except where indicated. The research was conducted between October 1981 and September 1984 at the Department of Aeronautics and Fluid Mechanics, University of Glasgow; and Westland Helicopters, Yeovil.

Stewart S. Houston

December 1984.

Abstract

Possible helicopter flight mechanics benefits associated with the use of an actively controlled horizontal tailplane are identified, influencing the areas of agility and manoeuvrability. In both cases, control strategies are postulated and implemented by means of control laws. They are then used with mathematical descriptions of the helicopter in digital computer simulations of manoeuvres to quantitfy the benefits.

In the field of helicopter agility, use of a relatively small horizontal tailplane is shown to enhance agility, relative to the helicopter with a fixed tailplane. Popup maneouvres to 50m can be flown up to 7% faster with the active tailplane; alternatively, geometrically tighter manoeuvres can be flown to the extent of reducing manoeuvre distance by up to 10%. The control law moves the tailplane proportionally with the contributions of the three rotor controls and helicopter pitch rate to the longtitudinal component of hub moment. It is however suggested that a tailplane control law based on functions of pitch attitude would be applicable to a wider range of manoeuvres than the popups simulated.

Helicopter manoeuvrability is enhanced by using the tailplane to decouple the pitch attitude from the flight path. The benefits are demonstrated by simulation of the acquisition and tracking of an airborne target. For a helicopter with the conventional pattern of control, significant changes in flight path result when the target is tracked with fuselage pointing; by comparison, the helicopter with a decoupled flight path and attitude controller changes flight path and speed by a negligible amount. It is suggested that this mode of control may be more generally applicable to control of the helicopter, in that it mitigates the speed/flight path/attitude compromise the pilot faces in flying his aircraft, or the possibly large hub moments when accelerating or decellerating.

The philosophy behind the use of the active tailplane differs from that of contemporary applications of moveable tailplanes, in that it is an integrated element of the flight control system, endowing (in its own right) control capabilities on the helicopter that are otherwise precluded by configuration. The addition of this extra control demands active control technology for several reasons: the applications require full control authority; the control laws are multivariable and change with speed; and the cockpit control setup would have to be simplified to the extent of the radical changes facilitated by active control technology.

Nomenclature

Notes 1/. Where a name or symbol has been used more than once, the sense in which it is used can be understood from the context.

2/. Names and symbols in the text that are subsets of, and applied to the same generic variable as those given here, are defined in the text at the appropriate point.

3/. The " θ_{1s}, θ_{1c} " and "β_{1s}, β_{1c}" scheme of notation is adopted here. The analyses were however conducted using the now less widely accepted " B_1, A_1 " and " a_1, b_1 " notation. Simply changing the sign of these latter four variables gives them as θ_{1s} etc. However this was not done with either the feedback matrix or the feedforward matrix results, which are therefore relative to the "old" scheme of notation.

4/. All angular quantities are in radians, unless specified otherwise. All velocities are in ms^{-1} unless specified otherwise.

5/. Bars over some variables denote normalised quantities

6/. Matrix elements are denoted $_{ij}$, where i indicates the row and j the column.

A ----- System matrix; coefficient of longitudinal stability quartic; disc area

AR ---- Agility rating

B ----- Control matrix, coefficient of longitudinal stability quartic

C ----- Matrix of coefficients in axis transformation equations; coefficient of longitudinal stability quartic

Cm_R --- Normalised rotor hub pitching moment

Cl_R --- Normalised rotor hub rolling moment

Cx_{ofus},

Cx_{fus},

etc --- Coefficients in linearised fuselage force and moment coefficients

D ----- Matrix of coefficients in axis transformation equations; drag; coefficient of longitudinal stability quartic

E ----- Matrix of coefficients in axis transformation equations; matrix of system eigenvectors; coefficient of longitudinal stability quartic

EI----- Stiffness of a beam

F ----- Matrix of coefficients in axis transformation equations

F ----- Generalised force

F_1----- Coefficient in rotor "spring stiffness" expression

I_x,I_y,

I_z ---- Helicopter moments of inertia

I_{zx} --- Product of inertia

J ----- Performance index

K ----- Feedback matrix

K ----- Tailplane hub moment gain

K_p ---- Precompensator matrix

K_f ---- Feedforward matrix

L,M,N - Roll, pitch and yawing moments

L',M',

N' ---- Perturbation roll, pitch and yawing moments

M_u,etc. Derivative with respect u, etc.

M_h ---- Longitudinal component of rotor hub moment

L_h ---- Lateral component of rotor hub moment

P_h ---- Total hub moment

$P_1(\Psi)$ - Azimuthal coordinate in blade deformation expression

Q ----- State weighting matrix

R ----- Control weighting matrix

R_t ---- Tail rotor radius

$S_m(x)$ - mth. mode shape of flapping blade

S_{flong} Normalised fuselage plan area

S_{flat} - Normalised fuselage side area

T ----- Axis transformation matrix; thrust; blade centrifugal loading

U,V,W - Total velociy components along body axes

U_P, U_T Blade velocity components

V_f ---- Flight speed

V_{fe} --- Trim flight speed

V_{ftg} -- Target flight speed

V_t ---- Tailplane volume ratio

W ----- Aircraft weight

X,Y,Z - Forces along body x,y,z, axes respectively

Y ----- Blade deflection

$X',Y',$

Z' ---- Perturbation forces along x,y,z axes respectively

a ----- Blade lift-curve slope

a_t ---- Tailplane lift-curve slope

a_{fin} -- Fin lift-curve slope

b ----- Number of blades

diag -- Indicates a matrix whose off-diagonal elements are null

e ----- Equivalent flapping hinge offset of a hingeless blade

g ----- Gravitational constant

h_c ---- Normalised rotor inplane X-force

h_R ---- Normalised height of rotor above x-y plane

h_f ---- Final altitude achieved

h_{fin} -- Normalised height of fin centre of lift above x-y plane

h_o ---- Initial altitude in Earth axes

h_t ---- Height of tailplane above x-y plane

h_{tr} --- Normalised height of tailrotor above x-y plane

k_s ---- Rotor "spring stiffness" term in hub moment expressions

k_λ ---- Wake induced velocity factor

l_t ---- Distance of tailplane from c.g.

l_{fin} -- Distance of fin centre of lift from c.g.

l_{tr} --- Distance of tail rotor from c.g.

m ----- Aircraft mass

m_o ---- Blade mass per unit length

p,q,r - Perturbation roll, pitch and yaw rates

r ----- distance along undeflected blade

q_c ---- normalised rotor torque

s ----- Rotor solidity

s_f ---- Final distance flown in Earth axes

s_o ---- Start position in Earth axes

s_t ---- Tail rotor solidity

t ----- time

t_c ---- Normalised thrust

t_{ctr}--- Normalised tail rotor thrust

t_f ---- final time

u,v,w - Perturbation translational velocities along x,y,z axes respectively

u_e,v_e,

w_e ---- Trim translational velocities along x, y, z axes respectively

u ----- Control vector

u_x, u_z Rotor velocity components

w_c ---- Normalised weight

x,y,z - Body axes

x ----- State vector; normalised distance along undeflected blade

x_{cg} --- Normalised location of c.g. relative to fuselage reference point

$x_e, y_e,$

z_e ---- Perturbation distances from trim point in Earth axes

y_c ---- Normalised rotor sideforce

$y_{box},$

z_{box} -- Dimensions of target box

α ----- Angle of attack

α_{fus} -- Fuselage angle of attack

α_t ---- Tailplane angle of attack

α_s ---- Tailplane incidence angle

α_{sh} --- Hub angle of attack

β ----- Blade flapping angle; sideslip angle

β_{fus} -- Fuselage sideslip angle

β_{cant} - Fin cant angle

β_o----- Rotor coning angle

β ----- Rotor disc longitudinal tilt

β_{1c}---- Rotor disc longitudinal tilt

β_{1s}---- Rotor disc lateral tilt

ν_o ---- Initial flight path angle; Lock Number

ν_f----- Final flight path angle

γ_s----- Shaft tilt

γ ----- Flight path angle

γ_s ---- Shaft tilt

ΔV_f --- Perturbation flight speed

δ ----- Blade drag coefficient; differential operator

ΔV_f --- Perturbation flight speed

μ ----- Tip speed ratio

χ ----- Wake angle

Ω ----- Rotor angular velocity

Ω_t ---- Tail rotor angular velocity

ρ ----- Air density

$\phi, \theta,$

ψ ----- Body perturbation roll, pitch and yaw angles; azimuthal position around disc

ϕ_e, θ_e Body trim roll, pitch and yaw angles

θ_{1s} --- Longitudinal cyclic pitch (perturbation only in time histories)

θ_{1c} --- Lateral cyclic pitch (perturbation only in time histories)

θ_0 ---- Main rotor collective pitch (perturbation only in time histories)

θ_{0tr} -- Tail rotor collective pitch (perturbation only in time histories)

λ ----- Rotor inflow ratio; system eigenvalue

λ_i ---- Rotor induced velocity

λ_β ---- Rotor flap frequency ratio

ACM --- Air Combat Manoeuvring

ACT --- Active Control Technology

ASE --- Automatic Stabilisation Equipment

CAC --- Computer Acceleration Control

NOE --- Nap-Of-the-Earth

SAS --- Stability Augmentation System

SISO -- Single Input, Single Output

Chapter 1

Active Control Technology and the Horizontal Tailplane

1:1 Introduction

Throughout the history of helicopter flight, distinct developments have enabled quantum improvements in all aspects of the helicopter's capabilities, influencing the areas of stability and controllability, handling qualities and performance. Such developments have included the introduction of hinged blades, the rotor swashplate for control, turboshaft engines and autostabilisation systems. At each stage, new roles and applications have been found for the helicopter, further expanding its usefulness. Today helicopters fulfil a plethora of functions in both the military and civilian fields. The helicopter is again at a milestone in its development, with two new technologies awaiting application: the use of composite materials, which allows the manufacture of complex and optimised blade sections and planforms, not previously achievable with metal construction; and the use of microelectronics in flight control, ranging from fast high capacity computers for processing, to electric actuators and the replacement of hydro- or electro-mechanical systems with digital electronic or optical signalling. In addition to the benefits in rotary-wing technology that have always paced rotorcraft development, for the first time a set of roles or specific applications exist that are also forcing the development of the helicopter. These roles are demanding tough, survivable battlefield helicopters, a requirement forced by the

number and sophistication of battlefield weapons systems not only in service, but also forseen.

The application of microelectronics to the control of any aerospace vehicle impacts flight mechanics in two distinct, although interdependent ways. Firstly, the programmable nature of the FCS allows the implementation of control laws or algorithms that can vary to suit flight state, vehicle loading or even the mode of control required (eg. for a combat helicopter there could be an NOE mode, a cruise mode and an ACM mode). Such an FCS would have an electro- or hydro-mechanical analogue of impossible complexity, not to mention weight. Secondly, the miniaturization of today's electonics allows multiple lanes or channels with sophisticated monitoring, to give systems of very high integrity. The latter will allow the former to use full control authority to fulfil a given task, if the system "decides" that this is necessary. The net effect of these features will be to allow manoeuvres to be performed that cannot currently be done, either because the FCS does not have the authority to allow stable and accurate manoeuvring beyond a certain point, or because it lacks the flexibility to signal the full range of the forces and moments capable of being produced, that would allow the pilot, for example, to fly in a certain mode; or to fly a desired path and attitude, with acceptable workload.

It should not be difficult to understand why the generic term for such technology is ACT, nor why vehicles that might utilise it are sometimes called CCV's - the control inputs can be configured, in a sophisticated manner if necessary, to generate forces and moments to produce the manoeuvre demanded by the pilot.

Given that a future helicopter control system will use ACT and exhibit the features just described, an analysis is required of the role that the horizontal tailplane would occupy within such a system. An advanced helicopter FCS should remove the need to consider traditional stability, controllability and handling qualities criteria that normally require a horizontal tailplane. On the other hand, the flexibility that ACT allows in all aspects of its application, including the resulting revolution possible in cockpit inceptors, might enable the tailplane to be used to produce control forces and moments in a manner that would enhance manoeuvrability or allow new and unconventional modes of control. The following literature survey and review puts the use of horizontal tailplanes on helicopters into perspective, and provides a useful database on which some assessment of the possible benefits of an actively controlled tailplane can be made.

1:2 A Review of the Literature

From the previous section it can be appreciated that the FCS and ultimately the handling qualities and flight dynamics of a future helicopter will be considerably different (perhaps fundamentally so) from the rotorcraft of the past. However it is important to reflect on the flight mechanics problems of previous helicopters, and to understand the way in which the tailplane has been used to correct them.

An early study of helicopter flight mechanics by Gessow and Amer, ref. [1], provides an insight into the physical aspects of helicopter stability that is easily understood. In this work the stability of the helicopter was split into considerations of static and dynamic stability,

in a manner analogous to a similar examination of fixed wing aircraft stability. The static stability of the helicopter, ie. that initial tendency to return to or diverge from the trim condition, is assessed in terms of individual stability derivatives. The speed stability of the helicopter rotor, represented by the derivative M_u, is normally positive with M_u greater than zero - an increase in the translational velocity u will result in a nose-up pitching moment, tending to slow the translational motion and hence oppose the initial disturbance. The angle of attack stability is negative, with M_w greater than zero - an increase in angle of attack will result in a nose-up moment, tending to further increase the initial perturbation. The pitch stability M_q is positive with M_q less than zero - a positive pitch rate gives a nose-down moment, tending to reduce the initial pitch rate disturbance. These simple "single degree of freedom" models are represented in figure 1:1. To understand these diagrams it is essential that the reader knows that a flapping rotating blade can be modelled as a second order system, and as such, there will be a 90 degree phase lag between output and input. This is adequately explained in standard helicopter texts such as Bramwell, ref. [2] and Johnson, ref. [3]. Further, it should be appreciated that the rotor can be represented as a disc, and the thrust assumed perpendicular to that disc. An assessment of the influence of fuselage aerodynamics on the static stability is also made in ref. [1]. Generally the fuselage will contribute to the angle of attack instability. As for speed stability, the conventional helicopter fuselage will have a nose-down moment coefficient in steady flight and any increase in speed will increase the magnitude of this moment, tending to increase the speed, ie. the fuselage aerodynamics will worsen speed stability. The contributions of the fuselage aerodynamics to helicopter static stability will more generally

be configuration specific, and may stabilise or destabilise the static speed stability, depending on the trim state of the helicopter. This may be understood from fuselage aerodynamic data as used by Padfield, ref. [4] for example, in developing a generalised mathematical model for flight mechanics work. This data is reproduced in figure 1:2. Note that the fuselage pitching moment coefficient can be positive or negative, depending on the angle of attack. Generally in the lower half of the speed range the angle of attack will be positive, the pitching moment will be positive and the fuselage contribution to speed stability will be stabilising.

One of the fundamental helicopter flight mechanics problems, viz. the longitudinal instability, can therefore be attributed to the rotor and body pitching moments, and how they vary with perturbations. The principal aerodynamic effect of a tailplane is a pitching moment on the helicopter and therefore it might be expected that the tailplane is capable of influencing the longitudinal stability by directly modifying the overall system of pitching moments, made up of the destabilising rotor and fuselage moments. A series of flight experiments was conducted by Gustafson et al, ref. [5] to assess the longitudinal flying qualities of three helicopter configurations. Although not aimed primarily at studying the effect of adding a tailplane (such a configuration was merely one to be evaluated competitively with two others), it was found that the influence of the tailplane was positive and significant - the helicopter with the tailplane demonstrated important handling qualities benefits over the aircraft without the tailplane. A brief examination of the results of these experiments helps to explain why most single main and tail rotor helicopters have horizontal tailplanes. The results are

probably best understood if explained in the context of the NACA divergence requirement, developed as a result of these experiments and which in fact influenced for many years helicopter handling criteria. The first part of the requirement states that following a displacement of the longitudinal cyclic pitch, the normal acceleration time history should become concave down within two seconds. The second part requires essentially that there should be no features of the normal acceleration response at the start of the manoeuvre that might render the pilot's task more difficult, in that he might be unable to predict what the peak normal acceleration might be, or when it might occur. Of the three helicopters (denoted A, B and C for convenience) A and B were identical, except that B had a horizontal tail assembly, figure 1:3, taken from ref. [5]. Configuration C was a different helicopter altogether, without a horizontal tailplane but with a gyroscopic device that served to increase the damping moments produced by angular rate pitching or rolling of the aircraft. Helicopter A did not meet either of the requirements, while aircraft C did. The tailed configuration met the first, although the authors expressed some doubt as to whether it met the second. It might appear so, considering the normal acceleration time histories, figure 1:4, also reproduced from ref. [5]; the pilot however did complain of an objectionable delay in the buildup of "g", but the removal of the divergent tendency in the growth of normal acceleration compared with the helicopter without the tailplane, was still believed to be more important than any further improvements.

An analytical study of the influence of the tailplane on helicopter flight dynamics was made by Bramwell, ref. [6], within a wider framework of an analysis of helicopter longitudinal stability and controllability.

Two terms in the longitudinal stability quartic

$$A\lambda^4 + B\lambda^3 + C\lambda^2 + D\lambda + E$$

were related to static stability (the E coefficient) and manoeuvre margin (the C coefficient). Expressions are given for these coefficients in terms of stability derivatives, and explicit expressions are given for the derivatives themselves. As a result the influence of a tailplane on stability and controllability is easily identified. Bramwell's paper concluded that the addition of a relatively small tailplane could vastly improve the manoeuvre qualities of the helicopter, but warned that the static stability could become negative at high tip-speed ratios. In fact, the question of whether or not static stability is desirable is not as straightforwards for the helicopter as it is for the fixed-wing aircraft because of the variation in the derivatives Z_u, M_u and M_w with speed, the effect of this on E, and the need for dynamic stability. For example, at high speed the tailplane is usually fitted to provide dynamic stability. This has the effect of reducing M_w, perhaps making it negative. Now E, from Bramwell, ref. [6] is

$$E = M_w Z_u - M_u Z_w$$

and Z_u is positive at high speed. Reducing M_w therefore reduces the static stability and could even make it negative. There is some provision for redressing this balance by modifying M_u, which can be varied by changing the tailplane incidence angle. This could however compromise the helicopter's trim state throughout the speed range. Bramwell concluded that such undesirable effects could probably be eliminated through careful

design.

The consequences of fitting a horizontal tailplane to single main and tailrotor helicopters has been well understood since the early days of the development of such aircraft. The influence on flight dynamics and handling qualities had been identified both qualitatively and quantitatively by flight experiments and analytical modelling. It is obvious, from even the brief literature survey presented, why most single main and tailrotor helicopters have a fixed horizontal tailplane; it offers a cheap and simple solution to the stability and controllability problems that helicopters face, and any undesirable effects (such as those on static stability and trim) are understood, and can thus be taken into account during design.

The use of moveable tailplanes on helicopters has been mainly to correct some inherent deficiency in the vehicle's flying qualities that the fixed surface cannot influence. In some cases, the fixed tailplane configuration has even contributed some handling problems, which are removed by making the tailplane moveable. There are several instances of this, detailed in the literature, where this is the case, as will be described later.

One of the first uses of a moveable tailplane was to provide a control pitching moment on helicopters with a teetering main rotor, and to this end the tailplane was geared to the longitudinal cyclic pitch. For such a rotor configuration, a major handling qualities problem can occur in low or zero thrust situations - that of inadequate or zero control pitching moment. It is instructive to describe the mechanism by which this

problem occurs, its influence on vehicle handling and the way in which the tailplane improves the situation. Consider two helicopters, each with a different rotor configuration - teetering (or with zero-offset flapping hinges), and one for which the blades are attached to the hub by flapping hinges offset from the hub centre. The latter can generate a pitching moment independently of the thrust - the centrifugal forces on opposite blades produce a couple. This cannot be done with the former configuration, and the only way in which a pitching moment can be generated is by thrust offset from the c.g. The effect this can have on flight dynamics and handling qualities is illustrated in figure 1:5. The first diagram shows the variation in controllability with load factor and rotor stiffness. For softer rotors, ie. those described by $\omega_b \simeq 1$, the control power and damping tends to zero as load factor is reduced, and can eventually reverse the control moment with respect to the sense of the pilot's input for low and negative load factors. The addition of a moveable tailplane, geared to the longitudinal cyclic pitch, has the effect of shifting the load factor curves upwards, by virtue of its contribution to control pitching moment. The onset of reversed control is thus delayed until lower values of load factor. The second diagram shows the pitch manoeuvre response diagram with the boundaries proposed by Edenborough and Wernicke, and taken from ref. [7]. The teetering rotor helicopter fails to fulfil the manoeuvrability requirements but the additional control power of the moveable tailplane helps to move the response characteristics closer to the desired area.

A study of the possible benefits of employing a moveable "stabilator" or horizontal tailplane on the Sikorsky S67 attack helicopter was made by Kaplita, ref. [8]. This tailplane configuration was not used

to correct any vehicle deficiencies, but rather to investigate any handling or flight mechanics benefits that might have been obtained using three modes; "free-floating", coupled to the longitudinal cyclic pitch, and trimmable in flight. The conclusions drawn in ref. [8] were that both the free-floating and in-flight trimmable modes provided little or no benefit, especially when the additional complexity of the control system was taken into consideration. The coupled mode was a feature recommended to be retained. This was because it confirmed results obtained with the NH3A research helicopter - the coupled tailplane contributed to improved handling qualities, reduced main rotor loads and produced a more manoeuvrable aircraft as a result, ref. [9]. It is important to note that this mode of tailplane control is different to that on helicopters with teetering or zero-offset flapping hinge rotors - both the S67 and the NH3A had offset flapping hinge rotor systems, and therefore did not suffer the handling qualities limitations at low thrust. The tailplane simply provided additional control power, rather than *all* control power, at zero thrust. The ability to trim the stabilator in flight was originally incorporated to vary the fuselage pitch attitude independently of the main rotor. This allows the longitudinal cyclic position, and therefore control margins and static stability, to be varied in flight. In addition, main rotor flapping can be reduced. As stated in ref.[8] an optimum setting was obtained for the S67, rendering the trimmable feature redundant. An additional design feature to note, especially when considered in the context of ACT, was the "design for failure" approach, and its effect on the operation of the tailplane. A tailplane actuator hardover failure resulted in an uncommanded pitching moment, produced by the tailplane travelling through its full incidence range of 10 degrees in 7 seconds. This had to be counteracted by application of longitudinal cyclic, of

which there had to be a sufficient margin. Now the fairly limited authority and very slow speed of response allowed control to be retained in the event of an actuator hardover. These characteristics are unlikely to be adequate for ACT applications (as will be shown), and so the philosophy of implementing a controllable tailplane using ACT will need to be different from that used in the past, in that there will no consideration of design for failure in the sense just described for the S67.

As mentioned prevously, the use of a horizontal tailplane has in some instances contributed new difficulties to the inherent problems associated with handling helicopters, caused primarily by the wake impinging on and moving over the tailplane, especially during transitions from the hover. This problem has come to light during the development programmes of several helicopters and different solutions have been implemented in each case cited here.

Hester et al, ref. [10] describe handling qualities aspects behind the Bell 222 development. Abrupt nose-up pitching during transitions from the hover in the original T-tailed configuration were caused by the main rotor downwash impinging on the tailplane as the wake moved aft. This is illustrated in figure 1:6, taken from ref. [10]. Note the wake angle at the given speeds - it is quite steep, and because of this the tailplane "sees" a significant change in angle of attack as it becomes immersed in the wake, causing the large uncommanded pitching moment. The solution was to position the tailplane on the tailboom, in the more conventional Bell location. At the speeds of concern the tailplane is then always immersed in the wake and the effects of the tailplane moving into and out of the

wake are absent. There was recognition of the possible occurence of this handling qualities problem during a phase of the development of the AH64 attack helicopter, ref. [11]. Three different solutions were considered, two of them shown in figure 1:7. At that stage in the program it was decided to implement a T-tail solution, thus placing the tailplane above the rotor disc and away from the wake. It is interesting to note that the production helicopter has a low mounted swivelling tailplane. In this case the tailplane incidence angle is varied as a function of flight speed, in order that its angle of attack is minimised when the wake passes over it. The possibility of large pitching moment variations during transitioning flight is therefore largely absent. Figure 1:8 shows this configuration in application on the UH60 helicopter.

The state of the art in moveable tailplane applications for helicopters can be found in the systems employed on the Bell 214ST and Sikorsky UH60 helicopters. The system employed on the 214ST improves longitudinal static stability, pitch dynamic stability, controls c.g. effects on pitch attitude and minimises the trim change with power. This electronic FBW tailplane provides these benefits basically through control of the attitude throughout the speed range (except for the dynamic stability improvements, which are obtained by means of feedback of airspeed perturbations to the tailplane). The electronic programmable nature of the system allows far greater flexibility in its design, allowing an optimum solution throughout the speed range. The electronic gains, both for feedback and to provide the required trim flight state, vary with speed, and the tailplane responds to control inputs not only in longitudinal cyclic, but also collective pitch, as well as speed perturbations. Control system authority (25 degrees) is significantly

greater than that of the S67, only 9 years previously. Although the benefits of this tailplane control system are significant (especially when compared with the mechanically geared tailplane on previous Bell helicopters), it should be appreciated that the flexibility endowed by the programmable nature of the system has been used to provide an optimum solution to "traditional" rotorcraft problems, and as an extension to the conventional stability augmentation system (SAS). Indeed consideration of static longitudinal stability (stick position with speed) and dynamic stability should not be of concern to the pilot of an advanced rotorcraft with ACT - the traditional controls in the cockpit are likely to disappear and be replaced with *inceptors* that may be of the spring return type with integral trimming, as studied by Morgan and Sinclair, ref. [12], for example; and dynamic stability will be taken for granted, with the FCS calling on full control authority if needed.

The UH60 Blackhawk helicopter has a moveable tailplane, ref. [13], normally operated automatically, but with reversion to pilot command if desired. The tailplane has been made moveable primarily to correct what would otherwise be undesirable features of the helicopter's response to controls or disturbances, due to its configuration - having a large canted tail rotor means that sideslip, either gust- or pilot-induced, or any tail rotor thrust change results in uncommanded pitching motions. The pitching moment capable of being produced by what is quite a large tailplane by helicopter standards, is commanded by a limited authority feedback system, the tailplane changing incidence either side of datum by only a few degrees in forward flight above 80 knots. Feedback signals are obtained from speed, attitude and sideslip motions, and the tailplane receives commands from main and tailrotor collective as well. In addition between

stabilisation task. Again it seems that no research is required in these areas - the tailplane is used as part of the stability augmentation system (SAS) on the Bell 214ST and UH60, and helicopters have been flown with the tailplane linked to the longitudinal cyclic for enhancing manoeuvres. However when considered in the context of the requirements of a future combat helicopter and the revolution in FCS design provided by ACT, the use of the tailplane to control attitude or provide a control pitching moment demands further study, as the helicopter is likely to be flown in environments quite unlike that of today eg. fast NOE or in ACM, and the ACT system could control it in a manner unlike that of current practice.

There is a considerable literature concerning the future roles of combat helicopters as well as the likely requirements, in terms of flight dynamics features needed to fulfil such roles. There has always been effort expended in studies aimed at enhancing helicopter manoeuvrability eg. ref. [14] dates from 1964, ref. [15] from 1968, and contemporary studies have concentrated on improving agility. Recently the roles of future combat helicopters have been more clearly defined, and phases of flight within such roles identified eg. by Steward, ref. [16], who describes three modes relating to the anti-armour mission; fast transit to the operating zone at a sensibly constant speed and height above the terrain, NOE flight in the operating zone to enhance survivability through maximum use of terrain features, and manoeuvring in the hover. In the first mode the high ground speeds over constantly changing and broken terrain would require low and even negative load factors to minimise exposure. In NOE flight the traditional hover-taxi airspeeds will be replaced by flight at speeds around the minimum power speed, giving

benefits such as improved agility through greater kinetic energy and power/thrust margins. Again low and negative "g" will be required although duration will be shorter. Flight may not be at constant speed as the terrain ahead and around will be masked by the very obstacles that the pilot is using for concealment, and such obstacles may present themselves suddenly, giving only limited room for manoeuvre. In conclusion Steward noted that current helicopters are not necessarily optimised for such operations, and that improved, including carefree, handling qualities will be required. In this respect, the author notes that ACT holds considerable promise.

Another mode of helicopter operation in the future that has recieved some attention is air combat. Lowson and Balmford, ref. [17] discussed this area, but with regard to helicopter versus high performance jet fighter. They concluded that provided the helicopter was engaged in a turning fight below 120 knots and was armed with an effective missile system, it could win against high performance aircraft. It was also noted that the helicopter can be pointed laterally and the authors expressed interest in investigating how far this capability could be used. Steward also tackled the concept of the helicopter in air combat, but concentrated on helicopter versus helicopter. This emphasised the need for increased agility for evasive manoeuvring and good target tracking capabilities at all speeds. The latter implies precise control of attitude and heading.

It can be understood from this brief description that the future combat helicopter will have to be operated to its performance limits and perhaps in new modes of operation. These requirements will force the helicopter to fly faster, manoeuvre more violently, rapidly change speed

and direction and to fulfil these requirements, unconventional control strategies could be required for optimum man/machine performance. Current helicopter types are unsuited for such operations for two main reasons; they lack the performance, and they do not have an FCS that will allow the pilot to manoeuvre the aircraft as required, with an acceptable workload. The current man-machine combination will not be able to perform the tasks of the future because the conventional helicopter FCS, which is essentially a limited authority stability augmenter, lacks the flexibility and authority that would allow precise control up to performance limits without excessive pilot compensation and resulting high (perhaps impossibly so) workload.

ACT will allow the implementation of a full authority high integrity FCS. If properly configured such a system should result in the future combat helicopter having the ability to manoeuvre as required without high pilot workload. Full authority control frees the pilot from his role as a stability augmenter, allowing him to *demand* motion without concern for stability. As a result the opportunity can at least in theory be taken to control the aircraft in different ways. Studies have been made to investigate different control strategies that could be called *manoeuvre demand strategies*, whereby movement of cockpit control inceptors is directly related to parameters of importance to the control of flight path; eg. pitch and roll rates, height and height rate, or indeed flight path parameters themselves giving direct control of the velocity vector. Ref. [18] describes various control strategies based essentially around two main systems: one is a "body rate" controller, the other a "flight path" controller. With the former system the pilot would command body angular rates to tilt the thrust vector and direct thrust control to vary

its magnitude. Cross-coupled responses to control inputs are absent. In a fundamental sense then such a controller is similar to the traditional pattern of helicopter control, but with undesirable features such as cross-couplings removed and a highly refined form of attitude control with control inceptor displacement more directly related to the desired perturbation in state. Tomlinson and Padfield, ref. [19], as part of a wider study of helicopter agility, investigated the influence of several forms of attitude controller on pilot rating while flying triple bend tasks. It was found that such modes of control improved the Cooper-Harper ratings - compared with the best raw helicopter results, these ratings were improved, in one case by 2. The other concept in manoeuvre demand FCS is the "flight path" controller, where cockpit inceptor movements are directly related to parameters of concern to trajectory in space ie. the velocity vector itself. Control movement may demand speed, height, height rate, turn rate, load factor etc. Body attitude control is thus taken from the pilot, who commands changes in the flight path directly. Bangen et al, ref. [20] investigated such a manoeuvre demand system and one of the most impressive results quoted was that an engineer with no previous helicopter piloting experience was able to fly the aircraft simulation successfully.

The future combat helicopter is likely to have a fairly stiff hingeless rotor configuration, certainly in the flapping degree of freedom. It is widely recognised that such a rotor system will confer upon the helicopter improved manoeuvrability, as has been demonstrated on Lynx and Bo105 helicopters for many years. Recently the benefits of this rotor configuration for agility tasks have been quantified, ref. [19]. Rotors with various stiffness and Lock number were assessed in the context of the agility courses flown in the piloted simulations. Generally pilots

preferred the stiffer rotors to fly triple bend tasks. Attlefellner and Sardanowsky, ref. [21] also described the benefits that could be obtained by using a stiff flapwise rotor, including improved control response, attainable load factor, turn performance and reduced exposure in NOE flight. These benefits are not without disadvantage however. In a wide review of hingeless rotorcraft flight dynamics, Hohenemser, ref. [22] pointed out that very large hub moments can result, eg. in trimmed flight due to an incorrectly set tailplane, or in manoeuvring flight with large control inputs, including collective pitch.

In summary then, the future combat helicopter is going to require improved agility over current configurations for better survivability and mission effectiveness. This enhanced agility will come through better performance and an FCS that will allow the pilot to fully utilise this performance. FCS requirements demand ACT, which in turn allows new control strategies that might further enhance the pilot's rating in particular tasks. The ability to perform new flight tasks eg. ACM will be required, together with a need to perform other "traditional" tasks such as NOE. Generally, the kinematics of future modes of flight need the swift response to control inputs that the stiff flapwise rotor can provide.

Armed with the information provided by this review, it is possible to reach some conclusions as to the application of an active tailplane on a future rotorcraft.

1:3 Conclusions, and Avenues of Research

The review has shown that traditional helicopter stability and

handling qualities problems can be solved by use of a relatively small fixed horizontal tailplane, whose pitching moment and its variation with perturbations in state will counteract the destabilising rotor and fuselage moments. Use of moveable tailplanes for control centred in the early years around consideration of an open-loop system, with the tailplane geared to the longitudinal cyclic pitch to produce an additional control pitching moment. The tailplane has also been used to vary the body attitude independently of the rotor, yielding various benefits including reduced drag, main rotor flapping, improved control margins and better static stability. The state of the art is shown by the FBW system on the Bell 214ST and UH60 helicopters. The FBW nature of the former system allows an optimum solution to the various flight mechanics problems by providing the desired body attitude throughout the speed range. The two main applications of a moveable horizontal tailplane are then to provide a control pitching moment for manoeuvring flight, and to give an optimum trim state throughout the speed range, through control of pitch attitude independently of the rotor. It might then seem at first sight that an ACT tailplane merits little investigation, as traditional rotorcraft flight mechanics problems should be absent on a helicopter with ACT. Indeed as described, with ACT there is a case for removing the tailplane altogether. The future combat helicopter is likely to have a stiff hingeless rotor, and so the need for additional control pitching moment is at first not apparent. Should the future helicopter require a tailplane for optimised trim performance, the technology for this already exists and has been applied to current production helicopters.

However, consideration of certain aspects of future combat helicopter operation, together with the ability of the tailplane to vary

pitch attitude independently of the rotor, or produce a pitching moment in manoeuvring flight, gives reason to study the use of the tailplane in a new context. Modes of operation are more severe than current helicopter practice; new flight tasks such as ACM, and a need to perform well known flight tasks such as NOE in a manner that will enhance mission effectiveness, presents a broad area of problems about which little is known. ACT, implemented to allow such modes of operation with acceptable workload, can allow unconventional control strategies - the helicopter may be flown differently with the result that the controls will move together quite unlike that of today's aircraft; and the stiff flapwise hingeless rotor while offering undoubted benefits in terms of response and controllability, can produce excessive hub moments. Within this context, there are two areas of control that an ACT tailplane could be used for. Firstly, it could produce a pitching moment in manoeuvres such that the rotor hub moment of the hingeless rotor helicopter is reduced. This would, for a given hub moment limit, allow more severe manoeuvres to be flown, thus contributing to enhanced agility. Secondly, the ability of the tailplane to vary the pitch attitude independently of the rotor could confer true CCV capabilities on the helicopter, rather than simply being used to optimise the trim. This latter function could be especially useful for acquisition and tracking of targets, especially in air to air work, complementing the ability of the helicopter to point laterally. There is no precedent for the uses of the tailplane just described, and the philosophy behind the use of the tailplane is quite different to that even on aircraft such as the 214ST or UH60 - the tailplane, as a control, would become an integrated element of the overall FCS, rather than an "add-on" to correct for inherent deficiencies in a given configuration. All aspects of the implementation of the active tailplane for the purposes just

described require investigation, including; basic design parameters (size, location), the required authority, control strategies and resulting control laws, and the aerodynamic and structural considerations that limit any benefits. In a given flight task, the benefits themselves need to be quantified vis a vis alternative configurations.

Chapter Two

A Mathematical Model of the Helicopter for Flight Mechanics Studies

2:1 Introduction

The capabilities offered by the modern computer are such that problems of quite considerable complexity can be solved in a reasonable time, without great expense. Given this situation, a major consideration in deciding the structure of a mathematical model is not the upper limit of the model's validity ie. how well can it represent how many phenomena, but its lower limit. Use of a mathematical model of given complexity to study a specific problem area could mask features in the results that are fundamental to the phenomena of concern, if the degree of sophisication is such that a physical interpretation of the model is difficult. This is not to say that complex mathematical descriptions of systems that could be more simply realised are not useful tools - in the design phase, where the physics of the system are understood, they are invaluable in obtaining accurate predictions of the system's behaviour. The art in developing a mathematical model of a system is in determining the simplest possible structure for the application in hand.

Having said that, mathematically modelling flight is a complex business, irrespective of the degree of sophisication of the resulting model. Features that have to be considered include aerodynamics - what

aerodynamic phenomena need be represented, and how is fundamental aerodynamic behaviour to be modelled; structure - what, if any, structural deformation is to be considered; dynamics - how do elements of the real system behave under the action of the aerodynamics, the structure and the controls; kinematics - leaving aside aerodynamic and gravitational forces and returning to the equations of motion of a rigid body, at and above terms of what order are simplifying assumptions made about the contributions of such terms to vehicle motion? For the helicopter, *dynamics* is of major concern, as the rotor with its flapping, lagging and feathering blades consitutes a dynamic system in its own right, with differential equations that describe its behaviour. It is fortunate that the area of modelling is extensively covered in the literature, and the experience of others with various levels of model in specific applications is available to be drawn on.

2:2 The Structure of the Model

The main assumptions made in the development of this model were

-- point representation of forces and moments
-- linear 2-D representation of the variation in aerodynamic force coefficients with sideslip or angle of attack
-- tip loss, compressibility, stall and unsteady aerodynamic effects are negligible
-- only the rotor flapping degree of freedom is included
-- rotor forces and moments generated by quasi-steady blade behaviour

There is evidence to suggest that these assumptions are probably valid for the determination of a model that is to represent accurately only *trends*. Padfield, ref. [23] investigated the influence of compressibility on rotor derivatives and concluded that general trends in the results may not be seriously distorted by assuming incompressible flow, but that there is a considerable difference in the values of thrust and coning angle, as well as the flapping derivatives, confirming earlier work.

Perhaps of greater concern are the latter two assumptions about blade behaviour. In a broad study of hingeless rotorcraft flight dynamics, Hohenemser ref. [22] analysed various levels of flight mechanics models, with increasingly complex representations of the main rotor. It was concluded that for most studies, a model consisting of rigid-body degrees of freedom plus rotor flapping only for generating rotor forces and moments, would be adequate - inclusion of the rotor's inplane degree of freedom had little effect on the rigid-body and rotor flapping modes, in the example cited by Hohenemser. For some rotor configurations, pitch/flap coupling can influence control and gust sensitivity, the angle of attack instability and the damping and control cross-couplings. This feature in not represented in this model, which will therefore be even more in error for such types than with other aircraft. The data set used however, represents a helicopter which can be assumed to have pitch/flap coupling minimised as a design aim.

The validity of the quasi-steady assumption about blade behaviour depends on the frequency separation of the rigid-body modes and the rotor modes. While describing this assumption as "adequate" for all flight

dynamics modes, Hohenemser points out that the approximations to the rigid-body modes for articulated and "soft" flapwise hingeless rotors can be considerably in error, but that such errors should become less important with increasing rotor stiffness. The helicopter used for the studies in this thesis had a rotor that was "soft" by Hohenemser's definition (λ_β^2=1.2), and it must therefore be assumed that some rigid body modes are poorly predicted. This can be put in some perspective by considering work done by Hansen, ref. [24] which compared the rigid-body eigenvalues obtained using the quasi-steady assumption, with those of higher-order models of the CH-53 helicopter, which has an offset-flapping hinge rotor. Using the longitudinal dynamics as an example, the eigenvalues most in error with the quasi-steady assumption were the short-period complex conjugate pair, whose imaginary parts were underestimated by 50%. Extrapolating this result to the stiff-flapwise hingeless rotor helicopter is difficult because its dynamics are quite different. Nonetheless, this example serves to illustrate the limitations of the assumption of quasi-steady blade behaviour.

These assumptions were used as the basis for development of a model that was of the linearised derivative type, where the perturbations from trim are assumed small enough for the perturbed forces and moments that result from motion away from the trim condition to vary linearly with the perturbations. The resulting simplification to the equations of motion is significant in that their coefficients are constant and this makes a physical understanding of the origin and effects of perturbed forces and moments on vehicle motion easy. However considerable critisism can be levelled against the linearised derivative approach, not the least of

which is that by definition, it is not valid for motions that are generally a large perturbation from trim. For a parametric study of flight mechanics where comparisons are drawn between various configurations, or a *trend* rather than absolute accuracy is required, then this type of model can be adequate, and provides a basis for clear insight into flight dynamics problems. Indeed, even when discussing quite complex motion phenomena, flight dynamicists will still refer to "derivatives" in an attempt to identify the underlying physical phenomena.

2:3 The Helicopter Model

The helicopter was assumed to consist of five individual elements whose forces and moments, and their variation with perturbations, could be added cumulatively to represent the resulting force and moment acting on the aircraft. The five elements are main rotor, tail rotor, fuselage, tailplane and fin. The rotor was modelled as stiff-flapwise for the reasons discussed in the preceeding chapter. The resulting equations of motion were relative to a set of orthogonal body-fixed axes, centred on the c.g., with the x-y plane lying in the floor of the helicopter, and the x-z plane perpendicular to this and forming the helicopter's plane of "symmetry", figure 2:1. The trim was calculated for the condition of steady "level" flight, and the resulting equations of motion were for perturbations from this trimmed state. The full description of the model, including expressions for the derivatives and the working required to arrive at them is not included. Such descriptions are normally very lengthy and involved and are really only of use when the author intends that his document be used as a reference, or if it contains sufficient new

material to merit detailed descriptions. The model was developed for these studies on the basis of recognised helicopter flight mechanics theory and, in particular, the following approach of Bramwell, refs. [2],[6] and [25] posesses neither of these qualities - as a result only the expressions for the forces and moments produced by each component are given, and the method of calculation of the trim and derivatives described. The aim in this is to give the reader a broad overview of the model that will allow him to place it in some perspective and thus assess its validity and limitations. It is however sufficiently complete for the reader to calculate the trim state and all the derivatives, if so desired. Initially the model's validity was checked qualitatively by ensuring that trends in control positions, the major derivatives and system eigenvalues were representative of a hingeless rotor helicopter. Baseline data for this helicopter is given in table 2:2. Later a more comprehensive model than the one written for this study was obtained and used as a benchmark against which a quantititative agsessment of HELSIM was made. The forces and moments were all normalised according to the scheme adopted by Bramwell in refs. [2] and [6] for example.

2:3.1 The Main Rotor Forces and Moments

The main rotor force coefficients according to Bramwell, ref. [25] are given by

$$\left.\begin{aligned} t_c &= a/4\ [\ 2/3\Theta_0(1+3/2\mu^2) + \lambda + \mu\Theta_{1s} - \mu e\beta_{1c} + 1/2\mu p\ ] \\ h_c &= 1/4\mu\delta - t_c\beta_{1c} - a/4\ [\ \mu\lambda_i\Theta_0 + 1/2\lambda(\Theta_{1s}+\beta_{1c}) + 1/8\mu q\Theta_{1c}\ ] \\ y_c &= -\ t_c\beta_{1s} + a\lambda/8\ [\ \Theta_{1c}-\beta_{1s}] \end{aligned}\right\} \text{---- (2:1)}$$

These coefficients are relative to shaft axes. The main rotor torque coefficient, from Bramwell, ref.[2] was taken to be

$$q_c = \delta(1+3\mu^2)/8 - t_c\lambda - \mu h_c \quad \text{----- (2:1a)}$$

The main rotor hub pitching and rolling moments are given by

$$Cm_R = - \frac{3\,(\,\lambda_\beta^2 - 1\,)aF_1}{2\,\gamma_0}\,\beta_{1c} \quad \text{---- (2:2)}$$

$$Cl_R = - \frac{3\,(\,\lambda_\beta^2 - 1\,)aF_1}{2\,\gamma_0}\,\beta_{1s} \quad \text{---- (2:3)}$$

$$\text{where } F_1 = \int_0^1 x\, S_1(x)\, dx$$

and x is the non-dimensional distance along the blade from the root, $S_1(x)$ the first mode shape. The expression for F_1 assumes that the blade mass per unit length is constant - γ_0 is calculated on the basis of this being the case. Ref. [25] contains a comprehensive description of the rotor model, which is not repeated here. However the salient points are now given. From the differential equation of blade bending (obtained using figure 2:2a)

$$\frac{\delta^2}{\delta r^2}\left[\,EI\,\frac{\delta^2 Y}{\delta r^2}\,\right] - \frac{\delta}{\delta r}\left[\,T\,\frac{\delta Y}{\delta r}\,\right] + \frac{\delta^2 Y}{\delta t^2} = \frac{\delta F}{\delta r}$$

the moment at the blade root of the aerodynamic, centrifugal and inertia loading is

$$M(0,\psi) = (\,\lambda_\beta^2 - 1\,)\Omega^2 R^3 P_1(\psi) m_0 F_1$$

where $P_1(\psi) = \beta_0 + \beta_{1C}\cos\psi + \beta_{1S}\sin\psi$. Note that only the first blade mode shape is used, and Bramwell justifies this in his analysis. $P_1(\psi)$ can be interpreted as the flapping angle of a rigid blade joining the root to the tip, figure 2:2b. The mean value of the hub moment for the rotor as a whole is obtained by resolving M in the pitching plane to give Cm_R; Cl_R is also obtained in this way.

The remaining problem is to find expressions for β_0, β_{1C} and β_{1S}, which is done by solving

$$\frac{d^2P_1}{d\psi^2} + \lambda_\beta^2 P_1 = \frac{1}{\Omega^2 R^2 f(1)} \int_0^1 \frac{dF}{dx} S_1(x)\, dx \quad \text{---- (2:4)}$$

which is itself obtained as the solution of the equation of blade bending using the orthogonal properties

$$\int_0^1 m_0 S_m(x) S_n(x) dx = 0, \quad m = n$$

$$= f(n), \quad m = n$$

The aerodynamic loading distribution is obtained with consideration of figure 2:2c and assuming that the applied blade pitch is given by

$$\theta = \theta_0 + \theta_{1C}\cos\psi + \theta_{1S}\sin\psi$$

In the solution of equation 2:4, constant and harmonic terms in $\sin\psi$ and $\cos\psi$ are equated to give three equations in three unknowns, β_0, β_{1S} and β_{1C}. Now these equations include terms in the integral of blade mode shape $S_1(x)$. Considerable simplification of the analysis results if it is

assumed that the blade can be represented by an offset rigid blade, figure 2:2d, where e is the "equivalent" offset, given by

$$e = \frac{\lambda_\beta^2 - 1}{\lambda_\beta^2} \quad \text{-----} \quad (2:5)$$

Bramwell's justification for this approach was that for the blades he investigated, the deflection became almost linear over the outer part of the blade and thus they could be approximated as "offset" rigid blades. In validating this assumption against the true solution, he found that equation 2:5 was in error by about 10%, which showed that there was still some curvature at the tip. Using the offset blade approach, with e determined by the flapping frequency of the first mode shape, the coefficients β_0, β_{1s} and β_{1c} could be expressed simply as

$$\left.\begin{aligned} \beta_0 &= \gamma_0/8\ (k_8\theta_0 + 4/3k_9(\lambda+\mu\theta_{1s}) - \mu e\beta_{1c}) + 1/2\mu k_9 p \\ \beta_{1c} &= (\ 2\mu\ (4/3k_1\theta_0 + k_2\lambda) + k_3\theta_{1s} - k_4\theta_{1c} + k_5 p - k_6 q\ )\ /\ k_0 \\ \beta_{1s} &= 4/3\mu k_{10}\beta_0 - k_{11}\theta_{1c} - k_{12} q\ -16/\gamma_0 k_{13} p + 8/\gamma_0 k_{14}\beta_{1c} \end{aligned}\right\} \text{---- (2:6)}$$

where k_i, i = 0, 14 are functions of e, μ and γ_0. A point of detail must now be mentioned, and that concerns the nature of β (and therefore the coefficients in this expression): β is the flapping angle of a centrally hinged rigid blade, and not that of the equivalent offset blade, figure 2:2d. Rather than calculate the "correct" flapping angle, β was retained as the angle described in figure 2:2b, because then it, and its coefficients can be directly compared with those of the equivalent centre-spring rotor model. Also, the hub moment coefficients Cm_R and Cl_R are directly proportional to β_{1c} and β_{1s} and not the "correct" angle.

2:3.2 The Tail Rotor Force

For the purposes of calculating derivatives, the tail rotor was modelled merely as a scaled version of the main rotor viz.

$$tc_{tr} = \frac{s_t A_t}{sA} \cdot \frac{\Omega_t R_t}{\Omega R} t_c \quad \text{----- (2:7)}$$

where t_c and its derivatives were of course evaluated with tail rotor rather than main rotor parameters. This is the approach taken by Bramwell, ref. [25]. In the trim calculation, the tail rotor thrust coefficient was obtained explicitly from a simple torque balance, as shown in section 2:3.7. The effects of these crude representations is discussed in section 2:4.

2:3.3 The Fuselage Forces and Moments

The fuselage aerodynamic forces and moments were written as

$$\left.\begin{aligned}
X_{fus} &= 1/2\ \bar{V}_f^2\ \bar{S}_{flong} / \bar{l}_f\ [\ Cx_{ofus} + Cx_{fus}\alpha_{fus}\ ] \\
Y_{fus} &= 1/2\ \bar{V}_f^2\ \bar{S}_{flat}\ / \bar{l}_f\ [\ Cy_{ofus} + Cy_{fus}\beta_{fus}\ ] \\
Z_{fus} &= 1/2\ \bar{V}_f^2\ \bar{S}_{flong} / \bar{l}_f\ [\ Cz_{ofus} + Cz_{fus}\alpha_{fus}\ ] \\
M_{fus} &= 1/2\ \bar{V}_f^2\ \bar{S}_{flong}\ [\ Cm_{ofus} + Cm_{fus}\alpha_{fus}\ ] \\
N_{fus} &= 1/2\ \bar{V}_f^2\ \bar{S}_{flat}\ [\ Cn_{ofus} + C_{nfus}\beta_{fus}\ ]
\end{aligned}\right\} \quad \text{----- (2:8)}$$

Such a linear representation of fuselage forces and moments is likely only to be valid over a limited range of angles of attack and sideslip, and is unlikely to model aerodynamic phenomena that are experienced with

helicopter fuselages such as flow breakdown and reattachment. Such aerodynamics however are likely to be non-linear in nature, and so their inclusion in linear model can be considered inconsistent. This model was unlikely to be used in flight conditions that result in the aerodynamic angles falling outside the range $-15° \leq \alpha_{fus}, \beta_{fus} \leq +15°$. As a result the fuselage forces and moments are likely to be adequately modelled.

2:3.4 The Tailplane Force

The validity of the results of studies into the effects of an active tailplane on helicopter flight dynamics depends on adequate modelling of the tailplane aerodynamics. For the development of this model, tailplane X and Y forces were assumed negligible - deleting the X-force (drag) is a valid assumption within the unstalled range of angle of attack, as the drag of the rest of the helicopter is so much greater. The tailplane Z-force by comparison can be a significant proportion of the overall Z-force. The tailplane Z-force is given by

$$Z_t = - 1/2 \, \bar{V}_f^{\,2} \bar{V}_t / \bar{l}_t \, a_t \alpha_t \quad \text{----- (2:9)}$$

The expression above is strictly true only for a limited range of angle of attack if a_t is assumed constant, as it was in this case. This limiting range is fixed by the angles of attack at which the tailplane will stall. Generally then the above expression is valid only for the range $-15° \leq \alpha_t \leq +15°$, but this will vary with section used.

In a study by Huber and Polz, ref. [26], features of rotor/fuselage/tail interactional aerodynamics were described, and it is

possible to model two of them that influence the tailplane linearly - the effect of upwash or downwash associated with the fuselage Z-force, and the impingement of the main rotor wake on the tailplane. The former reduces the tail lift-curve slope a_t while the latter modifies the tailplane angle of attack. The reduced lift-curve slope effect is normally that quoted in any data that is synthesised from tunnel results. The rotor wake impingement modelling is more involved however, and requires the calculation of flight conditions for which the tailplane is immersed in the wake, and also the wake contributions to velocity components at the tail. Considering the latter first, the wake was assumed to be 2-D, with no "spanwise" variation, and the induced velocity component λ_{it} to vary in magnitude, depending on the location in the wake viz.

$$\lambda_{it} = k_\lambda \lambda_i \text{ ----- (2:9a)}$$

where k_λ is a constant which varies according to position in the wake to represent how far it has developed. For a fully-developed wake derived from momentum considerations, k_λ=2. Some effort has gone into deriving k_λ empirically from test results, ref.[27] and from classical wake theory, ref.[28]. Bramwell synthesised the results of ref. [27] and used them for tandem rotor studies, ref. [29]. In this model however k_λ was specified *a priori*. The tailplane angle of attack can then be written

$$\alpha_t = \theta + \alpha_s + (w - k_\lambda \lambda_i + q l_t) / V_f^2 \text{ ----- (2:9b)}$$

Calculation of whether or not the tailplane is immersed in the wake was

made using expressions from ref. [4], derived on the basis of wake angle and airframe geometry, figure 2:3, viz.

$$\lambda_{it} = k_\lambda \lambda_i \iff x_1 < x < x_2 \text{ where}$$

$$x_1 = \left[\frac{l_t - R}{h_R R - h_t} \right], \quad x_2 = \left[\frac{l_t + R}{h_R R - h_t} \right]$$

2:3.5 The Fin Force

Calculation of the fin aerodynamic force was restricted to the Y-component. Wake impingement effects were neglected as the wake was assumed 2-D, with no "spanwise" component, and the fin vertical. Then

$Y_{fin} = 1/2\ \bar{V}_f\ \bar{V}_{fin}\ /\ \bar{l}_{fin}\ a_{fin}\ \beta_{fin}$, ----- (2:10) where

$B_{fin} = -\beta_{cant} + (v - r\ l_{fin})\ /\ V_f$ ----- (2:10a)

The same comment regarding a_t in the preceeding section can be applied to a_{fin}.

2:3.6 The Induced Velocity Calculation

The induced velocity calculation is very important in helicopter flight mechanics studies. It appears in the expressions for flapping, thrust and control angles, and can change the tailplane angle of attack as previously described. For this model the induced velocity was assumed to be uniform, and obtained from momentum considerations, ref. [30] viz.

$$v_i = \frac{T}{2\ \rho\ A\ (u_x^2 + (u_z - v_i)^2)^{1/2}} \text{ ----- (2:11), figure 2:4}$$

If u_z is neglected, a reasonable assumption for steady, "level" flight, then v_i, normalised as λ_i, can be obtained explicitly as the real and positive solution of the normalised equation

$$\lambda_i^4 + \lambda_i^2\mu^2 - (t_c s/2)^2 = 0$$

Hohenemser, ref.[22] discussed the importance of correct induced velocity modelling, as the hingeless rotor is more sensitive to errors in its calculation; non-uniform inflow can affect the control and some other derivatives. The next level of induced velocity model includes higher harmonics in ψ to give spanwise and longitudinal variation in λ_i, but this was not included in the model. The uniform induced velocity distribution, whose value is given by the expression above, must be regarded as the most elementary, and the possible effect on the derivatives kept in mind.

2:3.7 Calculation of Trim

As already stated the model was used only to generate a helicopter model for the steady level flight condition. With reference to figure 2:5 then, the equations of force equilibrium resolving along and perpendicular to the flight path, and moment equilibrium about the c.g. are

$$t_{cR}\sin\theta_e\cos\phi_e + h_{cR}\cos\theta_e - y_c\sin\theta_e\sin\phi_e - X_{fus}\cos\theta_e - Z_{fus}\sin\theta_e - Z_t\sin\theta_e = 0$$

$$t_{cR}\sin\phi_e + y_c\cos\phi_e + t_{ctr}\cos\phi_e + Y_{fin}\cos\phi_e + Y_{fus}\cos\phi_e = 0$$

$$t_{cR}\cos\theta_e\cos\phi_e - h_{cR}\sin\theta_e - y_c\cos\theta_e\sin\phi_e - w_c - Z_{fus}\cos\theta_e + X_{fus}\sin\theta_e - Z_t\cos\theta_e = 0$$

$$Cl_R + t_{ctr}h_{tr} + y_c h + Y_{fin}h_{fin} = 0$$

$$Cm_R + M_{fus} + Z_t l_t - t_{cR}x_{cg} + h_{cR}h_R = 0$$

$$q_c - Y_{fin}\bar{l}_{fin} - t_{ctr}\bar{l}_{tr} = 0$$

----- (2:12)

The forces t_{cR} and h_{cR} are the resolved components of the thrust and inplane rotor forces that take into account longitudinal shaft tilt viz.

$$t_{cR} = t_c \cos\gamma_s + h_c \sin\gamma_s$$

$$h_{cR} = -t_c \sin\gamma_s + h_c \cos\gamma_s$$

Implicit in these trim equations is a condition of zero sideslip. The solution of the equations is generally non-linear. To ease calculation of the trim in this model, simplifying assumptions were made - body attitude and rotor control angles were assumed small and any products in these variables was assumed negligible. The resulting "linear" equations give 5 equations in 8 unknowns (t_c, θ_e, ϕ_e, β_{1c}, β_{1s}, θ_{1s}, θ_{1c} and $\theta_0 - h_c$ and y_c from 2:1 already being substituted in as they can be expressed in terms of these 8 unknowns). The equations for t_c, (2:1), β_{1c} and β_{1s}, (2:6) were added to give 8 equations in 8 unknowns. These trim equations are linear only for a known value of the thrust coefficient. The solution therefore remains non-linear, and the method used for their solution was iterative. This is quite straightforwards, because the equations of longitudinal and lateral force and moment equilibrium are decoupled by the "linearisation". The equations of horizontal force and pitching moment equilibrium can be solved iteratively to yield t_c, β_{1c} and θ_e, if the term in θ_{1s} in the equation for h_c, (2:1) is neglected. This was done purely to allow the method of solution adopted here, and not on the assumption that this term

is small - in fact, it can be of the same order of magnitude as the terms retained. The term in θ_0, could however be neglected, as it will be an order of magnitude smaller than the rest. The remaining system of equations of longitudinal trim can then be solved for t_c, β_{1c} and θ_e. This was done by choosing an initial value of tc, $t_{ci}=0.9w_c$; the now linear simultaneous equations of horizontal force and moment equilibrium were solved to yield β_{1c} and θ_e, and together with t_{ci} substituted into the equation of vertical force equilibrium. If this equation was not satisfied, t_{ci} was updated and the process repeated until it was satisfied, ie. the sum of vertical forces equalled zero. These values of t_c, β_{1c} and θ_e were then substituted into the remaining system of five simultaneous linear equations to solve for the lateral trim and the control angles.

2:3.8 Calculation of the Derivatives and Equations of Motion

The expressions for the derivatives can all be calculated from the equations given in the preceeding sections. The equations of force and moment equilibrium (2:12) were differentiated (after being set equal to X, Y, Z, L, M and N respectively, rather than zero) with respect to all perturbations to obtain the aerodynamic derivatives. What must be remembered is that the rotor forces are relative to shaft axes, while the fuselage, tailplane and fin forces are relative to the total wind velocity (flight speed for zero gust velocities). Derivatives for rotor variables t_c, h_c, y_c and λ_i relative to body axes velocity components can all be obtained as for the following example for t_c, viz.

$$\frac{\delta t_c}{\delta u} = \frac{\delta t_c}{\delta \mu} \cdot \frac{\delta \mu}{\delta u} + \frac{\delta t_c}{\delta \lambda} \cdot \frac{\delta \lambda}{\delta u}$$

where $\mu = \bar{V}_f \cos\alpha_{sh}$ and $\lambda = \bar{V}_f \sin\alpha_{sh} - \lambda_i$. The fuselage, fin and tailplane forces are all relative to the flight speed V_f and it was assumed that

$$\frac{\delta \bar{V}_f}{\delta u} \simeq 1, \quad \frac{\delta \bar{V}_f}{\delta w} = \frac{\delta \bar{V}_f}{\delta v} \simeq 0$$

The reader is referred to Bramwell, ref. [25] for the derivative expressions themselves, especially for those with respect to v as their derivation has not been made obvious. Bramwell assumes that with a sideslip perturbation, rotor forces and moments do not change in magnitude, but merely alter their orientation relative to the body axes.

The small perturbation rigid-body equations of motion were obtained from the total-velocity expressions given by Babister, ref. [32] as

$$\dot{u} - v_e r + w_e q = - g\cos\theta_e\, \theta + X'$$

$$\dot{v} - w_e p + u_e r = g\,(\cos\phi_e\cos\theta_e\, \phi - \sin\phi_e\sin\theta_e\, \theta) + Y'$$

$$\dot{w} - u_e q + v_e p = -g\,(\sin\phi_e\cos\theta_e\, \phi + \cos\phi_e\sin\theta_e\, \theta) + Z'$$

assuming that the helicopter is symmetric about the x-z plane then $I_{xy} = I_{yz} = 0$, and

$$I_x\dot{p} - I_{zx}\dot{r} = L'$$

$$I_y\dot{q} = M'$$

$$I_z\dot{r} - I_{zx}\dot{p} = N'$$

where X', Y' etc. are the perturbed forces and moments. All of the preceeding elements were combined in the computer program HELSIM, written in FORTRAN and run on PDP 11/45 and VAX 11/750 computers. The output (system and control matrices, and eigenvalues) are denormalised.

2:4 Validation of the Model

In the absence of a comprehensive and detailed set of flight-test data, the model HELSIM was compared with the Royal Aircraft Establishment's HELISTAB, ref. [31], which is of the total force type with no linearising assumptions, and uses the equivalent centre-spring rotor model. From these total forces and moments however, a linearised state-space description of the helicopter can be produced. Accordingly, it can be considered if not *level* of modelling higher than HELSIM, then certainly a more complete and detailed representation of the helicopter.

The data set used to compare the two models represented a Westland Lynx helicopter, mass 4314kg and c.g. 127mm aft of the datum position. For a more direct comparison with HELISTAB, HELSIM assumed no wake impingement on the tail (which HELISTAB does not model), and HELISTAB was run with no blade twist, (which HELSIM does not model). The flight conditions considered were 60 to 160 knots at 10 knot intervals, in "level" flight.

The comparisons are shown in figures 2:6 to 2:9 (trim) and 2:10 and 2:11 (flight dynamics). The body pitch attitude, Θ_e, obtained using HELSIM is almost exactly the same as that for HELISTAB, figure 2:6, as is the longitudinal flapping angle β_{1C}, figure 2:7. This validates the linearising assumptions made to the equations of longitudinal equilibrium,

and the iterative method of solution adopted, ie. varying the rotor thrust coefficient until the vertical force equation is satisfied. Almost identical rotor inflow ratios, λ are obtained with each model figure 2:9, and so by implication are the induced velocity contributions λ_i; this is because

$$\lambda = \bar{V}_f \sin (\theta_e - \gamma_s) - \lambda_i$$

This validates the assumption that the term u_z in equation 2:11 is negligible for the steady level flight case. This in turn implies that the iteratively calculated thrust coefficient t_c compares well with HELISTAB, because it has an important role to play in the calculation of λ_i.

The comparisons between the rotor control angles show discrepancies in longitudinal cyclic and collective that worsen with speed - at 160 knots both are about 25 to 30% less with HELSIM, while the lateral cyclic pitch compares really quite well with HELISTAB, especially above 80 knots. The *trends* of the rotor control angles with speed is similar with the two models. These differences in the magnitudes of the control angles, especially θ_0 and θ_{1s} could come from two sources; firstly, the much more sophisticated non-linear total force trim calculation of HELISTAB, which could be taking into account the sum of small terms discarded in the derivation of HELSIM as negligible; and secondly the different rotor models. In fact it seems that the latter is the dominant influence on the difference between the results; it is not within the scope of this to discuss the two rotor models in detail, but inspection of the coefficients in the longitudinal flapping equation of both models serves to show the

significance of the differences, table 2:2. It can be seen that there are considerable (of the order of 30%) differences throughout the speed range studied, between corresponding coefficients. Bramwell's model does however give Cm_R and Cl_R that correspond closely with that of the equivalent centre-spring rotor viz.

$$C_{mR} = -0.0561\beta_{1C} \text{ ----- Bramwell}$$

$$C_{mR} = -0.0541\beta_{1C} \text{ ----- Centre-spring model}$$

This is the only element of the rotor model used in the calculation of the longitudinal trim (t_c, β_{1C} and Θ_e), and its good comparison here helps explain the similarly good comparison of the longitudinal trim parameters β_{1C} and Θ_e.

The lateral trim as expressed in the roll angle Φ_e, figure 2:6, and lateral flapping angle β_{1S}, figure 2:7, shows that the trend with speed of Φ_e and β_{1S} is adequately represented by HELSIM, but does not compare in magnitude. The difference is however consistent in the sense that the more level roll angle obtained with HELSIM is held with more lateral tilt of the disc, β_{1S}. The reason for this difference in the lateral trim of the two models was not, as might be imagined, due to lack of a good tail rotor model - remember, t_{ctr} was calculated only implicitly from a torque balance. The calculation of tail rotor thrust in HELSIM actually compares very well with HELISTAB; for example at 60 knots the tail rotor thrust with HELISTAB is 1.31kNm while with HELSIM it is 1.41kNm. Similarly at 160 knots HELISTAB gives tail rotor thrust as 2.86kNm, HELSIM as 2.82kNm. The difference was in fact traced to the fact that the lateral trim equations (sideforce and rolling moment), are solved simultaneously with the

flapping equations, unlike the longitudinal trim calculation for t_c, θ_e and β_{1c}; and as just described, the two rotor models display significant differences in the coefficients of the longitudinal flapping equation - it must be assumed that similar differences exist with the equation for lateral flapping. The equations of lateral trim, in their simultaneous solution with the flapping equations, couple with the latter through the term in θ_{1c} in the expression for y_c, equation (2:1), and through the term β_{1s} in C_{lR}.

The flight dynamics comparison is made in figures 2:10 and 2:11, comparing the rigid-body eigenvalues and selected derivatives* (those considered by the author to be of major importance in reflecting hingeless rotorcraft characteristics). Generally the eigenvalues compare well except for the low modulus non-oscillatory mode in the last graph of figure 2:10. The third graph of figure 2:10 shows the upper-half plane of the "dutch roll" complex pair of modes, and it can be seen that while the imaginary parts compare well throughout the speed range, the real part is consistently about 15% in error with the model HELSIM. The upper-half plane of the unstable longitudinal complex pair is shown above the dutch

the elements of the system and control matrices; not really the "aerodynamic" derivatives

roll comparison, and although these eigenvalues of each model lie along the same locus, close inspection reveals that HELSIM underestimates the instability of this mode at low and high speed, and overestimates the complex part at high speed - in fact with HELSIM, this mode seems to be

shifted back along the locus described by the modes obtained with HELISTAB, at low and high speed.

The derivatives obtained using HELSIM compare favourably with those of HELISTAB, especially those that lie along the diagonal of the system matrix (X_u, Z_w, M_q, Y_v, L_p and N_r). The other derivatives shown generally compare well, but with some discrepancies that help to explain the differences in the eigenvalues obtained. M_w for example, is less with HELSIM at low and high speed, especially so at high speed - this would explain why the instability of the complex pair of longitudinal modes is less at high speed with HELSIM. The comparison in the derivative L_v is very poor, and this explains the error in the real part of the dutch roll mode, and the very poorly predicted low modulus non-oscillatory mode. The strong pitch/roll cross-coupling (as expressed by the derivatives L_q and M_p) is greater with HELSIM, although the trends with speed are the same. This cannot be said to be the case with the derivatives L_u and L_w, although in magnitude L_u is probably a good enough approximation to that of HELISTAB at all speeds, L_w above about 100 knots only.

The control derivatives of the two models, figure 2:11a, compare very well, and illustrate the large amounts of control power, as well as the strong control cross-coupling, of the stiff-flapwise hingeless rotor.

The model HELSIM gives a similar representation of the hingeless rotor helicopter as R.A.E.'s HELISTAB. Trends in the trim, stability and derivatives with speed generally compare well, and the differences in the magnitude of trimmed roll and rotor lateral flapping angles traced to inadequate representation of the tailrotor in HELSIM. Although not

investigated any further than an examination of the coefficients of each longitudinal flapping equation, there seem to be significant differences between the rotor model described in ref. [25], and that of the equivalent centre-spring rotor. It is expected, from the magnitude of the differences in these coefficients, that the different representations of the rotor in each model is the major source of any discrepancies between HELISTAB and HELSIM. Some of the errors will however be due to the fact that HELISTAB is a model of the total force type, taking into account all of the small terms discarded as negligible in the process of linearisation of the equations used in HELSIM. HELSIM can be considered, however, to represent adequately the major features of hingeless rotor helicopter flight mechanics, viz. the angle of attack instability, large angular rate damping, strong pitch/roll cross-couplings, and the control power and control cross-coupling.

2:5 The Effect of Main Rotor Wake Impingement on the Horizontal Tailplane

It is likely that an accurate assessment of the effect of the main rotor wake impinging on the tailplane would be very difficult without three-dimensional flow modelling. Difficulties in considering the problem at any lower level than this are compounded by design idiosyncrasies eg. UH-60, AH-64 and A109 helicopters have suffered dynamic yaw/pitch coupling effects during development, identified as being caused by a lateral distribution of main rotor induced velocity. This is in addition to the pitch response problems during transitions from the hover, already cited in the preceeding chapter. As well as being impossible to represent in a simple fashion suitable for a linearised derivative model, such effects were not the ones of concern in this study. What was of concern, was the effect on helicopter stability of having the tail either uniformly immersed in the wake, or operating in the free stream. This was investigated by varying the factor k_λ in HELSIM, from 0 to 2, and therefore modelling the induced velocity in the wake at various stages of development, and therefore position in the wake. k_λ=2 identifies the wake as being fully developed.

A qualitative assessment of the effect on helicopter stability of the tailplane operating in the wake, can be obtained by examining the tailplane derivative M_{wt}, obtained easily from equation 2:9 as

$$M_{wt} = -1/2\ \bar{V}_f\ \bar{V}_t\ a_t\ \left(1 - k_\lambda \frac{\delta\lambda_i}{\delta w} \right)$$

Now for perturbations from steady "level" flight, $\delta\lambda_i/\delta w$ will be positive, thus reducing the stabilising contribution of M_{wt}; M_w overall will, for the stiff-flapwise hingeless rotor, therefore become more positive, ie. more destabilising. The effect on stability of the tailplane operating in the wake is shown quantitatively in figure 2:12 for the eigenvalues of the rigid-body dynamics that it significantly affects. These three eigenvalues are all longitudinal, two being the unstable complex-conjugate pair shown as the second plot in figure 2:10 for k_λ=0, the other one being the subsidence shown as the second-last graph of figure 2:10. The complex conjugate pairs for variations in speed and k_λ are all plotted together, while the corresponding non-oscillatory modes are plotted separately, but this is simply for clarity. What in fact happens is that with increasing speed for any non-zero k_λ, the real part of the complex pair becomes more positive while its imaginary part gets smaller, until the pair meet the real axis, where they split and become two real modes. With increasing speed one becomes more unstable, the other less unstable. Meanwhile the subsidence mode has been getting less stable, and the stable complex conjugate modes shown in figure 2:12 are the result of this mode ultimately coalescing with the least unstable of the other two modes. The discontinuity of the curves in the second graph of figure 2:12, spread over a 10 knot interval in each case, represents the speed range in which the unstable complex pair meets the real axis, splits and then coalesces with the original stable subsidence. The speed at which this occurs is reduced with increasing k_λ, as is obvious in the second plot of figure 2:12. This has a significant implication for longitudinal stability, because for k_λ non-zero, the helicopter is more unstable than that with k_λ=0. This is especially true for the cases where the original unstable

pair has already met the real axis. Then movement of one of the resulting real eigenvalues to the right is rapid with increase in speed: at 160 knots, for example, and with k_λ=0, the time to double amplitude of the unstable complex pair (given in figure 2:10) is about 2 seconds (the real part is approximately 0.365); with k_λ=2, the time to double amplitude of the unstable non-oscillatory divergence is less than 1 second, figure 2:12.

It was for this reason that in the simulations of chapters 4 and 5, k_λ=2, because it results in greater longitudinal instability. Now given that a result of a desired set of closed-loop response characteristics is that the closed-loop system eigenvalues take up certain values; and further, that it was taken to be the case that higher gain would be required to move a more unstable eigenvalue from its open-loop value to a given position, than a less unstable eigenvalue; then higher feedback control authority would be required with a given perturbation, if the helicopter had its tailplane operating immersed in the wake.

2:6 Conclusions

An adequate model to describe hingeless rotorcraft flight mechanics behaviour has been developed. It was decided to include the effect of wake impingement, as it worsens the instability of the helicopter.

Chapter 3

A Methodology for Obtaining Reduced Order Models for Helicopter Flight Mechanics Studies

3:1 Introduction

The search for greater insight into factors that affect handling qualities has led in recent years to analysis using reduced order models. To achieve a simplified model, it is generally possible to make simplifying assumptions based on experience and a knowledge of the system's dynamics. Reduced order models are of benefit primarily because they allow a view of the overall system as a sum of conceptually simpler models, which will hopefully lead to a greater understanding of the system's dynamics. These simpler models can reflect particular areas of interest, eg. longitudinal motion, lateral/directional motion or short-period pitch response. Milne, ref. [33] presented a method of obtaining reduced order models based on the assumption of widely separated roots, qualified by conditions on the coupling matrices such that they satisfy a condition of weak coupling. The analysis allows suitable lower order models to be obtained from a defined sequence of mathematical steps. Padfield, ref. [34] applied the analysis to the study of the short-period response of articulated and hingeless rotor helicopters. Reduced order models have also found application in system identification studies relating to helicopter flight mechanics, ref. [35]. In the context of this

thesis, the need for a reduced-order model was driven by the way in which the helicopter equations of motion are solved in the next chapter.

Unlike the dynamics of fixed wing aircraft, those of the helicopter are coupled, sometimes very closely. Two examples of note are the cross-couplings between lateral/directional and longitudinal modes, and also the couplings within the longitudinal dynamics between traditional short- and long-period modes. As a consequence, arbitrarily neglecting the lateral/directional modes to give a reduced model for longitudinal dynamics, for example, may not have any foundation. Using the eigenvectors of the modes of concern to discover the states of importance to that mode can become bewildering for coupled interconnected systems of high order. Further, such an approach will not reveal exactly which coupling terms in the system matrix have the greatest influence on the modes of concern. The method about to be described is an attempt to formalise the procedure used to identify an improvement to a proposed reduced model, and also to gain insight into terms of significance to the dynamics of the system, given *a priori* knowledge of the eigenvalues and eigenvectors of the full system. The method is based on an examination of the contributions that each derivative makes to each mode or eigenvalue of the full model, by means of a set of identities. The method is illustrated with the example of an improved longitudinal model of a hingeless rotor helicopter. Some insight is gained into the nature of the coupling terms that affect the modes of the subsystem. The method requires simply that the equations of motion be ordered in such a manner that the proposed subsystem is a submatrix of the full system description, which can then be partitioned on this basis.

3:2 The Theory

The state-space description of a linear invariant system is

$$\dot{x} = Ax + Bu \quad \text{----- (3:1), where}$$

x is the n-dimension state vector,

u is the m-dimension control vector,

A is the nxn system matrix,

B is the nxm control matrix.

The description (3:1) is transformed to a new reference frame using the canonical transformation

$$x = Ez \quad \text{----- (3:2)}$$

where E is an nxn matrix of the eigenvectors of A such that E(j,i) is the jth vector of the ith mode, λ_i. z is the n-dimension transformed state vector. Equation (3:1) thus becomes

$$E\dot{z} = AEz + Bu$$

$$\dot{z} = E^{-1}AEz + E^{-1}Bu$$

$$\dot{z} = \Lambda z + Ru \quad \text{----- (3:3)}$$

The autonomous form of (3:3) is

$$\underline{\dot{z} = \Lambda z} \quad \text{----- (3:4)}$$

Now the system matrix of the transformed equations is

$$\Lambda = \text{diag}\,[\lambda_i]\ ,\ i = 1,n$$

ie. a diagonal matrix whose elements are the eigenvalues of the system matrix A. Thus the transformation (3:2) has resulted in a new system description such that each state z_i is uniquely related to each mode λ_i, and the transformed system is thus decoupled.

From (3:3), it can be seen that

$$\Lambda = E^{-1}AE$$

$$E\Lambda = AE \text{ ----- } (3:5)$$

Suppose that it is desired to partition the system matrix A into two subsystems and coupling terms, as follows.

$$A = \begin{bmatrix} A_{11} & A_{12} \\ A_{21} & A_{22} \end{bmatrix}, \text{ where}$$

A_{11} = kxk matrix,

A_{22} = 1x1 matrix,

A_{12} = kx1 matrix,

A_{21} = 1xk matrix.

A_{11} and A_{22} are the system matrices of the subsystems, with A_{12} and A_{21} being the coupling matrices. Provided the equations of motion have been suitably rearranged, the partitioning is made simply and on any basis eg.

to partition longitudinal and lateral/directional motions.

Expression (3:5) can be partitioned to reflect that above ie.

$$\begin{bmatrix} E_{11} & E_{12} \\ E_{21} & E_{22} \end{bmatrix} \cdot \begin{bmatrix} \Lambda_1 & 0 \\ 0 & \Lambda_2 \end{bmatrix} = \begin{bmatrix} A_{11} & A_{12} \\ A_{21} & A_{22} \end{bmatrix} \cdot \begin{bmatrix} E_{11} & E_{12} \\ E_{21} & E_{21} \end{bmatrix} \quad \text{----- (3:6)}$$

The partitioning of E and Λ *must* be the same as that of A. From equation (3:6) we get

$$E_{11}\Lambda_1 = A_{11}E_{11} + A_{12}E_{21} \quad \text{----- (3:7a)}$$

$$E_{21}\Lambda_1 = A_{21}E_{11} + A_{22}E_{21} \quad \text{----- (3:7b)}$$

Post-multiplying both sides of (3:7b) by Λ_1^{-1} gives

$$E_{21} = (A_{21}E_{11} + A_{22}E_{21})\Lambda_1^{-1}$$

so that (3:7a) becomes

$$E_{11}\Lambda_1 = A_{11}E_{11} + A_{12}(A_{21}E_{11} + A_{22}E_{21})\Lambda_1^{-1} \quad \text{----- (3:8)}$$

$$\Lambda_1 = E_{11}^{-1} (A_{11}E_{11} + A_{12}(A_{21}E_{11} + A_{22}E_{21})\Lambda_1^{-1}) \quad \text{----- (3:8a)}$$

At this stage, there are several important aspects of the developments to be noted:

1/. Equation (3:8) does not give an explicit closed-form expression for "good" subsystem modes. It uses the eigenvectors of the full system

description and indeed the full system matrix itself;

2/. In this sense then, (3:8) is more accurately described as a set of *identities*, which are satisfied for any given full system matrix;

3/. The partitioning and resulting matrix algebra has been used to separate the identities of the proposed subsystems from one another, and it has also separated the terms defined as coupling terms (the second expression on the RHS of (3:8)) from terms defining the subsystem itself. If there is no coupling between the proposed subsystems then

$$E_{11}\Lambda_1 = A_{11}E_{11} \text{ ----- (3:9a)}$$

$$A_{12}(A_{21}E_{11} + A_{22}E_{21})\Lambda_1^{-1} = [0] \text{ ----- (3:9b)}$$

4/. When cross-coupling between A_{11} and A_{22} does exist, it is obvious that the magnitudes of the elements of the LHS of (3:9b) relative to those of the LHS of (3:9a) indicate the level of coupling between the proposed subsystems. By definition all the elements of A_{11} are of importance to the reduced order model, and therefore the degree of cross-coupling is determined by the relative magnitudes of *each* element of the LHS of (3:9b) and the corresponding element of $E_{11}\Lambda_1$. This in fact is the basis of the methodology developed to use the identity (3:8).

As a consequence, it is not essential to use (3:8) in the form of (3:8a) as E_{11}^{-1} is a common factor of both the expressions on the RHS of (3:8). In essence, it is the significance of the *products* AE on the modes of the proposed subsystem that is being determined - the reasoning behind their use in identifying elements of A_{12}, A_{21} and A_{22} that are of significance to the modes Λ_1 is explained in the next section.

3:3 Analysis of a Reduced Order Model

3:3.1 Methodology

Consider the eigenvalue λ_i in Λ_1. It has to satisfy an identity formed by the ith. row of E_{11}^{-1} multiplied by the ith. column of $A_{11}E_{11}$, plus the same row of E_{11}^{-1} multiplied by the ith. column of $A_{12}(A_{21}E_{11}+A_{22}E_{21})\Lambda_1^{-1}$. Thus when examining terms of importance to the eigenvalue λ_i only elements of the ith. column of the coupling expression are compared with the corresponding elements of the ith. column of $E_{11}\Lambda_1$. Now the ith. column of the expression $A_{12}(A_{21}E_{11}+A_{22}E_{21})\Lambda_1^{-1}$ is made up of successive rows of A_{12} multiplied by the ith. column of the coupling part of the identity, and because Λ_1^{-1} is a diagonal matrix, its ith. column is simply the ith. column of $A_{21}E_{11}+A_{22}E_{21}$ divided by the eigenvalue under investigation, λ_i. What this means in plain language is that when considering the identity involving the eigenvalue λ_i, the eigenvector of that mode *and that mode alone* is the only one that is required, and simple row by column multiplication of the A_{ij} and this eigenvector builds up the contributions of coupling to the elements of $E_{11}\Lambda_1$. Further details are best described by means of an example.

3:3.2 A Reduced Order Model of the Longitudinal Dynamics of a Stiff-Flapwise Rotor Helicopter

The helicopter model HELSIM described in the last chapter was used to produce the state-space description of the rigid-body dynamics of the Lynx helicopter at 100 knots with c.g. 127mm aft of datum, and no wake

impingement on the horizontal tailplane. The system eigenvalues are given in table 3:1. The eigenvalues of the reduced order model consisting purely of the longitudinal degrees of freedom is given in table 3:2 together with the corresponding eigenvalues of the full system. It is obvious that the reduced order model needs improvement, as only the imaginary part of the complex conjugate pair is adequately predicted - to within 2%; the real part is underestimated by 20%. There are errors of similar magnitude in the prediction of the two real modes. Normally, one would now look to the eigenvectors of the eigenvalues to determine their composition, in an attempt to identify significant states in each mode. The difficulty in selecting an improvement to the reduced model on this basis is well illustrated in table 3:3 for the two real modes - of the large mode it can really only be said that yaw rate and yaw angle are of little importance, while sideslip is very prominent in the low modulus eigenvalue.

For the purposes of illustrating the use of the identity 3:8, the state vector was ordered

$$x = [\ u\ w\ q\ \Theta\ v\ p\ \Phi\ r\ \Psi\ ]^T$$

Partitioning the A-matrix such that A_{11} is a 4x4 gives

$$A_{11} = \begin{bmatrix} -0.0389 & 0.0589 & 0.0820 & -9.8146 \\ 0.0165 & -0.8345 & 51.7417 & -0.0935 \\ 0.0249 & 0.0293 & -2.0889 & 0.0 \\ 0.0 & 0.0 & 0.9999 & 0.0 \end{bmatrix}$$

$$A_{12} = \begin{bmatrix} 0.0007 & -0.1619 & 0.0 & -0.0015 & 0.0 \\ 0.0 & -0.8798 & -0.1212 & -0.0084 & 0.0 \\ 0.0058 & 0.6403 & 0.0 & 0.0067 & 0.0 \\ 0.0 & 0.0 & 0.0 & -0.0123 & 0.0 \end{bmatrix}$$

$$A_{21} = \begin{bmatrix} 0.0606 & 0.0105 & -0.1204 & -0.0012 \\ -0.0110 & 0.1784 & -2.5817 & 0.0 \\ 0.0 & 0.0 & 0.0001 & 0.0 \\ -0.1524 & 0.0294 & -0.4297 & 0.0 \\ 0.0 & 0.0 & 0.0123 & 0.0 \end{bmatrix}$$

$$A_{22} = \begin{bmatrix} -0.2082 & -0.6020 & 9.8139 & -50.6211 & 0.0935 \\ -0.0959 & -10.7884 & 0.0 & -0.3394 & 0.0 \\ 0.0 & 1.0 & 0.0 & 0.0095 & 0.0 \\ 0.1296 & -1.6153 & 0.0 & -1.5456 & 0.0 \\ 0.0 & 0.0 & 0.0 & 1.0 & 0.0 \end{bmatrix}$$

For the purposes of illustration, only the make-up of the identities that the two real eigenvalues must satisfy will be used. The mode -3.2741 has eigenvectors as shown in table 3:3 so that

$${}^1E_{11} = [\ 0.0278 \quad 0.9937 \quad -0.0462 \quad 0.0141\ ]^T \text{ and}$$

$${}^1E_{21} = [\ 0.0890 \quad 0.0381 \quad -0.0117 \quad 0.0030 \quad -0.0007\ ]^T$$

where the superscript on E_{11} and E_{21} denotes the column of E. Now each element in the relevant column of $A_{21}E_{11}+A_{22}E_{21}$ is made up of a summation of the rows of A_{21} and A_{22} multiplied by the columns ${}^1E_{11}$ and ${}^1E_{21}$ respectively. The elements of the first column of $A_{21}E_{11}+A_{22}E_{21}$ in the identity for λ_1 are shown below, broken down into constituents

$$\begin{aligned}
&0.002+ 0.010+ 0.006+ 0.0 -0.019 -0.023 -0.114 -0.154 +0.0=-0.292 \\
&0.0 \ + 0.177+ 0.119+ 0.0 -0.009 -0.412 +0.0 \ \ -0.001 +0.0=-0.126 \\
&0.0 \ + 0.0 \ + 0.0 \ + 0.0 +0.0 \ \ +0.038 +0.0 \ \ +0.0 \ \ +0.0= 0.038 \quad \text{(A3:1a)} \\
&-0.004+ 0.029+ 0.020+ 0.0 +0.012 -0.062 +0.0 \ \ -0.005 +0.0= 0.002 \\
&0.0 \ + 0.0 \ - 0.001+ 0.0 +0.0 \ \ +0.0 \ \ +0.0 \ \ +0.003 +0.0= 0.002
\end{aligned}$$

Note that each element above is the product of a derivative with respect to a state, and the component of the eigenvector representing that state in the eigenvalue. In this case, the sum of the sideforce derivatives multiplied by the respective elements of the eigenvector is the most significant element of the column, although the rolling moment terms are also large.

The elements of the relevant column of $(A_{21}E_{11}+A_{22}E_{21})\Lambda_1^{-1}$ are given by simply dividing the column (A3:1a) by the eigenvalue -3.2741, with the result

+0.0892

-0.0385

-0.0116

+0.0031

-0.0006

The column that is the result of multiplying that above by A_{12} is given by

DOMINANT TERMS

$$\begin{array}{lcl} 0.0001 + & \lceil\ 0.0062\ \rceil & + 0.0000 + 0.0 + 0.0 = \ 0.0063 \\ 0.0 & |-0.0298\ | & + 0.0014 + 0.0 + 0.0 = -0.0284 \\ 0.0005 + & |\ 0.0247\ | & + 0.0 \quad + 0.0 + 0.0 = \ 0.0252 \\ 0.0 \quad + & \lfloor\ 0.0\ \quad \rfloor & + 0.0 \quad + 0.0 + 0.0 = \ 0.0 \end{array}$$

----- (A3:2a)

A3:1a and A3:2a are the worked examples of the expressions A3:1 and A3:2,

respectively, given in the appendix 1 to this chapter. Note that the resulting column (A3:2a) forming part of the identity for $\lambda_1 = -3.2741$ is dominated by the product of the rolling moment terms (L-derivatives times corresponding element of the eigenvector) and coupling derivatives X_p, Z_p and M_p ie. derivatives with respect to roll rate. Terms in sideforce and sideslip, and yaw moment and yaw rate, are at least an order of magnitude smaller.

Thus we now have all the terms that appear in the identity involving $\lambda_1 = -3.2741$. The RHS of (A3:2a) as a percentage of the corresponding elements of $E_{11}\Lambda_1$ in the identity for λ_1 is given in table 3:4. At this stage, what represents a significant amount of coupling in terms of a percentage, can really only be determined by trial and error. However in these examples, the elements of (A3:2a) were considered to be important to the mode if they were greater than 5% of the corresponding element of $E_{11}\Lambda_1$. The analysis suggests that the first and third elements of (A3:2a) make a significant enough contribution to satisfying the identity for $\lambda_1 = -3.2741$. These terms are made up of the derivatives X_p and M_p multiplied by the second element of $(A_{12}E_{11}+A_{22}E_{21})\Lambda_1^{-1}$ this in turn being made up of row by column multiplication of the rolling moment derivatives and the elements of the eigenvector of λ_1. Therefore, the rolling equation should be added to the proposed model A_{11}, together with the derivatives X_p and M_p. Returning to (A3:1a) and with reference to A3:1, it can be seen that the derivatives L_w, L_q and L_p should be included in the rolling degree of freedom - the derivative L_u has negligible influence on satisfying the identity involving λ_1, as the product of L_u and the u-element of the eigenvector of λ_1 is zero. The eigenvalue of the new subsystem

corresponding to -3.2741 is -3.2696 ie. only 0.14% in error over the full system value.

Repeating the analysis for $\lambda_4 = -0.3706$ gives a similar result, table 3:4a, except that this time only M_p of A_{12} need be included, but with L_u in the rolling moment. The latter's significance in the identity for λ_4 is small, but unlike that for λ_1, not insignificant. Without L_u the eigenvalue of the modified subsystem corresponding to -0.3706 is -0.3736, but with L_u it becomes -0.3708. In addition, sideslip terms are no longer as small, relative to roll terms, as in the identity for λ_1, but still small enough to be neglected.

The resulting structure for the improved reduced order model for longitudinal dynamics, taking into account the complex pair of eigenvalues as well, is given by

$$\begin{bmatrix} X_u & X_w & X_q & X_\theta & X_p \\ Z_u & Z_w & Z_q & Z_\theta & Z_p \\ M_u & M_w & M_q & 0 & M_p \\ 0 & 0 & 0 & k & 0 \\ L_u & L_w & L_q & 0 & L_p \end{bmatrix}, \text{ where k is a constant}$$

(The fourth row, that of zeros and k, forms the kinematic relationship between q and θ.)

The eigenvalues of the modified subsystem are compared with those of the original reduced order model and those obtained using the full system description in table 3:5. To all intents and purposes the differences between the modes obtained using the modified lower order model and the

full system are insignificant. An extra degree of freedom, that of roll has been added. This has not been given in any of the tables, because strictly speaking, it is a better approximation only to the longitudinal eigenvalues that is required, and this has been obtained. In fact the additional eigenvalue is a very good approximation to that of the full system.

3:4 Discussion

The analysis that has been described allows an assessment of the validity of a reduced order model and identifies the terms that are of significance to a mode, and which therefore should be included in a modified version of the original reduced order model, if an improvement in the approximate dynamics originally obtained is required. In order to do this it is necessary only to relocate the equations of motion such that the system can be partitioned in such a manner that one of the sub-matrices of A represents the reduced system under study. The influence of the other elements of A on the modes of the proposed subsystem can then be identified.

The essence of the method is *simplicity*, both in understanding the analysis and in its application. As formulated, inspection of the identities (3:8) makes an understanding of the results easy and their significance obvious, as the magnitudes of the coupling terms are directly related to the influence of such coupling on the eigenvalues. Inspection of the identities (3:8) allows a clearer understanding of the significance of the elements of the eigenvector of a mode, and the method would be

especially useful when dealing with unfamiliar dynamics, especially of high order. The analytic framework of this method formalises the search, made normally through a study of the eigenvectors of the modes, to identify states or motions of significance to the modes of concern.

While the formalised structure of the method allows the identification of significant coupling terms, it must be remembered that this is based on *inspection* of identities that the dynamics of the *full* system fulfil. Unlike that of Milne, ref. [33] therefore, the analysis does not result in expressions for "good" approximations to the eigenvalues of proposed subsystems, and this in effect reduces the analysis to that of a methodology, based on the set of identities. Nonetheless, this analysis *will* suggest improvements to a proposed lower order model (if they exist), that will give good approximations to the full system eigenvalues of interest. The reason for this can be explained by viewing the methodology simply as a means of reordering the system matrix such that new subsystems are produced with one or both of the coupling matrices null, or in some sense close to null.

It is normal practice in studies of fixed-wing aircraft dynamics to discard the lateral/directional degrees of freedom when studying the longitudinal motion, and vice versa. This cannot be done with the single main and tail rotor helicopter, because of considerable cross-coupling - as was shown, the longitudinal eigenvalues of the rigid-body model are poorly predicted when the lateral/directional equations of motion and cross-coupling terms are neglected. Use of the set of identities developed, (3:8) allowed the terms of significance to the longitudinal

eigenvalues in the full system to be identified. The resulting modifications that were made to the longitudinal model gave eigenvalues that were almost identical to those of the full system. The longitudinal eigenvalues are poorly predicted using only longitudinal degrees of freedom, and this is due entirely to the absence of coupling with roll - terms in sideslip and yaw have negligible influence on the longitudinal modes.

3:5 Conclusions

The method that has been described represents in effect a formalised statement of the analysis one would use when investigating the makeup of a mode by examination of the eigenvector of that mode.

The result of this formalisation is that greater insight into the effects of coupling terms in the equations of motion on the eigenvalues of the system is achieved.

Improvements to a reduced order approximate model can be readily identified; this has been demonstrated through the use of examples, and the improvements shown to be effective

The methodology is a different and easy to use approach to reduced order modelling.

Chapter 4

The Active Tailplane, and its Influence on Helicopter Agility

4:1 Introduction

The emerging requirements of future combat helicopters have resulted in studies to investigate ways in which agility, and therefore survivability, can be improved. Future *modes* of operation have been identified, ref. [16], two of which will involve manoeuvres in the vertical plane: high speed, low level transit to the operating zone; and nap-of-earth (NOE) flight when there, at speeds considerably greater than currently possible. This could place heavy demands on the airframe (in terms of speed and "g" capability) and the pilot. Design studies undertaken in the context of these requirements have demonstrated the suitability of the stiff-flapwise rotor configuration, ref. [21], and the desirability of advanced, integrated flight control systems (FCS) for reducing pilot workload, refs. [19], [20]. A disadvantage of this type of rotor system is that it can pose metal fatigue problems due to potentially large hub moments associated with blade flapping; as will be shown however, the hub moment limitation can be made less restrictive by use of an actively controlled horizontal tailplane. This study assesses the implications for helicopter agility of using the stiff rotor configuration along with different levels of tailplane control. It is assumed that some kind of advanced FCS is available of the type that dispenses with the

traditional pattern of control to give the pilot direct control of flight path parameters such as speed, load factor or climb angle. This study makes use of an inverse solution of the helicopter equations of motion, which obviates the need to consider the design and implementation of the FCS in detail.

4:2 Agility and the Flight Path

The question of what agility is must be addressed before any progress can be made with its analysis. When something is described as agile, the intuitive idea is that it can change *speed* and *position* rapidly, even violently, but with absolute precision, in order that its task may be fulfilled in the shortest possible time. This is generally true of aerospace vehicles and so agility, as pointed out by Tomlinson and Padfield, ref. [19], embraces aspects of two, sometimes separate, areas of aircraft design, namely performance and handling qualities. In this study the emphasis is on performance, in its widest sense, rather than handling qualities. In particular, agility is evaluated through consideration of longitudinal manoeuvring performance, which may be limited not simply by installed power or rotor thrust, but by parameters like rotor hub moment or blade flapping angle. In general, then, given that agility is limited by the need to keep a number of performance-related parameters within bounds, the aim is firstly to quantify agility and secondly to determine its value for several helicopter configurations.

For this work, agility was quantified through use of an *agility rating*, which was based on features the author considers to be fundamental

to the concept of agility, namely the geometry of the manoeuvre and the time taken to manoeuvre. The former reflects the tightness of the manoeuvre while the latter is a measure of how swiftly it is performed, and the two together can be a good guide to the overall loading on the helicopter. In effect the path in space is assigned a rating, *not* the helicopter, and the relative capabilities of several configurations are reflected in whether or not they can execute the path without exceeding a performance limitation. The concept of applying ratings to paths in space as a means of quantifying agility is discussed briefly in ref. [19]. For the agility studies of this thesis, the rating was defined as

$$AR = t_f \int_{x_e=s_o}^{x_e=s_f} z_e . d(x_e)$$

The rating was assigned to each member of a family of paths in space, which are shown in figure 4:0. It needs to reflect the increased level of agility required to fly a path that is more demanding than another, in that it occupies less space and/or is flown in less time. It can be seen that with this rating, as the required level of agility increases, then the rating will tend to zero. The family of paths cannot be *completely* general, but rather must be associated with a fairly well defined task so that the ratings assigned to different paths are directly comparable. In the present study it was sufficient to define the task in terms of a set of boundary conditions

$$\gamma_o = \gamma_f = 0$$

$$h_o = 0, \; h_f = 50$$

Speed is not included as a condition because incorporating time into the rating takes account of variations in speed. The paths can be seen to represent obstacle-clearing manoeuvres, or popups. It is important to investigate measures of agility associated with this type of manoeuvre as it is a basic element of manoeuvring flight, especially in an NOE environment. Quantifying agility in geometric terms is not new. Brotherhood and Charlton, ref.[36] for example, define a turn agility factor in terms of speed and geometric features of the turns flown in a series of flight experiments.

The assessment of agility used here has to be put in some perspective, because as yet there seems to be no uniformly accepted measure of helicopter agility. Indeed the very *nature* of agility seems to vary from author to author. The work of this chapter is based on that of Houston and Caldwell, ref.[37], which was to a large extent influenced by the brief statement in ref.[19] relating to the assigning of ratings to paths in space as a means of quantifying levels of agility. Refs. [19], [36] and [37] assess the nature of agility similarly in that they ultimately relate agility to the flight path, and the latter two references use geometric features of the flight path to quantify agility. Recently, other statements on the nature of agility have been made by Curtiss and Price, ref. [38] and Pausder and Sanders, ref. [39], and are concerned more with the *acceleration* capabilities of the helicopter (angular and translational). Curtiss and Price associate agility with the time taken to establish a specific flight path. Pausder and Sanders describe agility demands in terms of "geodetic" accelerations and quantify the agility required for a *task* (rather than a specific path in space) by

use of geodetic acceleration histograms. Whether or not this author's assessment of agility is a valid one is therefore open to question. It is felt however that the premise of agility being ultimately related to the flight path is better than defining it in terms of accelerations. Accelerations will certainly tell one how quickly the helicopter is changing state, but not *how* this capability is used to change the flight path. There is at least only a qualitative relationship between peak accelerations and the specific flight path that results. The author does appreciate that his statements are being made at an early stage of the analysis of agility, and can only qualify his assessment of agility by saying that it is an adequate measure of longitudinal manoeuvring performance that quantifies at least some intuitive idea of the nature of helicopter agility.

The geometry of the paths and the way in which they were assumed to be flown were selected with a particular FCS in mind. It was assumed that the FCS provided the pilot with the capability to command speed and flight path angle independently - ie. it was a "manoeuvre demand" system. Thus the flight paths are flown at constant speed and their geometry is such that they are piecewise-linear in the rate of change of flight path angle $\dot{\gamma}$. A typical function of $\dot{\gamma}$ is shown in figure 4:1 with the resulting time history of γ in figure 4:1a. The trajectory defined by this function of γ is given in figure 4:2. It is feasible that the FCS could schedule control inputs to the helicopter in such a way that movement of a single control inceptor by the pilot would result in the helicopter flying the specified path. Of course, this is an over-simplified representation of obstacle clearance in that it ignores the detailed dynamics of the pilot/

helicopter/ FCS interaction, which would depend both on the pilot's perception of the task and on the design of the FCS. But these factors impinge more on handling qualities than performance. In this study, it is taken for granted that the FCS confers handling qualities which allow maximum advantage to be taken of the available performance.

Forcing a mathematical model of a helicopter to fly desired manoeuvres has been undertaken successfully in the past. Wood et al, ref.[40], describe a *Maneuver Criteria Evaluation Program* which models the execution of certain manoeuvres by a helicopter, based on general features of the manoeuvres that are specified. Haverdings, ref.[41], defines idealised manoeuvres in which the trajectories are tightly constrained, but allows for deviation from the ideal in the execution of the manoeuvres. The approach taken here is different from both of these: not only is the geometry of each flight path exactly specified, but the helicopter is assumed to stick rigidly to the desired path. While this is not achievable in practice, it is adequate for the purpose of assessing the relative agility of different helicopter configurations.

4:3 Inverse Solution of the Vehicle Equations of Motion

The vehicle equations of motion used in this study represented the Lynx helicopter, mass 4314kg and c.g. fully aft. Previous studies, chapter 3, had indicated that a very good approximation to the longitudinal modes of the helicopter configurations tested here could be obtained by adding the rolling moment equation and associated cross-coupling derivatives to the 4th. order

system that represented purely longitudinal motion. The resulting system of order 5 can be written in state-space form as

$$\dot{\mathbf{x}} = A\mathbf{x} + B\mathbf{u} \text{ ----- (4:1), where}$$

$$x = [\ u\ w\ q\ \theta\ p\ ]^T$$

$$u = [\ \theta_{1S}\ \theta_0\ \theta_{1C}\ ]^T$$

Equation (4:1) is normally solved for the vector of state variables **x** given the control vector **u**. Assuming that the trim state of the helicopter is known, the flight path and attitude time histories that result from the inputs **u** can be constructed. The inverse solution consists essentially of calculating **u** given **x**. At first sight then, the inverse solution appears to be algebraic in nature, but this is only the case for special classes of problem - where the number of independent controls is equal to the number of degrees of freedom, which is clearly not the case here. The case of the helicopter with a tailplane, *independently* controllable, is different: here the number of independent controls equals the number of degrees of freedom. Correspondingly the pitch attitude time history can be specified *a priori*. In this study, the tailplane is not independently controllable and only the velocity vector, ie. a combination of trajectory and speed, is specified. It might then appear that an inverse solution of equation (4:1) poses an intractable problem, having algebraically more unknowns than equations. However the system can be recast not algebraically but as a set of differential equations in state-space form. This is now described for the system given in equation (4:1).

A formalised statement of the inverse procedure is as follows: for purely longitudinal motion,

$$\dot{p} = p = 0$$

So the rolling moment equation is

$$L_u u + L_w w + L_q q + L_\theta \theta + L_{\theta 1s}\theta_{1s} + L_{\theta 0}\theta_0 + L_{\theta 1c}\theta_{1c} = 0$$

An expression for θ_{1c} may be obtained from this which can be substituted into the other equations in (4:1). The state-space description becomes on rearranging,

$$\dot{\mathbf{x}} = A_1\mathbf{x} + B_1\mathbf{u}, \text{ where}$$

$$\mathbf{x} = [\ q\ \theta\ u\ w\ ]^T \text{ and } \mathbf{u} = [\ \theta_{1s}\ \theta_0\ ]^T$$

Further, partitioning the resulting system gives

$$\begin{bmatrix} \dot{\mathbf{x}}_1 \\ \dot{\mathbf{x}}_2 \end{bmatrix} = \begin{bmatrix} A_{11} & A_{12} \\ A_{21} & A_{22} \end{bmatrix} \cdot \begin{bmatrix} \mathbf{x}_1 \\ \mathbf{x}_2 \end{bmatrix} + \begin{bmatrix} B_{11} \\ B_{21} \end{bmatrix} u$$

where $x_1 = [\ q\ \theta\ ]^T$ and $x_2 = [\ u\ w\ ]^T$. Then

$$\dot{\mathbf{x}}_1 = A_{11}\mathbf{x}_1 + A_{12}\mathbf{x}_2 + B_{11}\mathbf{u} \text{ ----- (4:3)}$$

$$\dot{\mathbf{x}}_2 = A_{21}\mathbf{x}_1 + A_{22}\mathbf{x}_2 + B_{21}\mathbf{u} \text{ ----- (4:4)}$$

Equation (4:4) can be written as

$$u = B_{21}^{-1}\dot{x}_2 - B_{21}^{-1}A_{21}x_1 - B_{21}^{-1}A_{22}x_2 \text{ ----- (4:4a)}$$

so (4:3) becomes

$$\dot{x}_1 = (A_{11} - B_{11}B_{21}^{-1}A_{21})x_1 + B_{11}B_{21}^{-1}\dot{x}_2 + (A_{12} - B_{11}B_{21}^{-1}A_{22})x_2 - (4:5)$$

Figure 4:3 shows the relationship between sets of body-fixed, flight path and earth axes, from which expressions for u and w are obtained, viz.

$$u = V\cos\alpha - V_e\cos\theta_e$$

$$w = V\sin\alpha - V_e\sin\theta_e$$

$$\alpha = \theta + \theta_e - \gamma$$

Thus both x_2 and $\dot{x}_2$ can be expressed in terms of x_1 and the variables that define the flight path at time t, giving

$$x_2 = Cx_1 + D$$

$$\text{----- (4:6)}$$

$$\dot{x}_2 = Ex_1 + F$$

The reader is referred to the appendix 2 for the coefficients that form the elements of C, D, E and F. On substitution into (4:5) the new state-space description is

$$\dot{x}_1 = A'x_1 + B' \text{ ----- (4:7), where}$$

$$A' = A_{11} - B_{11}B_{21}^{-1}A_{21} + B_{11}B_{21}^{-1}E + (A_{12} - B_{11}B_{21}^{-1}A_{22})C$$

$$B' = B_{11}B_{21}^{-1}F + (A_{12} - B_{11}B_{21}^{-1}A_{22})D$$

Note that the resulting system, while still described by a set of linear ordinary differential equations, may no longer be *invariant*, as A' can be a function of the velocity vector, itself some prescribed function of time. This is because elements of C and E depend on the variables that define the flight path, the speed and climb angle. The latter changes during the manoeuvres investigated here. The system will be invariant if it is assumed that γ and $\dot{\gamma}$ are small. This is obvious from inspection of the equations for C and E in the appendix, which are the expanded versions of equations (4:6). It can be seen that assuming γ small and then neglecting products of small terms, removes terms in $\gamma\theta$ and γq from the expansions of equations (4:6), and therefore the elements of C and E that result in the variability of the new system matrix, (4:7). The reader is referred to section 5:3.1 of the next chapter, equations 6:1, for the linearised form of these equations. Equation (4:7) can be solved by using a numerical integration technique, and the control time histories then obtained explicitly from (4:4a).

4:4 Results

A set of attitude and control time histories is presented in figures 4:4, 4:5 and 4:5a for this helicopter flying one of the family of popup manoeuvres. The main feature to note is that the collective pitch time

history corresponds in form at least, to that of the flight path angle. Lateral cyclic pitch inputs are not insignificant, which is not surprising considering the strong pitch/roll cross-coupling with this rotor configuration. The longitudinal cyclic pitch controls the pitching motion of the helicopter; in the pullup segement of the manoeuvre, attitude changes are fairly small, caused by the cyclic moving forwards opposing the sizeable pitching moment from collective inputs. In the pushover segement the cyclic moves relatively far forwards, creating a large nose-down pitching moment, as is reflected in the pitch attitude response. In figure 4:6 the longitudinal component of the total hub moment is given, and in figure 4:6a is broken down to show the contributions of the three rotor controls. It can be seen that all three contribute significantly to the overall hub moment. Although hub moment is taken to be the parameter which limits agility, a broader view of the problem is that thrust and hub moment limits must be considered together - the hub moment limit varies with rotor thrust. In this problem it was assumed that the thrust constraint is not active.

The main points to note from these results are that collective appears to be used to control the flight path angle, while longitudinal cyclic controls the pitching motion of the helicopter. Note that these inputs suggest that the manoeuvre is not necessarily the most severe in geometric terms - nontheless limiting manoeuvres can be reached by moving the controls in this fashion. Given that the tailplane contributes primarily a pitching moment; and further that any change in the overall pitching moment affects the position of the longitudinal cyclic, then it was postulated that the control strategy for the horizontal tailplane is

to contribute a pitching moment to modify the overall moment on the helicopter, causing the longitudinal cyclic to move in such a direction that the hub moment will be reduced. The general form of the control law investigated was

$$\alpha_s = k_1 q + k_2 \theta_{1s} + k_3 \theta_{1c} + k_4 \theta_0$$

This form of control law was chosen because it will deflect the tailplane only to terms that contribute to hub moment. As a consequence, the tailplane is only modifying longitudinal cyclic position and therefore hub moment, when there is a perturbation in hub moment from trim. A feedback law (tailplane incidence proportional to speed, angle of attack, pitch attitude for example), could deflect the tailplane when there is no hub moment perturbation, therefore causing a change in hub moment. It was hoped that this would make correlation of any reduction (or increase) in rotor hub moment with the tailplane control time history obvious through a simple analysis on the basis of observed cause-and-effect, and so any necessary change to the control law easier to identify. Generally the gains k_i could be varied individually, but it was found that the peak limiting hub moment during manoeuvres could be reduced, and an improvement in agility quantified, by making the tailplane pitching moment proportional to M_h by selecting the correct values of k_i. The longitudinal component of hub moment can be expressed as

$$M_h = k_s \, (-0.0698q + 1.1243\theta_{1s} - 0.2208\theta_{1c} + 0.6639\theta_0)$$

The lateral component is

$$L_h = k_s\ (-0.0298q + 0.1948\theta_{1s} - 1.0550\theta_{1c} + 0.2255\theta_0)$$

with the total hub moment given by

$$P_h = \sqrt{(M_h^2 + L_h^2)}$$

so for the tailplane control angle to be proportional to M_h,

$$\alpha_s = K\ k_s\ (-0.0698q + 1.1243\theta_{1s} - 0.2208\theta_{1c} + 0.6639\theta_0)$$

The largest value of K allowable, given tailplane authority of ±15 deg. and a limiting value of $M_h = \pm 30$ kNm is ± 3.2.

It may be important to reduce hub moment, as it can be considered a performance parameter that can reach a limit in manoeuvres and therefore by definition limit agility. For a given rotor, the use of the tailplane as a control is the only obvious way of reducing hub moment. As noted by Hohenemser, ref.[22], incorrect use of the tailplane can lead to excessive hub moments, the corollary being that correct use can reduce it.

The family of popup manoeuvres was flown at 100 knots, and the limiting manoeuvres for each helicopter configuration obtained. Agility ratings for these cases are shown in the "agility diagram" of figure 4:7, where the agility ratings are plotted against the respective values of

h_f/s_f. There are several interesting features of this diagram. Firstly, the limiting manoeuvres for all four configurations lie on a locus of points: this should not be surprising as the manoeuvres are all geometrically similar, with the same boundary conditions. Secondly, moving along this locus to the right requires higher levels of agility, as the rating is tending to zero and the ratio h_f/s_f is increasing. Thirdly, each helicopter has several limiting manoeuvres: this point is discussed in section 4:5 but for now it is the ultimate level of agility that each configuration can achieve that is desired. The points which are of interest are shown in the expanded view of figure 4:7, 4:7a. In this sense the least agile configuration is the helicopter with a fixed tailplane, the most agile that with the active tailplane. Of the other two configurations, the tailless helicopter is only slightly less agile than the active tail case, while the configuration with the tail geared to the longitudinal cyclic is only marginally more agile than the helicopter with the fixed tailplane. Tailless helicopter hub moment time histories are very similar to those of the active tail configuration, resulting in very similar agility ratings. The reason for this is that the derivative M_ω is double that of the tailed configurations. For any given popup manoeuvre, the ω-time histories of each configuration are very similar, and thus relative to the fixed-tail case, the tailless configuration experiences a greater nose-down moment; to "balance" this, the disc is tilted further aft during the popup, i.e., the longitudinal component of hub moment is more positive. A physical interpretation of the differences in agility is given in figure 4:8, where the limiting trajectories of the least and most agile helicopters are shown. The most agile helicopter can fly a popup to 50m that intuitively requires more agility than the least agile

configuration - the manoeuvre is tighter, requiring less airspace and can be started about 35m closer to the obstacle. This represents a saving in manoeuvre distance and time of about 10%. The tailplane control input during the limiting manoeuvre in figure 4:8 is given in figure 4:9, and it is obvious that the tail control system requires high authority, in order that the benefits in agility are achieved.

Another perspective on the improvement in agility capability that is achievable with the active tailplane configuration can be obtained by quantifying *how much faster* this helicopter can fly a given manoeuvre before reaching the hub moment limit. To this end, the helicopter with the active tailplane was flown through the limiting manoeuvres of the least agile configuration, that with the fixed tailplane, at 101, 103, 105, 107 and 109 knots to identify at which speed the hub moment limit is met. The improvement in agility already demonstrated is shown in a different form in figure 4:10; the locus of limiting manoeuvres lies closer to the x-axis. The agility ratings are smaller and hence by definition, the helicopter with the active tailplane is more agile. This configuration can fly the limiting manoeuvres of the fixed-tailplane helicopter at 107 knots, ie. 7% faster, including the "tightest" manoeuvre which lies farthest to the right of the locus.

The helicopter with the active tailplane, it was shown, was more agile in bobup-type manoeuvres than the other three configurations, by virtue of the fact that the peak hub moment during a given manoeuvre was smaller than that of the other helicopters, allowing a more severe manoeuvre to be flown before the limit was met. This reduction is

illustrated in the example of figure 4:11 for the least and most agile helicopters flying the manoeuvre from a starting point 300 metres from the obstacle. However note that during the first half of the manoeuvre, the hub moment of the helicopter with the active tailplane is greater than that of the fixed-tail configuration, and quite considerably so. This result is typical of the popup manoeuvres investigated here - although the active tailplane configuration suffered a larger hub moment during the first part of the manoeuvres than any of the other three helicopters, this peak was never the limiting peak, even during the more severe popups that this configuration could fly. The fact that the active tailplane does not reduce the hub moment overall was felt to be intruiging - more so when one considers figure 4:9 in comparison with figure 4:6. The tailplane control pitching moment is opposite in sense to that of the hub moment - rather than aiding the rotor with pitching the helicopter, the tailplane is *opposing* it. And yet the helicopter with the active tailplane has the lowest *peak* hub moment during a given manoeuvre. The answer to this curious result can be obtained with consideration of figure 4:12. The helicopter with the active tailplane flies the same path in space as the fixed-tailplane helicopter with a more nose-down attitude. This result *does* correlate with figure 4:9: during the first 3.25 sec. of the manoeuvre, the tailplane gives an additional nose-down moment to the helicopter, and figure 4:12 shows that until this point in the manoeuvre, the active tailplane helicopter's attitude is increasingly nose down relative to the aircraft with the fixed tailplane. After 3.25 sec. the tailplane pitching moment acts to raise the nose, and indeed the gap between the two attitude time histories narrows. Now the forces indicated in figure 4:13 must have the same value at any point in a given manoeuvre

irrespective of configuration and pitch attitude time history; the result of this (to a first approximation) is that the rotor disc angle of attack time history will be the same for each configuration flying this manoeuvre. Thus with the active tailplane, the rotor is more nose-up relative to the fuselage, the flapping angle β_{1C} is therefore more positive, and so the longitudinal component of hub moment is more positive during the manoeuvre, illustrated in figure 4:14. The effect this has on the total hub moment is to increase the magnitude of the first peak, and reduce that of the second, as illustrated in figure 4:9. The control law implemented in the simulations to demonstrate the effect of the active tailplane on longitudinal agility is therefore a compromise, reducing the hub moment only over some part of the manoeuvres. At the same time it does quantify the improvement in agility that is achievable, because the reduction in hub moment that it gives at the limiting peak is the largest that can be obtained, irrespective of control law, because the tailplane has reached probably its limiting angle of attack, figure 4:9.

4:5 Discussion

The three main aspects of this chapter require further discussion. They are however sufficiently self-contained to be dealt with separately.

It has been assumed that helicopter agility can be assessed by examining features of the flight path (the geometry and time taken to fly) which can then be combined in an "agility rating" that quantifies the level of agility required to fly a manoeuvre. The rating is not simply the

time to perform the manoeuvre specified by the boundary conditions, but includes an assessment of the "tightness" of a specific path. What results is a measure of helicopter agility that quantifies some intuitive idea of the level of agility needed to fly a given path. The rating in this form has advantages over others in terms of uniqueness, giving a measure of agility that is not qualified by speed, for example. This type of analysis seems particularly amenable to a computer-based study where performance limitations as they pertain to the kinematics of agility are examined. However, as was noted, each helicopter has a series of limiting manoeuvres, and each one is flown differently - those to the left on the locus in figure 4;7 are flown with gentle, relatively lengthy pullups and severe pushovers, while those to the right are the opposite. This tends to suggest that the *style* of the manoeuvre then becomes important to the analysis, if each helicopter is to be represented on the locus by a single point, and this will depend on the pilot's perception of the task and his interaction with the helicopter/FCS combination. In a wider analysis of helicopter agility then, handling qualities considerations should probably be included, and a kinematics-based study such as this will probably not sufficient, although likely to be necessary. In this case the agility rating may be based on features more removed from the actual geometry of the flight path and the kinematics of the manoeuvre, and closer to features important to the pilot such as achievable pitch and roll rates, time constants, stability and control power. The resulting agility diagram may then look like figure 4:15 reproduced from ref. [19].

By viewing the solution of the helicopter equations of motion as an inverse problem, different helicopters can then be made to fly identical

paths since the velocity vector in each case is a precisely defined input to the system, equation (4:7), with the attitude and control time histories the output. The inverse solution may at first sight appear algebraic in nature, but this is true only for special classes of problem. In any case, the differential equation form of the inverse method is neater, in that it allows an analytical, rather than numerical, study of the stability and dynamics of the solution. The principal advantage of inverse methods for generating control inputs is simplicity; no assumptions are necessary about the form of the control system or the control strategy required. As a result it can give a significant insight into the control strategies required to fly specific manoeuvres in any manner. What is in some sense a limiting feature of the inverse method as formulated in this study is that the inverse of the matrix B_{z_1} must exist. This can be overcome as done here by use of a valid reduced order model. In the general case of motion in three dimensions where there are 4 controls and 3 velocity components, it will be necessary to impose an additional constraint equation eg. a condition of zero sideslip (assuming that the 3 attitude variables remain unspecified).

It is shown that using a controllable horizontal tailplane to reduce hub moment in popups on a helicopter with a stiff rotor *can* require a control law that is a function of the three rotor controls and pitch rate. In the past on helicopters with articulated rotors, the tailplane has been geared to the longitudinal cyclic to reduce blade flapping during manoeuvres, refs. [8], [9] for example. This does not appear to be sufficient in these studies. Ref. [37], suggested that this was because of the use of a model of a stiff-flapwise rotor helicopter, and in this context seemed to be the

case because the hub moment is a function of, among other things, all three rotor controls; and during popups flown in the style presented in that paper (and this chapter), the rotor controls all vary, contributing different proportions of the total hub moment at different times during the manoeuvre. This aspect should however be looked at more closely for confirmation of this explanation. It could be thought however of merely academic interest, as gearing the tailplane to the cyclic was shown to have little impact on the hub moment for the manoeuvres studied here.

An investigation was made to ascertain why the active tailplane configuration flew popup manoeuvres with the hub moment reduced at the limiting peak, but increased at the start of the manoeuvre. This revealed that the more nose-down attitude flown by the active tailplane configuration resulted in the longitudinal component of the rotor hub moment being more positive throughout the manoeuvre, because the rotor disc angle of attack was the same irrespective of helicopter configuration. The difference in attitude during the manoeuvre was in turn correlated with the tailplane incidence angle (and therefore pitching time history. The original reason for choosing the tailplane control law discussed in section 4:4 is therefore based on the erroneous assumption that the tailplane control pitching moment and rotor hub moment are correlated. This does not however invalidate the results of the benefit of the active tailplane to helicopter agility as already mentioned in the previous section; the tailplane control law implemented is a compromise, giving enhanced agility at the expense of greater (but not limiting) hub moment elsewhere in the manoeuvre. Neither is the control *strategy* invalidated, as can be seen from figure 4:16 - the longitudinal cyclic is

indeed the only longitudinal control whose time history during the manoeuvre is significantly affected by the addition of the active tailplane - this is therefore where the differences in hub moment arise. The considerable change in lateral cyclic is in proportion to that of longitudinal cyclic, but this is an indirect effect of adding an active tailplane, and the magnitude of the change in lateral cyclic will depend on the size of the derivative $L_{\theta_{1s}}$. It should be noted that although very small, these differences in θ_0 and θ_{1s} with the active tailplane are such that they help reduce the hub moment at the limiting peak. It is worthwhile noting that as well as being a compromise, the tailplane control law implemented here will in general not offer similar agility benefits in other manoeuvres. For example, in a pullup manoeuvre to a steady climb, the first peak in figure 4:11 is likely to be the limiting hub moment, and therefore the helicopter with the tailplane control law implemented here will be less agile than than the fixed tailplane configuration. A more generally applicable tailplane control law for enhancing agility, is likely to be based on the control of pitch attitude.

In absolute terms, the improvements in agility attainable with the controllable tail do not seem significant - reducing manoeuvre time by about 0.7 of a second, and relative to the least agile configuration, this is an improvement of about 10%. Alternatively the limiting manoeuvres of the least agile helicopter can be flown at up to 107 knots, as opposed to 100 knots. In order that these benefits are obtained, the tailplane will have to be actively controlled, because irrespective of the control law finally chosen, the system requires high authority.

4:6. Conclusions

The kinematic definition of helicopter agility based on the geometry and time taken to fly a specific path in space, together with the inverse solution of the vehicle equations of motion, has provided a fruitful means of comparing the relative agility capabilities of several helicopter configurations. It is however suggested that some consideration needs to be taken of the pilot's perception of the task.

The inverse solution is only algebraic for certain classes of problem. Otherwise manipulation of the state-space description of the helicopter allows the system to be recast as a set of differential equations. In this form, the resulting system may no longer be invariant, depending on assumptions about the velocity vector and its rate of change with time.

The theoretical studies of agility in popup manoeuvres were made for four similar helicopter configurations. The measure of agility adopted was consistent in use, reflecting the need for higher levels of agility to fly paths in space that are intuitively more severe than others. The most agile helicopter configuration was that with a moveable horizontal tailplane which produced, for a given manoeuvre, some reduction in rotor hub moment. Correspondingly for a given limiting hub moment, the helicopter with the moveable tail could fly tighter popups. Although the controllable tailplane offered improved agility over the other configurations, the sophistication of the control algorithm and the

control authority required suggest that the benefits would be achieved only if the tailplane was actively controlled and a fully integrated element of the vehicle FCS.

A more detailed analysis of inverse methods in studies of helicopter flight mechanics is required to increase the level of experience with what appears to be a very useful tool for investigations of helicopter agility.

Chapter 5

The Use of the Horizontal Tailplane for Decoupled Attitude Control

5:1 Introduction

Recently the application of flight control systems to aircraft to allow unconventional manoeuvres to be flown has allowed the study of such manoeuvres in flight tasks. The vehicle of most note in this area is the AFTI (Advanced Fighter Technology Integrator) F-16, which has demonstrated that some tactical benefits can be obtained in tasks involving the acquisition and tracking of targets, ref. [42], through decoupling the vehicle's degrees of freedom. This allows the aircraft to fly along a path with the three attitudes (roll, pitch and yaw) not necessarily related to the velocity vector. To permit such manoeuvres, the basic vehicle configuration has been altered by the addition of a pair of near-vertical canards and wing flaps that deflect up as well as down, to permit direct lift control. For similar development of the single main and tail-rotor helicopter however, no changes to the basic configuration would be required, because such a helicopter already has the means of generating the forces and moments required for decoupled attitude control - due mainly to the fact that the main rotor integrates the functions of lift, propulsion and control. At an elementary flight mechanics level, (neglecting handling qualities considerations and exactly how the flight and attitude demands would be made) all that is required for the helicopter is the development of an FCS that will synthesise the control

inputs in such a manner that the attitude can be decoupled from the flight path. Having said that, the problem is not so straightforwards - there are structural and aerodynamic considerations, even in achieving small attitude changes; the inter-relationship between speed and attitude with the conventionally configured helicopter, together with the use of longitudinal cyclic to control speed and attitude, is a major influence on the structure and control strategies of the resulting controller; and due consideration has to be taken of coupling between higher-order rotor dynamics and rigid-body modes, which is made more acute as feedback gain is increased and the latter modes become faster.

Although a few helicopters, both in service and in the past, have horizontal tailplanes capable of being controlled by the pilot, they are used essentially as trimming devices. They are unsuited for use as a means of decoupling the attitude from the flight path for pointing tasks, for two reasons; firstly they lack the speed of response, and in some cases the required authority eg. the S67, ref. [8] whose tailplane travelled through its full range of 10 degrees in 7 seconds; secondly the pattern of helicopter control allied to the cockpit setup would prohibit using the tailplane to decouple the attitude - it would add another control that the pilot would have to use in an environment where his workload is already high. More fundamentally, even if he possessed the manual dexterity to utilise this extra control, he would have to discriminate between attitude perturbations that resulted from use of the tailplane, and those he would command with the rotor for flight path control. The mental agility required to fly a path with attitude commands using the rotor, and at the same time "superimpose" attitude commands with the tailplane independently of the flight path is probably outwith the capability of any pilot.

It seems logical therefore that some basic requirements of a viable decoupled flight path and attitude controller would include a low workload, command-type FCS; a tailplane that is a fully integrated element of this FCS; and control strategy that separates the flight path and the attitude ie. not the traditional pattern of control.

5:2 Applications, Capabilities and Constraints of Decoupled Flight Path and Attitude Control

The principal use of decoupled attitude control would be to acquire and track targets, although secondary uses could include reducing the hub moment in trimmed flight by selection of the optimum pitch attitude, or simply allowing the pilot to set an attitude that he finds comfortable, for whatever reason. Although helicopter armaments are increasingly of the type that do not require the aircraft to point at its target, there is a varied literature that mentions and indeed demonstrates the desirability of fuselage pointing, albeit laterally by sideslipping, to enhance manoeuvrability, refs. [43], [16], [17] and [38], the latter three of which mention it due to the growing consideration of the combat helicopter for anti-helicopter operations. Ref. [38] in particular was concerned with the development of simplified models for simulations studies once it became apparent that unlike fixed-wing aircraft, uncoordinated (decoupled) manoeuvring could be a central mode of control in helicopter versus helicopter air combat, ref. [44]. While the ability of the helicopter to point laterally is well known, no work appears to have been done on the contribution to be made to tracking manoeuvrability by releasing the pitch degree of freedom. This is probably because the implementation of such a mode of control has had to wait until the advent of ACT, for the reasons

discussed in the previous section.

The constraints on decoupling the pitch attitude from the flight path with the conventional single main and tail rotor helicopter derive form both aerodynamic and structural considerations. Some control other than the main rotor is needed to pitch the fuselage and the tailplane is the most effective means of doing so - the main rotor being used to change the flight path. The tailplane however can reach angle of attack limits and stall, reducing its effectiveness, and this is the aerodynamic constraint. For a given velocity vector, the rotor will have to maintain a certain attitude with respect to the flight path and pitching the fuselage underneath the rotor, like a pendulum, gives rise to the structural constraint, the nature of which varies with the rotor stiffness. For "soft" rotors (such as those that are teetering or have a zero flapping hinge offset), the fuselage pitch attitude can be varied over a large range as there is no reacting moment at the hub, and the structural constraint is then one of ensuring that there is adequate clearance between the rotor and fuselage when the latter is at its extreme attitudes. As the rotor stiffness increases, there is a reacting moment at the hub of increasing magnitude, and varying the fuselage attitude and its orientation to the rotor by whatever means, tailplane or not, changes this reacting hub moment which can reach limiting values for some pitch attitudes. Rotor hub moment is the major structural constraint for stiff-flapwise rotors.

To put the previous discussion in perspective, results are presented that demonstrate the effect of increasing rotor stiffness on the pitch attitude change that is achievable independently of the flight path. These

results were obtained using the model HELSIM described in chapter 2, and are for trimmed flight. Figure 5:1 shows the variation in pitch attitude that can be achieved with rotors of varying stiffness, represented by the flap frequency ratio squared of the first flapping mode, λ_β^2, and the tailplane incidence angle required to produce the change. The helicopter configuration is based on that of the Westland Lynx at 160 knots with the c.g. 127mm forwards of datum. As the rotor stiffness increases the slope of the attitude/tailplane incidence relationship becomes shallower, indicating that a smaller range of attitudes is achievable with a given tailplane incidence range. Increasing the tailplane size increases the pitching moment per unit angle of attack, and the influence of this on the attitude/tailplane incidence curves is shown in figure 5:2. The tailplane size required is fixed by the required peak variation in pitch attitude at the minimum speed for which decoupled attitude control is required.

The helicopter configuration chosen for this study was the Lynx, mass 4314kg and c.g. 127mm forwards of datum. It was assumed that the minimum speed at which decoupled attitude control might be required was 80 knots. This is roughly the minimum power speed and is taken to be representative of future NOE speeds. The tailplane area was trebled in order that it could pitch the helicopter at least ± 5° at this speed without stalling. From figure 5:2 it can be seen that even at 160 knots the conventional tailplane on the Lynx can only just fulfil this requirement. For a given helicopter at a given speed the variation in pitch attitude with tailplane incidence is almost linear, figure 5:1 as is the rotor hub moment figure 5:3. This is due to the linearised fuselage, wake and interactional aerodynamics, and the modelling of the rotor to represent hub moment as a linear function of blade flapping. This

near-linearity makes the calculation of the maximum attitudes achievable within given hub moment and tailplane angle-of-attack limits easy, by simple extrapolation or interpolation given any two points on the attitude/tailplane incidence and hub moment/tailplane incidence curves. The limiting tailplane angle of attack was taken to be ± 15° and the rotor hub moment limit 35kNm. The limiting trim attitudes are shown in figure 5:4 as a function of speed between 60 and 160 knots - the lower curve is the peak nose-down attitude achievable within the constraint of limiting hub moment, which is met before the limiting tailplane angle of attack. The upper curve is the maximum nose-up attitude achievable; above 100 knots it is limited by the hub moment, but between 60 and 100 knots by the limiting tailplane angle of attack. The datum trim attitude at each speed was taken to be midway between the two curves, and is shown in figure 5:5 as a function of speed, together with the required variation in the tailplane incidence angle to give this curve. Selection of the datum trim attitude was not made arbitrarily - above 100 knots it minimises the rotor hub moment in steady level flight.

5:3 Synthesis of the Flight Control System

The helicopter FCS was synthesised on the basis of producing a controller that would decouple the states that it was desired to control independently. Further, it was presupposed that a controller which would modify the pattern of flight path control from one based on attitude commands to one in which the changes in the velocity vector are demanded directly, would require speed, climb angle, bank angle and yaw rate to be decoupled; in addition, the ability to point the fuselage independently of the flight path would require decoupling pitch attitude and sideslip.

Stability in response to disturbances is not sufficient for such an FCS - wholly necessary is the need to have swift, non-oscillatory responses to commands so that only simple inputs need to be made to attain any desired state. The response characteristics that can be achieved are limited by the physical range of control available, and the effect of feedback on the closed-loop system eigenvalues. Simply increasing the feedback gains to improve the response, resulting in closed-loop eigenvalues of higher and higher modulus, would not have given a representative helicopter/FCS combination, without consideration of the dynamics of the rotor. It can reasonably be expected that these rotor modes would be more strongly coupled with high-modulus closed-loop rigid-body modes than with the unaugmented open-loop dynamics. For these various reasons, it was therefore of crucial importance that an adequate system regulator be determined, although its characteristics were to be somewhat more refined than those of a conventional SAS. It does however form only one part of the overall FCS, and the structure of the closed-loop helicopter/FCS combination is shown in figure 5:6 to include two other essential elements: a precompensator matrix and a feedforward matrix. The former is used to decouple the effect of control action, while the latter scales the control inputs to ensure that a commanded change in the helicopter's state in a given degree of freedom is achieved.

5:3.1 Transformation of the Equations of Motion

The task of synthesising the FCS was eased by having the variables that it was desired to control appear explicitly in the state-space description of the helicopter. Accordingly, a transformation was applied to the helicopter equations of motion produced by the model HELSIM, such

that the velocity components u and w become ΔV_f and γ. The transformation is achieved quite simply. From ref. [45], the matrix that expresses body-referenced velocity components in terms of aerodynamic axes velocities is given by

$$T = \begin{bmatrix} \cos\alpha\cos\beta & -\cos\alpha\cos\beta & -\sin\alpha \\ \sin\beta & \cos\beta & 0 \\ \sin\alpha\cos\beta & -\sin\alpha\sin\beta & \cos\alpha \end{bmatrix}$$

which transforms the vector of body-axis component velocities $[\ U\ V\ W\ ]^T$ to the flight path set $[\ U_a\ V_a\ W_a\ ]^T$. Note that in the flight path system, there are no lateral or vertical components of velocity. Then writing

$V_f = U_a$, $V_a = W_a = 0$, we get

$$U = V_f \cos\alpha\cos\beta$$

$$V = V_f \sin\beta$$

$$W = V_f \sin\alpha\cos\beta$$

It was decided to retain the velocity component V in the equations of motion as nothing is to be gained by having sideslip angle β appear explicitly - it is simply related to V. Assuming that β is small,

$$U = V_f \cos\alpha$$

$$W = V_f \sin\alpha$$

Now the linearised small-perturbation relationship between aerodynamic, Euler and flight path angles is given by $\alpha = \theta - \gamma$ so that

$$U = V_f\ (\ \cos\theta\cos\gamma + \sin\theta\sin\gamma\ )$$

$$W = V_f\ (\ \sin\theta\cos\gamma - \cos\theta\sin\gamma\ )$$

These expressions are now fully linearised by assuming that

$$U = u_e + u, \quad W = w_e + w$$

$$V_f = V_{fe} + \Delta V, \quad \gamma = \gamma_e + \gamma'$$

$$\theta = \theta_e + \theta'$$

(The primes serve to distinguish total from perturbation quantities in the linearisation - once the expressions are linearised, they are removed). Then making the small angle assumption and thereafter neglecting products of small quantities

$$u = \Delta V_f \cos\theta_e + \gamma V_{fe} \sin\theta_e - \theta V_{fe} \sin\theta_e$$

$$w = \Delta V_f \sin\theta_e - \gamma V_{fe} \cos\theta_e + \theta V_{fe} \cos\theta_e \quad \text{----- (5:1)}$$

Expressions for $\dot{u}$ and $\dot{w}$ are readily obtained form those above, and the transformation was implemented in a digital computer program TRANSFORM. A comparison of the system and control matrices before and after the transformation is made in figure 5:7, using data representing the Lynx at 100 knots, with tailplane area trebled.

5:3.2 Calculation of the Precompensator Matrix

As stated previously, the precompensator was used to decouple the effect of control action by modifying the control matrix such that actuation of a given control forced only the desired degrees of freedom.

Let $u = K_p u_p$ where K_p is the precompensator matrix. The vector u_p can then be considered a change of variable under the transformation K_p. Then

$$Bu = BK_p u_p \ , \ BK_p = B_p \text{ ----- } (5:2)$$

B_p is the precompensated B-matrix, and its desired structure is given in figure 5:8. No significance should be attached to the numerical values of the elements of B_p in this figure - zeros indicate elements that are to be *minimised* by K_p and the 1's the elements that are to be non-zero, preferably with the values of the corresponding elements of B. The inputs u_{pi}, i=1,5 correspond to collective, longitudinal and lateral cyclic, tail rotor collective and tailplane incidence angle. Figure 5:8 therefore indicates that they are to respectively control climb, forward speed, the roll degree of freedom, sideslip/yaw rate and the pitch degree of freedom. A unique solution of 5:2 to give a K_p that would produce a desired B_p does not exist, because there are only five controls to influence six degrees of freedom. The problem then becomes one of producing an optimum solution, optimum in the sense that the elements of B_p denoted by zeros in figure 5:8 are minimised. A solution was obtained by formulation of the control couplings as a linear least squares problem, as now described.

Given m functions f_j in n variables k_i, it is desired to minimise a function g given by

$$g(k) = \sum_{j=1}^{m} \langle f_j(k) \rangle^2 \text{ ----- } (5:3)$$

so that the solution yields the k_i that will minimise the sum of the squares of the m functions. The functions themselves have then, in some sense, been minimised. In the general case, the f_j are the elements of B_p and are in terms of the n variables that form the elements of K_p. Now the elements denoted by 1's in figure 5:8 are to have values as close as

possible to the corresponding elements of the B-matrix, and therefore are **not** to be minimised. However they form an essental part of the overall solution - consider as an example the element of B_p that controls the speed degree of freedom, B_{p12}. It is given by

$$B_{p12} = X_{\theta 0} K_{p12} + X_{\theta 1s} K_{p22} + X_{\theta 1c} K_{p32} + X_{\theta 0tr} K_{p42} + X_{\alpha s} K_{p52}$$

Now for $B_{p12} = B_{12}$, a possible solution is given by

$$X_{\theta 0} K_{p12} + X_{\theta 1c} K_{p32} + X_{\theta 0tr} K_{p42} + X_{\alpha s} K_{p52} = 0 \text{ ----- (5:4)}, \quad K_{p22} = 1$$

Similar solutions can be written for B_{p21} etc. In assuming that $K_{pij} = 1$, i=j the number of *variables* is reduced from 25 to 20, and expressions such as (5:4) become additional *functions* to be minimised, giving a total of 30 functions, an increase of six. This is beneficial for the minimisation algorithm, ref. [46], which requires that $m \geqslant n$, not the case before the assumption that $K_{pii} = 1$. The above problem was implemented in the digital computer program CROSSFEED. It was found however at an early stage that weighting terms on the functions gave much better results in that they allowed some control over a solution whose mechanism, to the observer, was essentially invisible. An additional benefit was that tendencies to numerical instability with B matrices for speeds above 120 knots were removed. Accordingly the function (5:3) becomes

$$g(k) = \sum_{j=1}^{m} \langle W_{ij} B_{pij}(k) \rangle^2 \text{ ----- (5:5)}$$

where W_{ij} is an element of the weighting matrix that weights element B_{pij} in the precompensated B-matrix.

The matrix K_p for the 100 knots flight condition is shown in figure 5:9, the B-matrix and resulting precompensated B-matrix B_p in figure 5:9a. The magnitude of the elements of K_p give some indication of the amount of control coupling in any degree of freedom. Consideration of figure 5:9a shows that the matrix K_p is generally very effective in producing the matrix B_p that is similar in form to that desired. Two elements in the sideslip degree of freedom are not minimised, but in fact increased quite considerably. More judicious selection of weighting elements would probably reduce these terms, although by the nature of the minimisation process this could be at the expense of the good minimisation of other elements in B_p. Nonetheless it was felt that the precompensator matrix K_p and the resulting matrix B_p were more than adequate, especially as the control couplings in the rotational degrees of freedom were reduced to insignificant levels.

It is interesting to compare the B and B_p matrices for two extremes of the flight envelope, 60 and 160 knots, because this will indicate the changing nature of the control strategy for forward speed. The comparisons are made in figure 5:10 and 5:11 for 60 and 160 knots respectively, and shows similar results to that for 100 knots - the rotational degrees of freedom are very well decoupled, while coupling within sideslip is worsened. At 160 knots however the effect of collective pitch and longitudinal cyclic on the speed and climb degrees of freedom in the matrix B_p is very similar to that in the uncompensated B matrix. This was because at and above 120 knots, the derivative X_{θ_0} is greater than $X_{\theta_{1S}}$, increasingly so with speed, and thus collective becomes more effective than cyclic in controlling the speed degree of freedom. Accordingly no attempt was made to minimise the element B_{p11} - both B_{p11} and B_{p12} were

not weighted. It was therefore assumed that collective and longitudinal cyclic could be used to control forward speed above 120 knots.

The variability of the elements of K_p with forward speed is shown in figures 5:12 to 5:16 - which illustrate that generally, K_p is a nonlinear function of speed. Further, it can be seen that the elements in the first and second columns of K_p do not lie on the hand-drawn best fit curves, being considerably displaced at 120 and 130 knots but less so at 140 and 150 knots. (The first and second columns contain gains that factor collective and longitudinal cyclic pitch). This is due to the fact that changes were made to the relevant elements of the weighting matrix to take into account the changing control strategy above 120 knots. However the changes were not made smoothly to match the smooth changes in $X_{\theta 1s}$ and $X_{\theta 0}$ with speed, figure 5:17, and it is likely that a better choice of weightings would help to draw these elements of K_p closer to the curve fits. The nonlinearity of the elements of K_p with speed is a result of the changing nature of the control couplings.

5:3.3 Calculation of the Feedback Matrix

As mentioned previously, determination of the feedback matrix is of crucial importance to the synthesis of an FCS that will give the desired performance, because it determines the stability, speed of response and the coupling between the degrees of freedom. The feedback matrix synthesis technique used here took no account of system performance (in terms of steady-state errors) in response to commands; the feedback matrix was therefore obtained as the solution of a regulator, rather than servo, problem.

Synthesis of a feedback matrix can be tedious and time-consuming, especially using classical techniques which are essentially single input/single output (SISO) in nature. For coupled multivariable systems, such as the helicopter, determination of the feedback matrix can then be a bewildering, complex iterative process. Use of a multivariable design technique can greatly ease the task of obtaining a feedback matrix, as it will generally calculate a controller simultaneously taking into account each degree of freedom. There are many to choose from however, including simple forms of eigenvalue (pole) assignment, modal control and optimal control, refs. [47] and [48]. More sophisticated multivariable theories exist, and are under investigation to assess their applicability to the helicopter problem, ref.[49]. It was decided however for this study to use the optimal control technique described for example in ref. [47], but widely described and the basis of much work in the '60's and '70's to determine its feasibility for aerospace applications.

Given a system described by

$$\dot{x} = Ax + Bu \text{ ----- } (5:7)$$

it is desired to calculate the optimal control u_0 that will minimise the quadratic performance index

$$J = 1/2 \int_0^{t_f} (x^T Q x + u^T R u) \, dt \text{ ----- } (5:8)$$

Note that the elements of the Q and R matrices penalise respectively perturbations in state and control. Given that the optimal control u_0 is an optimal *feedback* control given by

$$u_o = -Kx \text{ ----- } (5:9)$$

then it can be shown that

$$K = R^{-1}B^TM \text{ ----- } (5:10)$$

where M is the solution of a matrix-Riccati equation. There are several ways to arrive at this equation, but they are quite involved and outwith the scope of this thesis to describe. It should be noted that the matrix-Riccati equation is time-dependent where the regulation period t_f is finite. If it is assumed that the regulation period is infinite, $t_f=\infty$, the equation becomes algebraic viz.

$$MA - MBR^{-1}B^TM + Q + A^TM = 0 \text{ ----- } (5:11)$$

with the result that the matrix $\bar{K}$ is time-invariant. The computer program RICATI was written to solve the time-invariant matrix-Riccati equation using the Potter algorithm, ref. [50] and calculate the matrix K, given the matrices A, B, Q and R. Now the resulting closed-loop system will be optimal only in the sense that the index J is minimised over an infinite period of time, in response to a set of initial conditions as the disturbance; (because the optimal control was specified as a *feedback*, the closed-loop system is not optimal when forced by control inputs that are a result of commands). Further, it is obvious by inspection of equations 5:7 to 5:11 that different closed-loop systems result from selection of different performance indices, each one of which is optimal in the sense described above, but only one of which may be the "optimum" from the

designers' point of view, in that it gives the required response characteristics. As a result, the effort expended in utilising this means of obtaining a feedback matrix has centred on developing synthesis techniques that relate the elements of performance index (the Q and R matrices) to response characteristics of the closed-loop system, refs. [51], [52] and [53]. For this study, the methodology of Murphy and Narendra, ref. [53] was applied to the problem of obtaining the feedback matrix K using the optimal control method described.

The determination of a suitable Q-matrix was made as follows. The initial values of the elements of Q and R were determined as suggested in ref. [51], by the expressions

$$Q_{ii} = \frac{1}{x_{imax}^2}, \quad R_{ii} = \frac{1}{u_{imax}^2}$$

Note that this only gives a *qualitative* relationship between Q, R and the resulting response characteristics. For the values

$$\Delta V_{max} = 2.4 ms^{-1} \quad \gamma_{max} = 0.082 rad \quad q_{max} = 0.2 rads^{-1} \quad \theta_{max} = 0.045 rad$$

$$\theta_{omax} = \theta_{1smax} = \theta_{1cmax} = \theta_{otrmax} = \alpha_{smax} = 0.2618 rad$$

the initial Q and R matrices are

$$Q = \text{diag} [\ 0.175 \quad 150 \quad 25 \quad 500 \quad 0 \quad 0 \quad 0 \quad 0 \quad 0\ ]$$

$$R = \text{diag} [\ 131.3123 \quad 131.3123 \quad 131.3123 \quad 131.3123 \quad 131.3123\ ]$$

Synthesis of the K-matrix was then made one degree of freedom at a time. For the ith. state, the element Q_{ii} was varied about the initial value

given above, all other elements of Q and R remaining fixed. Sets of feedback equations were then obtained for each matrix Q, and the response of the resulting closed-loop systems to an initial condition in the ith. state determined. Characteristics of the response noted were the speed of response, t_0 (defined by the time taken for the perturbation in state i to reach 5% of the initial condition in that state), the peak controller output in the channel that was to control the state under investigation and the magnitude of any overshoot. In addition, the largest longitudinal mode (or modes if a complex pair) of each closed-loop system was noted.

This information, for the longitudinal degrees of freedom, is summarised in figures 5:18 to 5:21 and selection of the desired Q-matrix and therefore response characteristics was made on the basis of these figures. Note that this method in effect assumes that for the various Q, the response to different initial conditions is decoupled, so that variation of say Q_{11} will not affect the desired response in γ set by Q_{22}. This will generally not be the case: accordingly the variation in response characteristics of each degree of freedom with large changes in the elements that penalise deviation in other degrees of freedom, was calculated and is shown in figures 5:22 to 5:24. For each degree of freedom investigated, the value of Q_{ii} was that chosen initially. The other values selected for the elements of Q and R when examining their effect on the response characteristics of each channel, were in fact those finally chosen for the calculation of K (see below). It can be seen that to all intents and purposes, the three longitudinal degrees of freedom have been decoupled. The apparent sensitivity in the control input/t_0 relationship in pitch is due to the differences in the weighting Q_{33} - that penalising pitch rate - and not the other elements of Q. It can be

seen from figure 5:21 that the pitch speed of response is very sensitive to variations in the element Q_{33}. Therefore selection of the elements of Q required to give the desired response characteristics can indeed be made by inspection of figures 5:18 to 5:21. The process was repeated for the lateral/directional degrees of freedom and the final set of weighting matrices is given by

$$Q = \text{diag} [\ 0.175\ 275\ 65\ 800\ 0.1\ 2.5\ 100\ 25\ 0\ ]$$

$$R = \text{diag} [\ 131.3123\ 131.3123\ 5000\ 131.3123\ 131.3123\ ]$$

The resulting feedback matrix for the 100 knots flight condition is given in figure 5:25. It can be seen that generally, the longitudinal inputs are approximately functions of the longitudinal states ΔV_f, γ, q and θ, while the lateral/directional inputs are functions of lateral states. The exceptions are the longitudinal input gains proportional to bank angle. The closed-loop system eigenvalues with this feedback matrix are compared with the open-loop helicopter in figure 5:26. The closed-loop eigenvalues, as well as indicating a stable system, show that the feedback has significantly affected the magnitude of the eigenvalues. None are however, greater in magnitude than the largest open-loop eigenvalue.

The gains for the speed range 60 to 160 knots are presented in figures 5:27 to 5:31, and are intended simply to show the variability of the feedback with speed.

The longitudinal response characteristics of the resulting closed-loop system at 100 knots is given in table 5:1. In table 5:1, it can be seen that the speed of response to an initial

condition of $5ms^{-1}$ is fairly slow, taking 4.76s to decay to 5% of the initial condition. The peak perturbation in θ_{1s} is about 11.8°. The flight path angle and pitch attitude responses to initial conditions in γ and θ respectively of 10° are altogether much faster, with the pitch attitude decaying to 5% of the initial condition in just over 0.6s and the flight path angle to the same level in 0.58s. Large control inputs are required in each of these cases - about -12° collective for the initial condition in γ, and 9.5° of tailplane incidence for the initial condition in θ.

The level of coupling between degrees of freedom in response to the initial conditions in ΔV_f, γ and θ respectively is given in tables 5:2, 5:3 and 5:4. What can generally be noted is the very low level of coupling; for example, the peak perturbation in speed is -0.344 knots in response to the 10° initial condition in attitude; in flight path angle it is 1.033° in response to the initial condition of $5ms^{-1}$ in speed; and in attitude it is 0.186° in response to the initial condition of 10° in flight path angle. The aim of decoupling the pitch attitude from the flight path has to all intents and purposes been achieved. Cross-coupling is almost insignificant, except in roll, which has a peak perturbation of 1.368° in response to the initial condition in pitch attitude. All of the coupled response peaks occur very quickly - all but one (the insignificant roll angle in response to the initial condition ΔV_f) within 1s.

5:3.4 Calculation of the Feedforward Matrix

The feedforward matrix was used to calculate the control inputs that would result in the helicopter achieving the commanded change in state. The aim was to produce a set of control inputs given the command vector

$$x_d = [\ \Delta V_d\ \gamma_d\ \theta_d\ v_d\ \phi_d\ r_d\ ]^T$$

such that there was no steady-state error in response to step commands. The feedforward matrix K_f was calculated given a forcing function matrix B_f that was derived on a trial-and-error basis, as now described. For the system

$$\dot{x} = Ax + B_p u_p$$

let $u_p = u_{pd} + u_{pf}$. u_{pd} are the components of the control input that result from the command vector, and given by the relationship involving the feedforward matrix

$$u_{pd} = K_f x_d$$

and u_{pf} are the components of control that result from feedback

$$u_{pf} = -Kx$$

so that $$\dot{x} = (A - B_p K)x + B_p K_f x_d$$

thus the forcing function matrix is given by

$$B_f = B_p K_f \text{ ----- } (5:12)$$

Given B_f, determination of K_f is not straightforwards as a unique solution cannot be found: B_f is a 9x6 matrix, B_p is a 9x5 (and they both have three null rows) and K_f is a 5x6. Therefore there are 36 equations in 30 unknowns. However since only the response to longitudinal commands was investigated, and the longitudinal and lateral/directional submatrices of B_p are to all intents and purposes decoupled, fig. 5:9a, only the elements

that pertain to the longitudinal forcing functions were calculated. Thus only the longitudinal submatrices of B_f and B_p, denoted respectively as B_f' and B_p', were used in the analysis. Then the elements of B_f' were chosen as follows: considering each diagonal element of the 3x3 matrix B_f' in turn, the initial values chosen were scaled as necessary as a result of calculation of the steady-state response to a given step commanded change in each state, so that for say ΔV_d, $\Delta V_f = \Delta V_d$ in the steady state. Once the diagonal elements were obtained the off-diagonal elements were calculated, and they served to ensure that the steady-state response of degrees of freedom in which no change in state was desired, would be zero. For example, a command in pitch also commands a change in flight path angle and speed. The resulting matrix B_f' for the 100 knots flight condition is given in figure 5:32. Calculation of K_f' the longitudinal submatrix of K_f is then easy as it is a unique solution to the set of simultaneous equations 5:12, and it is shown in figure 5:33.

Generally, what amounts to a scaling of the control inputs in order that the desired steady-state response be achieved, cannot be adopted for coupled multivariable systems subject to many simultaneous inputs, as the effect on the transient response could be most undesirable. In this case however, there is considerable decoupling of the responses of individual degrees of freedom and the input to each channel can thus be scaled without adverse effect on the transient response. This rather empirical approach to the determination of K_f can be justified on two counts; firstly, although tedious and time consuming, it is simple and effective; secondly, the alternative is to integrate the calculation of the feedforward matrix with that of the feedback matrix, as done by Murphy and Narendra. They generated a wide class of inputs by means of a model

represented by a set of differential equations which they adjoined to the helicopter model and solved as a regulator problem. In this study modification of the theory of optimal feedback control to take into account commands was considered outwith the scope of the thesis. In any case as will be seen, the elemental, rather than integrated approach to design of the FCS provided good response characteristics to commands.

5:4 Simulation of a Target Tracking Manoeuvre

The simulations were carried out in the context of helicopter versus helicopter air combat. It was assumed that the target was flying 50m above the helicopter on a reciprocal track at 150 knots, and that it was 1000m away when the manoeuvre was started. This is a wholly realistic and demanding scenario - the helicopter is flying at a speed that is probably the limit at very low level (100 knots), and the target at a speed that would require it to fly at least 50m higher. For a given target range and vertical displacement, the combination of high closing speed and the fact that the other helicopter is on a reciprocal track presents a "worst case" for the helicopter with the decoupled flight path and attitude controller. This is because it then has less time to acquire and track the target before the relative positions of the two aircraft are such that the manoeuvre is outwith the pitch attitude limits set by the structural or aerodynamic constraints defined in section 5:2. The combination of target range and height in this simulation is such that the pitch attitude perturbation for acquisition at t=0 is not outwith these limits.

The target was assumed to be acquired and thereafter tracked, when the projection of the helicopter's x-axis lay within a rectangular box

about the target. It was assumed that this box was perpendicular to the plane of the flat earth, and with dimensions defined by the rotor diameter and overall height of a medium helicopter, figure 5:34. The location of the projection of the helicopter's x-axis is easily calculated knowing the pitch and yaw angles, and the relative location of helicopter and target. The simulations were run using the digital computer program MIMESIS, ref. [54]. State and position time histories were calculated, allowing reconstruction of the helicopter's trajectory. Calculation of the control angles also allowed some assessment to be made of the required level of control authority, and the rotor hub moment.

The desired attitude angles could not be expressed as continuous functions of time because some account had to be taken of any errors, however small, in the helicopter's desired speed and position during the manoeuvre. Given the helicopter and target's relative location at any time t, the desired attitude angle was calculated from the equation

$$\theta_d = \text{atan}\left[\frac{50 - z_e}{1000 - x_e - V_{ftg}.t}\right] \quad \text{----- (5:13)}$$

The commanded change in attitude was built up as a series of step inputs, whose magnitude at any time t was given by equation 5:13. The sequence of step inputs were calculated and commanded 1000 times per second and as a result the input was essentially continuous. The numerator in the above expression is the height difference between the helicopter and target at time t, while the denominator is the distance between the helicopter and the vertical projection of the target on the horizontal plane containing the helicopter.

5:4.1 Simulation Results

The results of the target tracking simulations are divided into three separate groups that are considered separately; firstly the attitude tracking. Figure 5:35 shows the pitch attitude perturbation necessary to acquire and track the target, and it can be seen that the limiting pitch attitude perturbation, 6.5 degrees, is reached after 4.25 seconds, thus defining the manoeuvre time. The target is acquired in 0.83s, and thereafter tracked. The pitch and yaw attitude error time histories are shown in figure 5:36, demonstrating that the two degrees of freedom are to all intents and purposes decoupled. The attitude errors are presented in a different form in the crossplot of figure 5:37, which illustrates the location of the projection of the x-axis relative to the box defining the target.

The helicopter's flight path during the manoeuvre is expressed in terms of speed and position in figures 5:38 and 5:39 respectively. An insignificant change in speed accompanies the acquisition and tracking of the target, important if it is desired to maintain kinetic energy. The helicopter's deviation in desired track is given in figure 5:39. The maximum height perturbation is a loss of only 0.2m, occuring at the end of the manoeuvre, as does the peak lateral displacement, reaching a similarly insignificant 0.15m

The control position time histories are given in figure 5:40 together with the resulting rotor hub moment. The tailplane element requires full authority, deflecting to about 12.5° leading edge down at the end of the manoeuvre. The magnitude of the perturbation of the main

rotor controls demonstrates the considerable coupling between the degrees of freedom in the raw helicopter that the FCS is compensating for. The collective pitch is reduced by about 0.2° from trim, although there is an initial step to 0.6° caused by the feedforward matrix commanding a change in flight path. The longitudinal cyclic moves forwards over 3° and the lateral cyclic pitch perturbation is almost 0.6° - there is considerable pitch/roll cross-coupling with the stiff-flapwise rotor configuration. Tail rotor collective pitch perturbation is only -0.08°. As expected there is a large change in the rotor hub moment during this manoeuvre, reaching a peak of 30 kNm at the end of the manoeuvre ie. where the attitude perturbation is greatest.

The conventional helicopter could also acquire and track targets, but it must do so by using the main rotor. The result of this is that some change in flight path must also occur. This was quantified by carrying out a simulation of the same helicopter as that used above, but with an FCS that retains the traditional pattern of control - thrust by means of collective, and flight path by attitude, appendix 3. With such a pattern of control, the target can be acquired and tracked with two consequences for flight path: firstly, the desired attitude commands could be made using the rotor, and with constant collective setting. The aim in this might be attempt to keep as much kinetic energy as possible for manoeuvring - the helicopter will however climb quite quickly. Secondly, the collective and therefore lift could be reduced during the manoeuvre, in an attempt to minimise the gain in height. The former of the two options was simulated here, and the results are given in figures 5:41, 5:42 and 5:43. The performance in acquiring and tracking the target is similar to that of the helicopter with the decoupled controller; the

change in flight path is not however, with this helicopter losing about 5 knots in forward speed and gaining 13m in height, both within 5 sec.

5:5 Discussion

It has been shown that a helicopter of conventional configuration can be modified with a suitably sized horizontal tailplane and FCS that will allow the fuselage pitch attitude to be decoupled from the flight path, within identified structural and aerodynamic constraints. Unfortunately this novel mode of control poses more questions than any that it answers, as the magnitude of the benefits achieved are specific to the task scenario simulated. The significance of what has been achieved can be more generally quantified if one considers how the speed/attitude relationship of the conventionally configured helicopter is used. Pilots can fly fairly accurately from one speed to another at a given height, by flying at an attitude they know from experience the helicopter will adopt at the new speed. For the Lynx helicopter, the speed/attitude relationship was shown in figure 2:6, and it can be seen that a change in attitude of only 3.5° nose-up at 100 knots would eventually slow the helicopter to 60 knots. In the simulations carried out for this study, an attitude change of 6.5° nose-up at 100 knots results in almost no change in speed. The tailplane and FCS therefore is very effective at forcing the helicopter to do something that, for its configuration, is traditionally impossible and quite unnatural.

Within the context of the simulations presented the decoupled flight path and attitude mode of control offers significant benefits. The alternative, more traditional mode of control permits the helicopter to

perform the same tracking task, but with some change in speed and flight path - the consequences of breaking concealment in an environment that demands NOE, to the extent of 13m over anything up to 5 seconds, could be fatal. In addition, thereafter the helicopter would be continuing the manoeuvre having lost, and indeed continuing to lose, a considerable amount of kinetic energy. By comparison, the helicopter with the decoupled flight path and attitude controller would have lost an insignificant amount of kinetic energy and concealment up to the same point. Beyond the point where the limiting pitch attitude precludes futher tracking of the target independently of the flight path, the helicopter would have to manoeuvre in space to continue tracking. Even so, it would only be starting to lose energy and concealment, and thus has retained for the first 4-5 seconds of the manoeuvre, the advantages it sought in operating NOE.

The synthesised FCS requires high gain in the feedback element, significantly affecting the magnitudes of the eigenvalues representing the rigid-body modes of the helicopter. Higher gain, for faster response, would almost certainly require consideration of rotor dynamics. However for the purposes of demonstrating the benefits of this mode of control, the resulting FCS is adequate as it provides the required speed of response while largely eliminating coupling between the degrees of freedom. The three-element structure of the FCS is largely a result of the fact that the feedback matrix synthesis technique did not allow a quantitative measure of coupling to be specified. The amount of decoupling which results is partly due to the use of a precompensated B-matrix and partly to the fact that the response characteristics of the degrees of freedom (over which there is a direct influence through the performance

index J) are sufficiently fast (or well enough damped) for their response to disturbances other than commanded changes, to be small. More sophisticated means of obtaining a system regulator, such as those under investigation, ref. [49], allow specification of the stability, speed of response and coupling through desired assignment of both eigenvalues *and* eigenvectors. Use of such a technique could therefore obviate the need for a precompensated B-matrix, certainly as part of the feedback element, and therefore change the structure of the closed-loop system, figure 5:6. It is therefore in no sense definitive of that required for this mode of control. Nonetheless the resulting FCS can be regarded as *representative* of that required to obtain the reponse characteristics of the helicopter/FCS combination simulated here. It is merely an algorithm to move the controls in the desired manner, and any other FCS that will give similar response characteristics would have to move the controls in a similar fashion. Therefore there are features of this, and by deduction any other FCS that will implement this mode of control that indicate the need for ACT: firstly, the relatively high gain significantly modifes the helicopter's dynamics; secondly the sophistication of the FCS and its variability with speed; and thirdly the high level of authority required - and not just of the tailplane element. As was demonstrated, flying the decoupled manoeuvre simulated resulted in movement of the rotor controls that are in fact close to the authority limits of the current Lynx ASE/CAC system. Further demands on the rotor controls, eg. to change the flight path or suppress gust-induced response, would be likely to more than saturate a limited authority system.

Using the horizontal tailplane as a control on the conventionally configured helicopter allows decoupling of the three longitudinal degrees

of freedom as the number of controls is increased to three. However it is by no means the panacea for control of the helicopter - thrust compounding would also add the necessary extra control and change the control strategies that a decoupled flight path and attitude mode would require. Speed would be controlled by using thrust, and pitch attitude by the longitudinal cyclic pitch; such a control strategy would in fact have benefits over that implemented in this investigation. Firstly, pitching moment per unit longitudinal cyclic is almost insensitive to speed, allowing independent control of the attitude *throughout* the speed range; by comparison, the tailplane moment per unit control diminishes as speed is reduced, requiring larger control inputs for a given desired attitude. Secondly, the rotor attitude would no longer need to be related to the desired flight path, (this is why disc tilt through cyclic can be used to pitch the fuselage) as engine thrust rather than the longitudinal component of the thrust vector would be used to control speed. As a result large hub moments would be avoided and bigger changes in attitude achievable.

5:6 Conclusions

The addition of a moveable horizontal tailplane to the conventionally configured single main and tail rotor helicopter allows the three longitudinal degrees of freedom to be decoupled, within structural and aerodynamic constraints.

Synthesis of an adequate FCS allowed full advantage to be taken of the extra control, conferring on the helicopter the ability to fly a novel and unconventional manoeuvre. Computer simulations of the helicopter/FCS

combination in a tracking manoeuvre showed that targets could be acquired and tracked with an insignificant change in the helicopter's velocity vector (flight path). By comparison, a helicopter/FCS combination that retained the traditional pattern of control, loses considerable forward speed and gains some height in performing the same manoeuvre. In the context of operations in an NOE environment, there is therefore some tactical benefit to be achieved through implementing a decoupled flight path and attitude controller.

The helicopter FCS needed to give the required level of performance, in terms of speed of response and the amount of coupling, requires relatively high gain that significantly modifies the open-loop rigid-body dynamics. The rotor modes may have to be taken into account if faster response or a greater degree of decoupling is required. The resulting FCS demands ACT because of the high level of control authority required, the relative sophistication of the controller and its variability with speed.

The decoupled flight path and attitude mode of control using the horizontal tailplane, could be more generally applicable to the helicopter with a flight path or velocity vector demand type of FCS. However the use of thrust compounding would also add the extra control necessary to decouple the longitudinal degrees of freedom. With such a configuration, the control strategies implemented would be different to those simulated here, and could render the applicability of the horizontal tailplane to the overall scheme of control redundant.

This novel application of the horizontal tailplane is reflected in the design philosophy of sizing the tailplane, which marks a departure

from the tradition of sizing it from considerations of dynamic stability. Main rotor stiffness, the required range of pitch attitude and the minimum speed at which the decoupled flight path and attitude mode is required determines the size of the tailplane.

Chapter 6

A General Discussion and Summary

The results of chapters 4 and 5 indicate that the horizontal tailplane offers some flight mechanics benefits if actively controlled. These benefits could not have been obtained if the tailplane were either pilot controlled; geared, for example to the longitudinal cyclic pitch; or part of a conventional SAS. This is because it requires full authority and deflection is a function of many variables, including speed. In addition, the tailplane is an integrated element of the FCS, with a command function to fulfil, rather than simply stabilisation. This would be impossible to obtain with conventional cockpit control setup. The simplification possible with ACT in the area of control inceptors (including helmet-mounted sights), is likely to overcome the limitations of adding this extra control.

Of course the aim of research in a topic such as this is to investigate firstly, whether or not the tailplane can actually be used to fulfil the functions desired of it; and secondly, given that it can, do the results obtained suggest that the benefits are likely to be achieved in more general situations. If the answer to the latter is "yes", then it will point way to future work in this area.

The influence of the active tailplane on helicopter agility that is limited by rotor hub moment can be considered significant, as given popup manoeuvres can be flown up to 7% faster than the 100 knots reference

speed; alternatively, tighter paths in space can be flown at 100 knots, to the extent of reducing the distance over which the manoeuvre is flown, and this reduces the time taken for the task by about 10%. As described in chapter 4, the control law implemented to quantify these benefits is a compromise, but it does reduce the peak, manoeuvre-limiting hub moment significantly, allowing enhanced agility which is quantified above. It was demonstrated that the initial postulation of the tailplane pitching moment being correlated with hub moment was wrong. This is unfortunate as the control law implemented was based on applying tailplane pitching moment proportional to the contributions of each rotor control and the pitch rate, to the longitudinal component of the hub moment. However, the fact that the control law was a compromise prompted a search for the true mechanism by which the tailplane affects the hub moment. This in fact was so simple that is should have been clear from the start - for a given flight path, the rotor disc angle of attack time history is the same irrespective of configuration; the tailplane pitching moment results in the helicopter flying a given manoeuvre with a slightly different attitude relative to the fixed tailplane case, and so disc flapping relative to the fuselage and therefore the hub moment, is different. Since the benefit of having an active tailplane in this application is significant, further work should be undertaken to synthesis a control law (not based on functions of the rotor controls) that will reduce the hub moment everywhere during a given manoeuvre, and not just at the limiting peak. A law that reduces hub moment in this way is likely not to be manoeuvre-specific, and therefore will be more generally applicable to enhancing agility in a wider range of manoeuvres. It is recommended that such a control law should be based on functions of pitch attitude, given the mechanism by which the tailplane modifies the hub moment.

The other application of an active horizontal tailplane investigated was that of providing pitch attitude control independently of the flight path. This is possible in theory because addition of a controllable tailplane gives three independent controls for the three longitudinal degrees of freedom. However, the range of attitude achievable is limited principally by the main rotor hub moment, and for the stiff-flapwise rotor configuration, a sizeable tailplane is required in order that the fuselage can be pitched to the hub moment limit without stalling. Otherwise tailplane stall becomes another limitation on the range of pitch attitude that can be obtained independently of the flight path. The advantages to be obtained in a target acquisition manoeuvre of having a decoupled flight path and attitude mode of control have been demonstrated by simulation. Compared with such a helicopter, that with a control system offering the more conventional pattern of control will lose speed and gain height fairly quickly, when flying the manoeuvre that was simulated. Looking ahead, simulations of different tracking manoeuvres eg. in turning flight, climbing/descending, sideslipping etc. would help to more generally quantify the applicability of this mode of control. If the results of such simulations gave good results, the applicability of the mode from the pilot's point of view, would have to be investigated, marking the next stage in study of such a mode of control.

Simply demonstrating decoupled flight path and attitude control does however allow one to say that it will have a positive benefit in two applications that were not simulated, and therefore where the benefits were not quantified. Firstly, it solves the problem with the conventional helicopter in manoeuvring flight, of reconciling attitude, speed and trajectory demands, only two of which can be controlled independently.

With a future *conventional* yet actively controlled helicopter there may be a case for the decoupled flight path and attitude mode of control, simply because it would be straightforwards to implement in a FCS that is by nature programmable and capable of full authority control; because of this, there is no flights mechanics reason for the compromise in longitudinal control to remain. Secondly, the large hub moments that could occur when demanding changes in speed could be reduced, in fact to zero, by using the tailplane to pitch the fuselage at the same rate as the rotor. It should be noted however, that the thrust compounded helicopter, as mentioned in chapter 5, could obviate any need for the tailplane in this mode of control.

It can be concluded that the actively controlled horizontal tailplane on a future conventionally configured helicopter offers, in the isolation of this dissertation, significant benefits. Agility can be enhanced, and an unconventional mode of control implemented that allows control of the body attitude independently of the flight path. As well as giving the ability to acquire and track targets, without changing speed or trajectory such a mode of control would go some way to mitigating the traditional speed/climb/attitude compromise in controlling the single main and tail rotor helicopter. The benefits can only be achieved with ACT, as the control algorithms are sophisticated, require full authority, and the kind of cockpit setup that only ACT can provide. The tailplane in a future helicopter would become a fully integrated element of the FCS, taking on command functions that are an element of the overall controllability and manoeuvrability of the helicopter. This is not the case of current application of tailplanes on helicopters.

References

1). A. Gessow, K.b. Amer, An Introduction to the Physical Aspects of Helicopter Stability, NACA TN 1982, 1949.

2). A.R.S. Bramwell, Helicopter Dynamics, Edward Arnold, 1976.

3). W, Johnson, Helicopter Theory, Princeton U.P., 1980.

4). G.D Padfield, A Theoretical Model of Helicopter Flight Mechanics for Application to Piloted Simulation, R.A.E. TR81048, 1981.

5). F.B. Gustafson, et al., Longitudinal Flying Qualities of Several Single-Rotor Helicopters in Forward Flight, NACA TN 1983, 1949.

6). A.R.S. Bramwell, Longitudinal Stability and Control of the Single Rotor Helicopter, R. and M. 3104, 1959.

7). H.-J. Pausder, D. Jordan, Handling Qualities Evaluation of Helicopters with Different Stability and Control Characteristics, Vertica Vol. 1, 1976.

8). T.T. Kaplita, Investigation of the Stabilator on the S-67 Aircraft, USAAMRDL Technical Report 71-55, 1971.

9). J.J. Howlett, Flight Characteristics of the NH-3A Compound Helicopter with Integrated Control Surfaces, Naval Air Systems Command, Contract N00019-67-C-0513, 1969.

10). M.L. Hester, et al., Handling Qualities Aspects of the Bell Model 222 Design and Development Program, Paper presented at the 34th Annual National Forum of the American Helicopter Society, 1978.

11). K.B. Amer, et al., Handling Qualities of Army/Hughes YAH-64 Advanced Attack Helicopter,

12). M. Sinclair, M. Morgan, An Investigation of Multi-Axis Isometric Sidearm Controllers in a Variable Stability Helicopter, N.A.E Aeronautical

Report LR - 606, 1981.

13). M. Lambert, BlackHawk, LAMPS and AAH, Flight International, Vol.113 No.3597, 1978.

14). H.K. Edenborough, K.G. Wernicke, Control and Maneuver Requirements for Armed Helicopters, Paper presented at 20th. Annual National Forum of the American Helicopter Society, 1964.

15). H.L. Kelley, R.J. Pegg, R.A. Champine, Flying Quality Factors Currently Limiting Helicopter Nap-of-the-Earth Maneuverability as Identified by Flight Investigation, NASA TN D-4931, 1968.

16). W. Steward, Operational Criteria for the Handling Qualities of Combat Helicopters, AGARD CP333, 1982.

17). M.V. Lowson, D.E.H. Balmford, Future Advanced Technology Rotorcraft, The Aeronautical Journal, 1980.

18). P. Pryse-Davies, Control Modes for a Conceptual Simulation Study of Nap of the Earth Flight in an ACT Helicopter, Westland Helicopters Advanced Control Department ACN 15/82, 1982.

19). B.N. Tomlinson, G.D. Padfield, Piloted Simulation Studies of Helicopter Agility, Vertica Vol. 4 No's 2 - 4, 1980.

20). H. - J. Bangen, et al., Investigation of a Helicopter Manoeuver Demand System, Paper presented at 2nd. European Rotorcraft and Powered Lift Aircraft Forum, 1976.

21). S. Attlfellner, W. Sardanowsky, Meeting the Maneuverability Requirements of Military Helicopters, Paper presented at 2nd. European Rotorcraft and Powered Lift Aircraft Forum, 1976.

22). H. Hohenemser, Hingeless Rotorcraft Flight Dynamics, AGARD AG197, 1973.

23). G.D. Padfield, Longitudinal Trim, Stability and Response for

Helicopters, R.A.E. Tech. Memo Structures 990, 1981.

24). Raymond S. Hansen, Toward a Better Understanding of Helicopter Stability Derivatives, Paper presented at 8th. European Rotorcraft Forum, 1982.

25). A.R.S. Bramwell, A Method for Calculating the Stability and Control Derivatives of Helicopters with Hingeless Rotors, Research Memorandum City University London Aero. 69/4, 1969.

26). H. Huber, G. Polz, Studies on Blade-to-Blade and Rotor-Fuselage-Tail Interferences, Aircraft Engineering, 1983.

27). H.H. Heyson, S. Katzoff, Induced Velocities Near a Lifting Rotor with Non-Uniform Disc Loading, NACA Rep. 1319, 1958.

28). K.W. Mangler, H.B. Squire, The Induced Velocity Field of a Rotor, R. and M. 2642, 1950.

29). A.R.S. Bramwell, The Longitudinal Stability and Control of the Tandem-Rotor Helicopter, R. and M. 3223 Part I, 1959.

30). H. Glauert, A General Theory of the Autogyro, R. and M. 1111, 1926.

31). Jane Smith, An Analysis of Helicopter Flight Mechanics Part I - Users Guide to the Software Package HELISTAB, R.A.E. Memorandum, 1984.

32). A.W. Babister, Aircraft Dynamic Stability and Response, Pergamon, 1980.

33). R.D. Milne, The Analysis of Weakly Coupled Dynamical Systems, International Journal of Control, Vol. 2, No. 2, 1965.

34). G.D. Padfield, On the Use of Approximate Models in Helicopter Flight Mechanics, Paper presented at 6th. European Rotorcraft and Powered Lift Aircraft Forum, 1980.

35). G.D. Padfield, R.W. DuVal, Applications of System Identification Methods to the Prediction of Helicopter Stability, Control and Handling

Characteristics, American Helicopter Society Specialists Meeting on Helicopter Handling Qualities, 1982.

36). P. Brotherhood, M.T. Charlton, An Assessment of Helicopter Turning Performance During Nap-of-Earth Flight, R.A.E. Tech.Memo FS(B) 534, 1984.

37). S. Houston, A.E. Caldwell, A Computer Based Study of Helicopter Agility, Including the Influence of an Active Tailplane, Paper presented at 10th. European Rotorcraft Forum, 1984.

38). H.C. Curtiss, Jr., George Price, Studies of Rotorcraft Agility and Maneeuverability, Paper presented at 10th. European Rotorcraft Forum, 1984.

39). H. - J. Pausder, K. Sanders, DFVLR Flying Qualities Research Using Operational Helicopters, Paper presented at 10th. European Rotorcraft Forum, 1984.

40). T.L. Wood, et al., Maneuver Criteria Evaluation Program, NTIS AD - 782 209, 1974.

41). H. Haverdings, A Control Model for Manoeuvring Flight for Application to a Computer-Flight-Testing Program, Vertica Vol. 7 No. 3, 1983.

42). Col.D.W. Milam, F.R, Swortzel, Automating Tactical Fighter Combat, Aerospace America, 1984.

43). R.B. Lewis II, Huey-Cobra Manoeuvring Investigation, Paper presented at 26th. Annual National Forum of the American Helicopter Society, 1968.

44). Project D-318, U.S. Army Applied Technology Laboratories, U.S. Navy Test Pilot School.

45). B. Etkin, Dynamics of Atmospheric Flight, John Wiley and Sons, Inc., 1972.

46). Numerical Algorithms Group - NAG, Minimising or Maximising a Function, NAG Mk.7, Routine E04FCF, 1981.

47). R.J. Richards, An Introduction to Dynamics and Control, Longman, 1979.

48). N. Munro, Modern Approaches to Control System Design, Peter Peregrinus, 1979.

49). D.L.K. Parry, Helicopter Modal Control, University of Glasgow, 1984 (in preparation).

50). J.E. Potter, Matrix Quadratic Solutions, J. Siam Applic. Math., Vol. 14, No. 3, 1966.

51). P.M. Brodie, Use of Advanced Control Theory as a Design Tool for Vehicle Guidance and Control.

52). G.D. Padfield, Minimum Integral Control - A Synthesis Technique, Westland Helicopters Research Paper 461, 1974.

53). R.D. Murphy, K.S. Narendra, Design of Helicopter Stabilisation Systems Using Optimal Control Theory, J. Aircraft Vol. 6, No. 2, 1969.

54). I.W. Ricketts, MIMESIS - A Continuous System Simulation Language, Ph.D. Thesis, University of Dundee, 1977.

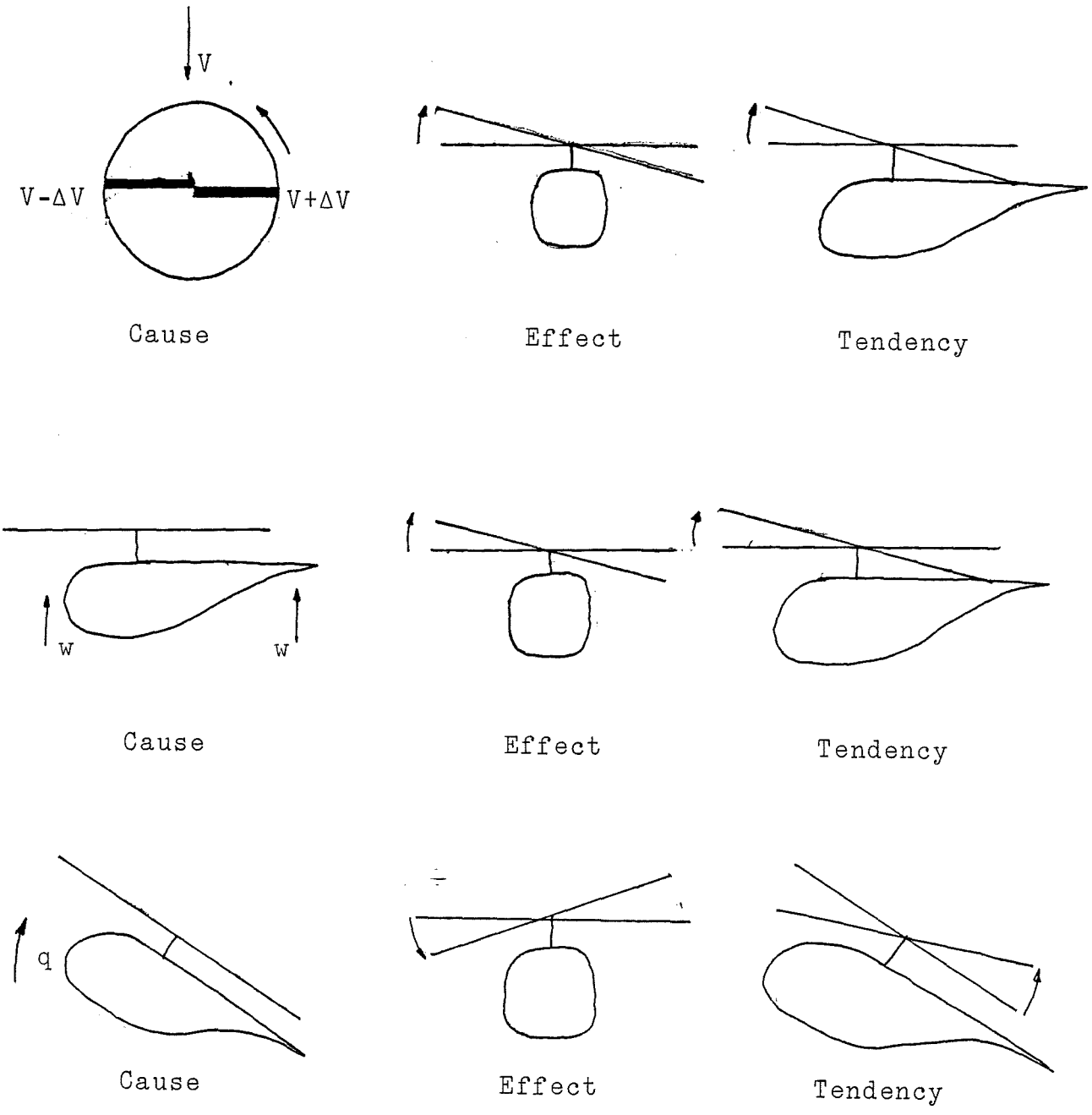

Figure 1:1 -- Simple concepts of rotor stability.

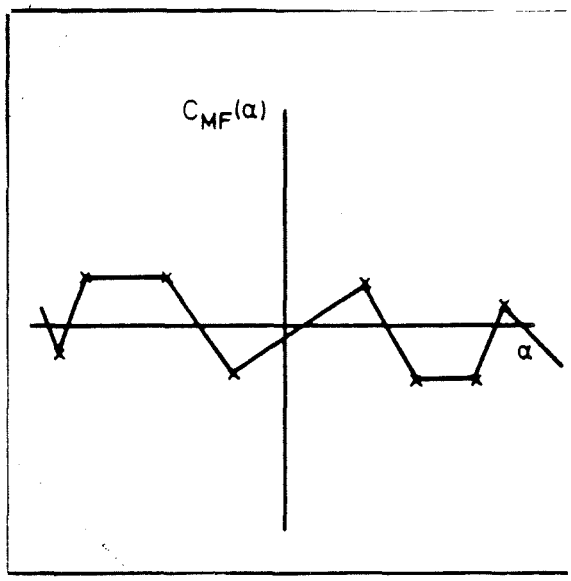

Figure 1:2 -- Typical variation of fuselage pitching moment coefficient with angle of attack; from ref. [4].

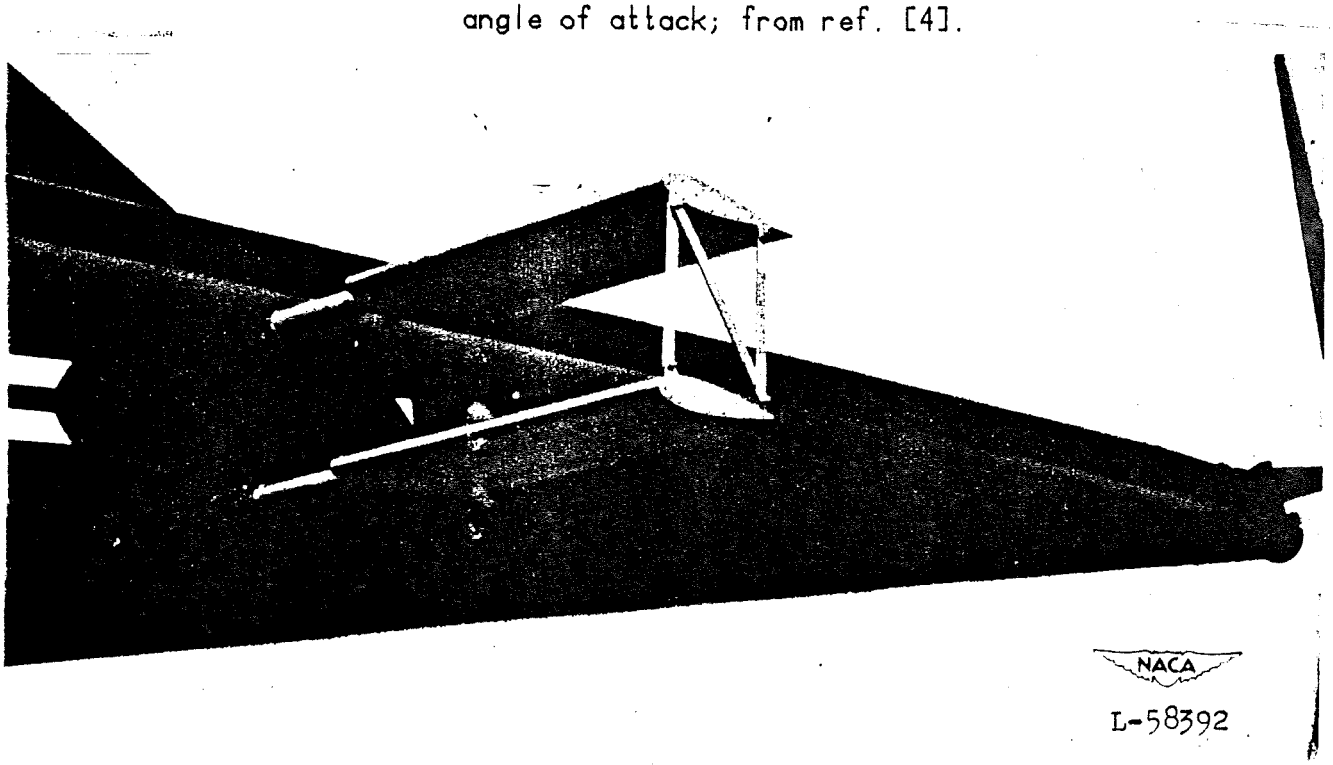

Figure 1:3 -- Experimental horizontal tailplane configuration; from ref. [5].

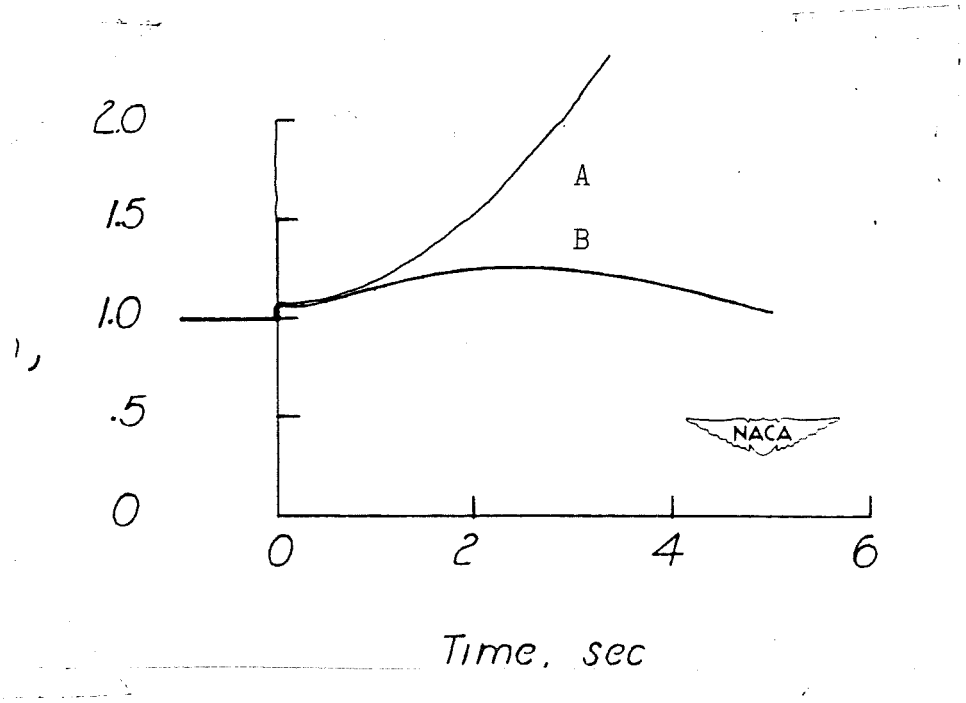

Figure 1:4 -- Normal acceleration time histories which helped development of the NACA divergence requirement; from ref. [5].

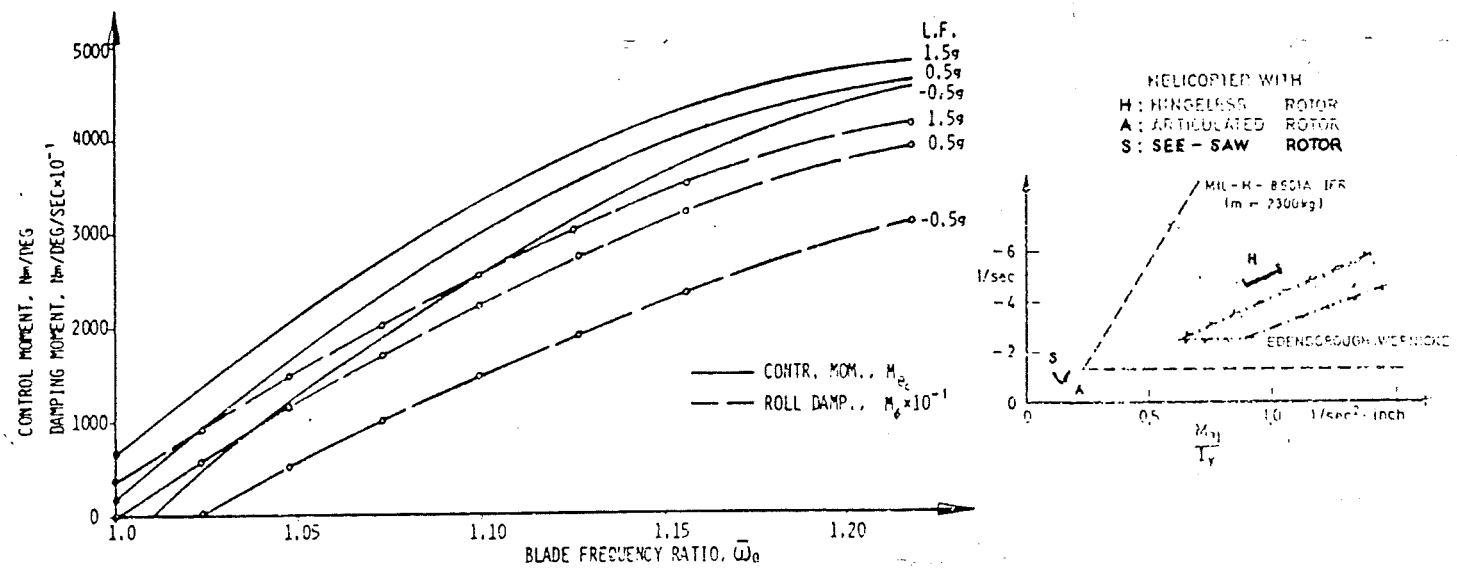

Figure 1:5 -- The effect of rotor stiffness on controllability and manoeuvre response.

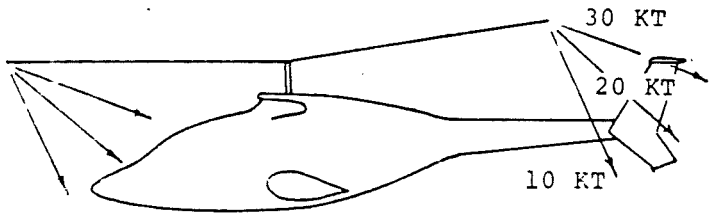

Figure 4. Main Rotor Downwash Impingement on the Horizontal Stabilizer During Acceleration from Hover.

Figure 1:6 -- Wake angle variation with speed in relation to Bell 222 tailplane location; from ref. [10].

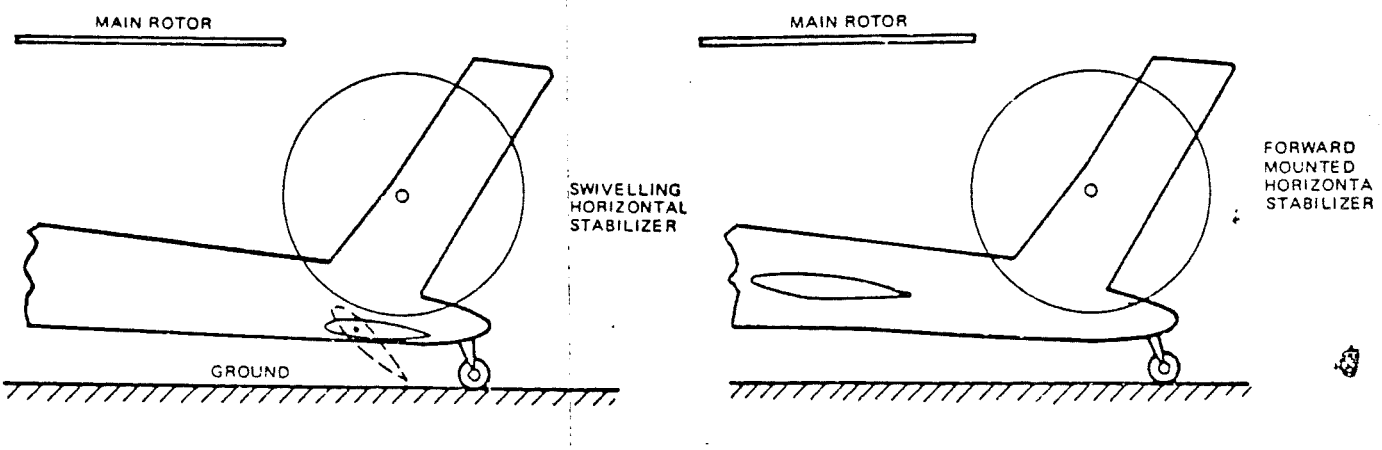

Figure 1:7 -- Solutions to the tailplane wake impingement problem, considered during YAH-64 development; from ref. [11].

Figure 1:8 -- Solution to the tailplane/wake impingement problem, in application on the UH-60 helicopter.

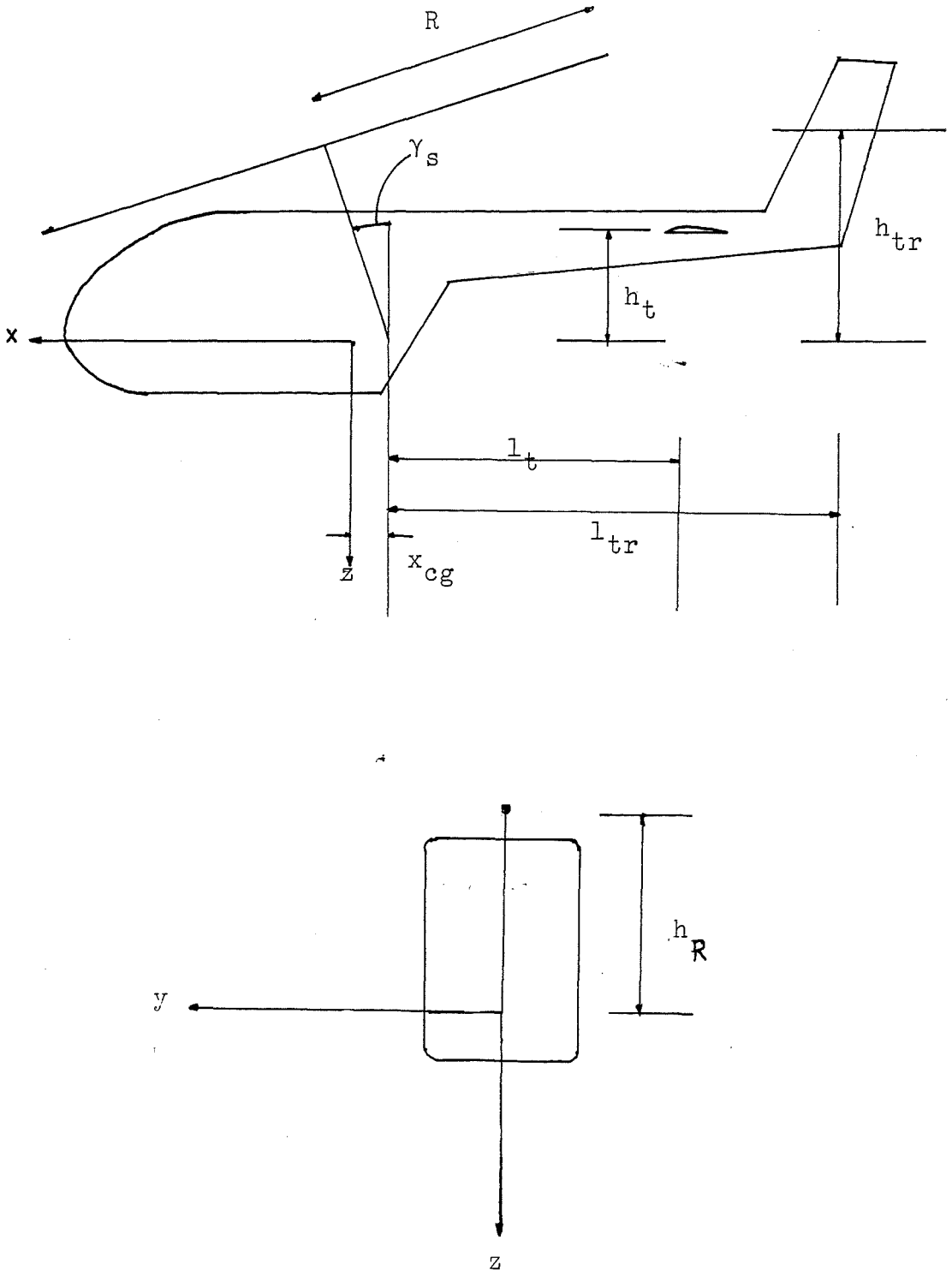

Figure 2:1 -- Helicopter geometry and the body axes system.

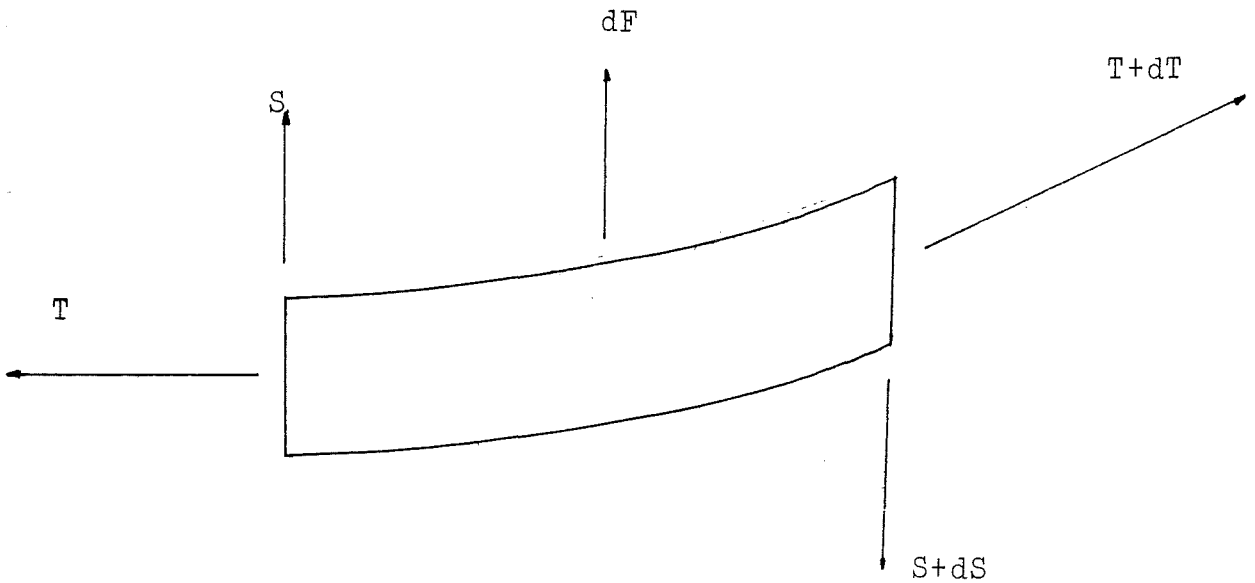

Figure 2:2a -- Forces acting on a blade element.

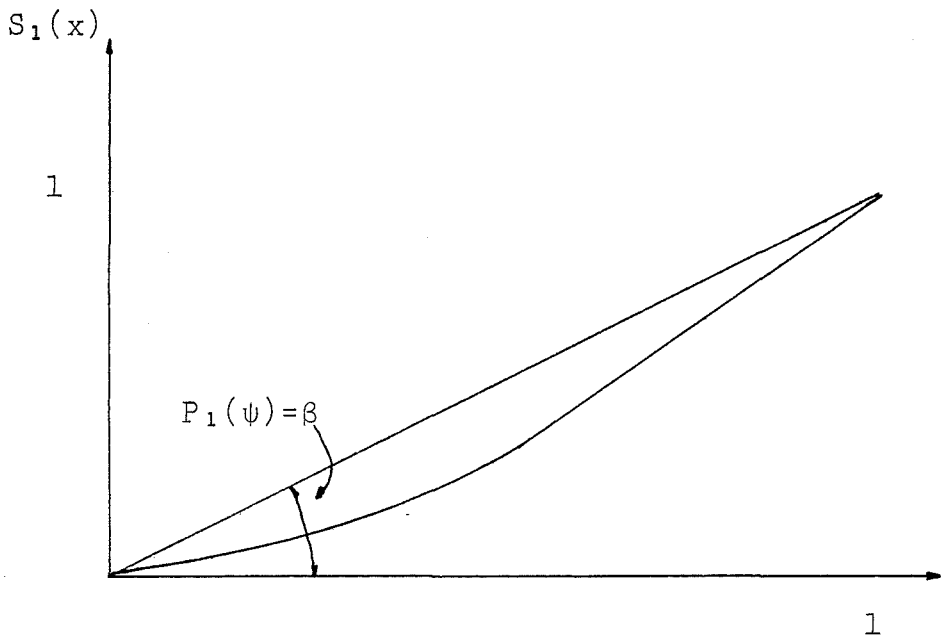

Figure 2:2b -- Interpretation of the azimuth coordinate $P_1(\psi)$.

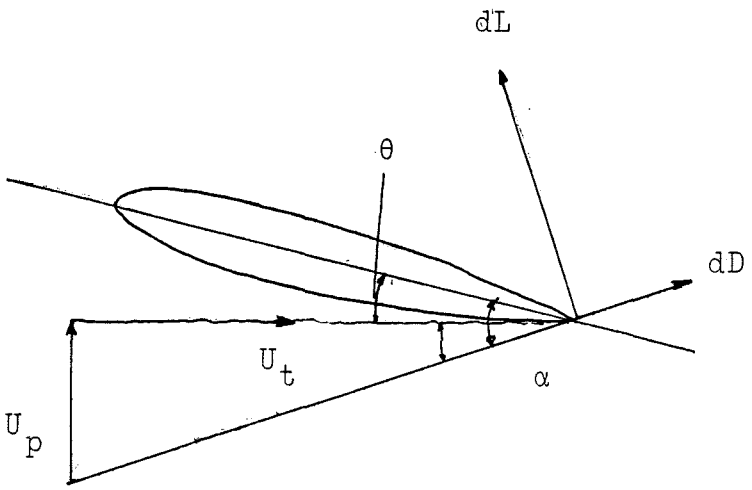

Figure 2:2c -- Velocity components "seen" by a 2-D aerofoil element of the blade.

$$S_1(x) = 0,\ 0 < x < e$$

$$S_1(x) = \frac{x - e}{1 - e},\ e < x < 1$$

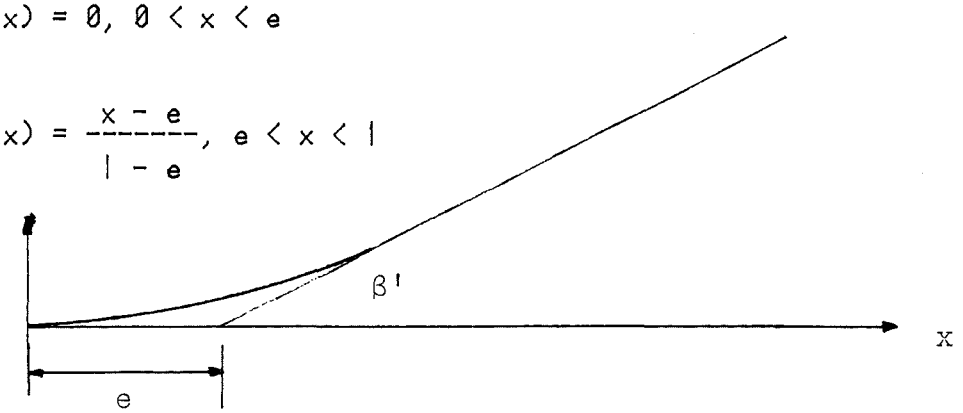

Figure 2:2d -- Bramwell's interpretation of the hingeless rotor blade as an equivalent "offset" flapping blade with the equivalent offset defined by the flapping frequency of the first flapping mode.

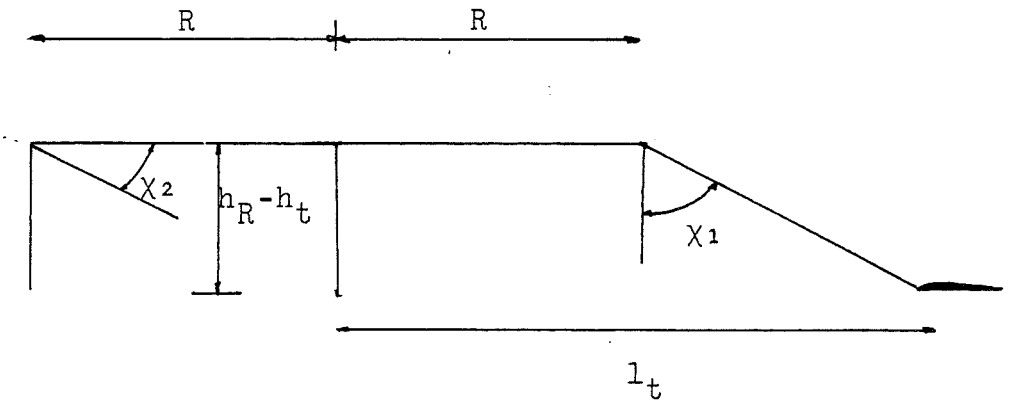

Figure 2:3 -- Schematic view of the relationship between airframe geometry and wake angle, on wake impingement with the tailplane.

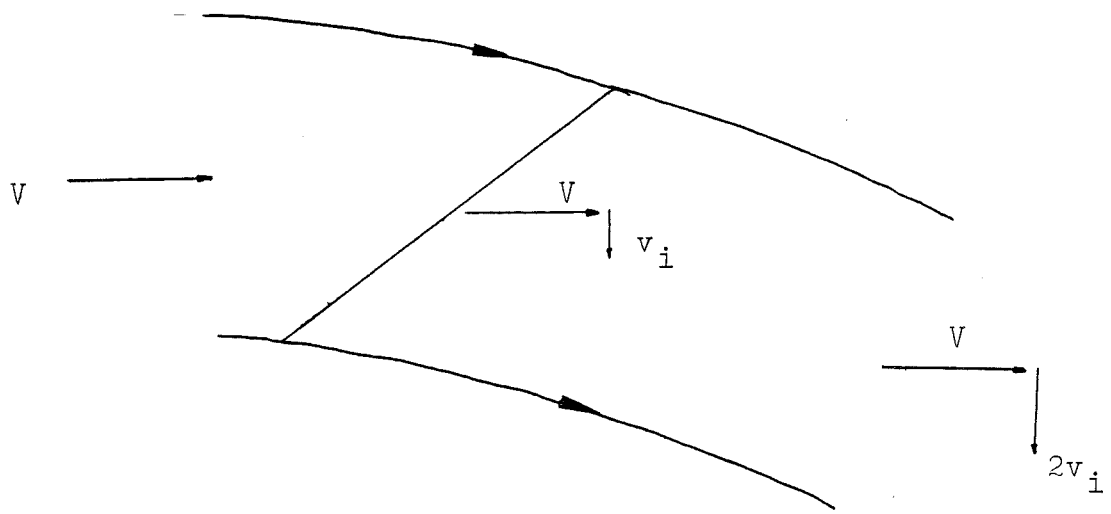

Figure 2:4 -- Schematic of Glauert's interpretation of the wake and the induced velocity component.

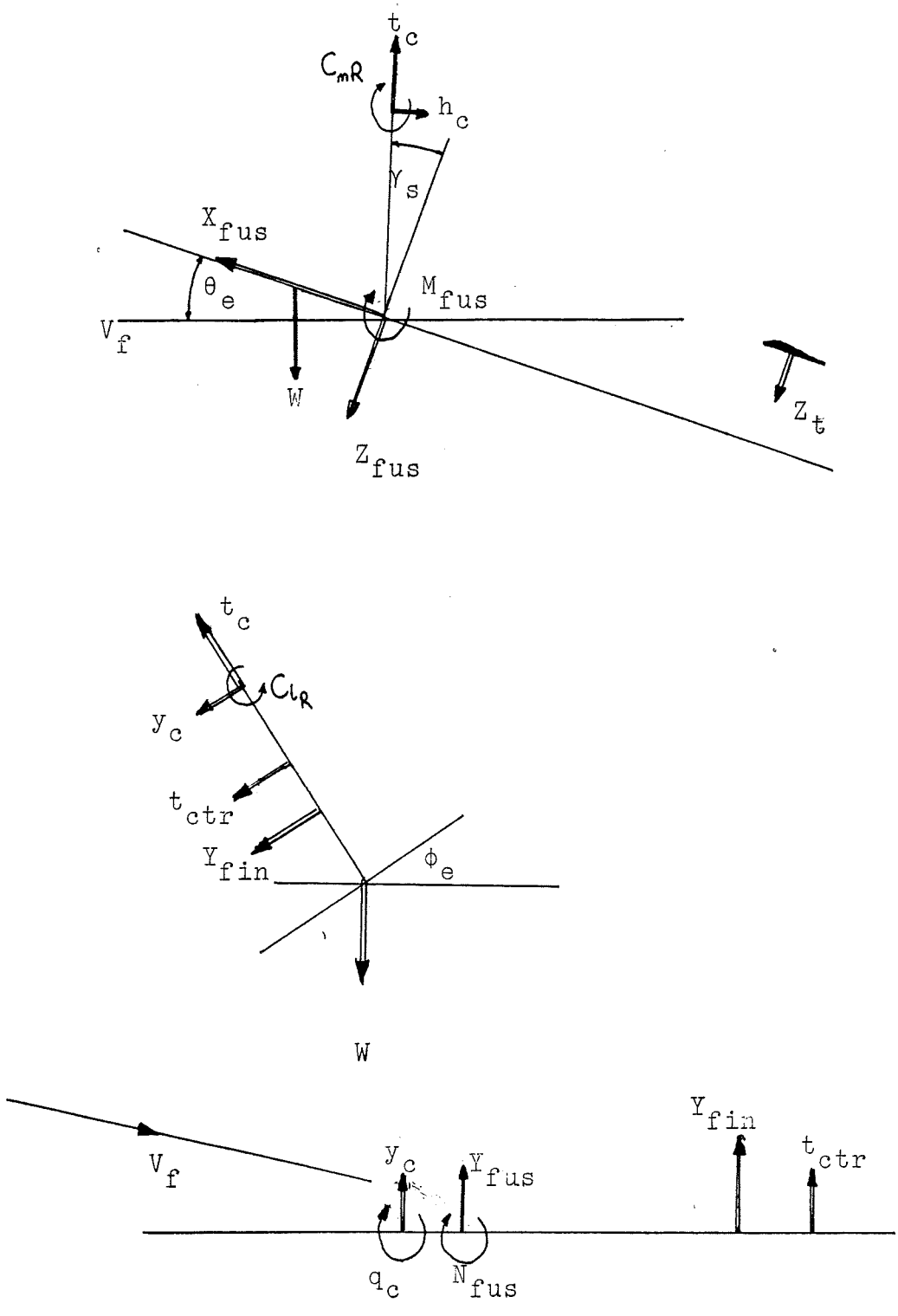

Figure 2:5 -- System of forces and moments acting on the helicopter.

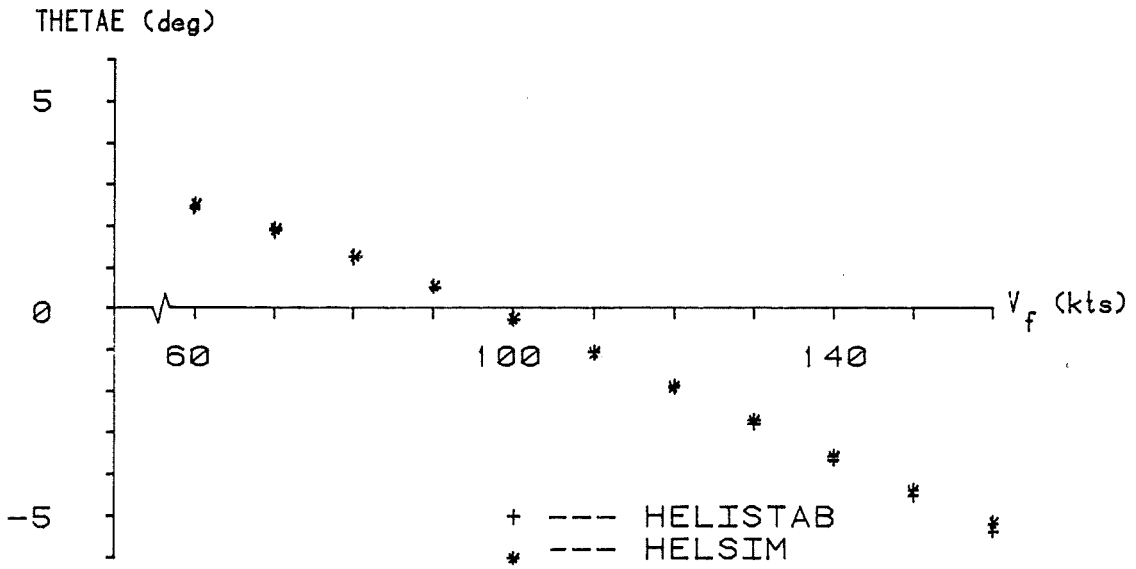

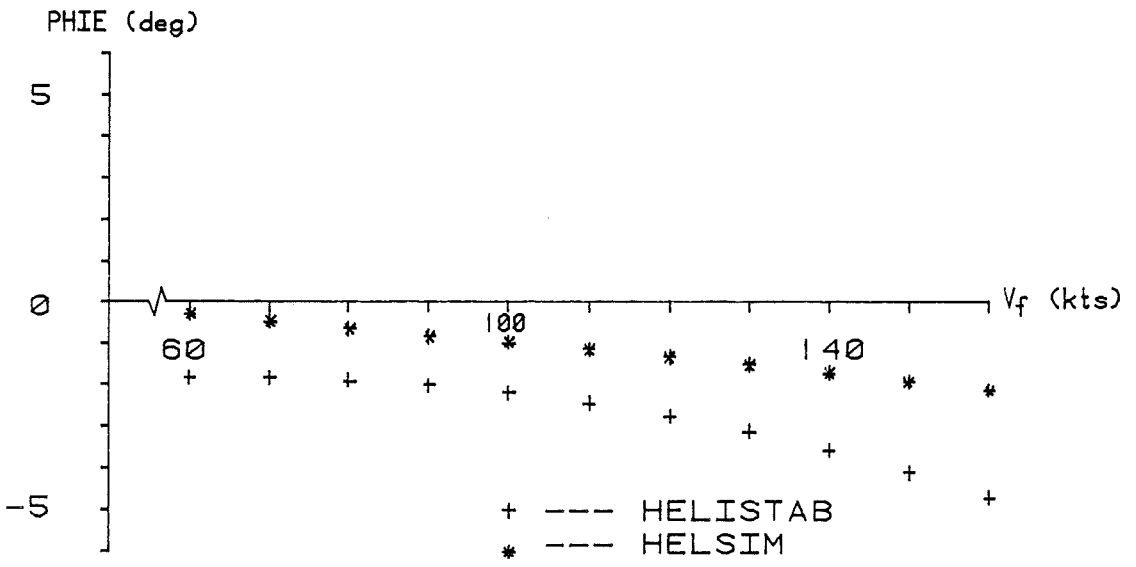

Figure 2:6 -- Comparison of trimmed body attitudes in level flight using the HELISTAB and HELSIM models.
Aircraft ---- Westland Lynx; mass=4314kg; xcg=-0.0198

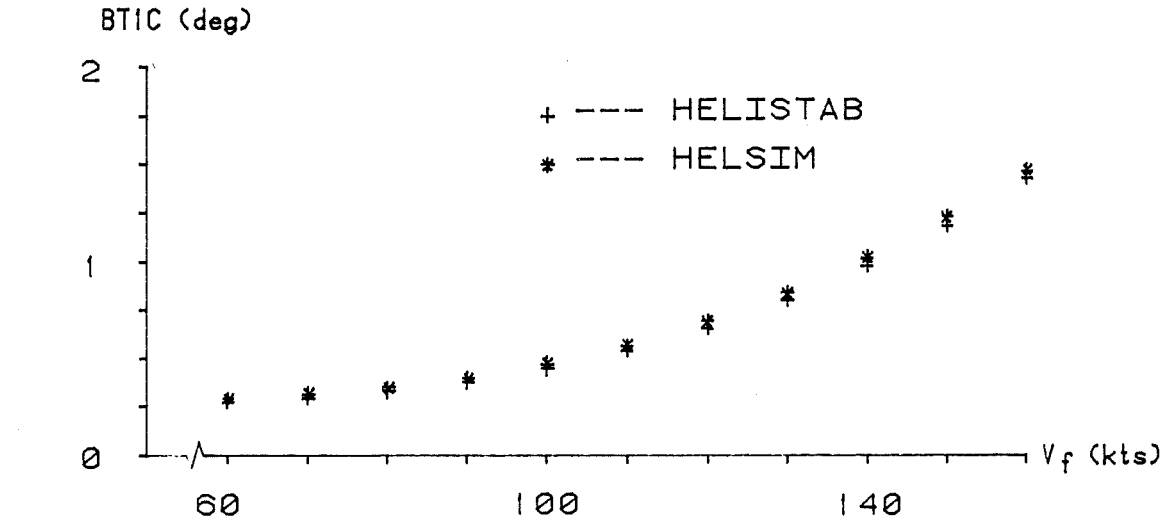

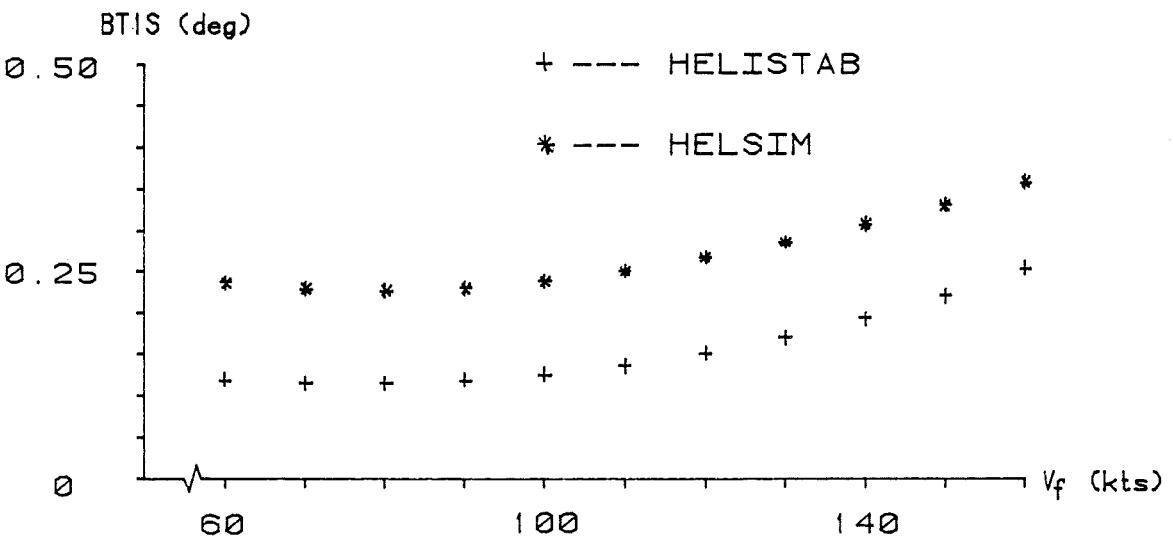

Figure 2:7 -- Comparison of trimmed flapping angles in level flight using the HELISTAB and HELSIM models.
Aircraft ---- Westland Lynx; mass=4314kg; xcg=-0.0198

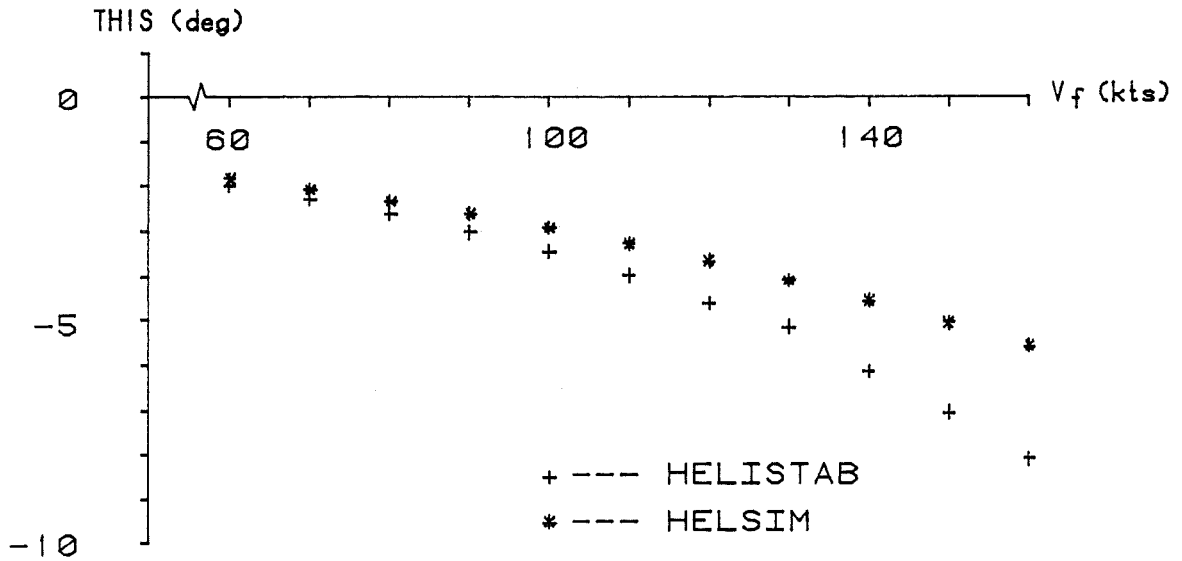

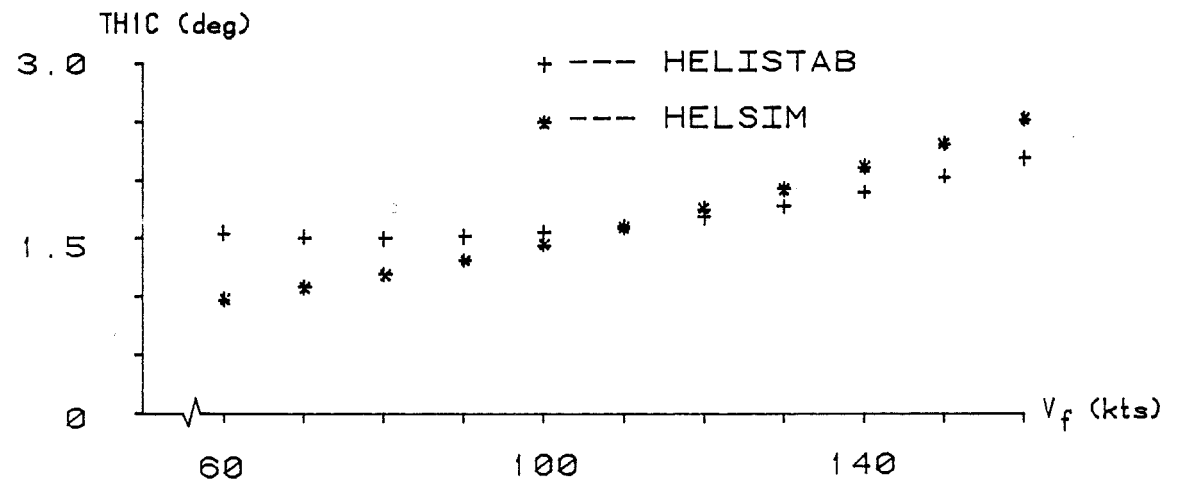

Figure 2:8 -- Comparison of trimmed cyclic pitch angles in level flight using the HELISTAB and HELSIM models.

Aircraft ---- Westland Lynx; mass=4314kg; xcg=-0.0198

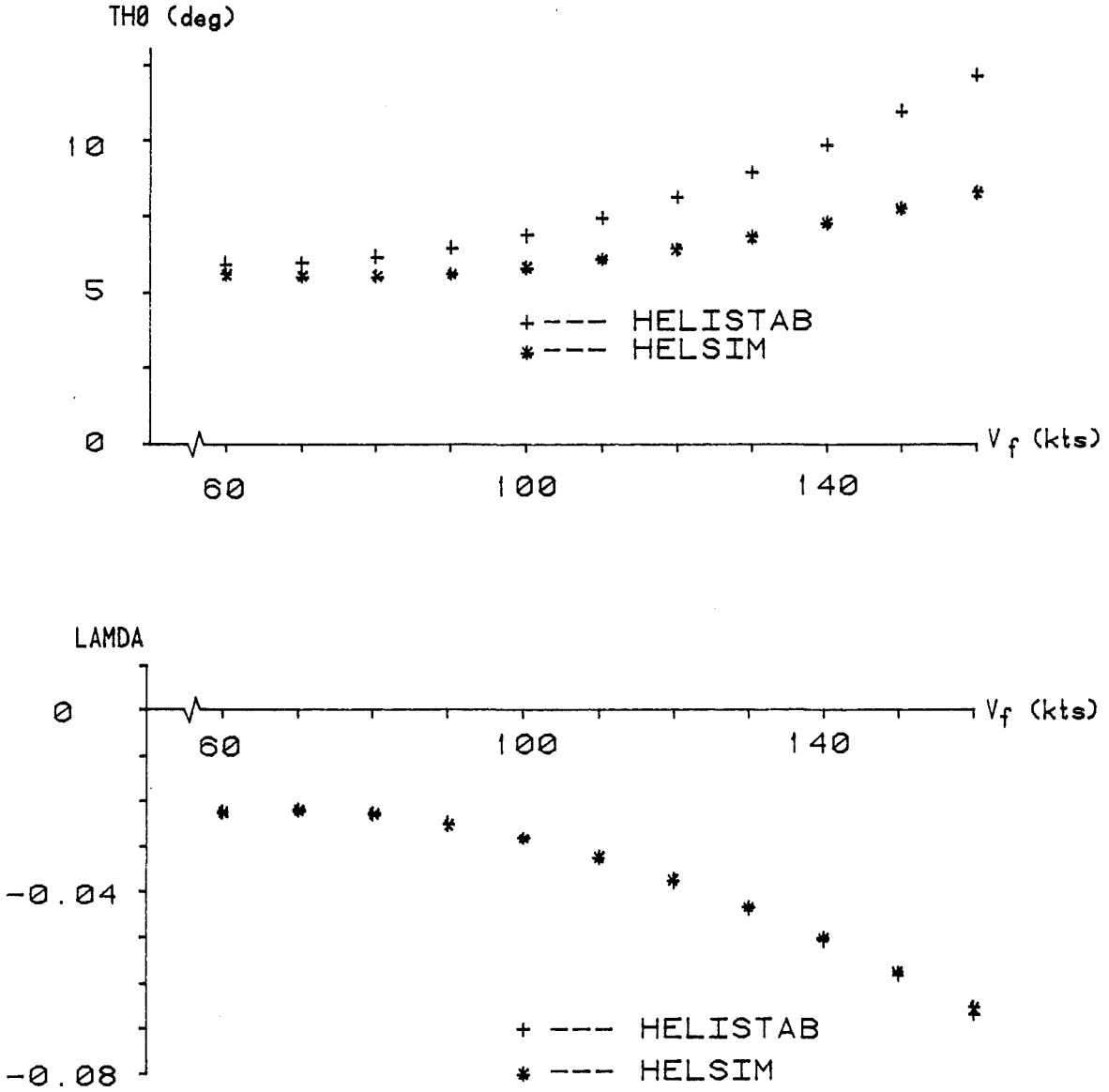

Figure 2:9 -- Comparison of trimmed collective pitch angle, and rotor inflow ratio in level flight using the HELISTAB and HELSIM models.
Aircraft ---- Westland Lynx; mass=4314kg; xcg=-0.0198

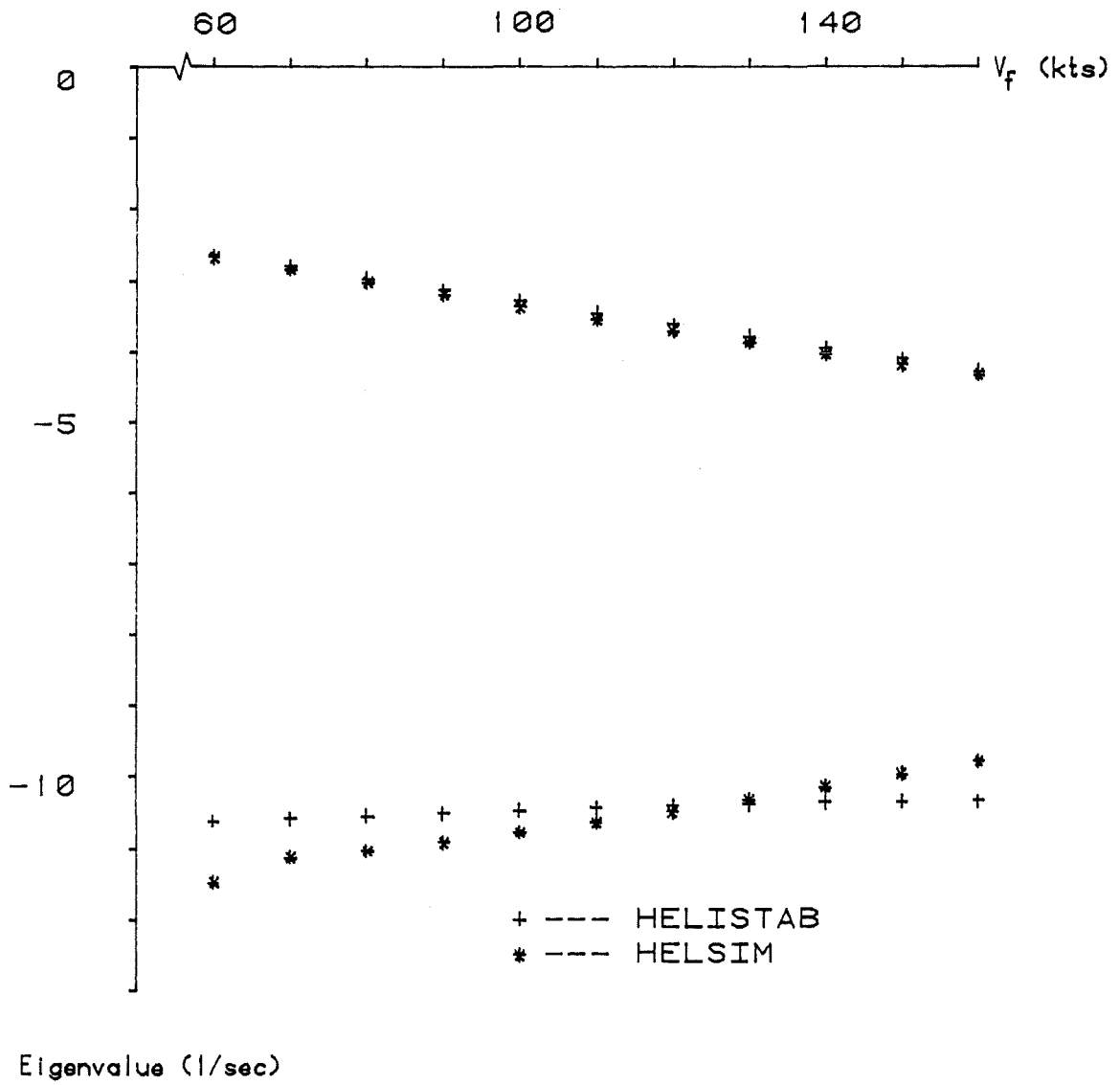

Figure 2:10 -- Comparison of rigid-body eigenvalues obtained using the model HELSIM with those from HELISTAB.
Aircraft ----- Westland Lynx; mass=4314kg; xcg=-0.0198

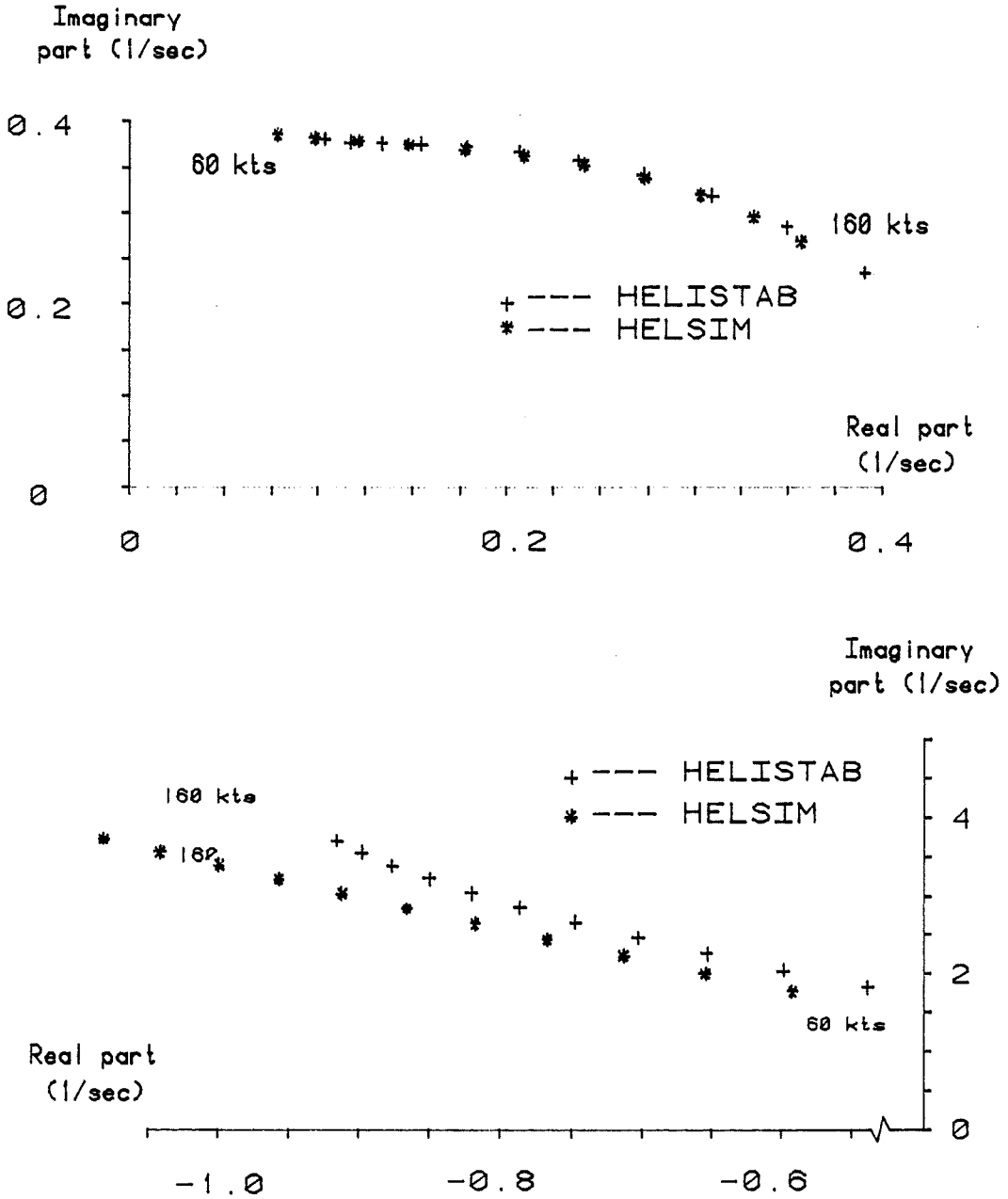

Figure 2:10 -- continued

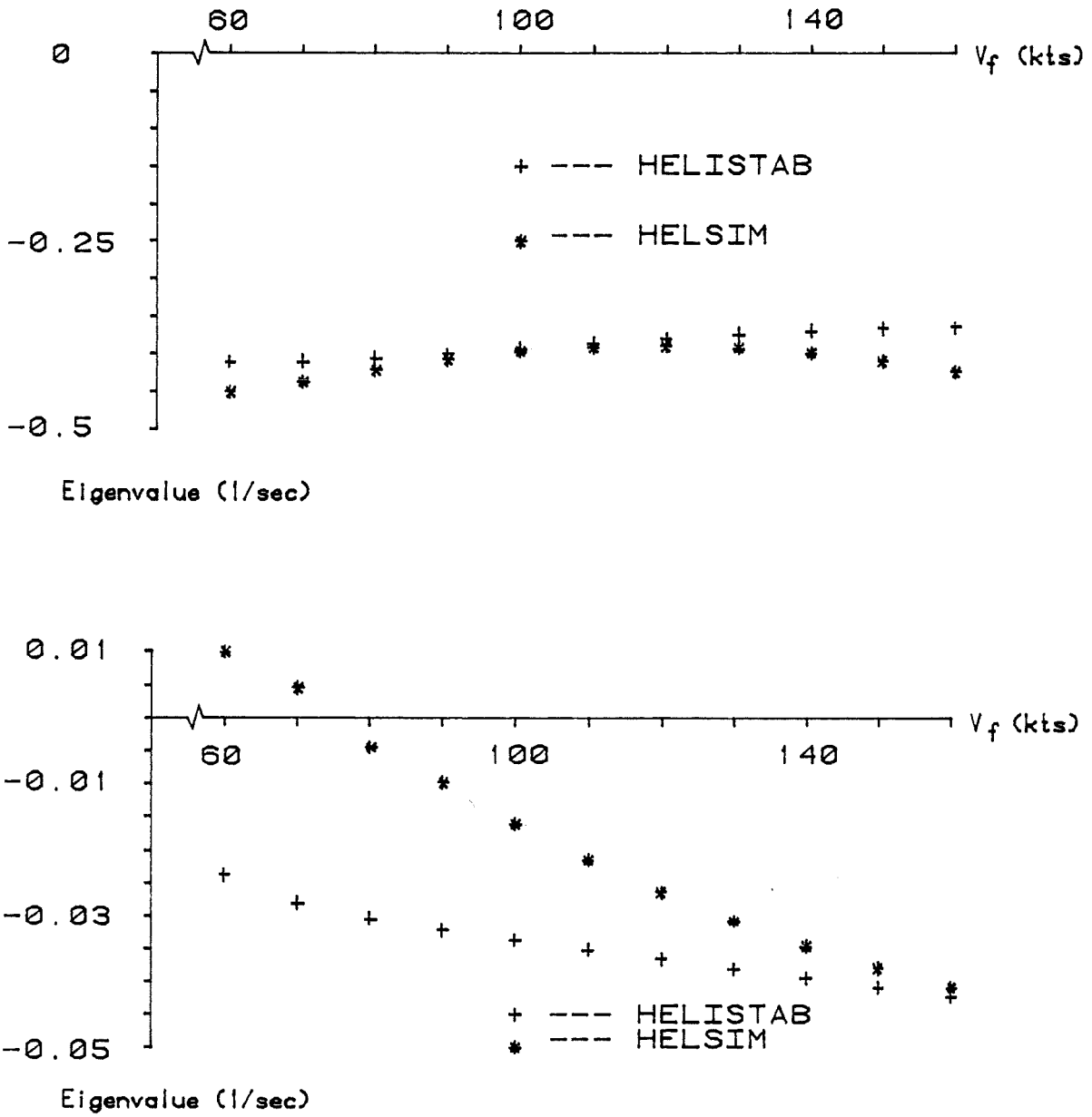

Figure 2:10 -- concluded

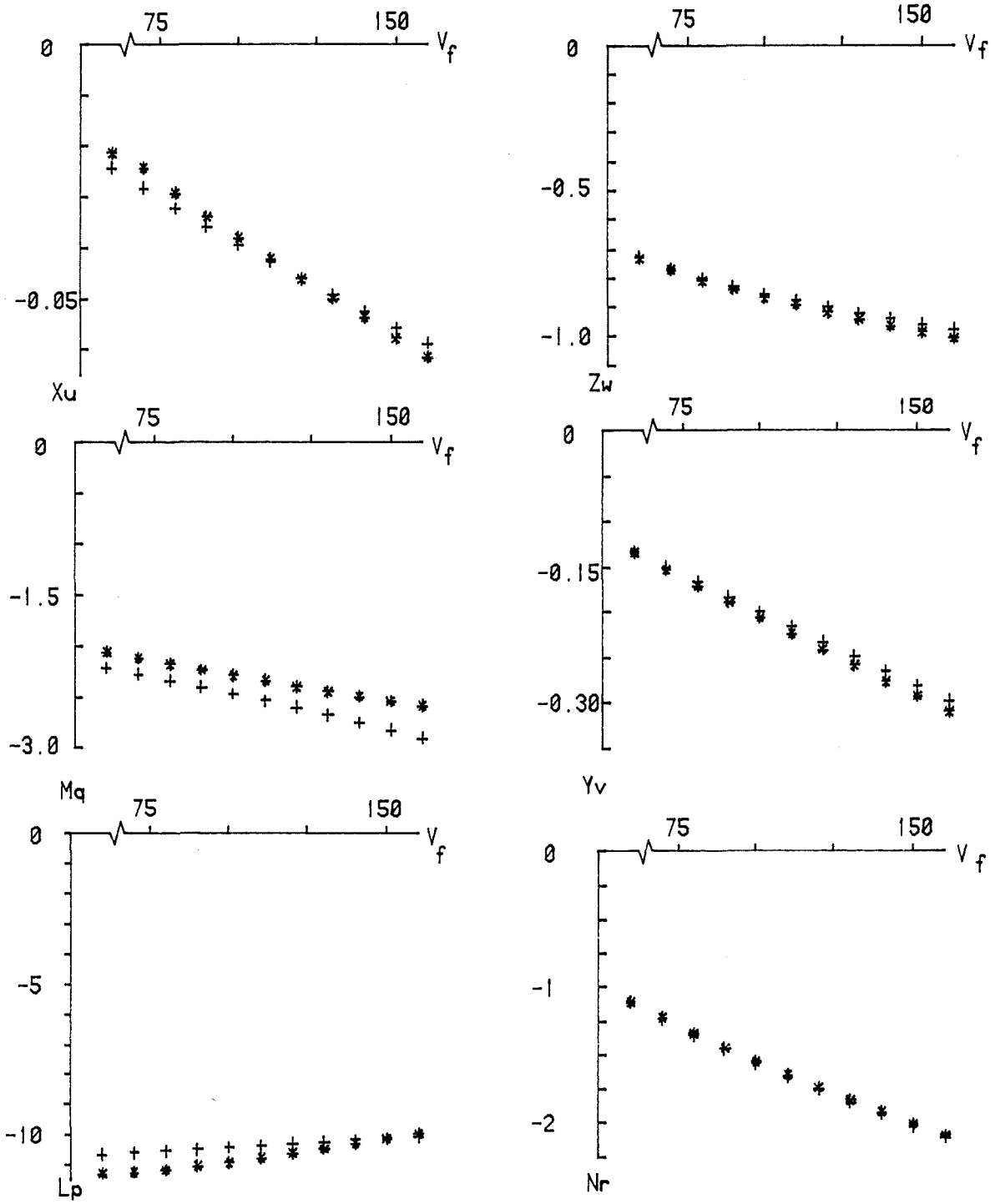

Figure 2:11 -- Comparison of "derivatives" about trim conditions of steady "level" flight using the HELISTAB and HELSIM models.

\+ -- HELISTAB

* -- HELSIM

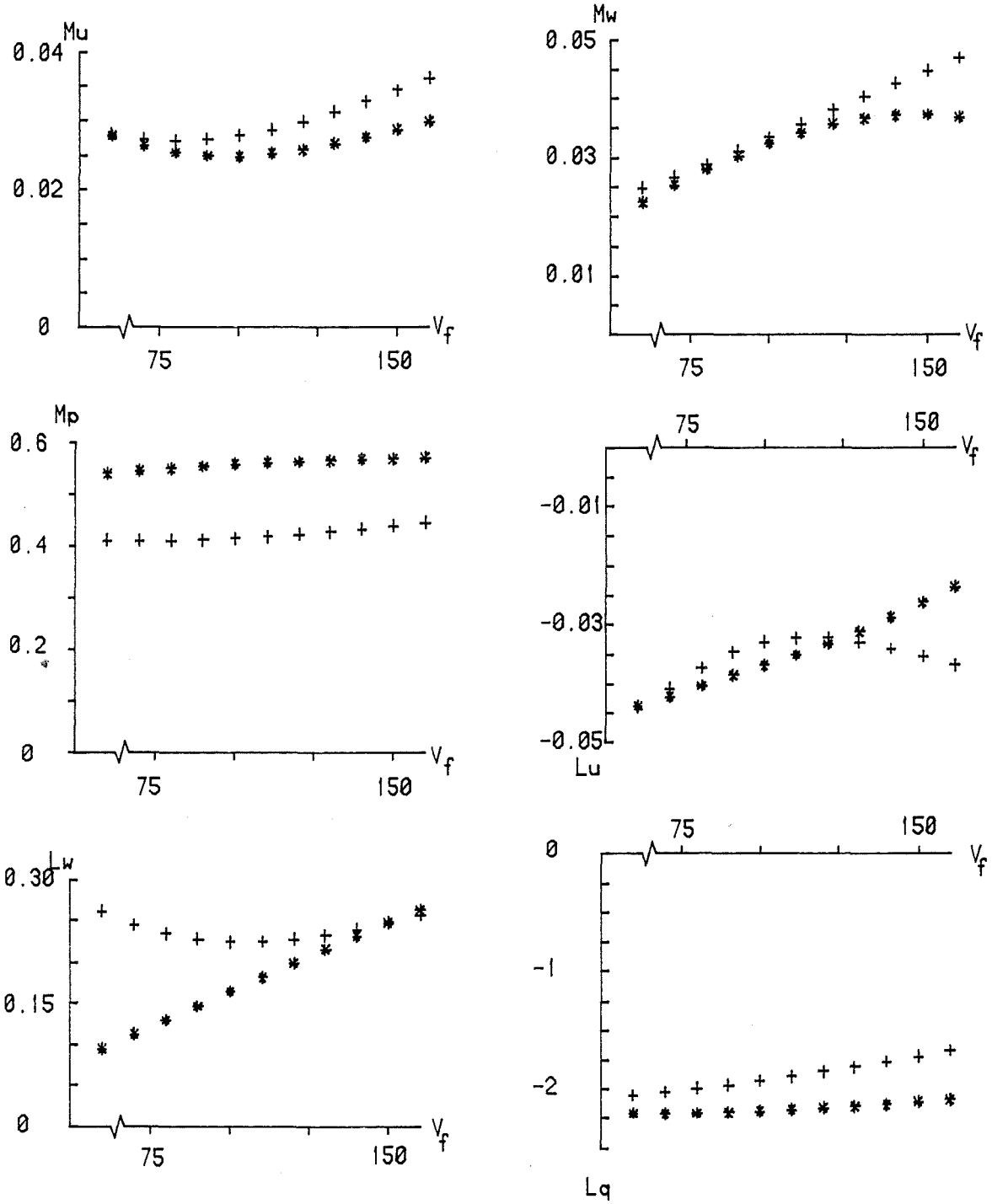

Figure 2:11 -- continued

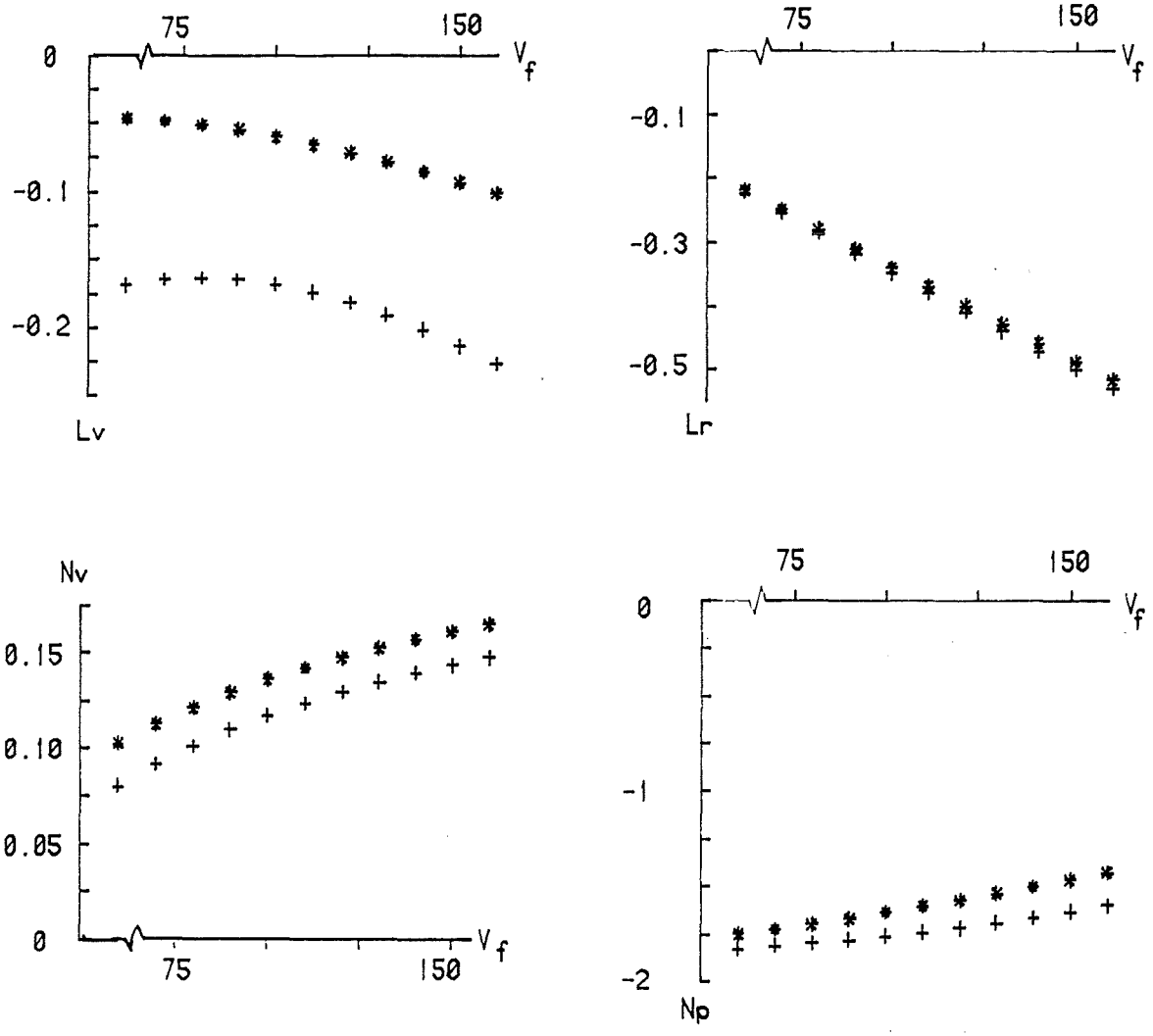

Figure 2:11 -- concluded

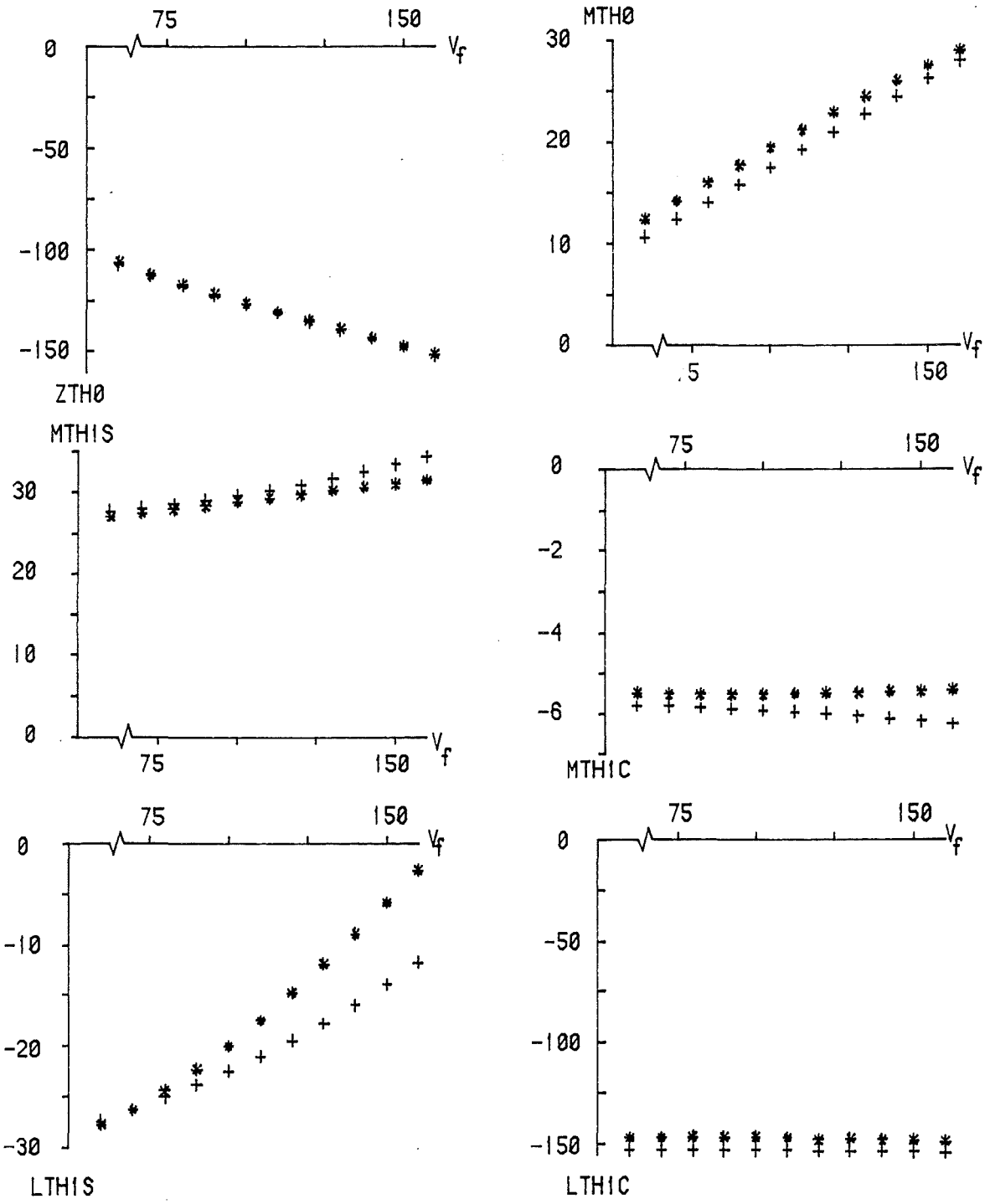

Figure 2:11a -- Comparison of control "derivatives"

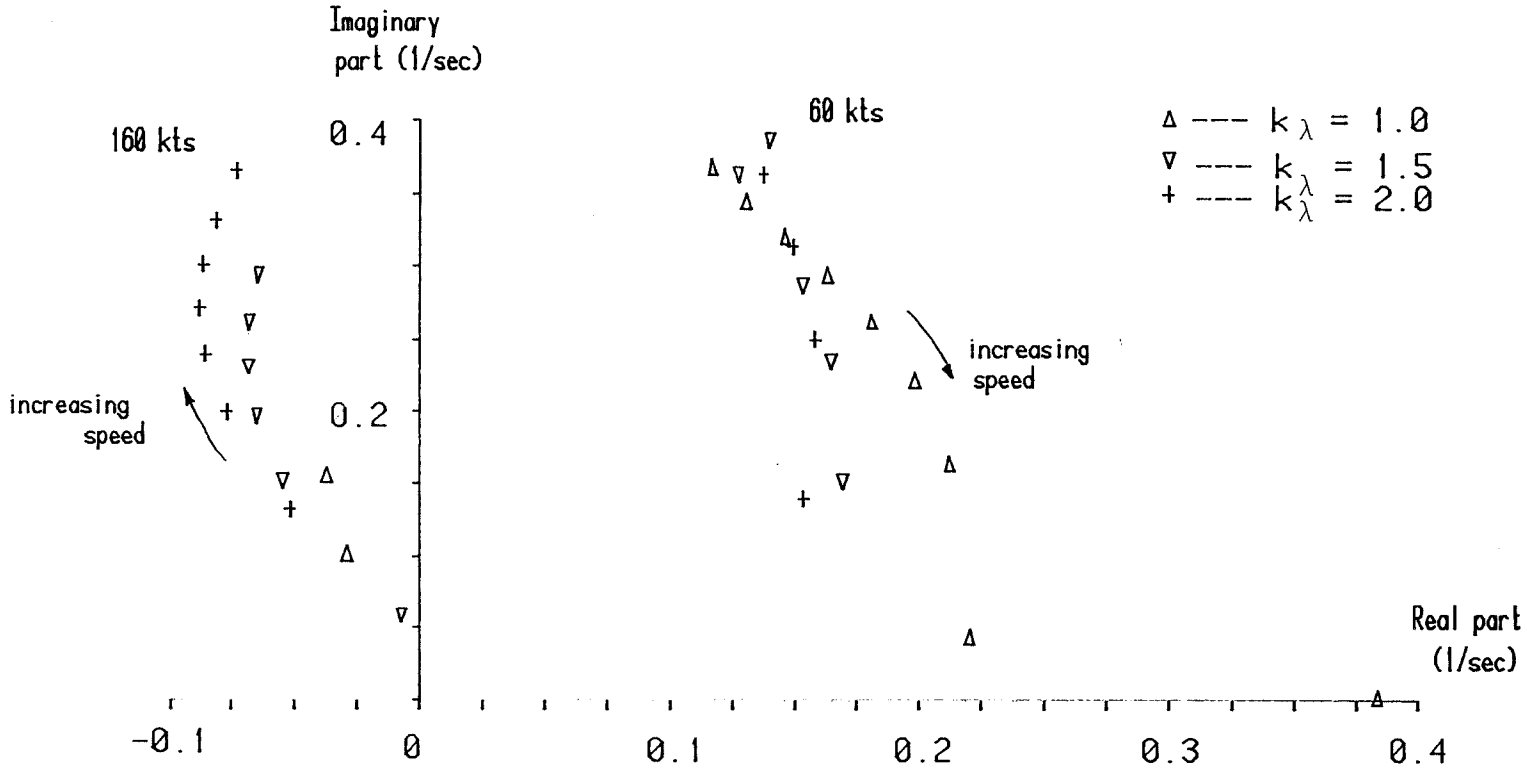

Figure 2:12 -- The effect of different values of wake impingement factor on the low-modulus longitudinal rigid-body eigenvalues.
Aircraft ----- Westland Lynx; mass=4314kg; xcg=-0.0198

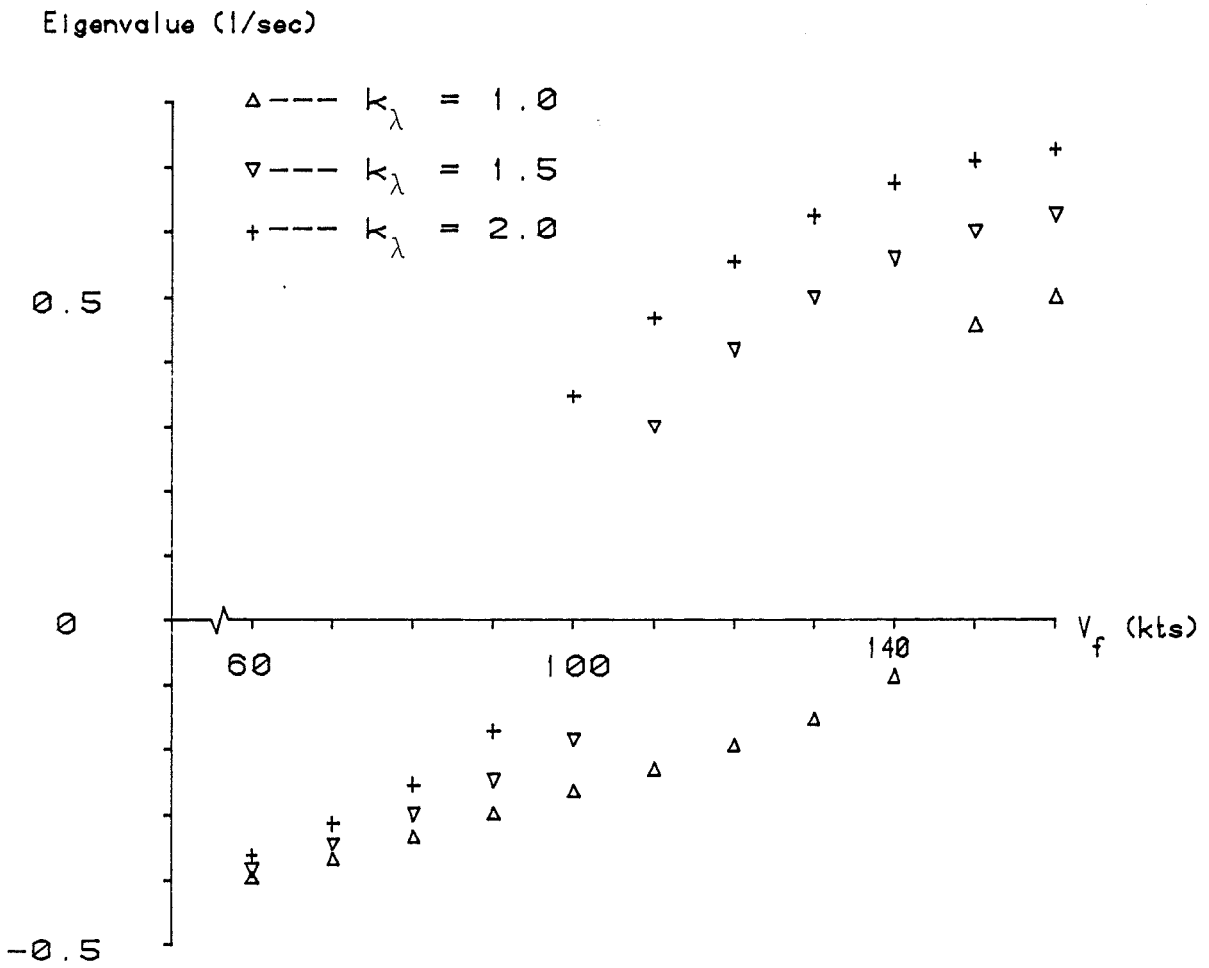

Figure 2:12 -- concluded

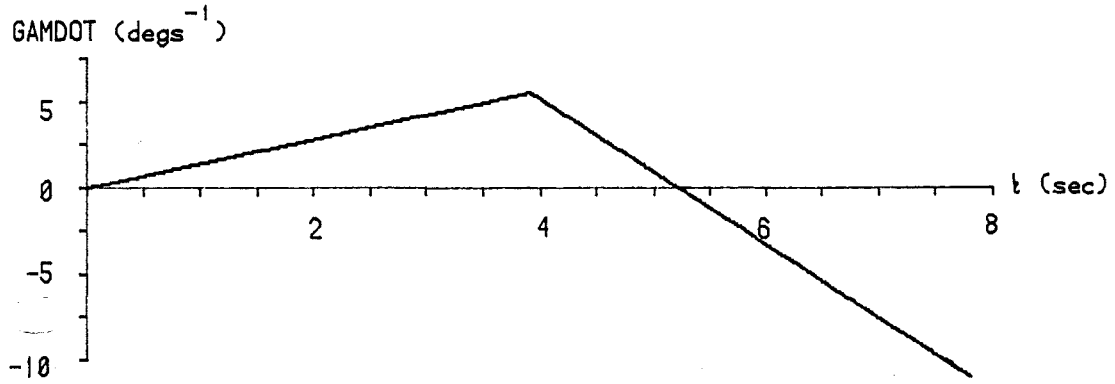

Figure 4:1 -- Piecewise linear function of the rate of change of climb angle that specifies a path to clear a 50m obstacle from 400m at 100 knots.

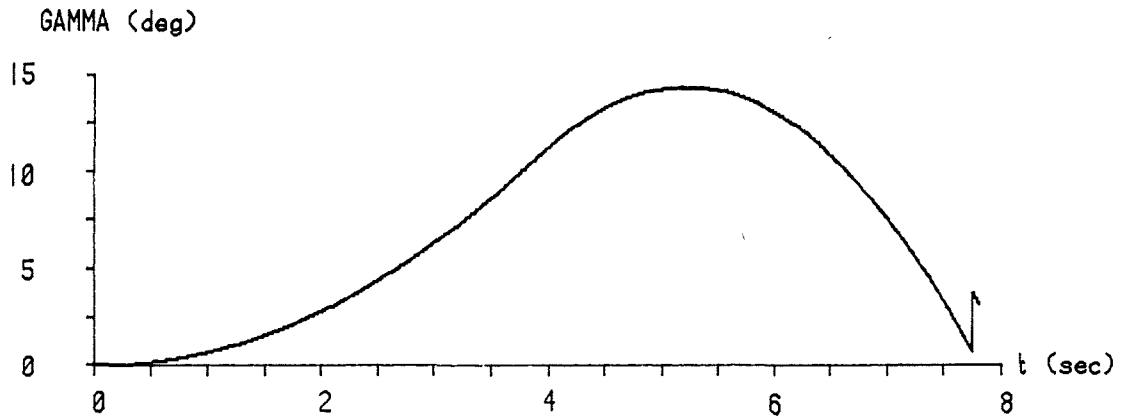

Figure 4:1a -- Resulting climb angle time history

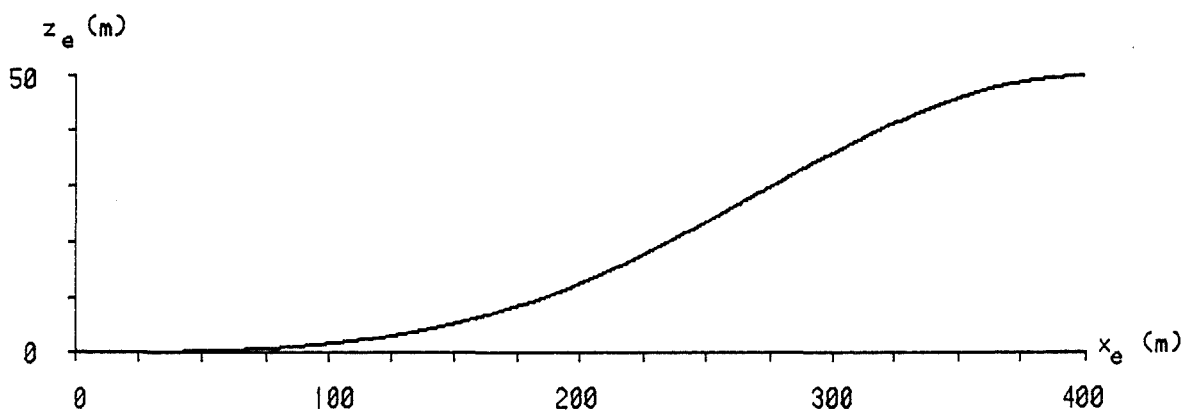

Figure 4:2 -- Trajectory specified by GAMDOT time history in figure 4:1 above.

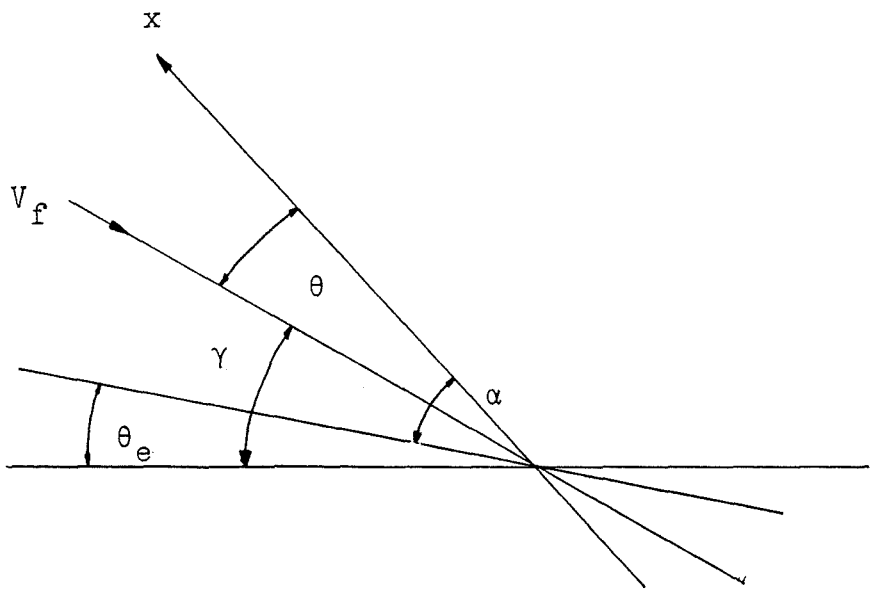

Figure 4:3

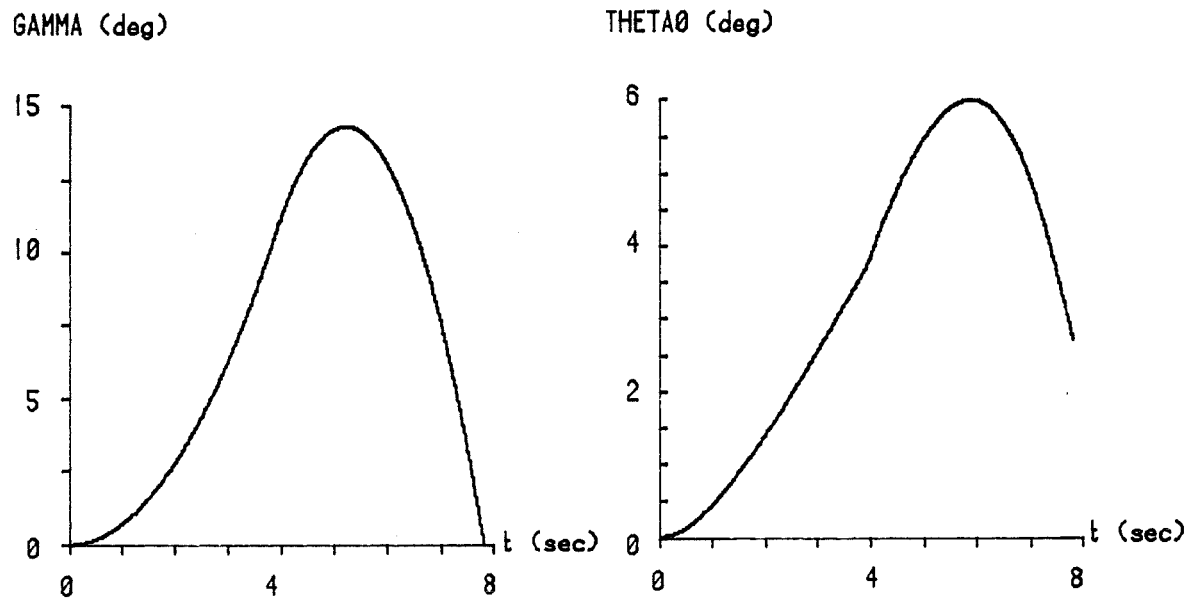

Figure 4:4 -- Comparison of climb and collective pitch angle time histories. Manoeuvre as specified by figure 4:1.

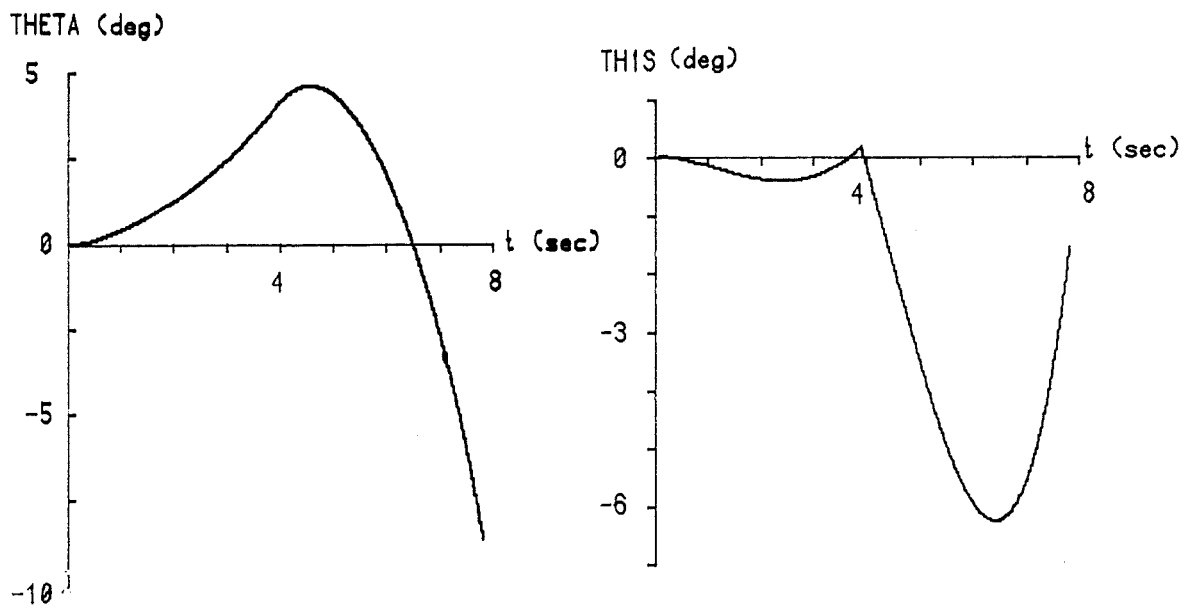

Figure 4:5 -- Comparison of pitch attitude and longitudinal cyclic pitch angle time histories. Manoeuvre as specified by figure 4:1.

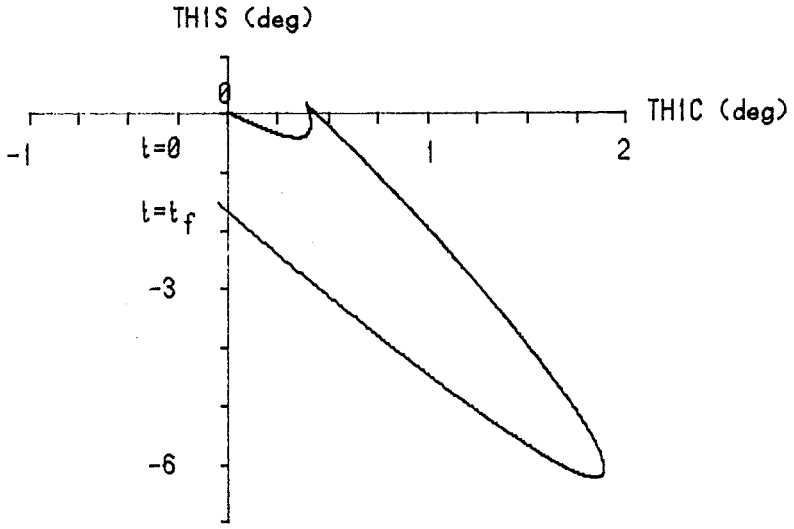

Figure 4:5a -- Locus of cyclic pitch position during the manoeuvre specified by figure 4:1.

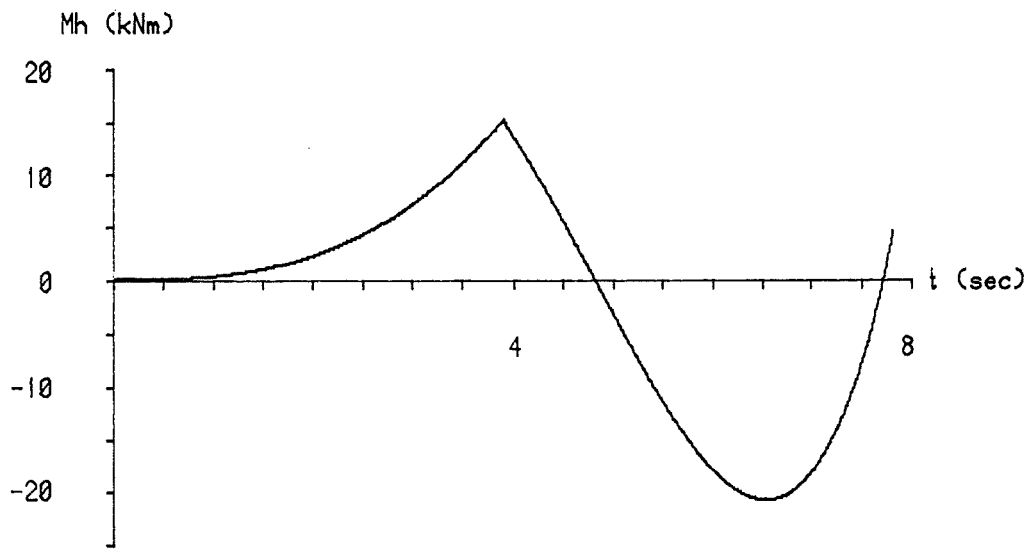

Figure 4:6 -- Time history of the longitudinal component of rotor hub moment during popup. Manoeuvre as specified by figure 4:1.

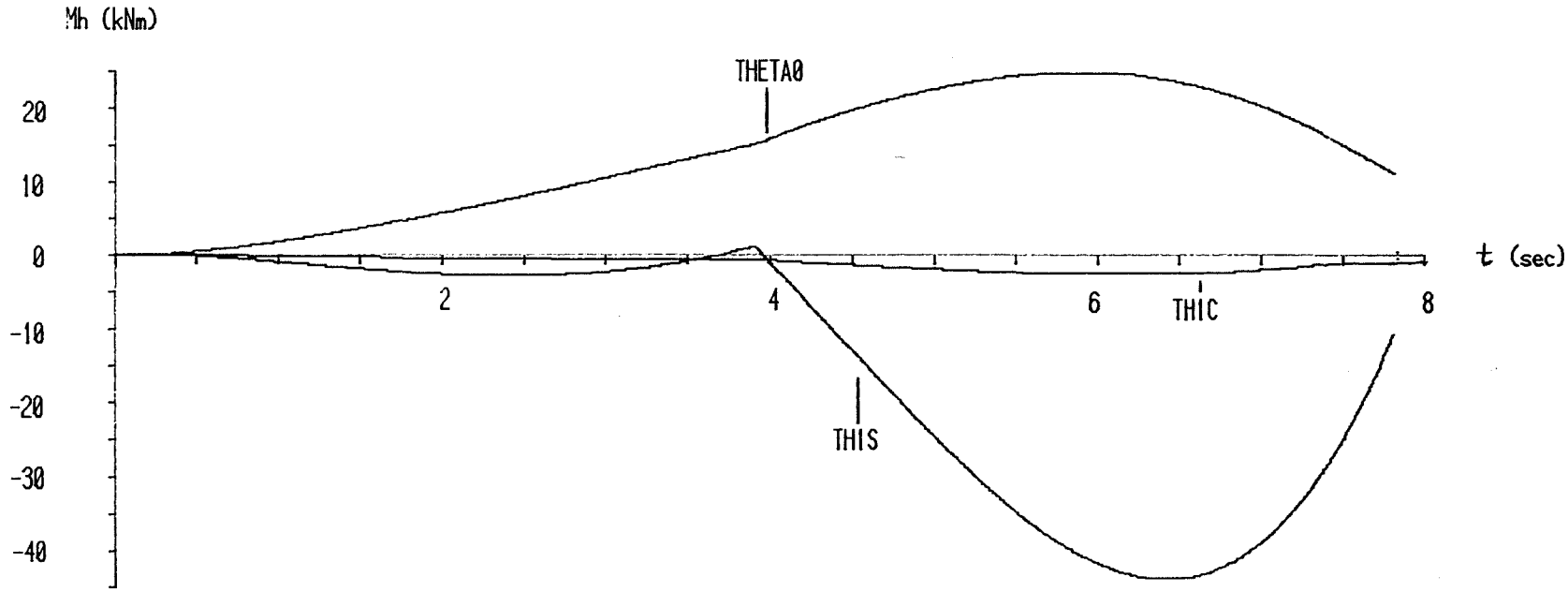

Figure 4:6a -- The longitudinal component of hub moment - contributions of the three main rotor controls.

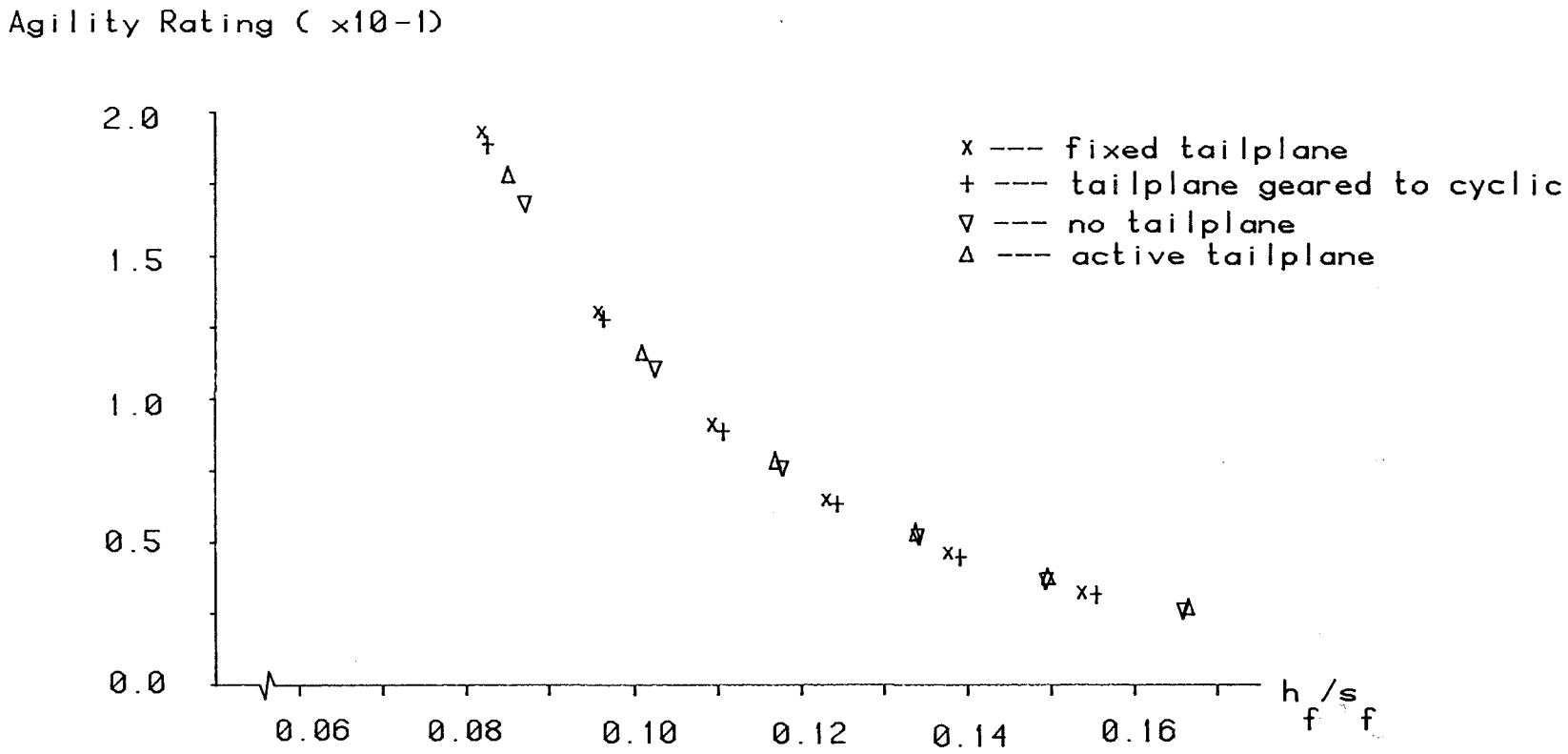

Figure 4:7 -- Agility ratings for each configuration flying popups manoeuvres at 100 knots.

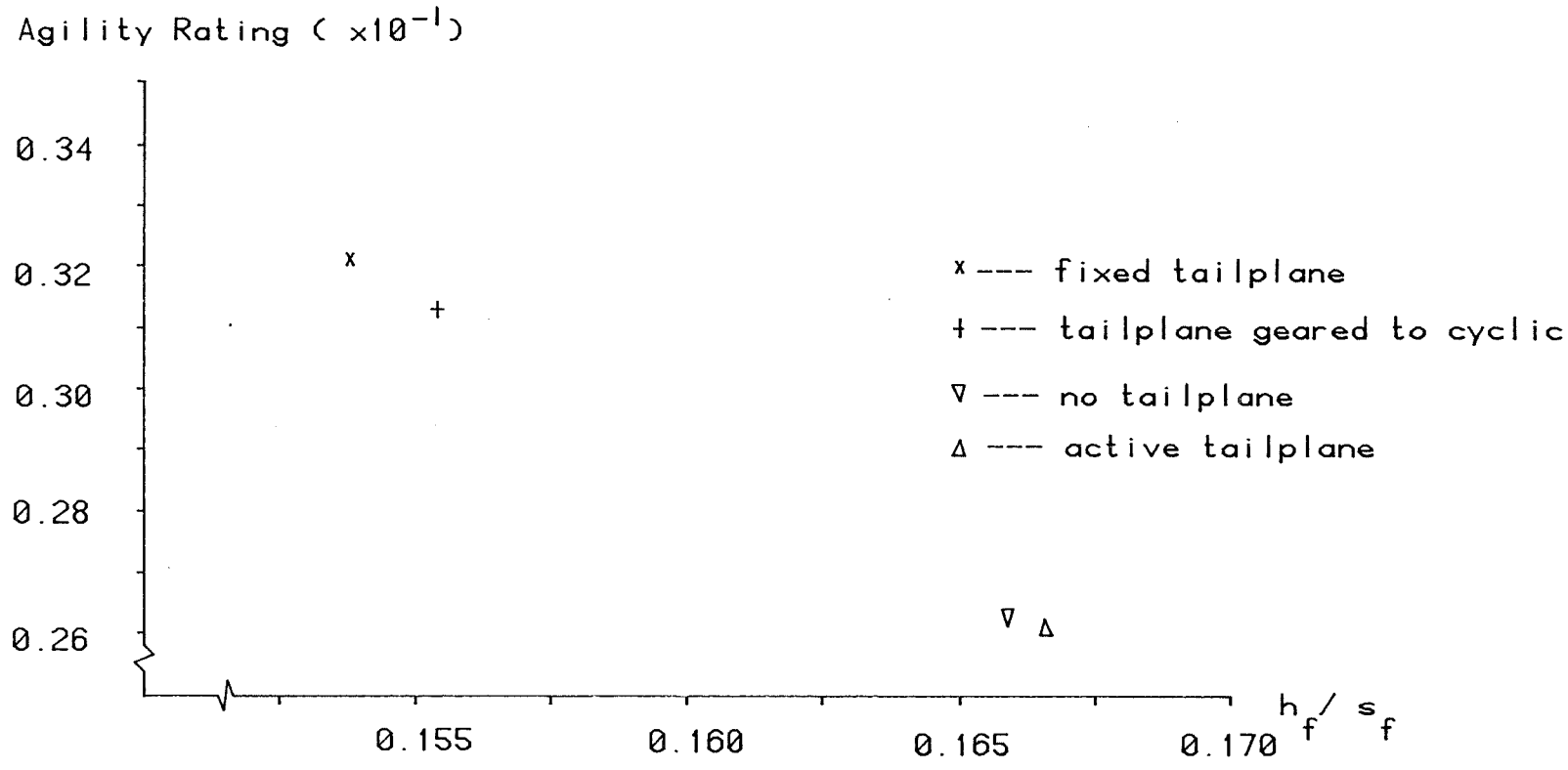

Figure 4:7a -- Exploded view of the full agility diagram, showing the limiting manoeuvres for each configuration furthest to the right of the locus

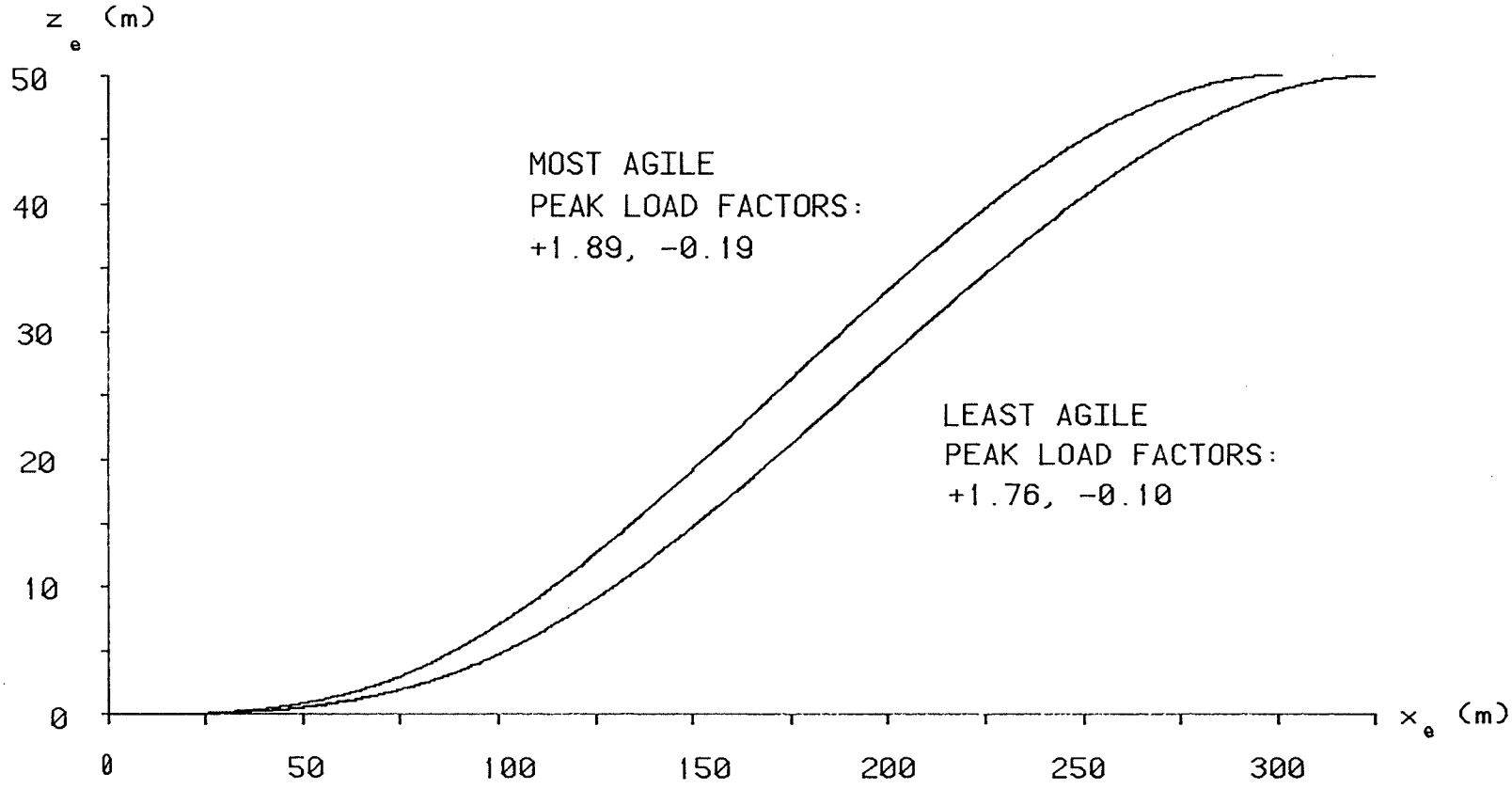

Figure 4:8 -- Comparison of the limiting trajectories of the most and least agile configurations, 100 knots.

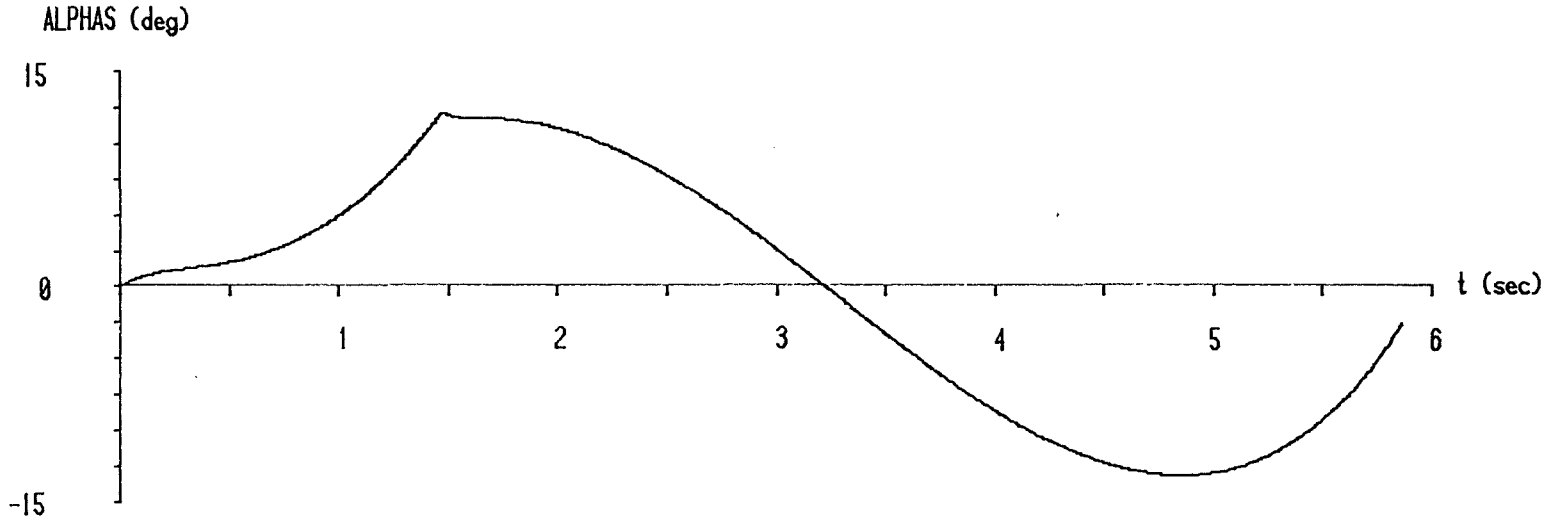

Figure 4:9 -- Tailplane incidence angle time history for the most agile configuration flying the limiting manoeuvre.

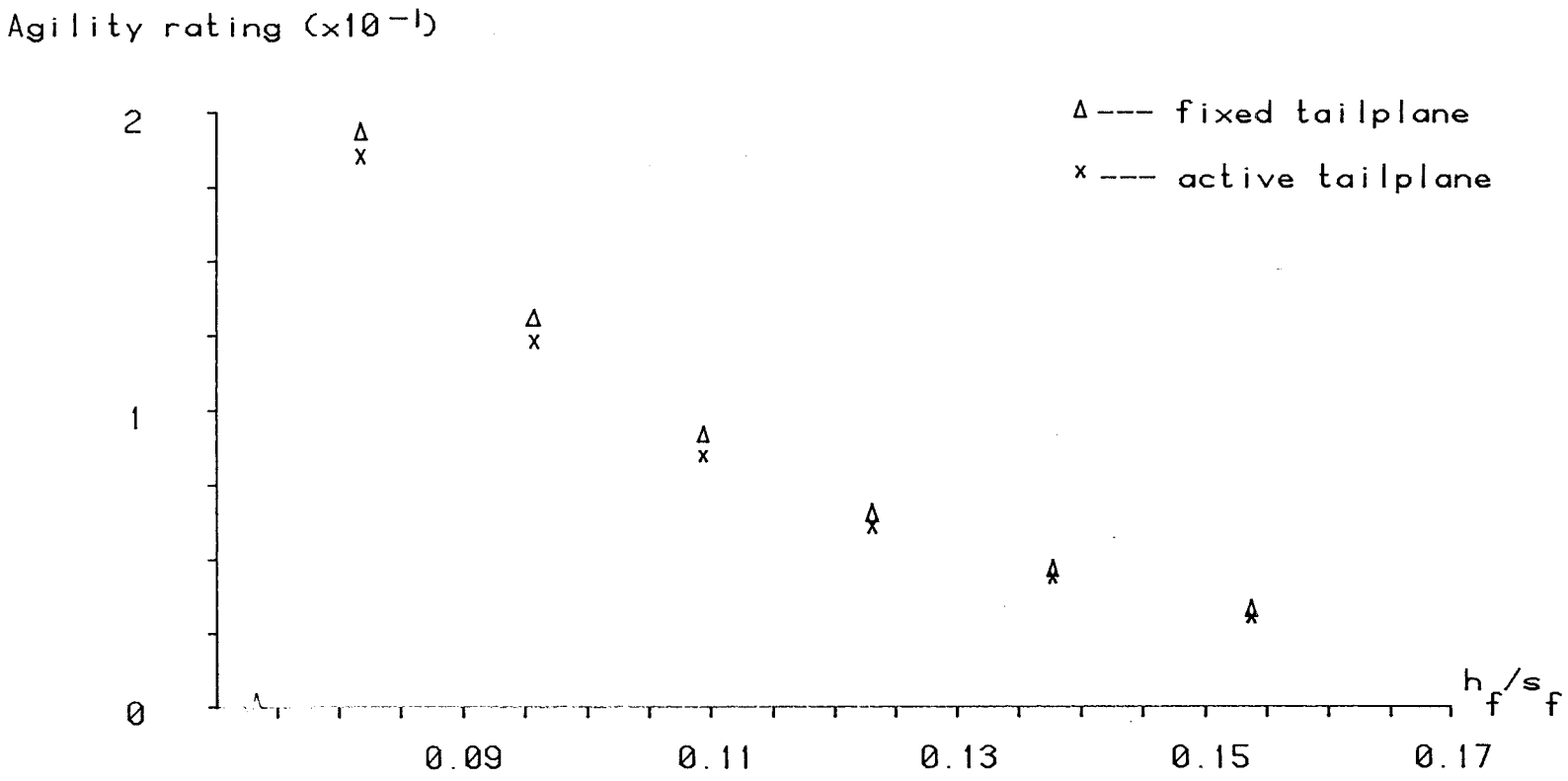

Figure 4:10 -- Comparison of the limiting agility ratings of the most and least agile helicopters, with the former reaching its own limiting manoeuvres 7 knots faster than the latter.

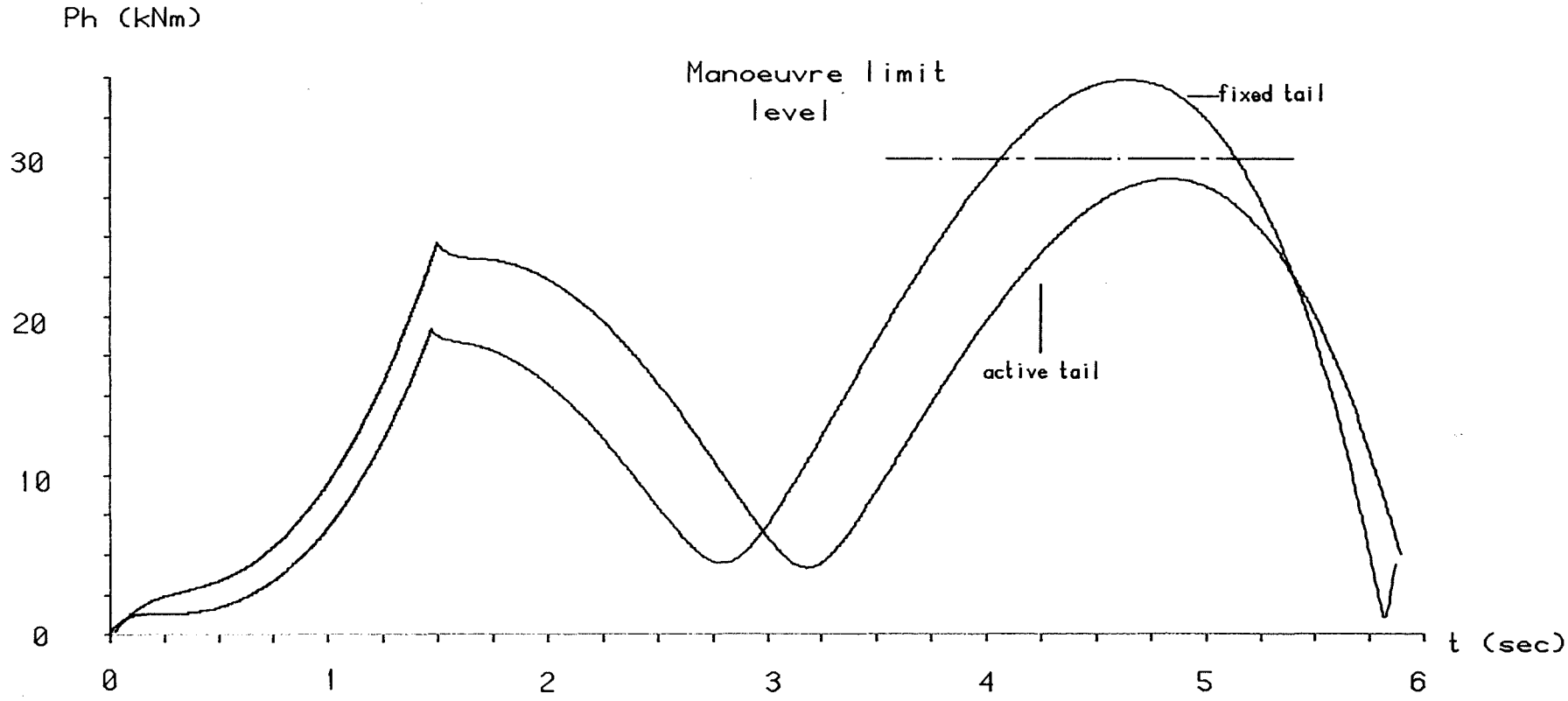

Figure 4:11 -- Comparison of the hub moment time histories of least and most agile helicopters, flying the limiting manoeuvre of the latter at 100 knots.

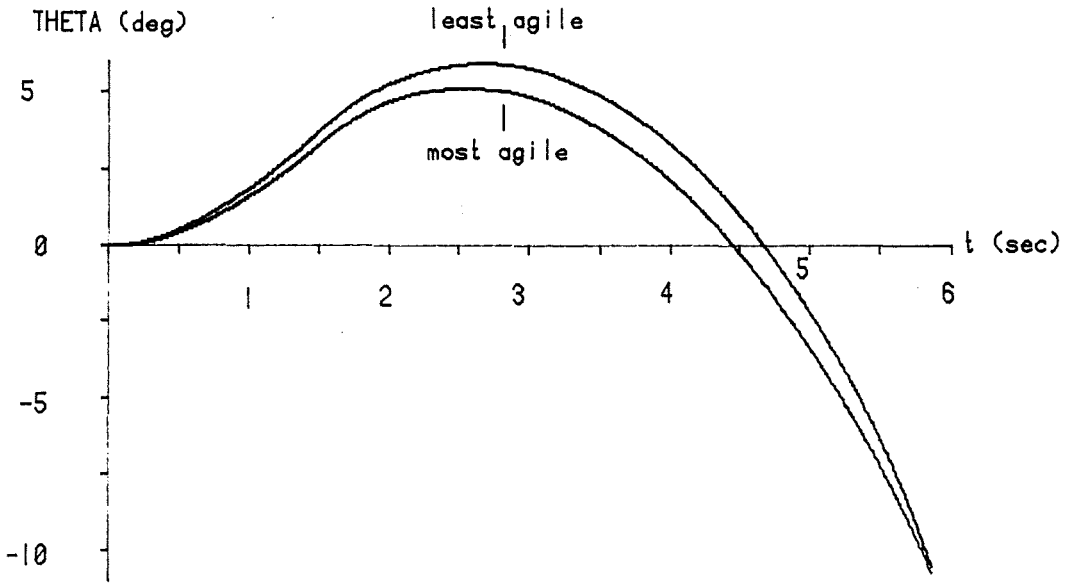

Figure 4:12 -- Comparison of the pitch attitude time histories of least and most agile configurations, flying the limiting manoeuvre of the most agile helicopter.

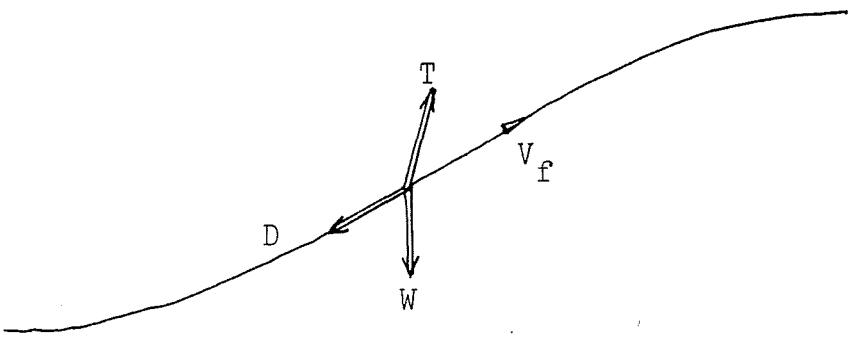

Figure 4:13 -- Forces acting on helicopter to produce the given change in flight path.

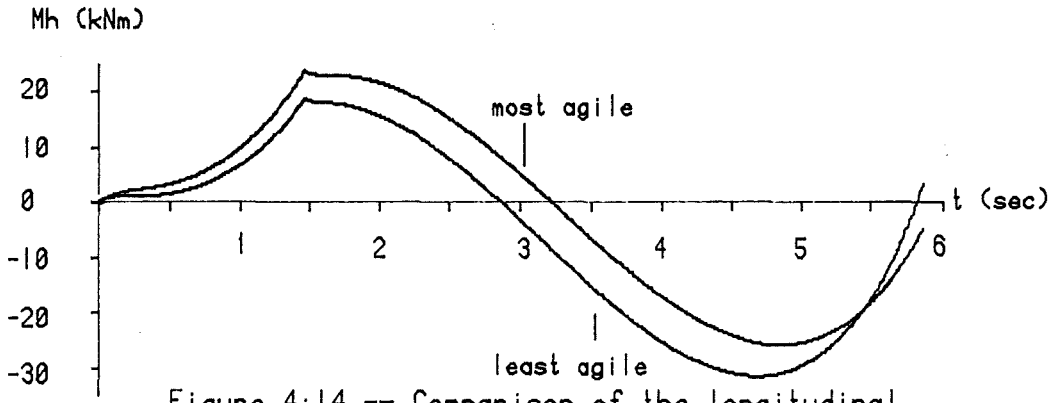

Figure 4:14 -- Comparison of the longitudinal component of hub moment of the least and most agile configuration when flying the limiting manoeuvre of the most agile helicopter.

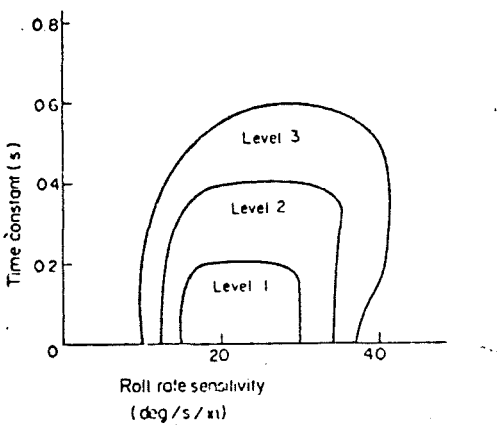

Hypothetical agility levels for roll response.

Figure 4:15

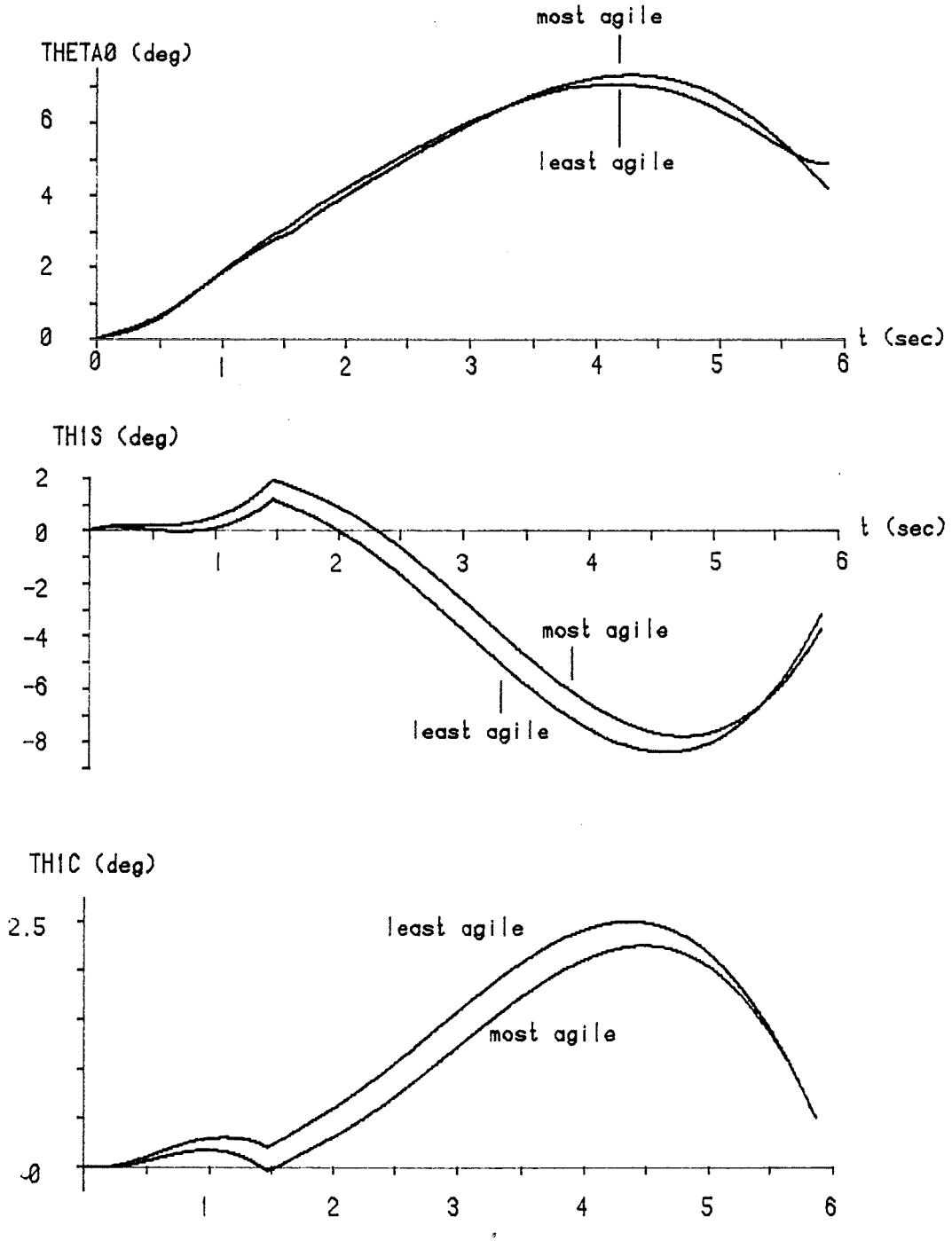

Figure 4:16 -- Comparison of the main rotor control time histories, of the least and most agile configurations flying the limiting manoeuvre of the most agile helicopter.

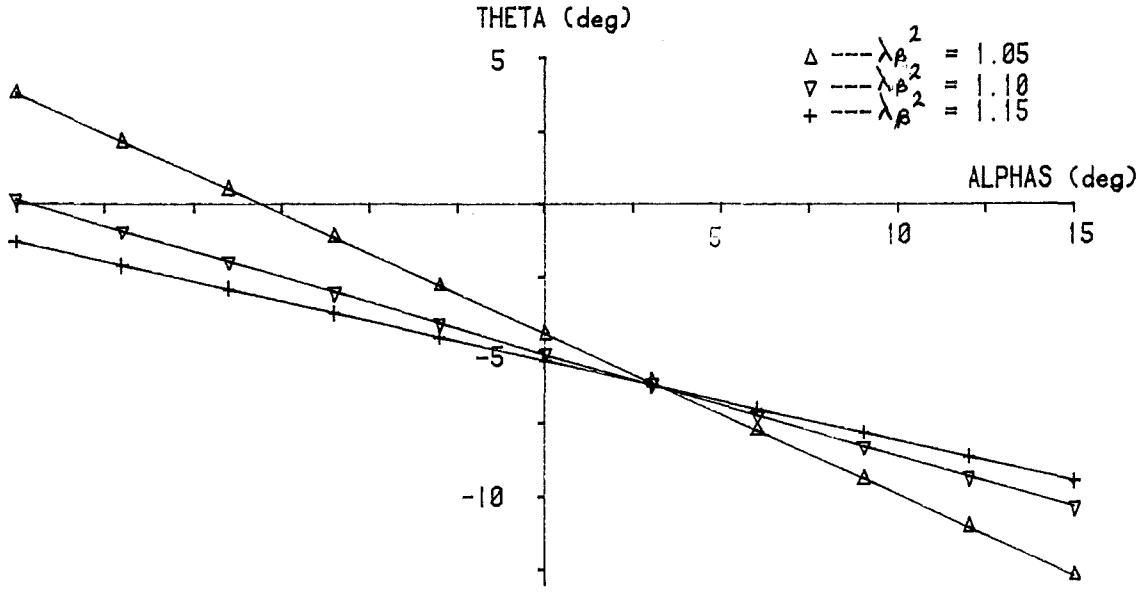

Figure 5:1 -- The influence of rotor stiffness on the pitch attitude/tailplane incidence relationship at 160 knots.

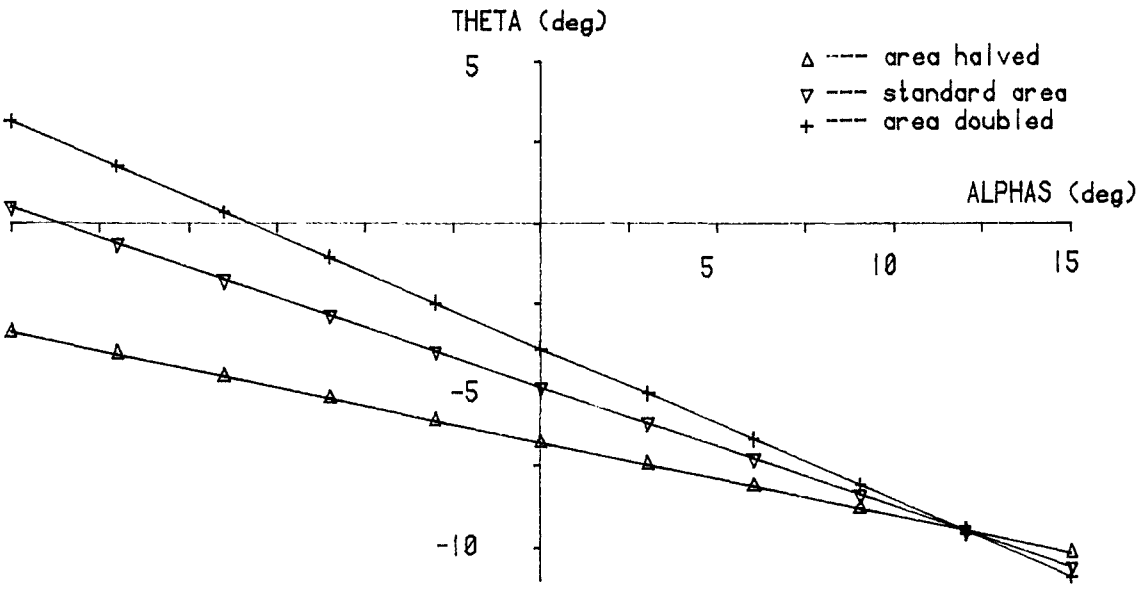

Figure 5:2 -- The influence of tailplane area on the pitch attitude/tailplane incidence relationship at 160 knots.

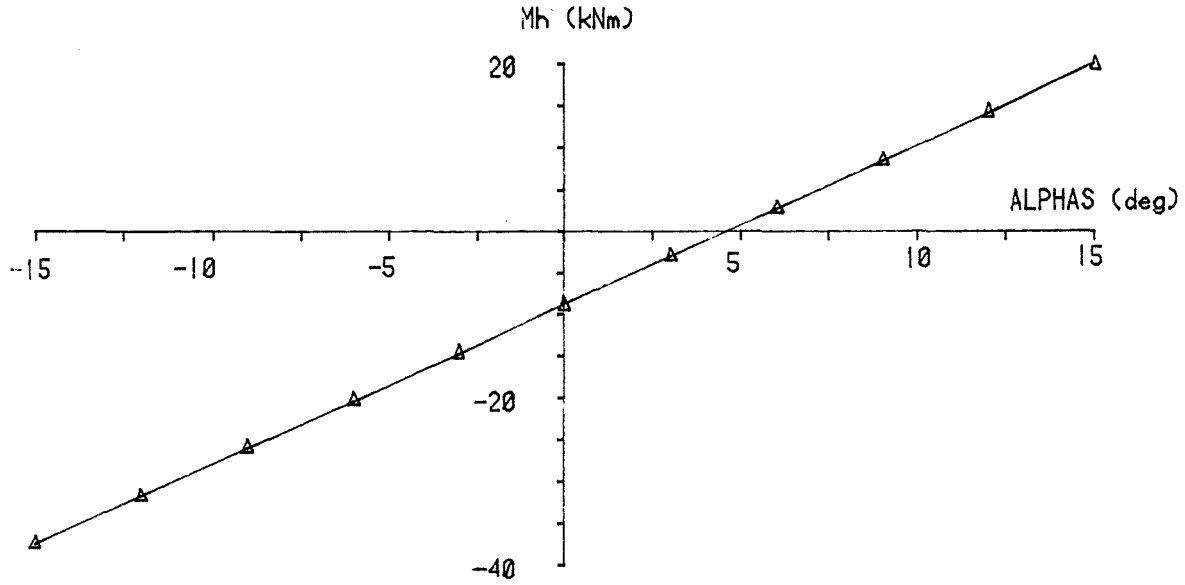

Figure 5:3 -- The variation in the longitudinal component of hub moment with tailplane incidence at 100 knots; tailplane area trebled.

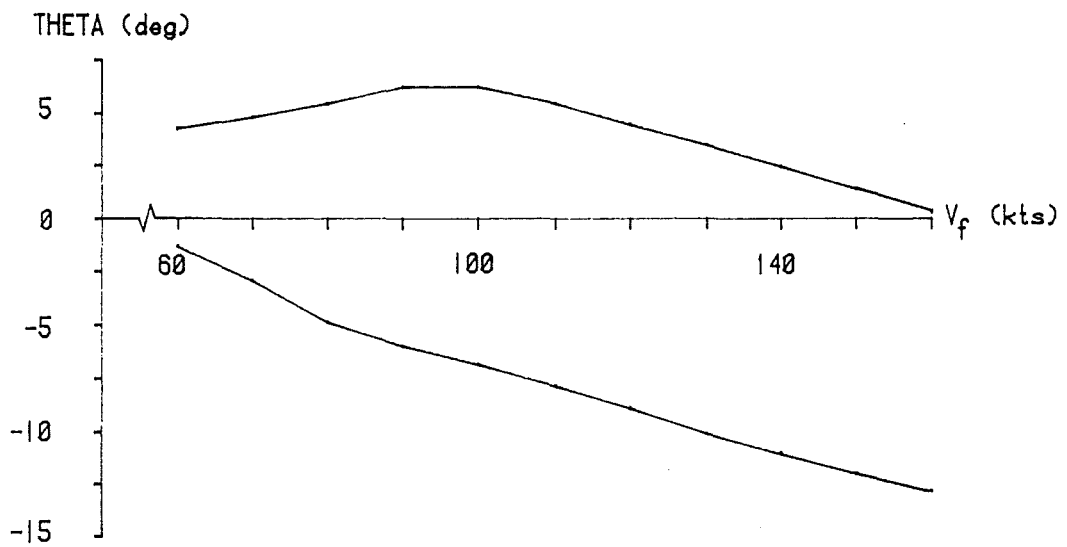

Figure 5:4 -- Limiting trim pitch attitudes in level flight, 60 to 160 knots. Limits defined by allowable tail aoa or rotor hub moment.

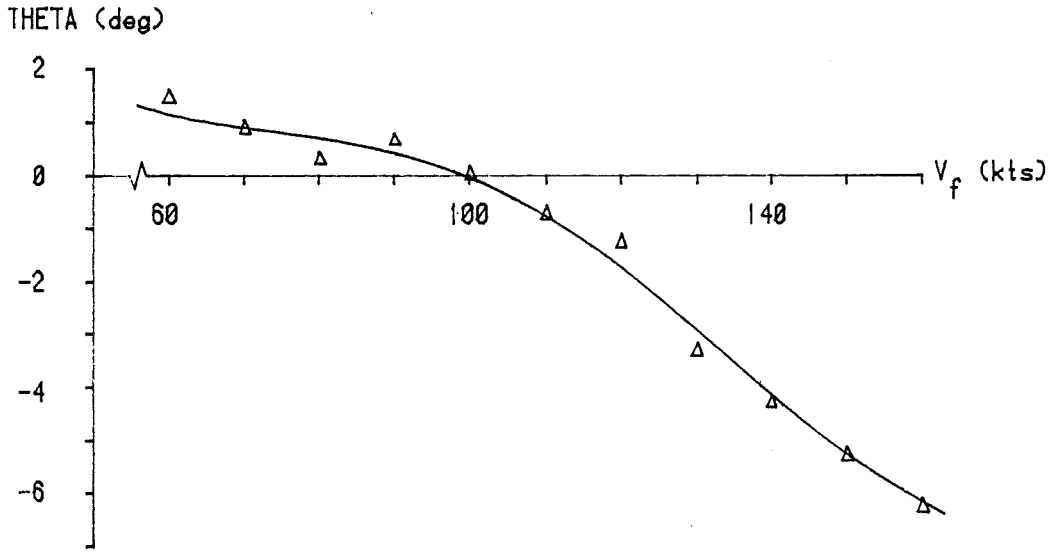

Optimum trim pitch attitude in level flight, 60 to 160 knots.

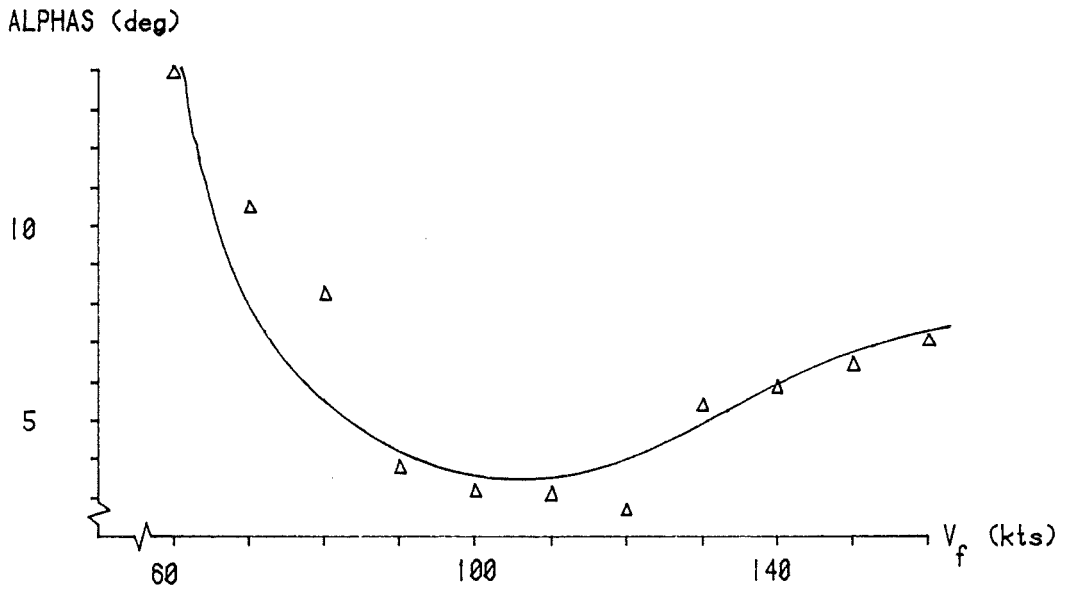

Variation in tailplane incidence angle required to produce the above trim pitch attitudes.

Figure 5:5

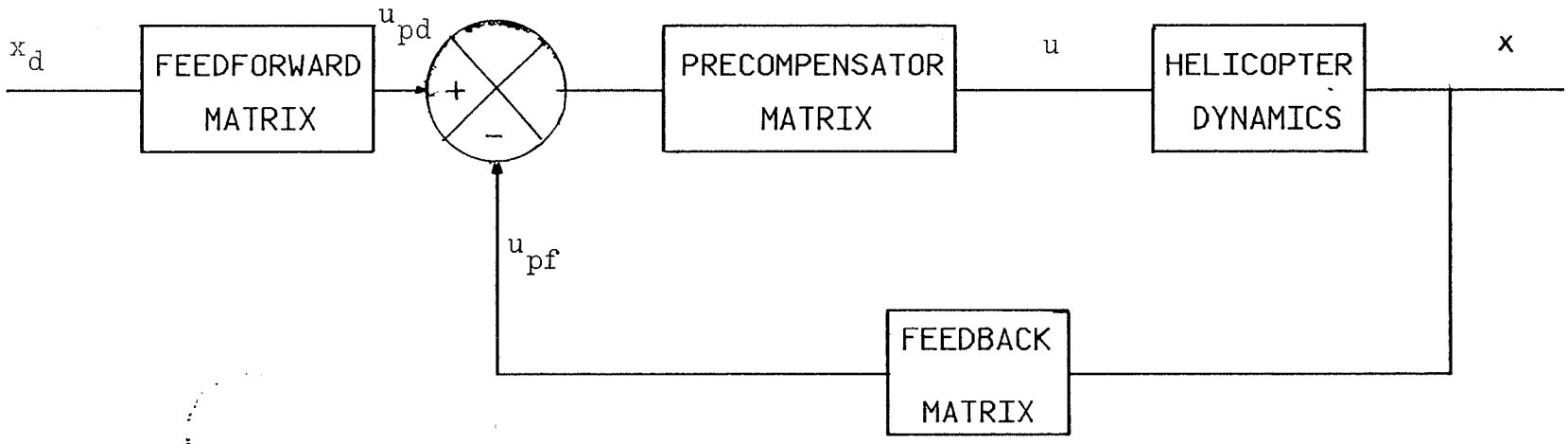

Figure 5:6 -- Block diagram of the closed-loop helicopter/FCS combination, showing the structure of the decoupled flight path and attitude controller

Ø.Ø38Ø	Ø.Ø438	Ø.9167	-9.8147	Ø.ØØØ5	-Ø.1546	Ø.ØØØØ	Ø.ØØ14	Ø.ØØØØ
Ø.Ø123	-Ø.8978	51.2836	Ø.Ø9Ø2	Ø.ØØØØ	-Ø.ØØ36	Ø.1426	Ø.ØØØ1	Ø.ØØØØ
Ø.Ø733	-Ø.Ø985	-3.96ØØ	-Ø.Ø555	Ø.ØØ26	Ø.4986	Ø.ØØØØ	-Ø.ØØ59	Ø.ØØØØ
Ø.ØØØØ	Ø.ØØØØ	Ø.9999	Ø.ØØØØ	Ø.ØØØØ	Ø.ØØØØ	Ø.ØØØØ	Ø.Ø145	Ø.ØØØØ
Ø.ØØ48	Ø.Ø123	-Ø.1Ø62	-Ø.ØØ13	-Ø.2Ø57	-Ø.5194	9.8136	-5Ø.82Ø8	-Ø.Ø9Ø2
Ø.Ø391	Ø.1618	-2.1829	Ø.ØØØØ	-Ø.Ø226	-1Ø.7Ø12	Ø.ØØØØ	-Ø.3954	Ø.ØØØØ
Ø.ØØØØ	Ø.ØØØØ	Ø.ØØØ1	Ø.ØØØØ	Ø.ØØØØ	1.ØØØØ	Ø.ØØØØ	-Ø.ØØ92	Ø.ØØØØ
Ø.Ø146	Ø.Ø272	-Ø.3585	Ø.ØØØØ	Ø.16Ø7	-1.5943	Ø.ØØØØ	-1.6611	Ø.ØØØØ
Ø.ØØØØ	Ø.ØØØØ	-Ø.Ø145	Ø.ØØØØ	Ø.ØØØØ	Ø.ØØØØ	Ø.ØØØØ	Ø.9999	Ø.ØØØØ

Original state-space system matrix.

(100 knots)

-Ø.Ø379	-2.6461	Ø.4453	-7.1695	Ø.ØØØ5	-Ø.1465	-Ø.ØØ13	Ø.ØØ13	Ø.ØØØØ
Ø.ØØØ2	-Ø.8979	-Ø.ØØ22	Ø.8962	Ø.ØØØØ	Ø.Ø173	-Ø.ØØ28	Ø.Ø144	Ø.ØØØØ
-Ø.Ø733	5.Ø755	-3.96ØØ	-5.131Ø	Ø.ØØ26	Ø.4986	Ø.ØØØØ	-Ø.ØØ59	Ø.ØØØØ
Ø.ØØØØ	Ø.ØØØØ	Ø.9999	Ø.ØØØØ	Ø.ØØØØ	Ø.ØØØØ	Ø.ØØØØ	Ø.Ø145	Ø.ØØØØ
Ø.ØØ48	-Ø.6317	-Ø.1Ø62	Ø.63Ø4	-Ø.2Ø57	-Ø.5194	9.8136	-5Ø.82Ø8	-Ø.Ø9Ø2
-Ø.Ø391	-8.2622	-2.1829	8.2622	-Ø.Ø226	-1Ø.7Ø12	Ø.ØØØØ	-Ø.3954	Ø.ØØØØ
Ø.ØØØØ	Ø.ØØØØ	Ø.ØØØ1	Ø.ØØØØ	Ø.ØØØØ	1.ØØØØ	Ø.ØØØØ	-Ø.ØØ92	Ø.ØØØØ
-Ø.Ø146	-1.3852	-Ø.3585	1.3852	Ø.16Ø7	-1.5943	Ø.ØØØØ	-1.6611	Ø.ØØØØ
Ø.ØØØØ	Ø.ØØØØ	-Ø.Ø145	Ø.ØØØØ	Ø.ØØØØ	Ø.ØØØØ	Ø.ØØØØ	Ø.9999	Ø.ØØØØ

Transformed state-space system matrix.

(100 knots)

Figure 5:7

$$\begin{bmatrix} 0 & 1 & 0 & 0 & 0 \\ 1 & 0 & 0 & 0 & 0 \\ 0 & 0 & 0 & 0 & 1 \\ 0 & 0 & 0 & 0 & 0 \\ 0 & 0 & 0 & 1 & 0 \\ 0 & 0 & 1 & 0 & 0 \\ 0 & 0 & 0 & 0 & 0 \\ 0 & 0 & 0 & 1 & 0 \\ 0 & 0 & 0 & 0 & 0 \end{bmatrix} \cdot \begin{bmatrix} u_{p1} \\ u_{p2} \\ u_{p3} \\ u_{p4} \\ u_{ps} \end{bmatrix}$$

Figure 5:8 -- Desired structure of precompensated B matrix, B_p. State vector is ordered $x = [\ \Delta V_f \quad \gamma \quad q \quad \theta \quad v \quad p \quad \phi \quad r \quad \psi\ ]^T$

$$\begin{bmatrix} u_{p1} \\ u_{p2} \\ u_{p3} \\ u_{p4} \\ u_{ps} \end{bmatrix} = \begin{bmatrix} 1.0000 & -0.3983 & -0.0333 & 0.0192 & -0.0019 \\ 0.5340 & 1.0000 & 0.1137 & 0.0084 & 0.0003 \\ 0.0427 & -0.2885 & 1.0000 & -0.0125 & -0.0004 \\ 0.0013 & -0.0016 & -0.8939 & 1.0000 & 0.0000 \\ 2.1501 & 2.0510 & -0.2436 & 0.0432 & 1.0000 \end{bmatrix} \cdot \begin{bmatrix} \theta_0 \\ \theta_{1s} \\ \theta_{1c} \\ \theta_{0tr} \\ \alpha_s \end{bmatrix}$$

Figure 5:9 -- Precompensator matrix K_p for 100 knots.

$$B = \begin{bmatrix} 6.4436 & -12.0747 & 1.7220 & 0.0000 & 0.0007 \\ 2.4632 & 0.9226 & -0.0024 & 0.0000 & 0.0913 \\ 10.6293 & 25.7794 & -5.3159 & 0.0000 & -11.2401 \\ 0.0000 & 0.0000 & 0.0000 & 0.0000 & 0.0000 \\ 0.1497 & -2.7582 & -10.0959 & 7.5142 & 0.0000 \\ 23.3375 & -32.1786 & -143.7148 & -2.0360 & 0.0000 \\ 0.0000 & 0.0000 & 0.0000 & 0.0000 & 0.0000 \\ 3.8840 & -5.3553 & -23.9178 & -21.0139 & 0.0000 \\ 0.0000 & 0.0000 & 0.0000 & 0.0000 & 0.0000 \end{bmatrix}$$

$$B_p = \begin{bmatrix} 0.0703 & -15.1364 & 0.1347 & 0.0012 & -0.0162 \\ 3.1521 & 0.1295 & -0.0017 & 0.0590 & 0.0868 \\ 0.0015 & 0.0262 & 0.0000 & 0.0005 & -11.2505 \\ 0.0000 & 0.0000 & 0.0000 & 0.0000 & 0.0000 \\ -1.7447 & 0.0828 & -17.1311 & 7.6211 & 0.0024 \\ 0.0092 & -0.0113 & -146.3295 & -0.0621 & -0.0001 \\ 0.0000 & 0.0000 & 0.0000 & 0.0000 & 0.0000 \\ -0.0259 & 0.0307 & -5.8724 & -20.6854 & 0.0009 \\ 0.0000 & 0.0000 & 0.0000 & 0.0000 & 0.0000 \end{bmatrix}$$

Figure 5:9a --- B and B_p matrices for 100 knots level flight condition.

$$B = \begin{bmatrix} -1.0622 & -11.5405 & 1.8698 & 0.0000 & -0.0422 \\ 3.4533 & 0.8109 & -0.0043 & 0.0000 & 0.0548 \\ 6.1944 & 25.6867 & -5.3081 & 0.0000 & -4.0423 \\ 0.0000 & 0.0000 & 0.0000 & 0.0000 & 0.0000 \\ -0.0166 & -2.4179 & -9.8151 & 5.6358 & 0.0000 \\ 13.7373 & -31.3217 & -143.0826 & -1.5270 & 0.0000 \\ 0.0000 & 0.0000 & 0.0000 & 0.0000 & 0.0000 \\ 2.2862 & -5.2127 & -23.8126 & -15.7606 & 0.0000 \\ 0.0000 & 0.0000 & 0.0000 & 0.0000 & 0.0000 \end{bmatrix}$$

$$B_p = \begin{bmatrix} 0.0205 & -11.9189 & 0.1444 & 0.0004 & -0.0470 \\ 3.4375 & 0.0101 & 0.1801 & 0.0258 & 0.0255 \\ -0.0054 & 0.0044 & 0.0009 & 0.0003 & -4.0639 \\ 0.0000 & 0.0000 & 0.0000 & 0.0000 & 0.0000 \\ -0.9320 & 0.0410 & -16.8762 & 5.7304 & 0.0070 \\ 0.0049 & -0.0054 & -145.5923 & -0.0475 & -0.0007 \\ 0.0000 & 0.0000 & 0.0000 & 0.0000 & 0.0000 \\ -0.0138 & 0.0152 & -5.7916 & -15.5144 & 0.0026 \\ 0.0000 & 0.0000 & 0.0000 & 0.0000 & 0.0000 \end{bmatrix}$$

Figure 5:10 --- B and B_p matrices for 60 knots level flight condition.

$$B = \begin{bmatrix} 23.5388 & -1.2204 & 0.7984 & 0.0000 & 1.3132 \\ 1.8629 & 1.0205 & -0.0007 & 0.0000 & 0.1470 \\ 18.5043 & 26.3542 & -5.1119 & 0.0000 & -28.8087 \\ 0.0000 & 0.0000 & 0.0000 & 0.0000 & 0.0000 \\ -0.0568 & -2.0584 & -11.0568 & 9.8528 & 0.0000 \\ 39.3887 & -30.5857 & -145.8775 & -2.6697 & 0.0000 \\ 0.0000 & 0.0000 & 0.0000 & 0.0000 & 0.0000 \\ 6.5553 & -5.0902 & -24.2777 & -27.5538 & 0.0000 \\ 0.0000 & 0.0000 & 0.0000 & 0.0000 & 0.0000 \end{bmatrix}$$

$$B_p = \begin{bmatrix} 24.5390 & -1.3048 & -0.0037 & 0.0257 & 0.0149 \\ 1.8987 & 1.0678 & -0.1105 & -0.0379 & 0.0823 \\ 0.0005 & 0.0064 & -0.0007 & 0.0010 & -28.8124 \\ 0.0000 & 0.0000 & 0.0000 & 0.0000 & 0.0000 \\ -2.9801 & 0.3419 & -17.3790 & 10.0357 & 0.1462 \\ 0.5058 & -0.1002 & -144.0613 & -0.0853 & -0.0199 \\ 0.0000 & 0.0000 & 0.0000 & 0.0000 & 0.0000 \\ -0.0111 & 0.1320 & -6.3904 & -27.1237 & 0.0542 \\ 0.0000 & 0.0000 & 0.0000 & 0.0000 & 0.0000 \end{bmatrix}$$

Figure 5:11 --- B and B_p matrices for 160 knots level flight condition.

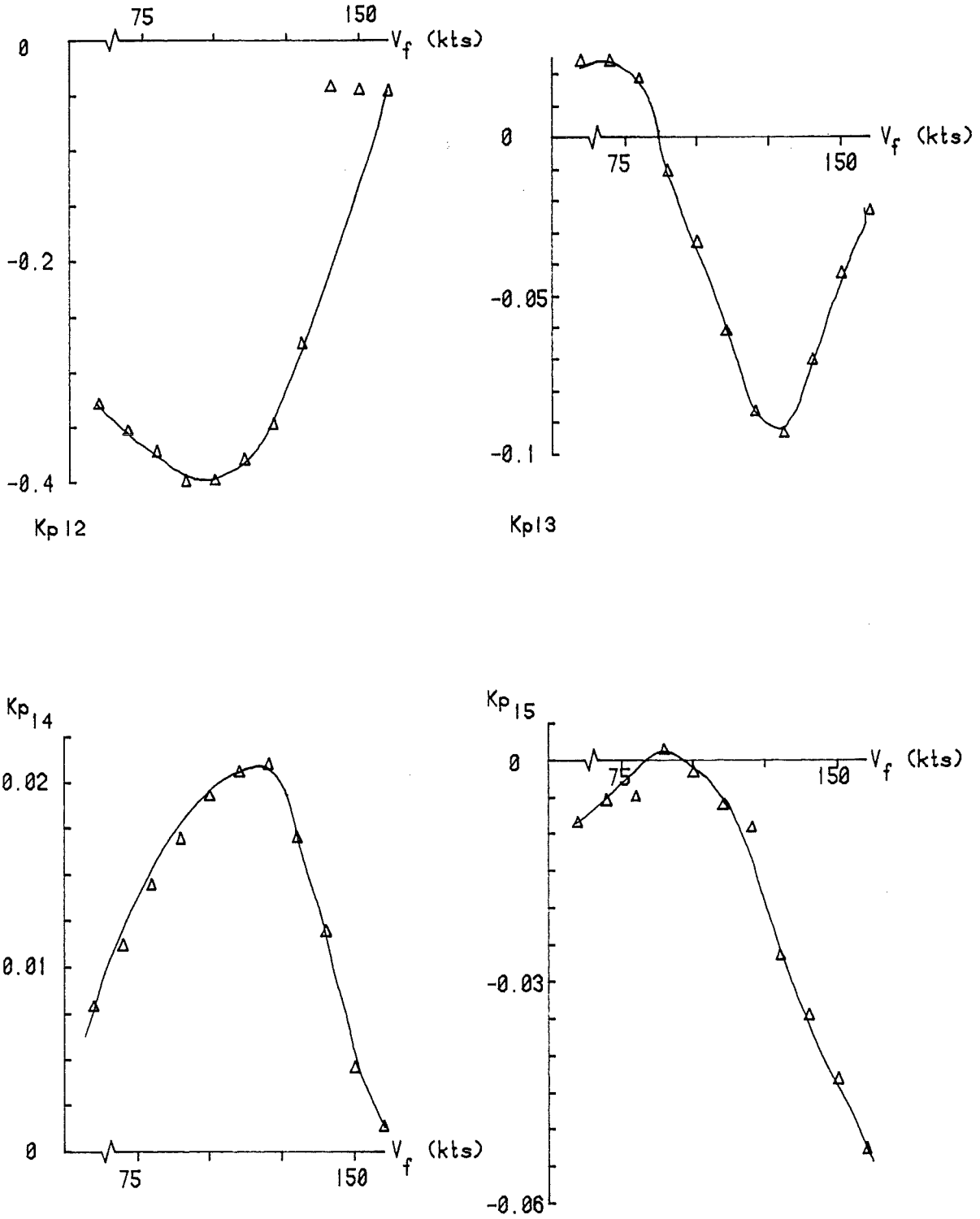

Figure 5:12 -- precompensator matrix gains; control Up1 ("collective") as a function of longitudinal cyclic, lateral cyclic, tail rotor collective and tailplane incidence.

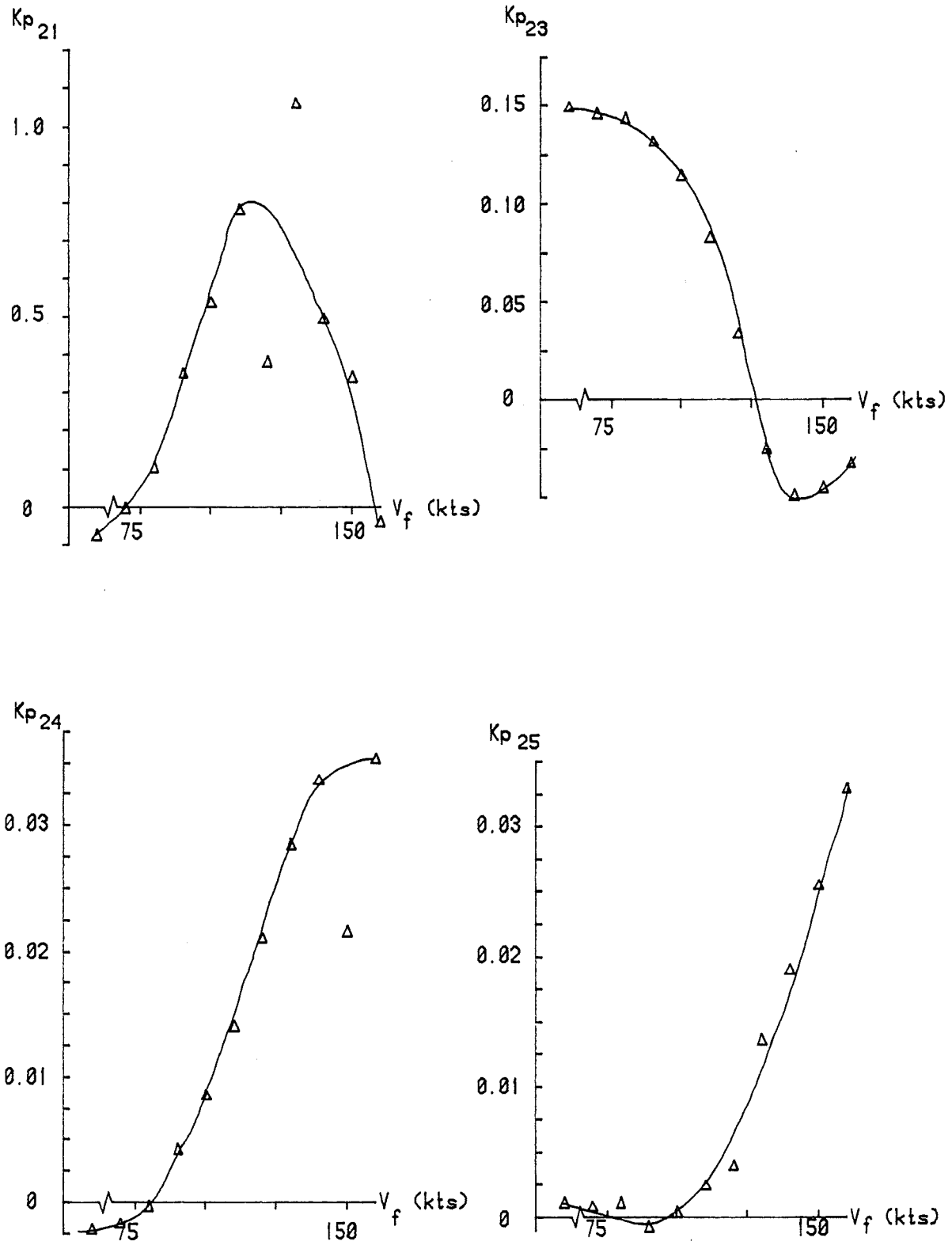

Figure 5:13 -- precompensator matrix gains; control Up2 ("long. cyclic") as a function of collective, lateral cyclic, tail rotor collective and tailplane incidence.

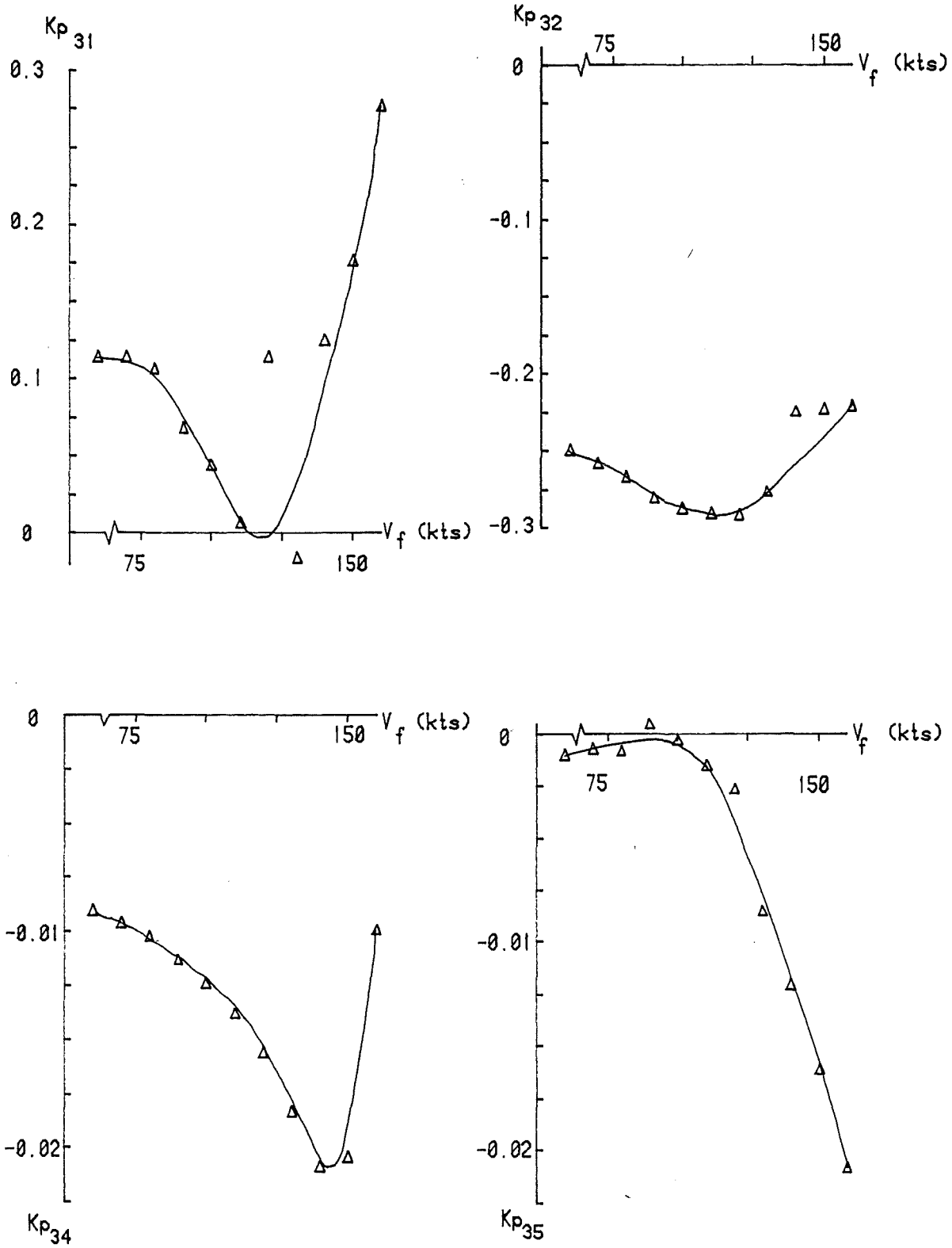

Figure 5:14 -- precompensator matrix gains; control Up3 ("lateral cyclic") as a function of collective, long. cyclic, tail rotor collective and tailplane incidence.

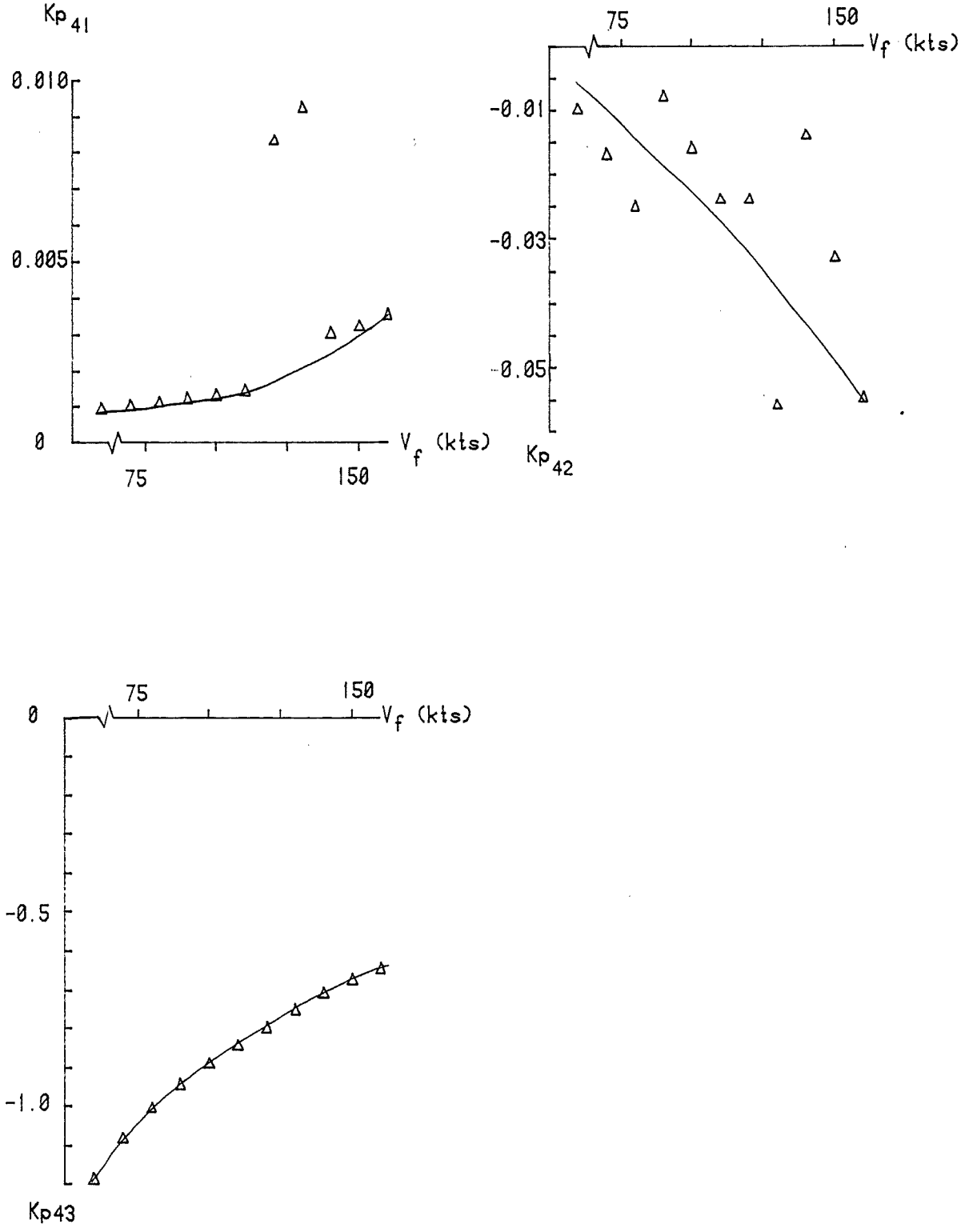

Figure 5:15 -- precompensator matrix gains; control Up4 (tail rotor "collective") as a function of collective, long. cyclic and lateral cyclic.

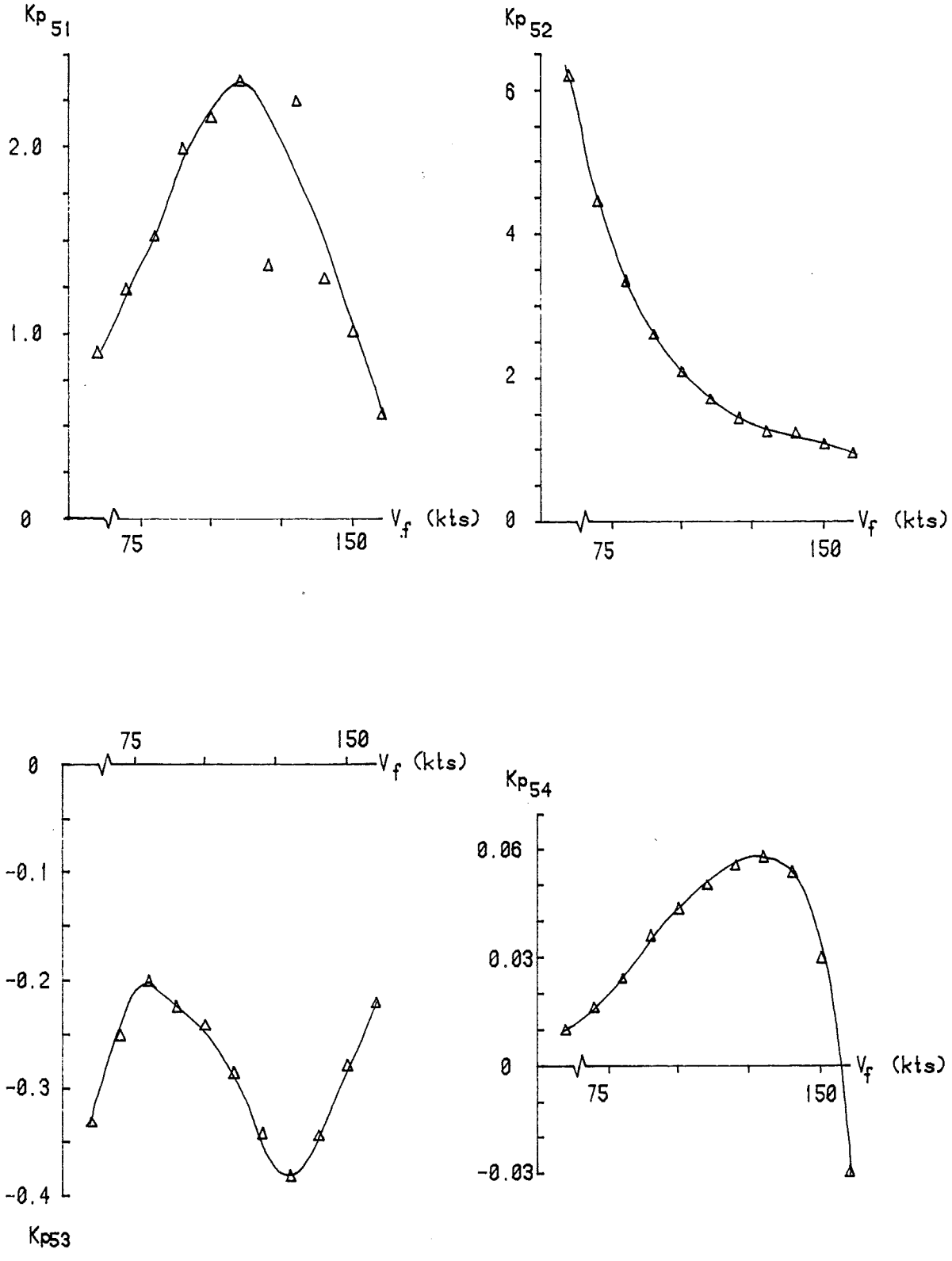

Figure 5:16 -- precompensator matrix gains; control Up5 ("tailplane incidence") as a function of collective, long. cyclic, lateral cyclic and tail rotor collective.

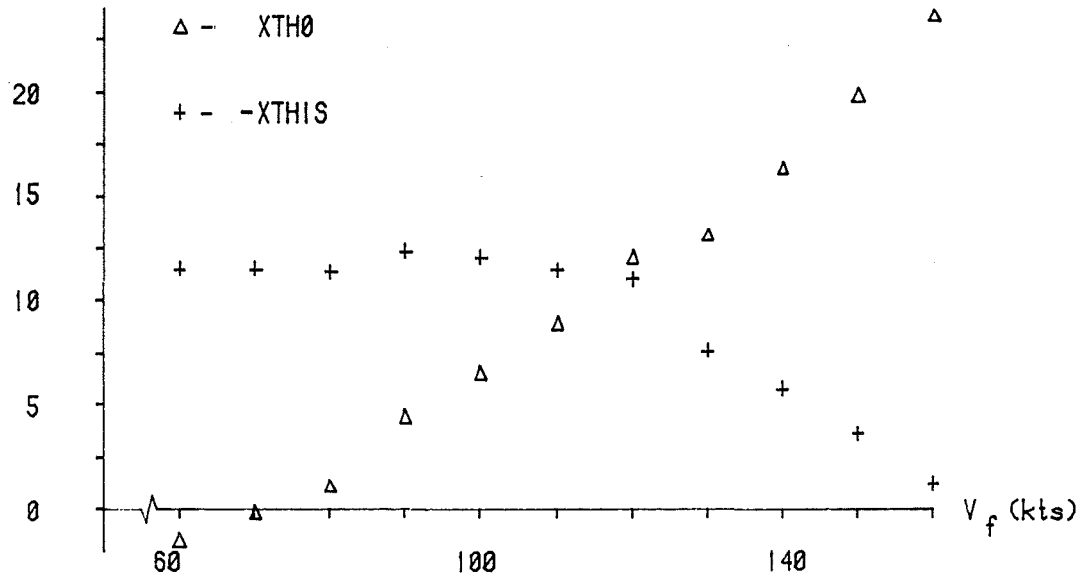

Figure 5:17 -- Variation in XTH0 and XTHIS with speed.

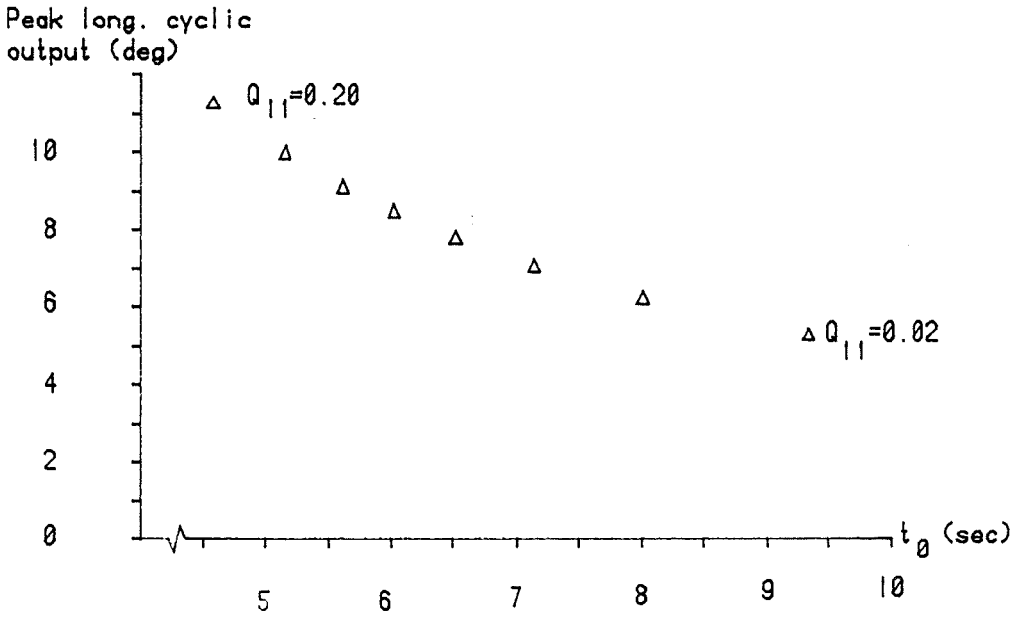

Figure 5:18 -- Relationship between response time and peak long. cyclic required; forward speed.

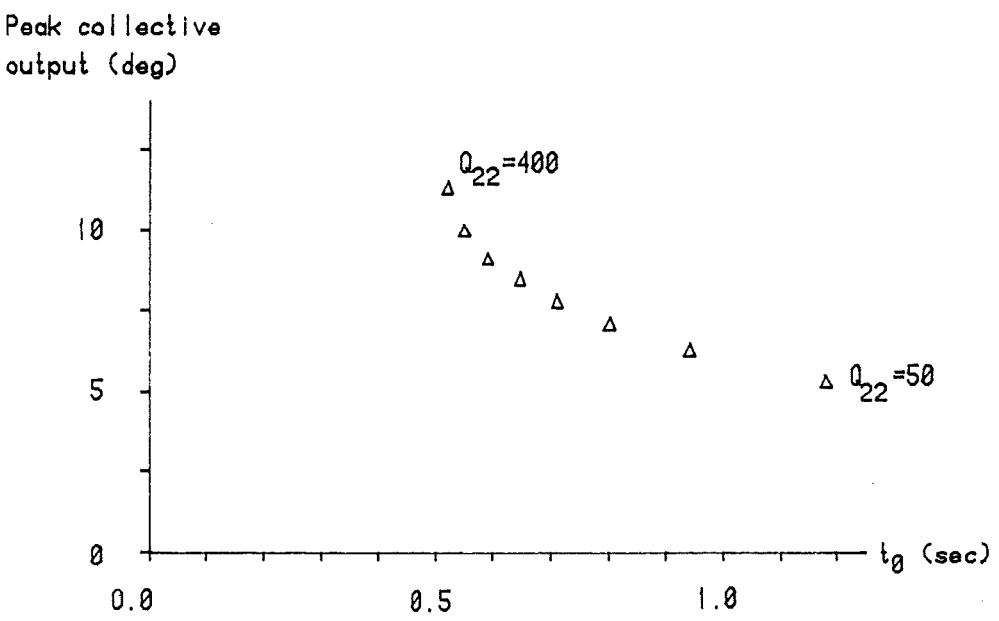

Figure 5:19 -- Relationship between response time and peak collective required; climb angle.

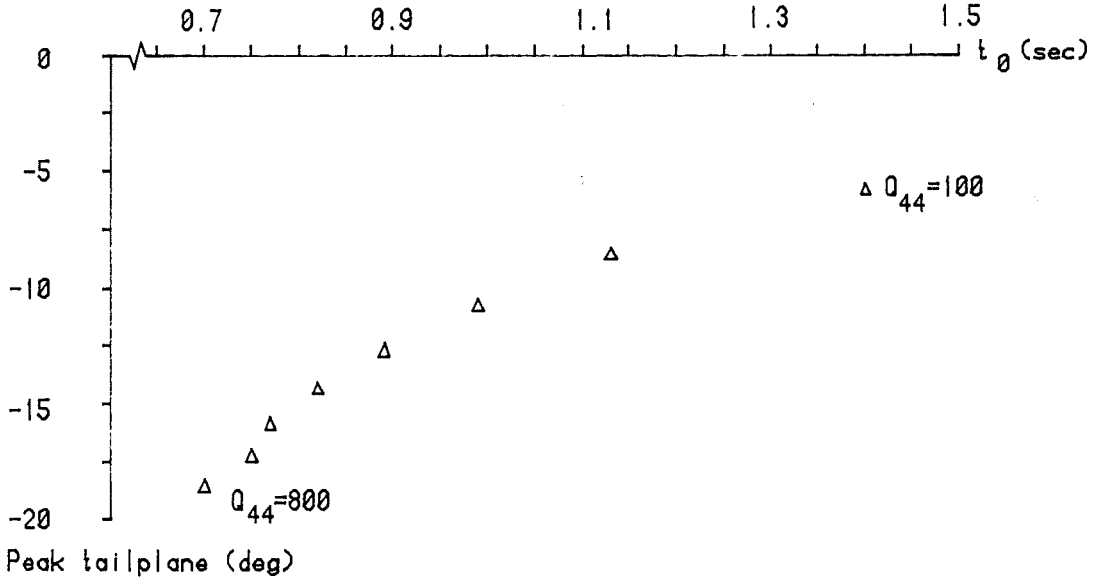

Figure 5:20 -- Relationship between response time and peak tailplane incidence required; pitch attitude.

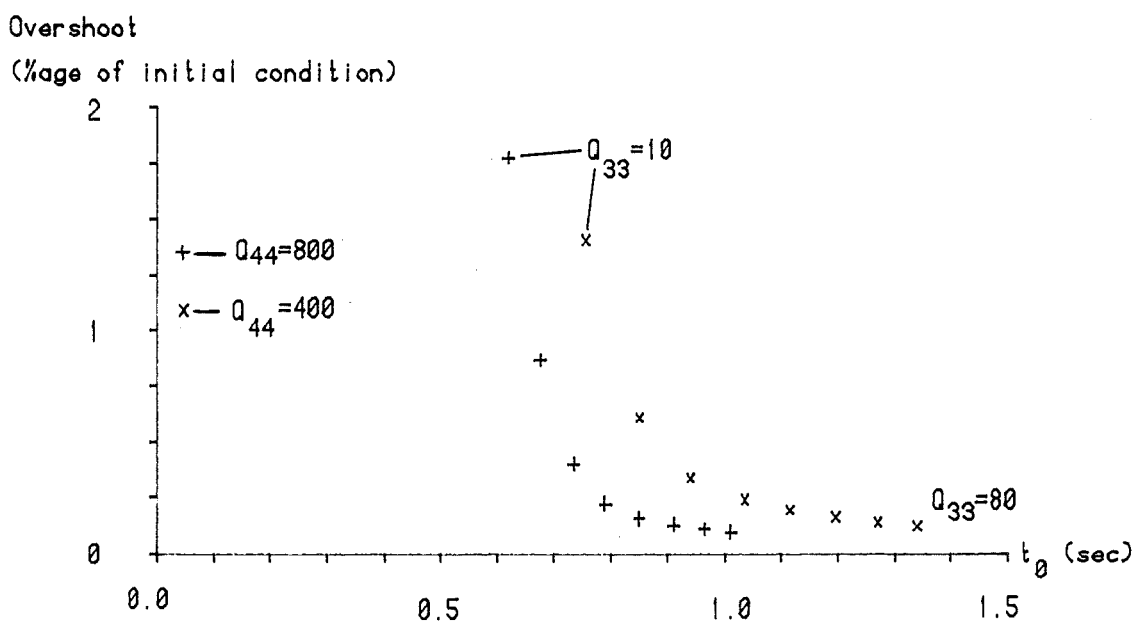

Figure 5:21 -- Relationship between overshoot and response time; pitch attitude

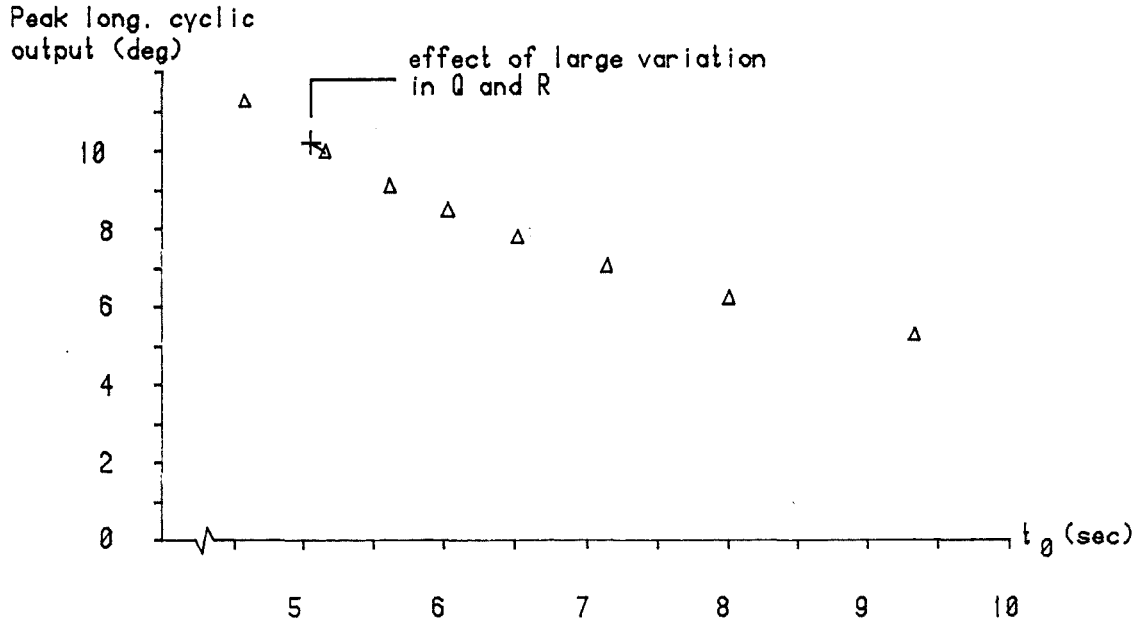

Figure 5:22 -- The effect on the relationship between response time and peak long. cyclic, of large variations in Q and R (see text).

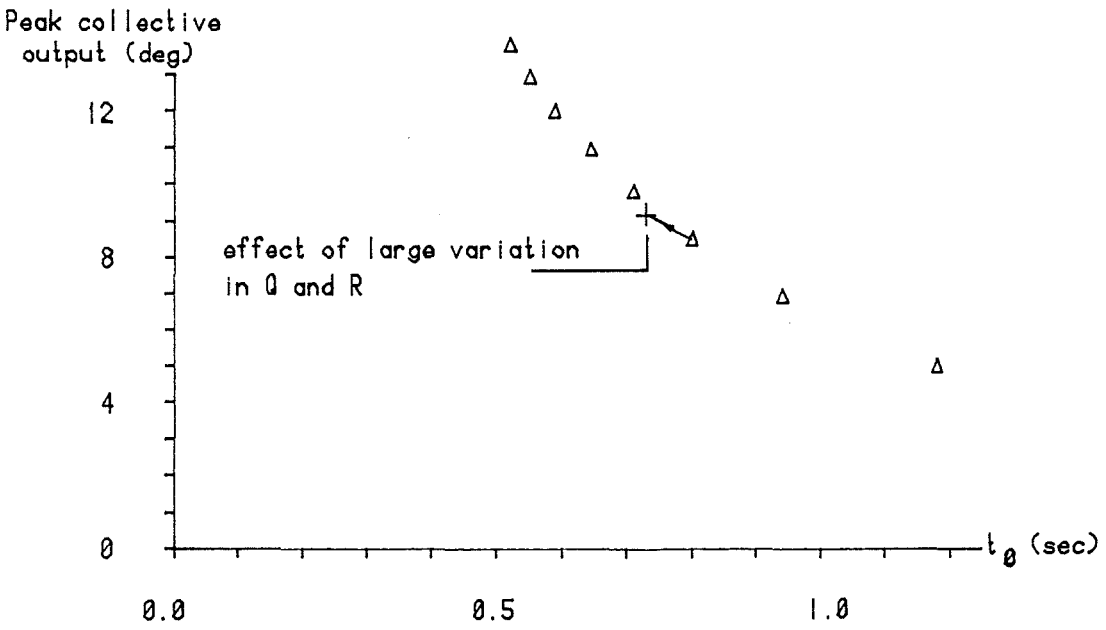

Figure 5:23 -- The effect on the relationship between response time and peak collective, of large variations in Q and R (see text); climb angle

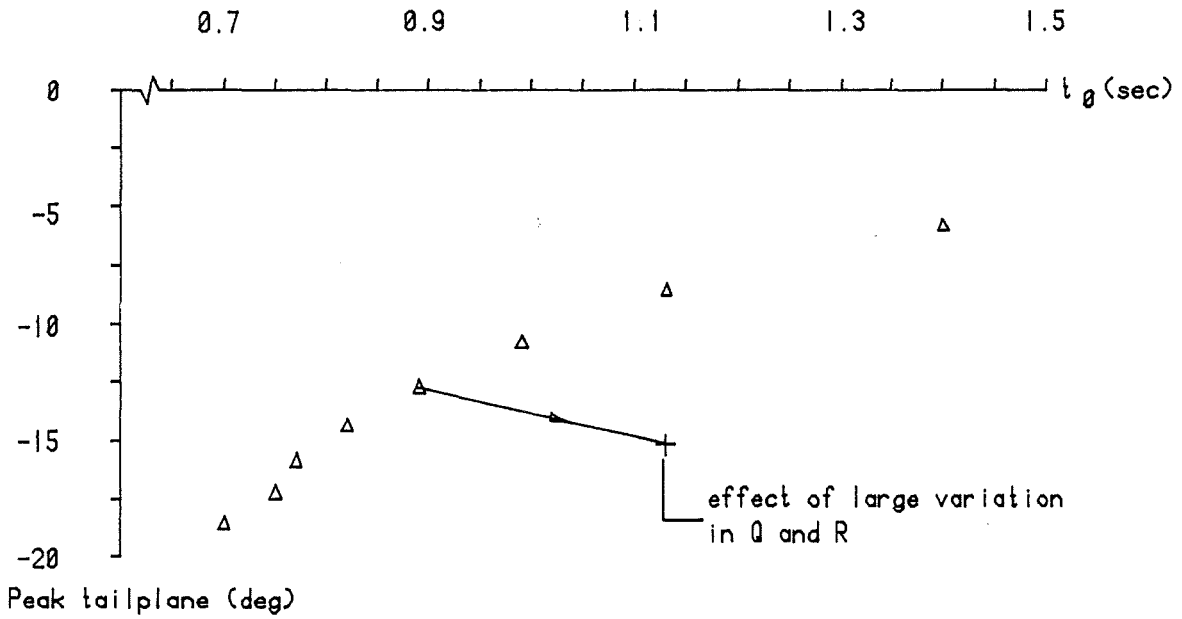

Figure 5:24 -- The effect on the relationship between response time and peak tailplane incidence, of large variations in Q and R (see text); pitch attitude.

$$u_{pf} = [\ u_{p1}\ u_{p2}\ u_{p3}\ u_{p4}\ u_{p5}\ ]^T$$

$$= -\begin{bmatrix} -0.0068 & 1.2865 & 0.0781 & 0.3208 & 0.0000 & -0.0109 & -0.1686 & -0.0034 & 0.0 \\ 0.0382 & -0.0873 & -0.0307 & -0.1845 & 0.0000 & -0.0006 & 0.0078 & -0.0045 & 0.0 \\ -0.0003 & -0.0135 & 0.0067 & 0.0637 & 0.0000 & 0.0154 & 0.1389 & -0.0035 & 0.0 \\ 0.0054 & 0.0533 & 0.0070 & -0.0199 & 0.0196 & 0.0342 & 0.0224 & -0.4529 & 0.0 \\ 0.0191 & -0.2432 & -0.6455 & -2.1425 & 0.0000 & -0.0200 & -0.0023 & 0.0030 & 0.0 \end{bmatrix} .$$

$$[\ \Delta V_f\ \gamma\ q\ \theta\ v\ p\ \phi\ r\ \psi\ ]^T$$

Figure 5:25 --- Feedback matrix for decoupled flight path and attitude controller, 100 knots.

OPEN LOOP

-10.6320

-0.8706 ± 2.7853i

-2.5044 ± 1.5069i

0.4499

-0.4430

-0.0150

0.0000

CLOSED LOOP

-10.6084

-7.6590

-7.0616

-5.0455

-4.4631

-3.6092

-1.9522

-0.6306

0.0000

Figure 5:26 --- Comparison of open and closed loop rigid-body eigenvalues with decoupled flight path and attitude controller, at 100 knots.

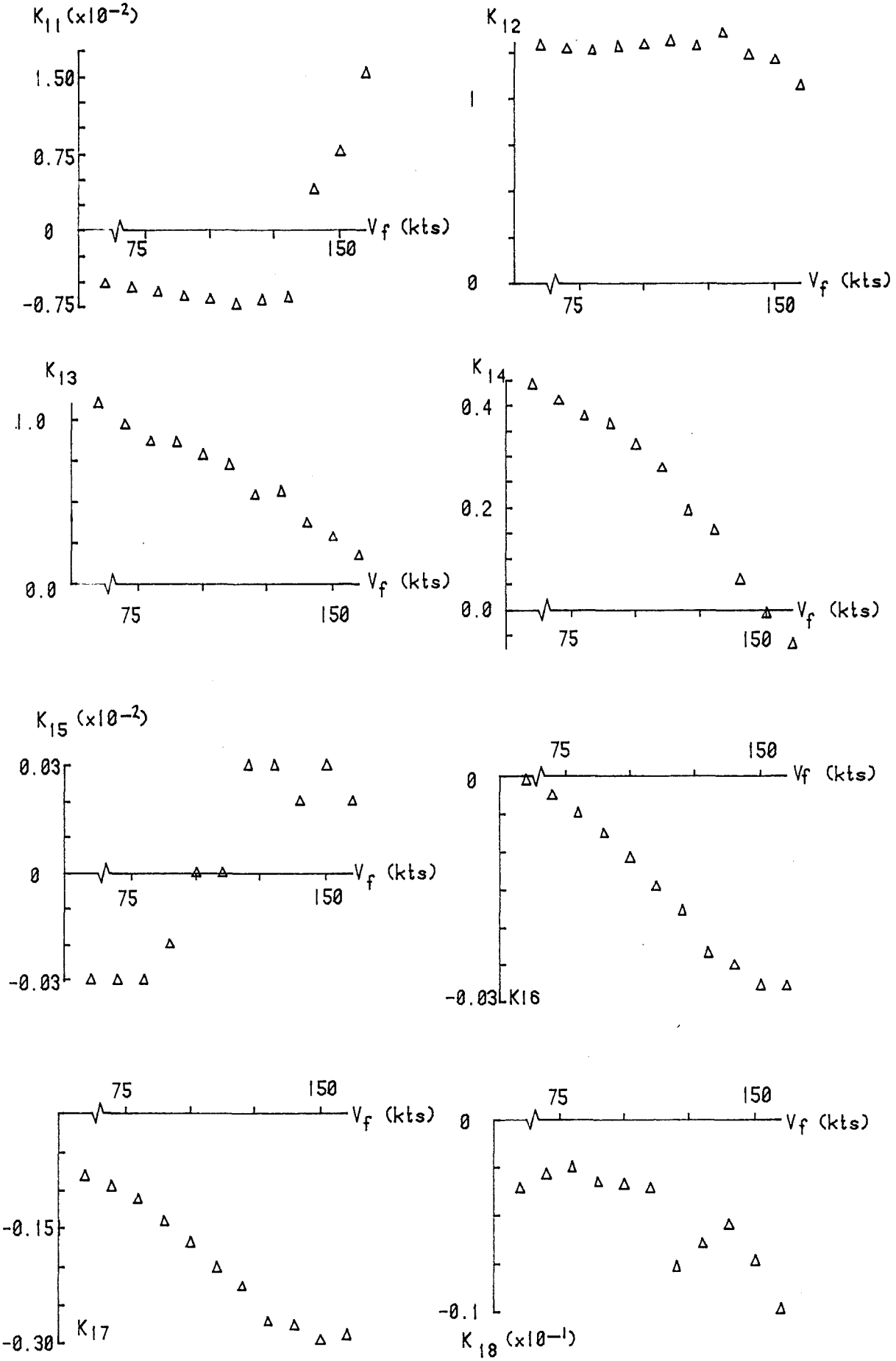

Figure 5:27 -- Control Upl "collective" gains.

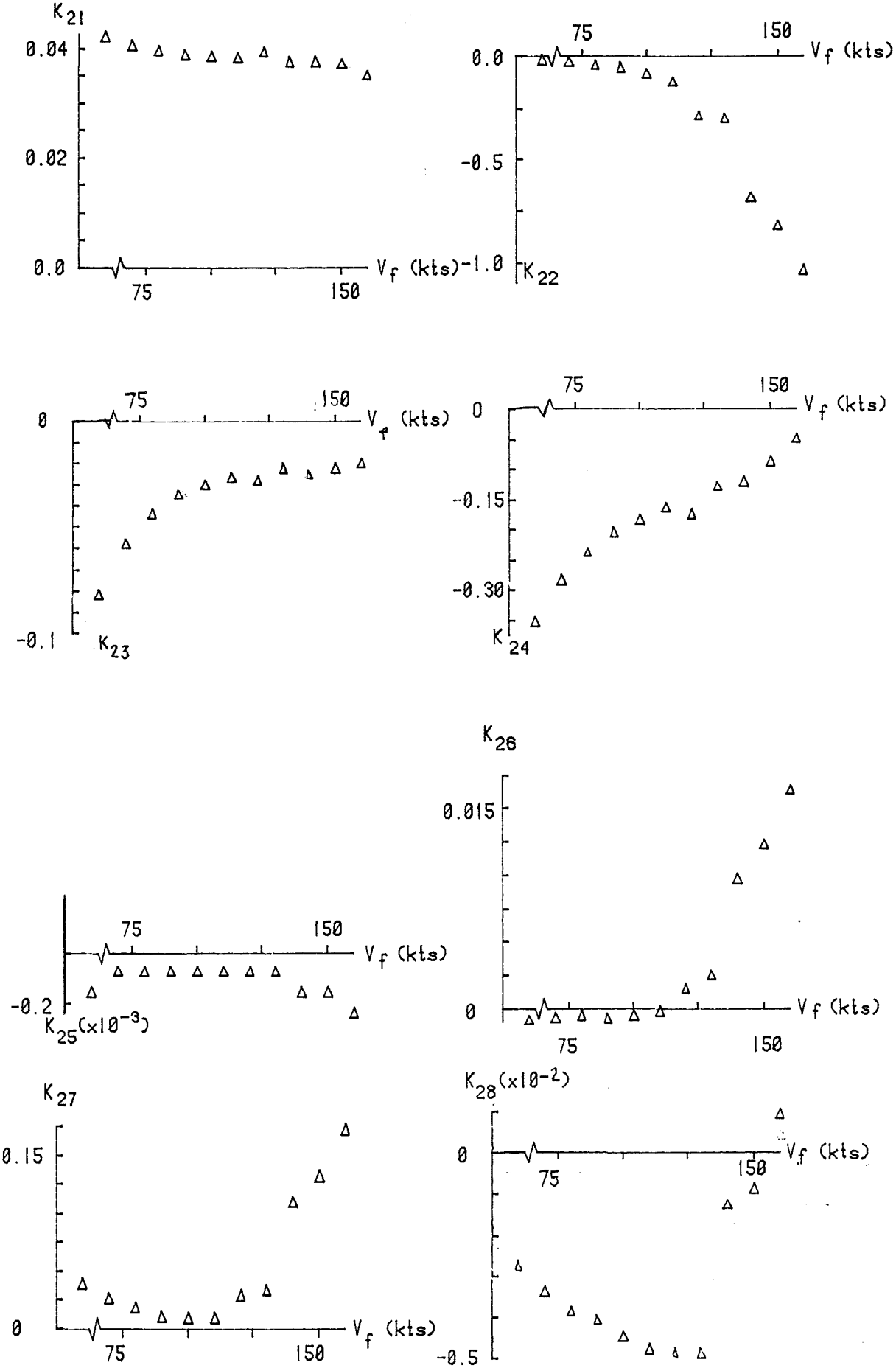

Figure 5:28 -- Control Up2 "long. cyclic" gains

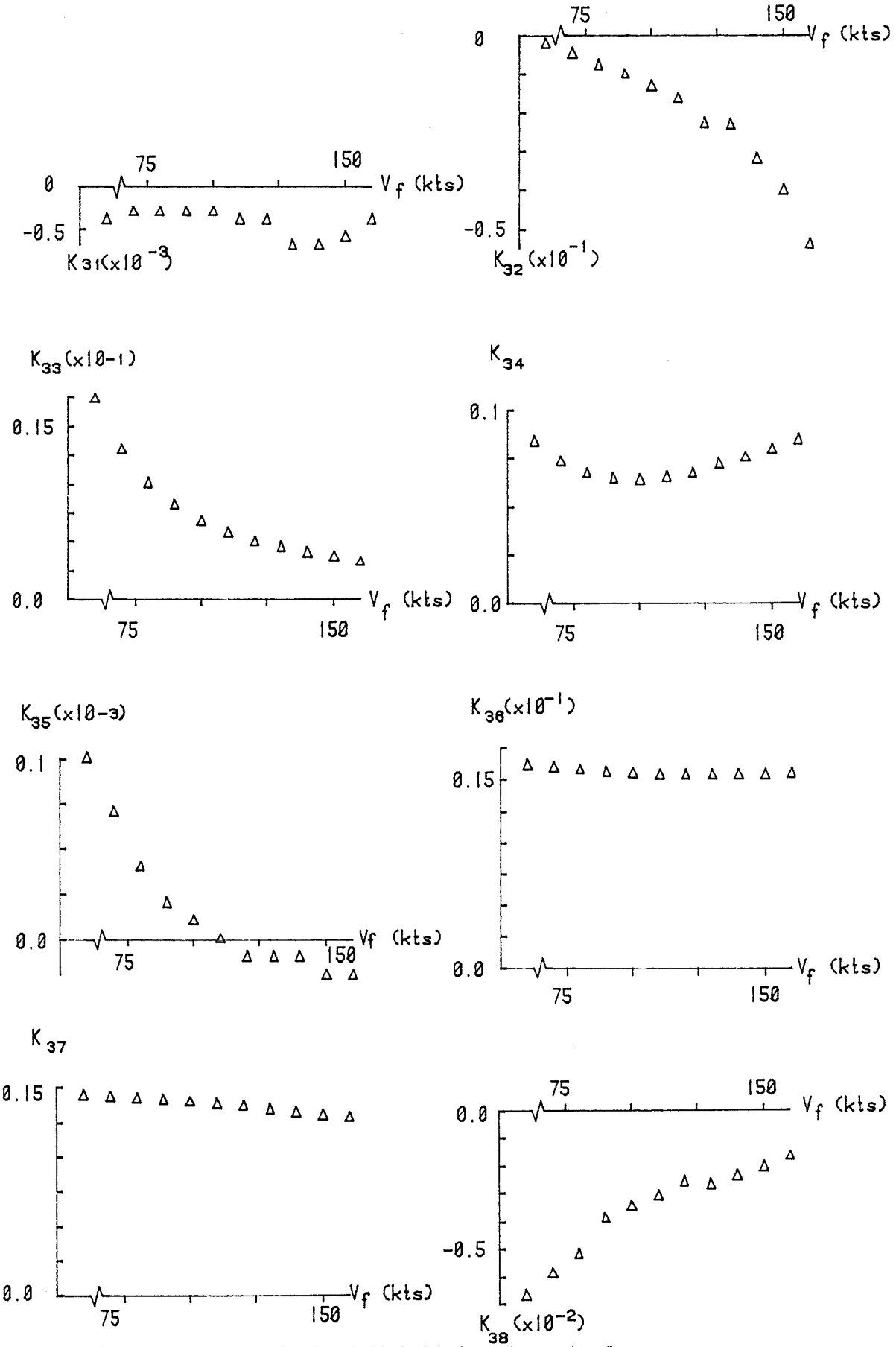

Figure 5:29 -- Control Up3 "lateral cyclic" gains

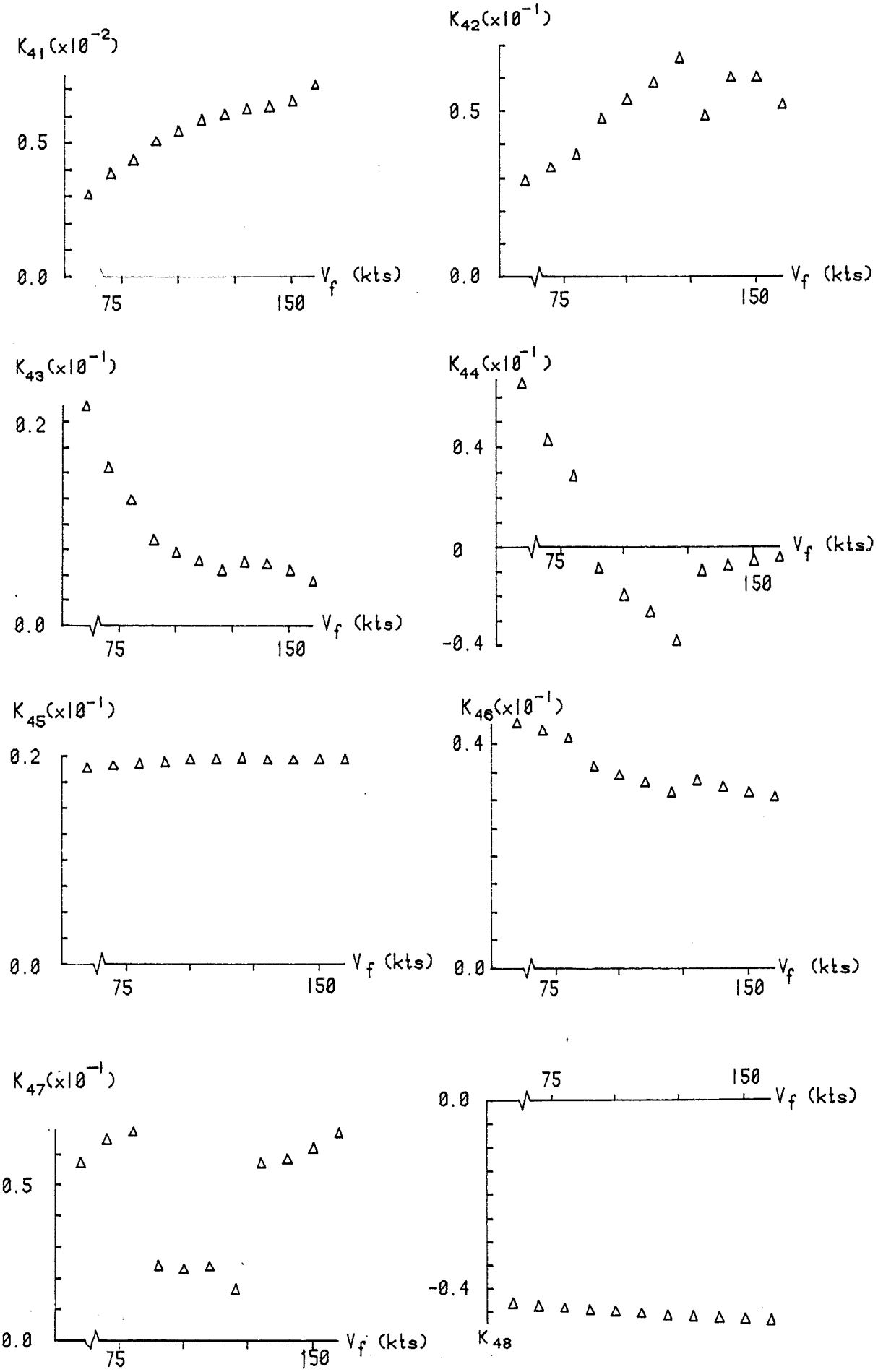

Figure 5:30 -- Control Up4 "tail rotor" gains

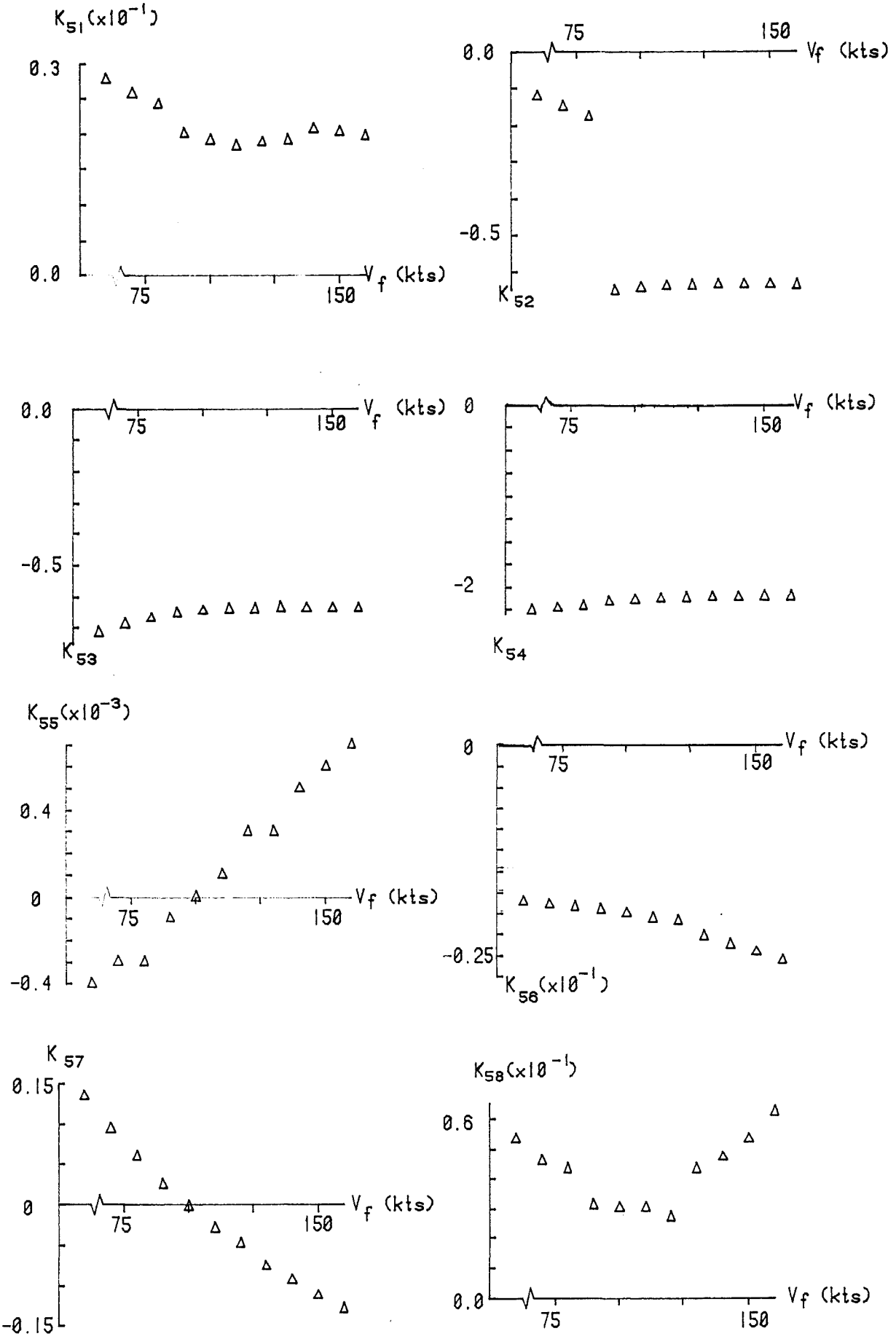

Figure 5:31 -- Control Up5 'tailplane' gains

$$\begin{bmatrix} 1.6110 & 0.6273 & 4.5751 \\ 5.1398 & -0.0250 & 0.0116 \\ -2.0793 & -0.0277 & 29.1610 \end{bmatrix}$$

Figure 5:32 --- Submatrix B_f' of the full forcing function matrix B_f, decoupled flight path and body attitude controller. Demand vector is ordered $x_d = [\ \gamma_d \quad \Delta V_{fd} \quad \Theta_d\ ]^T$.

$$\begin{bmatrix} u_{p2} \\ u_{p1} \\ u_{ps} \end{bmatrix} = \begin{bmatrix} 0.0415 & 0.0991 & 0.2989 \\ -0.0062 & 1.6296 & 0.0874 \\ -0.0024 & 0.1848 & -2.5927 \end{bmatrix} \cdot \begin{bmatrix} \Delta V_{fd} \\ \gamma_d \\ \Theta_d \end{bmatrix}$$

Figure 5:33 --- Submatrix K_f' of the full feedforward matrix K_f, decoupled flight path and body attitude controller.

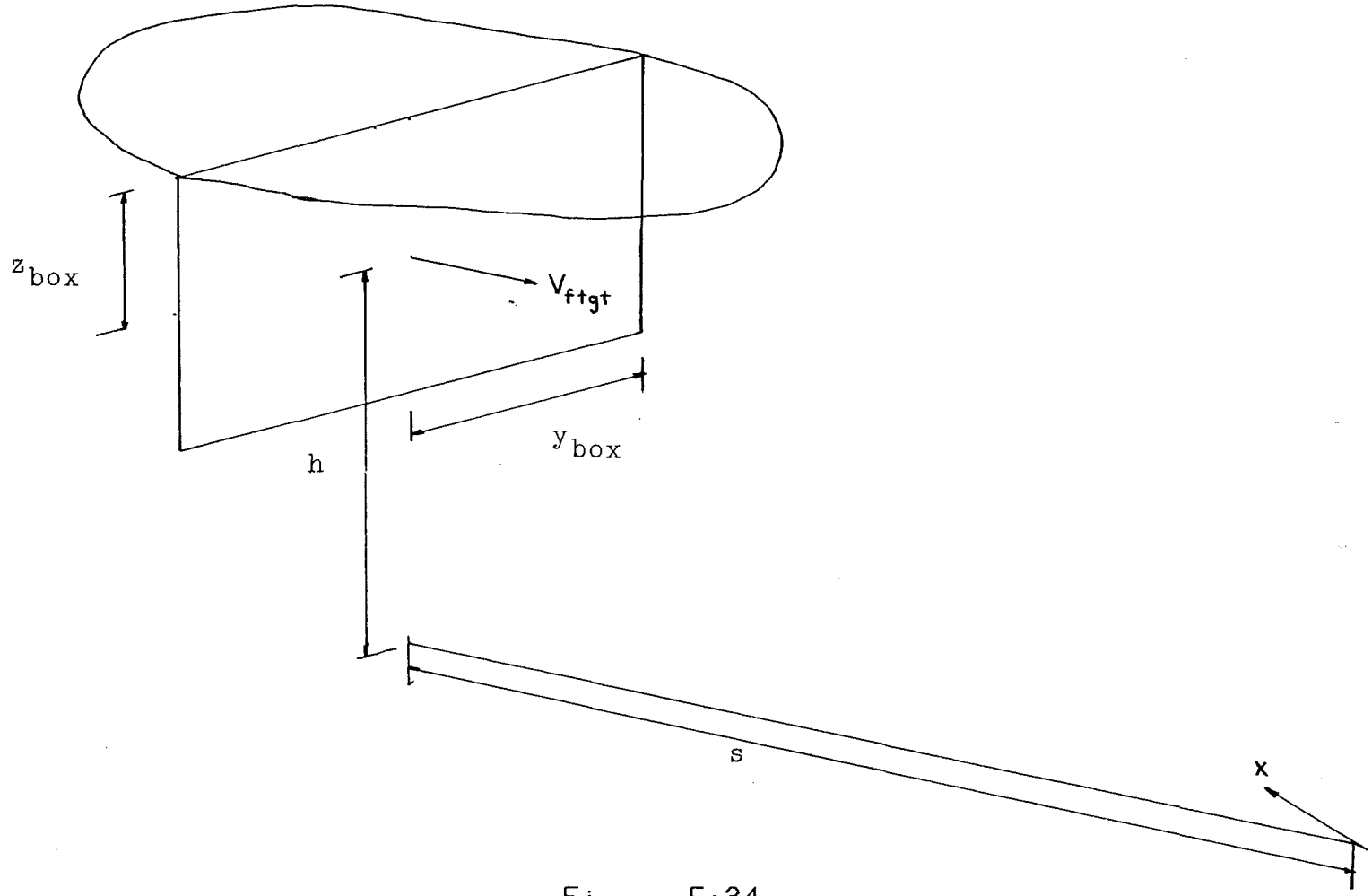

Figure 5:34

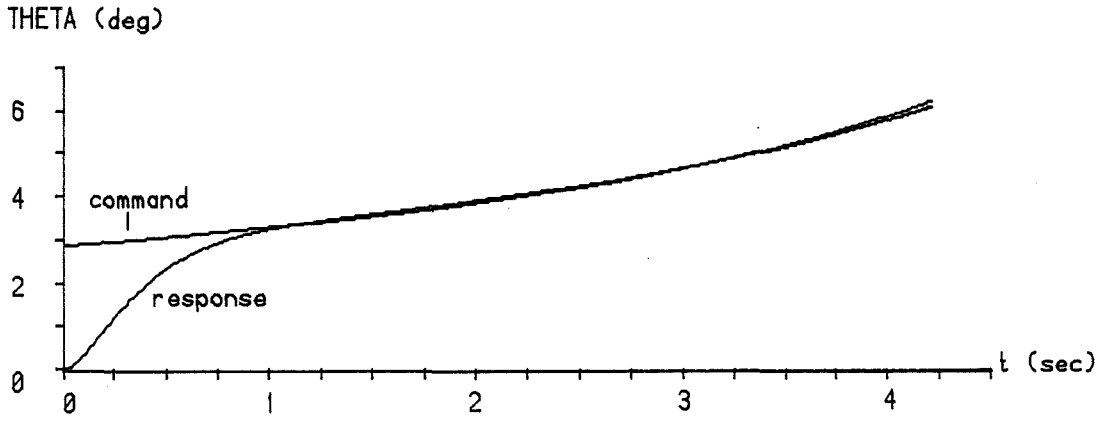

Figure 5:35 -- Pitch command and response to acquire and track given target.

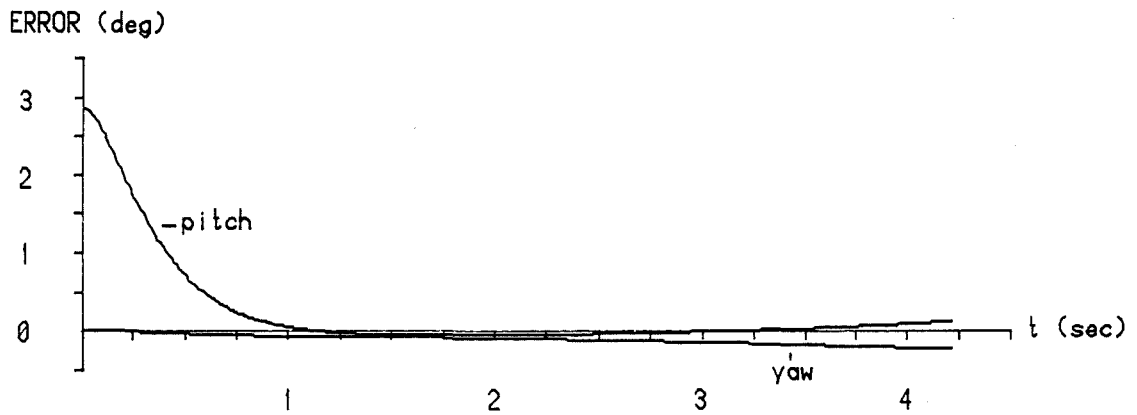

Figure 5:36 -- Pitch and yaw attitude errors in acquiring and tracking target.

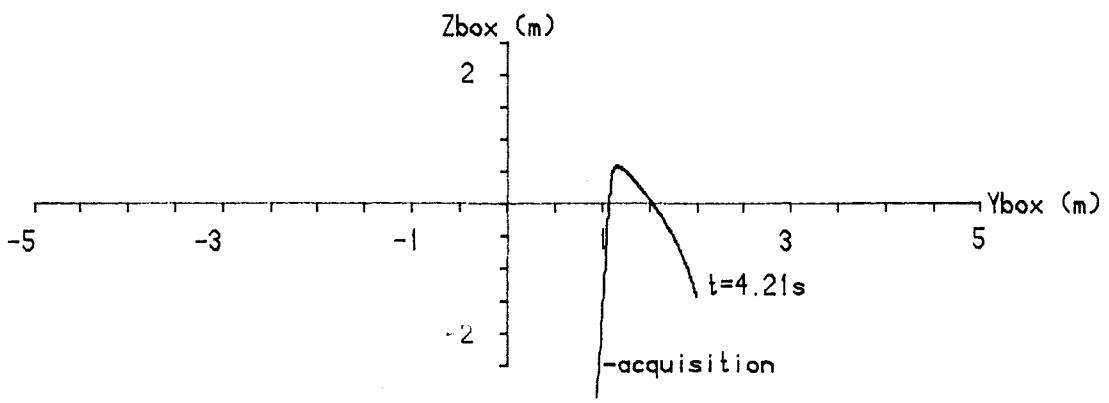

Figure 5:37 -- Projection of helicopter's x-axis on target plane during manoeuvre.

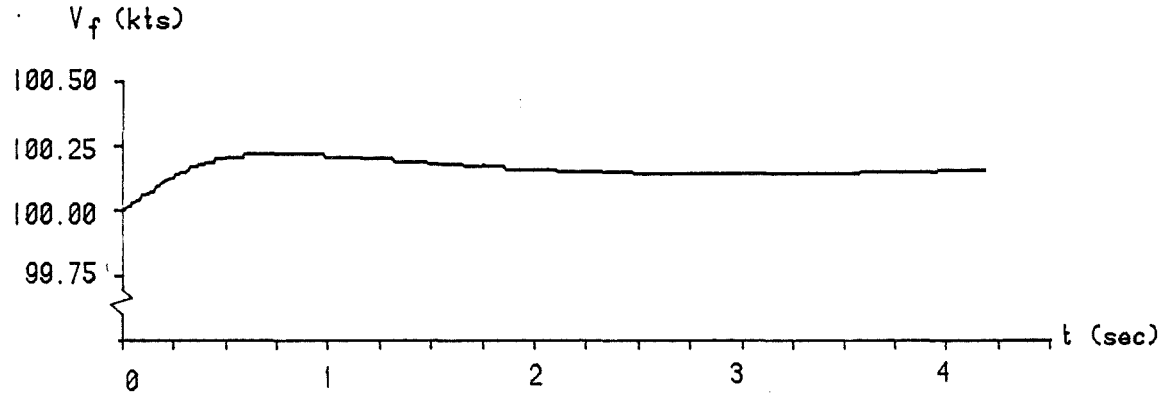

Figure 5:38 -- Helicopter flight speed during decoupled attitude tracking manoeuvre.

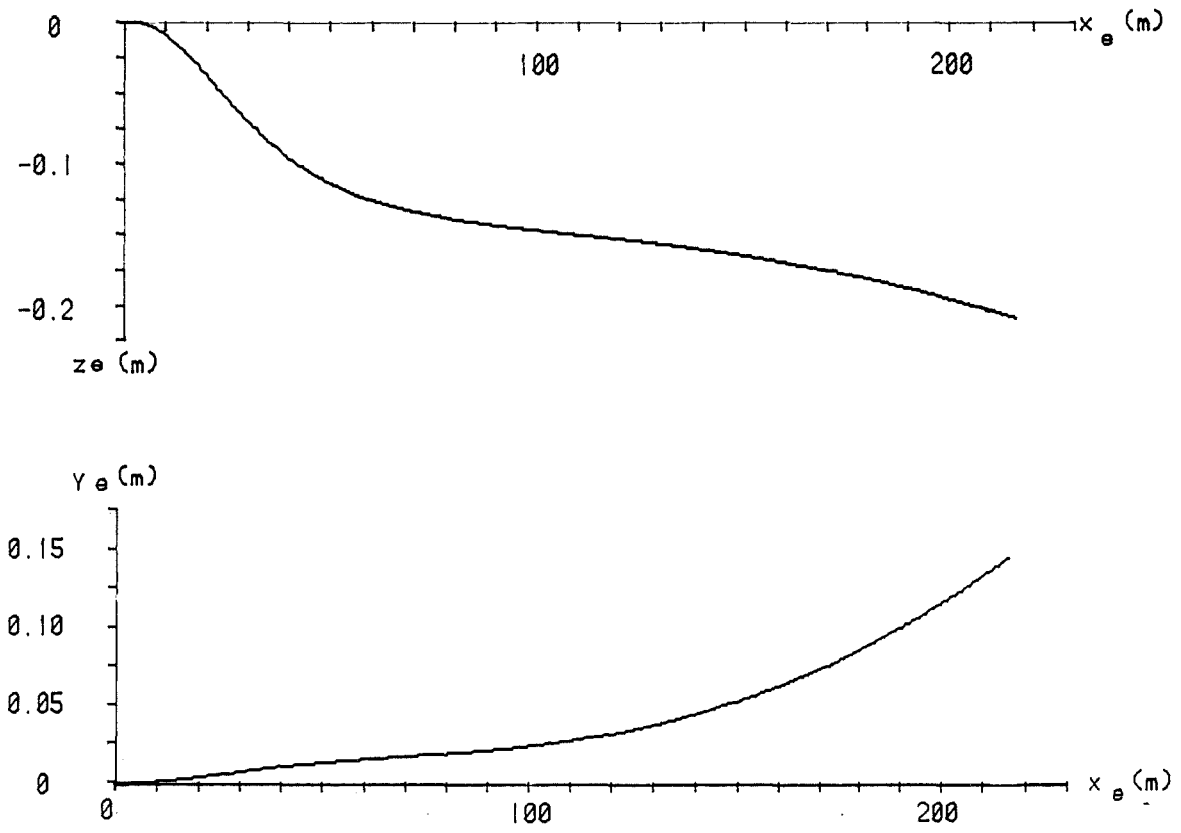

Figure 5:39 -- Helicopter trajectory during decoupled attitude tracking manoeuvre.

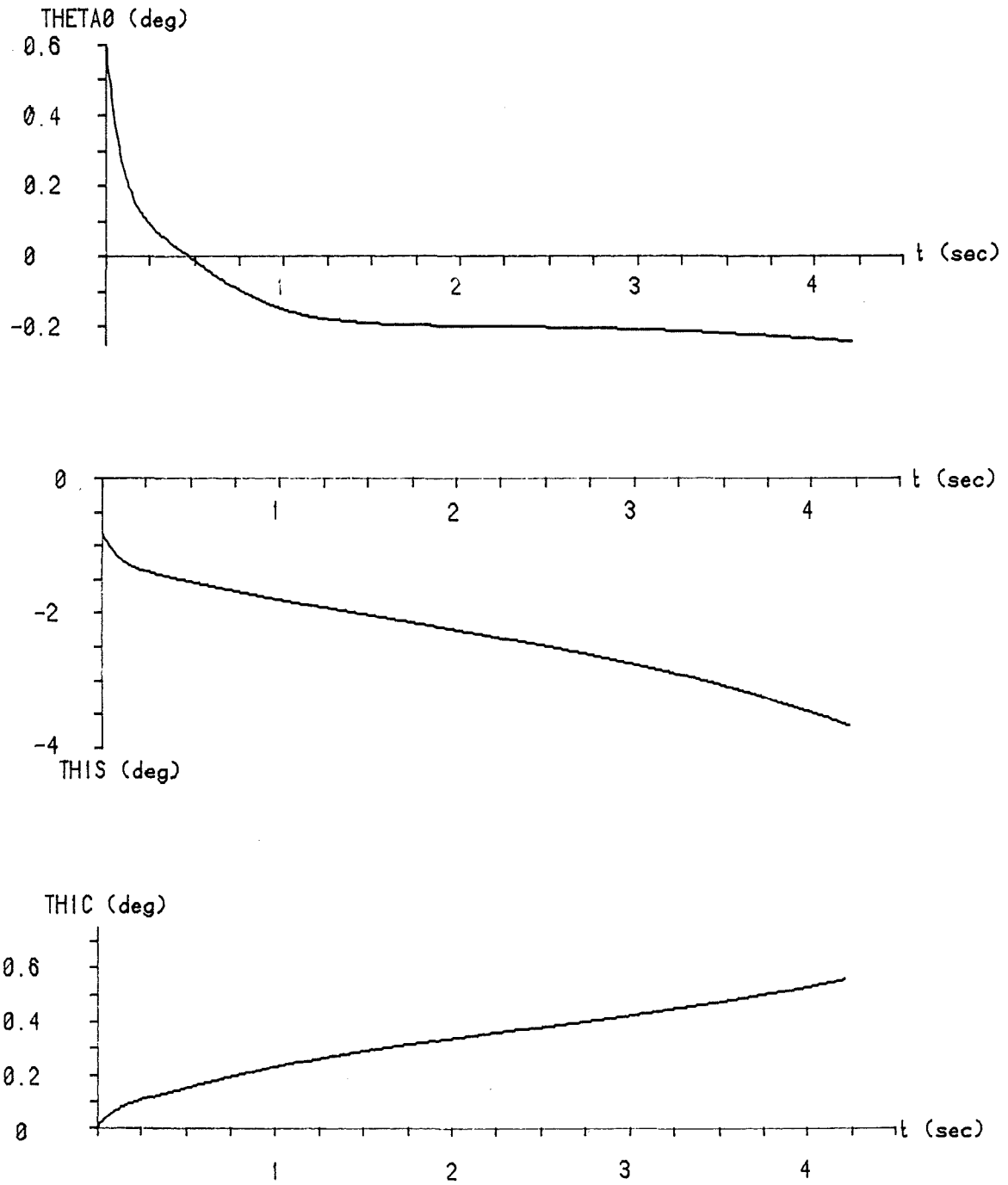

Figure 5:40 -- Control time histories for decoupled attitude tracking manoeuvre.

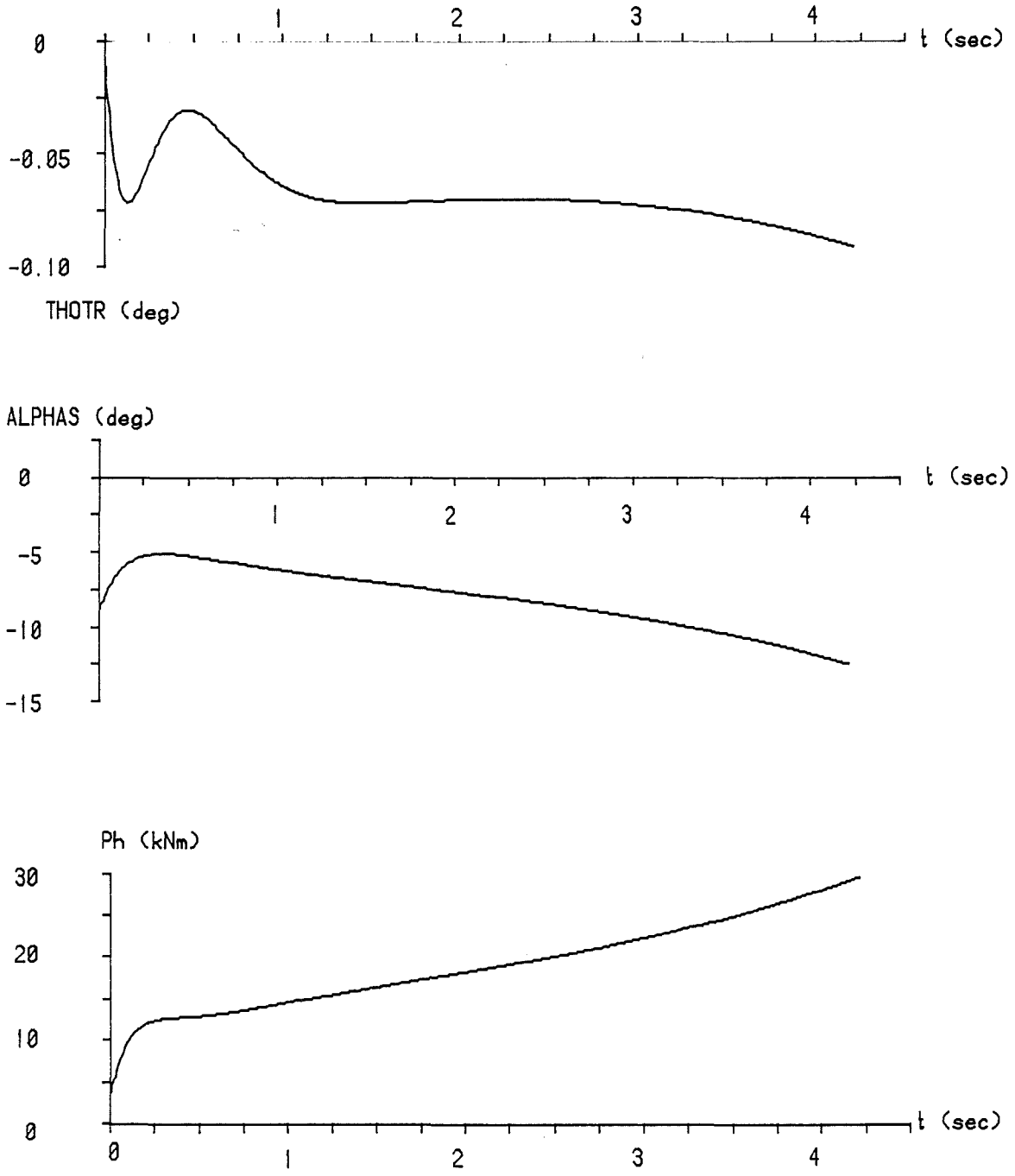

Figure 5:40 -- concluded

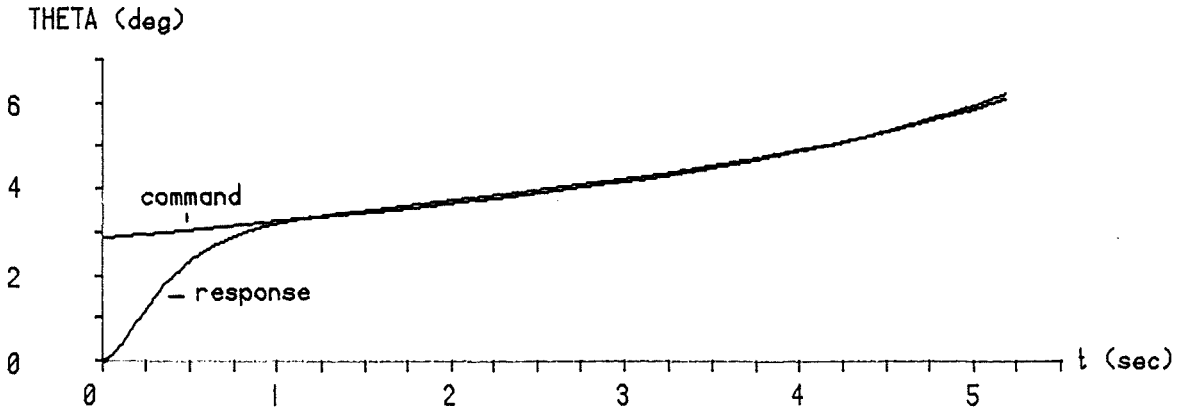

Figure 5:41 -- Pitch command and response to acquire and track given target.

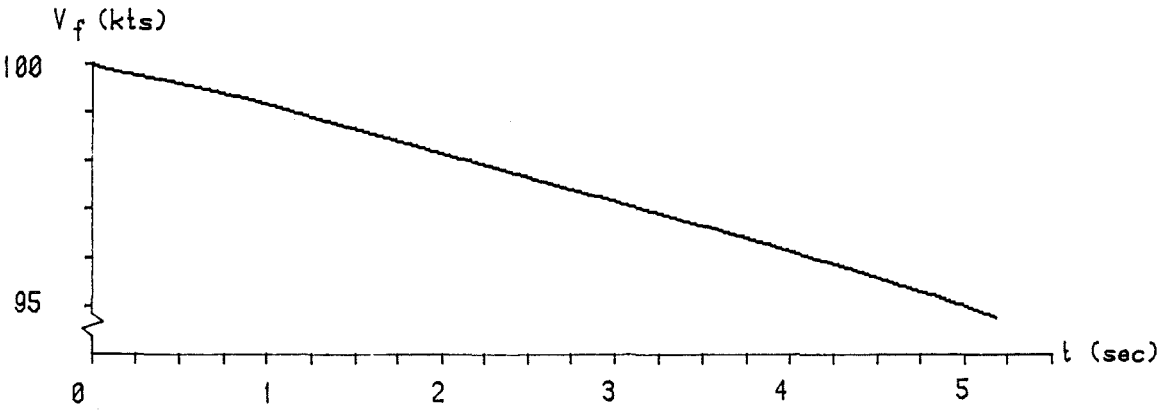

Figure 5:42 -- Helicopter flight speed during attitude tracking manoeuvre.

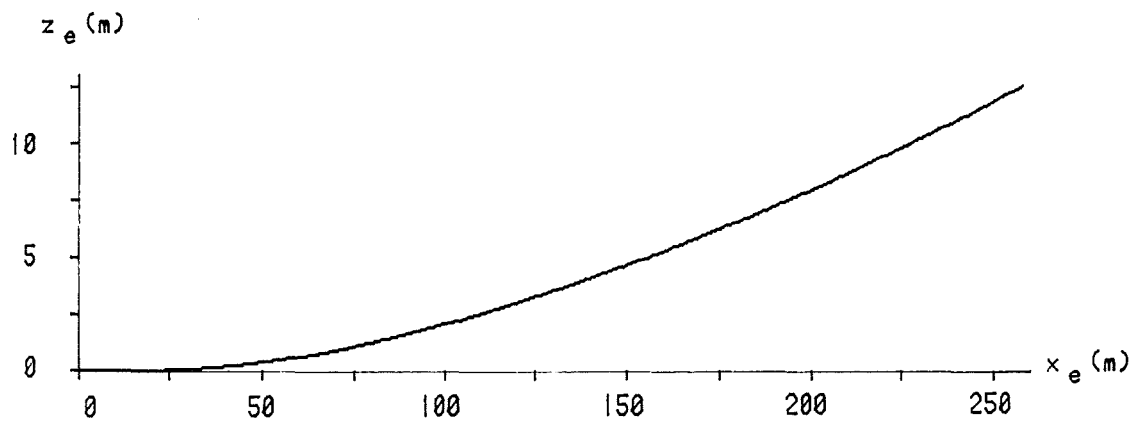

Figure 5:43 -- Helicopter trajectory during attitude tracking manoeuvre.

Aircraft mass	4314kg
I_x	2767kgm^2
I_y	13905kgm^2
I_z	12209kgm^2
I_{xz}	2035kgm^2
Ω	35.63kgm^2
R	6.40m
s	0.0778
a	6.00
γ_s	4 deg
h_R	0.1986
h_{tr}	0.1786
x_{cg}	-0.0198
a_t	-1 deg
β_{cant}	-3 deg
δ_o	7.119
$\lambda_\beta{}^2$	1.2
h_{fin}	0.0838
l_t	7.5341m
l_{tr}	7.5341m
l_{fin}	7.5533m
V_t	0.1407
s_t	0.208
Ω_t	206.654rads^{-1}

Table 2:1 - Table of helicopter leading data

	Model			
	Bramwell		Centre-Spring	
Coeff. of	θ_o	θ_{1s}	θ_o	θ_{1s}
Speed (kts)				
60	-0.4334	-1.1508	-0.3189	-0.8508
100	-0.7365	-1.2217	-0.5317	-0.9118
160	-1.2330	-1.4019	-0.8508	-1.0604

Table 2:2 - Comparison of two coefficients in the equation of longitudinal flapping given by different rotor models.

Type	Eigenvalue
Longitudinal	-3.2741
"	-0.3706
"	0.1992+0.3752i
"	0.1992-0.3752i
Lateral	-10.6425
"	-0.7968+2.6268i
"	-0.7968-2.6268i
"	-0.0225
"	0.0

Table 3:1 -- Rigid-body eigenvalues for Westland Lynx, 100 knots. Model HELSIM.

Full model	Reduced model	Error
-3.2741	-2.8567	-12.75%
-0.3706	-0.4252	+14.75%
0.1992+0.3752i	0.1598+0.3827i	-19.8%,+2%
0.1992-0.3752i	0.1598-0.3827i	-19.8%,+2%

Table 3:2 -- Comparison of longitudinal eigenvalues obtained using reduced order model in longitudinal dof's alone with those of the full system.

Eigenvalue	-3.2741	-0.3706
	Eigenvectors	
u	0.0278	0.5266
w	0.9937	-0.5606
q	-0.0462	-0.0053
θ	0.0141	0.0147
v	0.0890	0.6367
p	0.0381	-0.0150
ϕ	-0.0117	0.0403
r	0.0030	0.0105
ψ	-0.0007	-0.0281

Table 3:3 -- Eigenvectors of the two real longitudinal eigenvalues - full system description.

Eigen-value	Relevant column of $E_{11}\Lambda_1$	Relevant column of $A_{12}(A_{21}E_{11}+A_{22}E_{21})\Lambda_1$	Coupling as %-age of $E_{11}\Lambda_1$
-3.2741	-0.09102	-0.0061	6.7%
	-3.25347	-0.0284	0.87%
	0.15126	0.0297	19.64%
	-0.04616	0.0	0.0%

Table 3:4a -- Influence of coupling terms on the identity for

$\lambda_1 = -3.2741$

Eigen-value	Relevant column of $E_{11}\Lambda_1$	Relevant column of $A_{12}(A_{21}E_{11}+A_{22}E_{21})\Lambda_1$	Coupling as %-age of $E_{11}\Lambda_1$
-0.3706	-0.19516	0.0026	1.33%
	0.20776	0.0069	3.32%
	0.00196	-0.0103	525.5%
	-0.00540	0.0	0.0%

Table 3:4b -- Influence of coupling terms on the identity for

$\lambda_1 = -0.3706$

Model	Full	Reduced (Longitudinal)	Reduced (Long.+roll)
Eigenvalue	-3.2741	-2.8567	-3.2795
	-0.3706	-0.4252	-0.3708
	0.1992+0.3752i	0.1598+0.3827i	0.1980+0.3708i
	0.1992-0.3752i	0.1598-0.3827i	0.1980-0.3708i

Table 3:5 -- Comparison of longitudinal rigid-body eigenvalues of Lynx helicopter at 100 knots, with three levels of model.

Initial condition	Response time t_0 (sec)	Peak control output
$\Delta V_{f0} = 5ms^{-1}$	$\Delta V_f = 0.05\Delta V_{f0}$ at 4.76 s	$\theta_{1s} = 11.82°$
$\gamma_0 = 10°$	$\gamma = 0.05\gamma_0$ at 0.58 s	$\theta_0 = 11.95°$
$\theta_0 = 10°$	$\theta = 0.05\theta_0$ at 0.6 s	$\alpha_s = 9.41°$

Table 5:1 --- Response characteristics of the longitudinal degrees of freedom at 100 knots with decoupled flight path and attitude controller.

Initial condition: $\Delta V_{f0}=5ms^{-1}$		
state	peak perturbation	time of peak (sec)
γ	1.033°	0.48
θ	0.179°	0.83
v	$0.267ms^{-1}$	0.69
ϕ	-0.089°	1.40
ψ	-0.299°	0.72

Table 5:2 --- Coupled responses to the initial condition in forward speed.

Initial condition: $\gamma_0 = 10°$		
state	peak perturbation	time of peak (sec)
ΔV_f	$-0.035 ms^{-1}$	0.70
θ	0.186°	0.38
v	$0.033 ms^{-1}$	0.17
ϕ	-0.074°	0.42
ψ	0.047°	0.55

Table 5:3 --- Coupled responses to the initial condition in climb angle.

Initial condition: $\theta_0 = 10°$		
state	peak perturbation	time of peak (sec)
ΔV_f	$-0.344 ms^{-1}$	0.68
γ	0.603°	0.40
v	$-0.117 ms^{-1}$	0.41
ϕ	1.368°	0.62
ψ	0.100°	0.47

Table 5:4 --- Coupled responses to the initial condition in pitch attitude.

Appendix 1

These analytical expressions were used in the worked example in section 3:3.2, and therefore pertain to the given ordering of the state vector, and partitioning into subsystems. For the identity in λ_i, let the eigenvectors be denoted by

$$[\ e_{ui}\ e_{wi}\ e_{qi}\ e_{\theta i}\ e_{vi}\ e_{pi}\ e_{\phi i}\ e_{ri}\ e_{\psi i}\ ]^T$$

where e_{ui}, e_{wi} etc. are the vectors representing the states u,w, etc. in the mode λ_i. Then the relevant column of $A_{12}E_{11}+A_{22}E_{21}$ is given by

$$\begin{aligned}
&Y_u e_{ui} + Y_w e_{wi} + Y_q e_{qi} + Y_\theta e_{\theta i} + Y_v e_{vi} + Y_p e_{pi} + Y_\phi e_{\phi i} + Y_r e_{ri} + Y_\psi e_{\psi i} = Ye\\
&L_u e_{ui} + L_w e_{wi} + L_q e_{qi} + L_\theta e_{\theta i} + L_v e_{vi} + L_p e_{pi} + L_\phi e_{\phi i} + L_r e_{ri} + L_\psi e_{\psi i} = Le\\
&\qquad\qquad k_1 e_{qi} \qquad\qquad + k_2 e_{pi} \qquad\quad + k_3 e_{ri} \qquad\quad = k_1 e\\
&N_u e_{ui} + N_w e_{wi} + N_q e_{qi} + N_\theta e_{\theta i} + N_v e_{vi} + N_p e_{pi} + N_\phi e_{\phi i} + N_r e_{ri} + N_\psi e_{\psi i} = Ne\\
&\qquad\qquad k_4 e_{qi} \qquad\qquad\qquad\qquad\qquad + k_5 e_{ri} \qquad\quad = k_2 e
\end{aligned}$$

----- A3:1

Dividing each element of A3:1 gives $(A_{12}E_{11}+A_{22}E_{21})\Lambda_1^{-1}$. Then the relevant column of $A_{12}(A_{12}E_{11}+A_{22}E_{21})\Lambda_1^{-1}$ is given by

$$\begin{aligned}
&(\ X_v Ye + X_p Le + X_\phi k_1 e + X_r Ne + X_\psi k_2 e\ ) / \lambda_i\\
&(\ Z_v Ye + Z_p Le + Z_\phi k_1 e + Z_r Ne + Z_\psi k_2 e\ ) / \lambda_i\\
&(\ M_v Ye + M_p Le + M_\phi k_1 e + M_r Ne + M_\psi k_2 e\ ) / \lambda_i \qquad \text{----- A3:2}\\
&k_6 Ne\ /\ \lambda_i
\end{aligned}$$

The k_i are constants determined by the trim state of the helicopter. A3:1 is the analytic expression corresponding to (A3:1a), A3:2 is that corresponding to (A3:2a).

Appendix 2

The elements of the matrices C, D, E and F in chapter 4 are given in this appendix. They are obtained simply from

$$u = V_f\cos\alpha - V_{fe}\cos\theta_e$$

$$w = V_f\sin\alpha - V_{fe}\sin\theta_e$$

$$\alpha = \theta + \theta_e - \gamma$$

and assuming that $V_f=V_{fe}$, $\sin\theta\simeq\theta$ and $\cos\theta\simeq 1$. Then

$$C = \begin{bmatrix} 0 & V_{fe}\sin(\gamma - \theta_e) \\ 0 & V_{fe}\cos(\gamma - \theta_e) \end{bmatrix}, \quad D = \begin{bmatrix} V_{fe}\{ \cos(\gamma - \theta_e) - \cos\theta_e \} \\ -V_{fe}\{ \sin(\gamma - \theta_e) + \sin\theta_e \} \end{bmatrix}$$

$$E = \begin{bmatrix} V_{fe}\sin(\gamma - \theta_e) & V_{fe}\dot{\gamma}\cos(\gamma - \theta_e) \\ V_{fe}\cos(\gamma - \theta_e) & -V_{fe}\dot{\gamma}\sin(\gamma - \theta_e) \end{bmatrix}$$

$$F = \begin{bmatrix} -V_{fe}\dot{\gamma}\sin(\gamma - \theta_e) \\ -V_{fe}\dot{\gamma}\cos(\gamma - \theta_e) \end{bmatrix}.$$

Appendix 3

An FCS was synthesised, that retained the traditional pattern of helicopter control, viz. flight path and speed changes through control of the body attitudes. As well as conferring positive stability, the FCS gave similar attitude response characteristics to that of the helicopter with the decoupled flight path and body attitude controller. Synthesis of the FCS was made in two stages, and the overall process was crude compared with that adopted for the other FCS. The purpose of this appendix is to describe the synthesis technique. The controller was calculated only for the 100 knots flight condition.

The first stage was to decouple the attitude dynamics from translational dynamics. The state vector was reordered as

$$x = [\ q \quad p \quad r \quad \Theta \quad \Phi \quad \psi \quad \Delta V_f \quad v \quad \gamma\ ]^T$$

and the resulting system matrix partitioned thus;

$$A = \begin{bmatrix} A_{11} & A_{12} \\ A_{21} & A_{22} \end{bmatrix},$$

where A_{11} is a 6x6 matrix of attitude terms only, A_{22} a 3x3 of translational dynamics alone, and A_{12} and A_{21} the coupling terms. A_{12} is a 6x3 matrix, but three rows are null - the three rows that would form terms in the kinematic relationships between p, q, r and Φ, Θ, ψ. Denoting the submatrix of the remaining three rows A_{12}', then

$$A_{12}' = \begin{bmatrix} M_{\Delta Vf} & M_v & M_\gamma \\ L_{\Delta Vf} & L_v & L_\gamma \\ N_{\Delta Vf} & N_v & N_\gamma \end{bmatrix}$$

Now these terms represent cross-coupling in three degrees of freedom, and can be influenced by three controls - longitudinal and lateral cyclic, and tail rotor collective. A multivariable linear feedback can thus be constructed from ΔV_f, v and γ to these three controls that will set the cross-couplings above to zero, simply by solution of a set of simultaneous linear equations, viz.

$$B_{sub}K' = A_{12}'$$

$$\text{then } K' = B_{sub}^{-1}A_{12}'$$

where B_{sub} is a submatrix of B consisting of longitudinal and lateral cyclic and tailrotor derivatives in the pitch, roll and yaw degrees of freedom, and K' is a submatrix of K. Having decoupled the rotational dynamics from the translational degrees of freedom, adequate response characteristics and stability were obtained by feedback of pitch attitude and rate, roll attitude and rate and yaw angle and rate to respectively longitudinal cyclic, lateral cyclic and tail rotor collective. This was done on an iterative basis. The closed-loop eigenvalues of the resulting helicopter/FCS combination are

-8.1227

-6.4665

-4.3552

-3.2028

-2.6671

-0.8562

-0.1675

-0.1615

0.0000

That the closed-loop system gives the desired attitude response characteristics is shown in figure 5:41.